



**HAL**  
open science

## New recyclable catalysts for the formations of carbon-carbon and carbon-nitrogen bonds

Dong Wang

► **To cite this version:**

Dong Wang. New recyclable catalysts for the formations of carbon-carbon and carbon-nitrogen bonds. Organic chemistry. Université de Bordeaux, 2014. English. NNT : 2014BORD0128 . tel-01159007

**HAL Id: tel-01159007**

**<https://theses.hal.science/tel-01159007>**

Submitted on 2 Jun 2015

**HAL** is a multi-disciplinary open access archive for the deposit and dissemination of scientific research documents, whether they are published or not. The documents may come from teaching and research institutions in France or abroad, or from public or private research centers.

L'archive ouverte pluridisciplinaire **HAL**, est destinée au dépôt et à la diffusion de documents scientifiques de niveau recherche, publiés ou non, émanant des établissements d'enseignement et de recherche français ou étrangers, des laboratoires publics ou privés.

THÈSE EN COTUTELLE PRÉSENTÉE  
POUR OBTENIR LE GRADE DE  
**DOCTEUR DE**  
**L'UNIVERSITÉ DE BORDEAUX**

ÉCOLE DOCTORALE  
SPÉCIALITÉ : Chimie Organique

Par

**M. Dong WANG**

**NOUVEAUX CATALYSEURS RECYCLABLES POUR LES  
REACTIONS DE FORMATION DE LIAISONS  
CARBONE-CARBONE ET CARBONE-AZOTE**

Sous la direction de M. Didier ASTRUC

Soutenue le: 26 Septembre 2014

Membres du jury:

Mme Angela MARINETTI	Directeur de recherche au CNRS	Rapporteur
M. Noël LUGAN	Directeur de recherche au CNRS	Rapporteur
M. Jean-François LETARD	Directeur de recherche au CNRS	Examineur
M. Lionel SALMON,	Chargé de Recherche au CNRS	Examineur
M. Jaime RUIZ	Ingénieur contractuel à Université de Bordeaux	Membre invité
M. Didier ASTRUC	Professeur à l'Université de Bordeaux	Directeur de thèse

# Acknowledgement

This thesis was completed in the **Institut des Sciences Moléculaires** (ISM), UMR CNRS N °5255, Bordeaux University.

I would like to express my gratitude to all those who have helped me during the writing of this thesis. First of all, I would like to express my sincerest gratitude to my supervisor **Prof. Didier Astruc**, for his inspiring, patient instruction, insightful criticism and expert guidance on my thesis. Without his consistent and illuminating instruction, this thesis could not have reached its present form. His profound knowledge of chemistry triggers my love for this area, his earnest attitude tells me how to be an eligible chemist. I am also deeply grateful for his kind help in daily life. All help from him will be always engraved on my mind.

I am also greatly indebted to the two reporters for the thesis, **Angela Marinetti**, and **Mr. Noël Lugan**, and the other external jury members **Jean-François Létard**, and **Lionel Salmon** CNRS Director of Research for their time and energy in serving as referees and examiners of the PhD.

I am also deeply grateful to the engineer of our research group, **Dr. Jaime Ruiz**, for his patient guidance on experiment operation and excellent work on cyclic voltammetry. High tribute shall be paid to **Lionel Salmon**, **Sergio Moya**, **Dominique Denux**, **Mrs. Christine Labrugère**, and **Laetitia Etienne** for their excellent analyses on several samples.

My sincere gratitude also goes to my former and current colleagues, including **Amalia Rapakousiou**, **Yanlan Wang**, **Liyuan Liang**, **Christophe Deraedt**, **Pengxiang Zhao**, **Haibin Gu**, **Changlong Wang**, **Sylvain Gatard**, **Roberto Ciganda** and **Martin d'Halluin**, who kindly gave me invaluable advice and help to solve various problems in both study and life.

Last but not the least, my gratitude also extends to my family who have been assisting, supporting and caring for me all of my life. Special thanks should go to my wife **Na Li** who give me continuous support and encouragement during my thesis.

# Table of Content

<b>General Introduction.....</b>	<b>1</b>
<b>Chapter 1</b>	
<b>Overview on Dendritic and Magnetic Catalysts.....</b>	<b>5</b>
1.1 Introduction.....	6
1.2 Dendritic Catalysis – Basic Concepts and Recent Trends.....	7
1.3 Fast-Growing Field of Magnetically Recyclable Nanocatalysts.....	26
<b>Chapter 2</b>	
<b>Iron Oxide Magnetic Nanoparticle-Immobilized Ru Catalyst.....</b>	<b>62</b>
2.1 Introduction.....	63
2.2 Magnetically Recoverable Ruthenium Catalysts in Organic Synthesis.....	64
2.3 A recyclable Ruthenium(II) Complex Supported on Magnetic Nanoparticles: A Regioselective Catalyst for Alkyne–Azide Cycloaddition.....	83
<b>Chapter 3</b>	
<b>Magnetic Nanoparticle-Immobilized Tris(triazolyl) Cu(I) Catalyst for the Copper-catalyzed Alkyne Azide (CuAAC) "Click" Reaction.....</b>	<b>86</b>
3.1 Introduction.....	87
3.2 A Highly Active and Magnetically Recoverable Tris(triazolyl) Cu(I) Catalyst for “Click” Alkyne-Azide Cycloaddition Reaction.....	88
<b>Chapter 4</b>	
<b>Magnetically Recyclable Palladium Nanoparticles in C-C Coupling Reactions..</b>	<b>96</b>
4.1 Introduction.....	97
4.2 Highly Efficient and Magnetically Recoverable “Click” PEGylated $\gamma$ -Fe <sub>2</sub> O <sub>3</sub> -Pd Nanoparticle Catalysts for Suzuki-Miyaura, Sonogashira, and Heck Reactions.....	99
4.3 Impregnation of Dendritically Preformed Pd Nanoparticles on Magnetic Nanoparticles for Improved Catalyst Robustness, Efficiency and Recyclability..	131
<b>Chapter 5</b>	
<b>Mono- and Polymetallic Palladium Complexes Containing 2-Pyridyl-1,2,3-triazole Ligand or Nonabranched-derived Ligand.....</b>	<b>143</b>
5.1 Introduction.....	144
5.2 The Clicked Pyridyl-Triazole Ligand: From Homogeneous to Robust, Recyclable Heterogeneous Mono- and Polymetallic Palladium Catalysts for Efficient Suzuki-Miyaura, Sonogashira, and Heck Reactions.....	146
<b>Conclusion and Perspective.....</b>	<b>160</b>
<b><i>List of Published or Submitted Thesis Publications</i>.....</b>	<b>163</b>

## General Introduction

Increasing environmental concerns have pushed chemists to turn their attention from traditional concepts of process efficiency to “green” and sustainable chemistry that assign minimization of waste generation and avoid the use of toxic and/or hazardous substances.<sup>1,2,3</sup> Specifically, the guiding principle of green chemistry can be paraphrased as: *waste prevention instead of remediation, atom efficiency, less hazardous/toxic chemicals, safer products by design, innocuous solvents and auxiliaries, energy efficient by design, preferably renewable raw materials, shorter syntheses (avoid derivatization), catalytic rather than stoichiometric reagents, design products for degradation, analytical methodologies for pollution prevention and inherently safer processes.*<sup>4</sup>

Green catalysis, a key component of these principles, is extremely important in the modern development of green chemistry.<sup>5,6,7</sup> A green catalyst must possess specific features including low preparation cost, high activity, great selectivity, high stability, efficient recovery, and good recyclability.<sup>8</sup> To date, several effective strategies resulting in green catalysis have been discovered such as the recovery of catalyst, cascade reaction protocol, the use of “green” solvents (neat condition, water, ethanol, ionic liquids, supercritical liquids), flow conditions, photocatalysis and so on. Design and use of recoverable catalysts are the most promising and straight way to green catalysis, because the recovery of catalyst is not only a task of great economic and environmental importance in catalysis science, but also overcome the problem of metal contamination in products.

Catalyst recovery can be done by the experimental manipulations of precipitation, traditional filtration, nanofiltration with membranes, centrifugation, extraction and magnetic separation.<sup>5</sup> In general, to achieve these processes, organic and inorganic supports (including polymers, dendrimers, metal oxides, alumina, fluoros tag, zeolites, carbon nanotube, graphene, active carbon, silica, metal nanoparticles, ionic liquids, and so on) are needed for immobilizing free catalytic species forming heterogeneous or homogeneous catalysts.

We have long been interested in catalyst recovery, especially for dendrimer catalysts and magnetic nanoparticles-immobilized catalysts. Dendrimers are a family of nanosized, branched three-dimensional supramolecular, and possess monodisperse nature which retains the advantage of homogeneous catalysts in terms of showing fast kinetic behavior, easy tenability and rationalization.<sup>9-13</sup> Moreover, dendrimer catalysts can easily be removed from the reaction mixture by precipitation, traditional filtration, or nanofiltration techniques because of their large size compared with the products.<sup>11</sup>

Magnetic nanoparticles (MNPs) have attracted considerable interest as ideal supports, and the study in this field has been undergoing an explosive development.<sup>14</sup> Indeed, magnetic nanoparticles (MNPs) perfectly bridge the gap between catalytic activity and catalyst separation. Magnetically recyclable catalysts have the potential to approach catalysts benefiting from high activity, high selectivity, high stability, and easy separation, because MNPs-immobilized catalysts combine the advantages of nanocatalysts<sup>15,16</sup> with their inherent properties including non-toxicity, biocompatibility, facile assembling, and high accessibility of reusability through magnetic attraction.

As mentioned above, dendrimer catalytic and magnetic catalysts are two important modes of catalyst recovery. Their comparison should be deeply significant and useful in catalyst recovery science. Therefore, we reviewed both subjects and present these overviews in the first chapter.

The second chapter concerns magnetically recyclable Ru catalysts. First of all, the history, trends and prospects of MNPs-immobilized Ru catalysts involving the related design, synthesis and catalytic application are briefly described. This overview was published in the journal "*Molecules*". The second subsection is an experimental study that mainly focuses on the immobilization of pre-synthesized pentamethylcyclopentadienyl ruthenium complexes on iron oxide nanoparticles and its catalytic test in alkyne-azide cycloaddition regioselectively producing 1,5-disubstituted 1,2,3-triazoles.

The third chapter demonstrates that the versatile tris(triazolyl) ligand is readily deposited on MNPs, and subsequent complexation with CuBr salt generates a novel

MNPs-supported tris(triazolyl)-CuBr catalyst. This catalyst shows a high activity for Cu(I)-catalyzed alkyne-azide cycloaddition (CuAAC “click” reaction) in aqueous solution at room temperature, and more importantly copper recovery is achieved.

The fourth chapter provides a description of MNPs-anchored Pd nanoparticles (PdNPs). The efficiency of triethylene glycol (TEG)-terminated “click” dendrimers-stabilized metal NPs has been testified by our previous research.<sup>17,18</sup> Based on this, we turn our attention to the synthesis of MNP-immobilized PdNPs decorated with dendritic TEG-terminated “click” ligands. The syntheses were carried out through two strategies: reduction of pre-coordinated Pd salts immobilized on the MNP support, impregnation of pre-synthesized PdNPs into MNPs. Both kinds of MNPs-PdNPs performed well in carbon-carbon coupling reactions, and unprecedented dendritic effects were observed in various aspects.

The fifth chapter introduces the syntheses of palladium complexes containing single or nonbranched 2-pyridyl-1,2,3-triazole ligands. When a nonbranched ligand was used, partly- and fully- metalized Pd complexes showed various state in the given media. Their catalytic properties were also tested in classic coupling reactions.

At the end of the thesis, the “Conclusion and Perspectives” section summarizes the progress resulting from the research conducted during this thesis concerning heterogeneous and abundant catalysts for various classic reactions. In addition, perspectives are provided, indicating that development of new magnetic plasmonic photocatalysts based on AuNPs, AgNPs and CuNPs, exploration of magnetic bimetallic catalysts, and replacement of “noble” metal catalysts by abundant metal (so-called “biometals”) catalysts should be valuable goals of further work along this line.

## References

1. P. T. Anastas, J. C. Warner, *Green Chemistry: Theory and Practice*, Oxford University Press, New York, **1998**.
2. M. Doble, A. K. Kruthiventi, *Green Chemistry and Engineering*, Academic Press, London, **2007**.

3. S. K. Sharma, A. Mudhoo, *Green Chemistry for Environmental Sustainability*. CRC Press, Boca Raton, FL, USA, **2010**.
4. R. A. Sheldon, I. Arends, U. Hanefeld, *Green Chemistry and Catalysis*. Wiley-VCH, Weinheim, Germany, **2007**.
5. G. Ertl, H. Knozinger, J. Weitkamp, Eds. *Handbook of Heterogeneous Catalysis*. Wiley-VCH, Weinheim, Germany, **1997**.
6. A. Suzuki In. *Modern Arene Chemistry*. D. Astruc, Ed. Wiley-VCH, Weinheim, **2002**.
7. G. A. Somorjai, *Introduction to Surface Chemistry and Catalysis*. Wiley, New York, **1994**.
8. S. B. Kalidindi, B. R. Jagirdar, *ChemSusChem* **2012**, 5, 65.
9. G. R. Newkome, E. He, C. N. Moorefield, *Chem. Rev.* **1999**, 99, 1689.
10. G. R. Newkome, C. N. Moorefield, F. Vögtle, *Dendrimers and Dendrons: Concepts, Synthesis Applications*. Wiley-VCH, Weinheim, **2001**
11. D. Astruc, F. Chardac, *Chem. Rev.* **2001**, 101, 2991.
12. L. Gade (Ed.), *Dendrimer Catalysis*. Springer, Heidelberg, **2006**.
13. J. M. J. Fréchet, D. A. Tomalia, *Dendrimers and Other Dendritic Polymers*. JohnWiley & Sons, Ltd, **2001**.
14. V. Polshettiwar, R. Luque, A. Fihri, H. Zhu, M. Bouhrara, J.-M. Basset, Magnetically Recoverable Nanocatalysts, *Chem. Rev.* 2011, 111, 3036–3075.
15. Astruc, D. Ed. *Transition-metal Nanoparticles in Catalysis*. Wiley-VCH: Weinheim, **2008**.
16. B. D. Chandler, J. D. Gilbertson, In D. Astruc, (ed) *Nanoparticles and Catalysis*, Wiley-VCH, Weinheim, 2007.
17. E. Boisselier, A. K. Diallo, L. Salmon, C. Ornelas, J. Ruiz, D. Astruc, *J. Am. Chem. Soc.* **2010**, 132, 2729.
18. C. Deraedt, L. Salmon, L. Etienne, J. Ruiz, D. Astruc, *Chem. Commun.* **2013**, 49, 8169.

**Chapter 1**  
**Overview on Dendritic and Magnetic Catalysts**

## 1.1 Introduction

Dendrimer chemistry has attracted considerable interest and driven various promising applications in drug delivery, materials science and catalysis. This field is also an important part of the research of our group, and a variety of dendrimers were specifically prepared and applied therein in biology, catalysis, sensing and nanotechnology.

Since 2001, our group has published several review articles or overviews on the development of dendrimer chemistry. For example, in 2010, our group published a comprehensive review entitled “*Dendrimers Designed for Functions: From Physical, Photophysical, and Supramolecular Properties to Applications in Sensing, Catalysis, Molecular Electronics, Photonics, and Nanomedicine*”.<sup>1</sup> In 2012, a review on electron-transfer processes in dendrimers and applications was published.<sup>2</sup> Here, our attention is mainly focused on the developments and trend of dendrimers in catalysis.<sup>3-5</sup>

Dendrimer chemistry is still promising in catalysis, and many publications on dendritic catalysis emerged in the last few years. Thus it appeared necessary to write a new updated review on the recent breakthroughs and trends in this area.

In recent years, the development of magnetic catalysts is enormously accelerating.<sup>7</sup> A large number of new reactions, nanocatalysts, systems, and trends are appearing at a fast rate, and more than 400 publications have appeared in the last 2 years. Thus, in this chapter, we also summarize the basic concepts, seminal studies, new breakthroughs of magnetically recoverable catalysts.

### References:

1. D. Astruc, E. Boisselier, C. Ornelas, *Chem. Rev.* **2010**, *110*, 1857.
2. D. Astruc, *Nat. Chem.* **2012**, *4*, 255.
3. D. Astruc, F. Chardac, *Chem. Rev.* **2001**, *101*, 2991.
4. D. Astyuc, *Tetrahedron Asymm.* **2010**, *21*, 1041 (Henri Kagan issue).
5. V. Polshettiwar, R. Luque, A. Fihri, H. Zhu, M. Bouhrara, J.-M. Basset, Magnetically Recoverable Nanocatalysts, *Chem. Rev.* **2011**, *111*, 3036–3075.



## Review

## Dendritic catalysis—Basic concepts and recent trends



Dong Wang, Didier Astruc\*

ISM, Univ. Bordeaux, 351 Cours de la Libération, 33405 Talence Cedex, France

## Contents

1. Introduction .....	2317
2. Basic concepts and seminal studies .....	2319
3. Recent advances and trends .....	2321
3.1. Metallo dendritic catalysts .....	2321
3.1.1. Suzuki–Miyaura reaction .....	2321
3.1.2. Mizoroki–Heck reaction .....	2322
3.1.3. Cu-catalyzed alkyne–azide (CuAAC) reaction .....	2323
3.1.4. Hydrogenation .....	2324
3.1.5. Carbonylation and hydroformylation reactions .....	2327
3.1.6. Oxidation reaction .....	2327
3.1.7. Polymerization and oligomerization .....	2327
3.1.8. Arylation and alkylation reactions .....	2327
3.1.9. Asymmetric synthesis .....	2328
3.1.10. Other reactions .....	2328
3.2. Dendritic organocatalysts .....	2330
4. Conclusion and outlook .....	2332
Acknowledgments .....	2332
References .....	2332

## ARTICLE INFO

## Article history:

Received 5 March 2013

Accepted 28 March 2013

Available online xxx

## Keywords:

Dendrimer

Metallo dendritic catalysts

Catalysis

Organocatalysts

Nanoparticle catalysts

## ABSTRACT

In this review, attention is focused on briefly summarizing the main concepts of dendrimers in catalysis and essentially reviewing new breakthroughs and trends in this area that have appeared during the last few years. Dendrimers have been proposed to bridge the gap between homogeneous and heterogeneous catalysis, and dendritic catalysts have the potential to approach catalysts benefiting from high activity, high selectivity, high stability, and easy separation.

© 2013 Published by Elsevier B.V.

**Abbreviations:** ARO, asymmetric epoxide ring-opening; BINAP, 2,2'-bis(diphenylphosphino)-1,1'-binaphthyl; CM, cross metathesis; Cp, cyclopentadiene; CuAAC, copper-catalyzed alkyne–azide cycloaddition; DENS, dendrimer-encapsulated nanoparticles; DPA, dendritic phenylazomethine; DSNS, dendrimer-stabilized nanoparticles; EYM, enyne metathesis; FTSDPEN, fluorinated dendritic chiral mono-*N*-tosylated 1,2-diphenylethylenediamine;  $G_n$ , number of dendritic generation; HKR, hydrolytic kinetic resolution; MNP, metal nanoparticle; NBD, norbornadiene; NP, nanoparticle; PAMAM, polyamidoamine; PAMDMAM, polyamidodimethylamine; PdNP, palladium nanoparticle; POM, polyoxometalate; PPI, polypropylene imines; PTA, (1,3,5-triaza-7-phosphaadamantane); PPX, poly(*p*-xylylene); pyta, pyridyltriazole; RCM, ring-closing metathesis; SILC, supported ionic liquid catalyst; TEMPO, 2,2,6,6-tetramethylpiperidine-*N*-oxyl.

\* Corresponding author.

E-mail address: [d.astruc@ism.u-bordeaux1.fr](mailto:d.astruc@ism.u-bordeaux1.fr) (D. Astruc).

## 1. Introduction

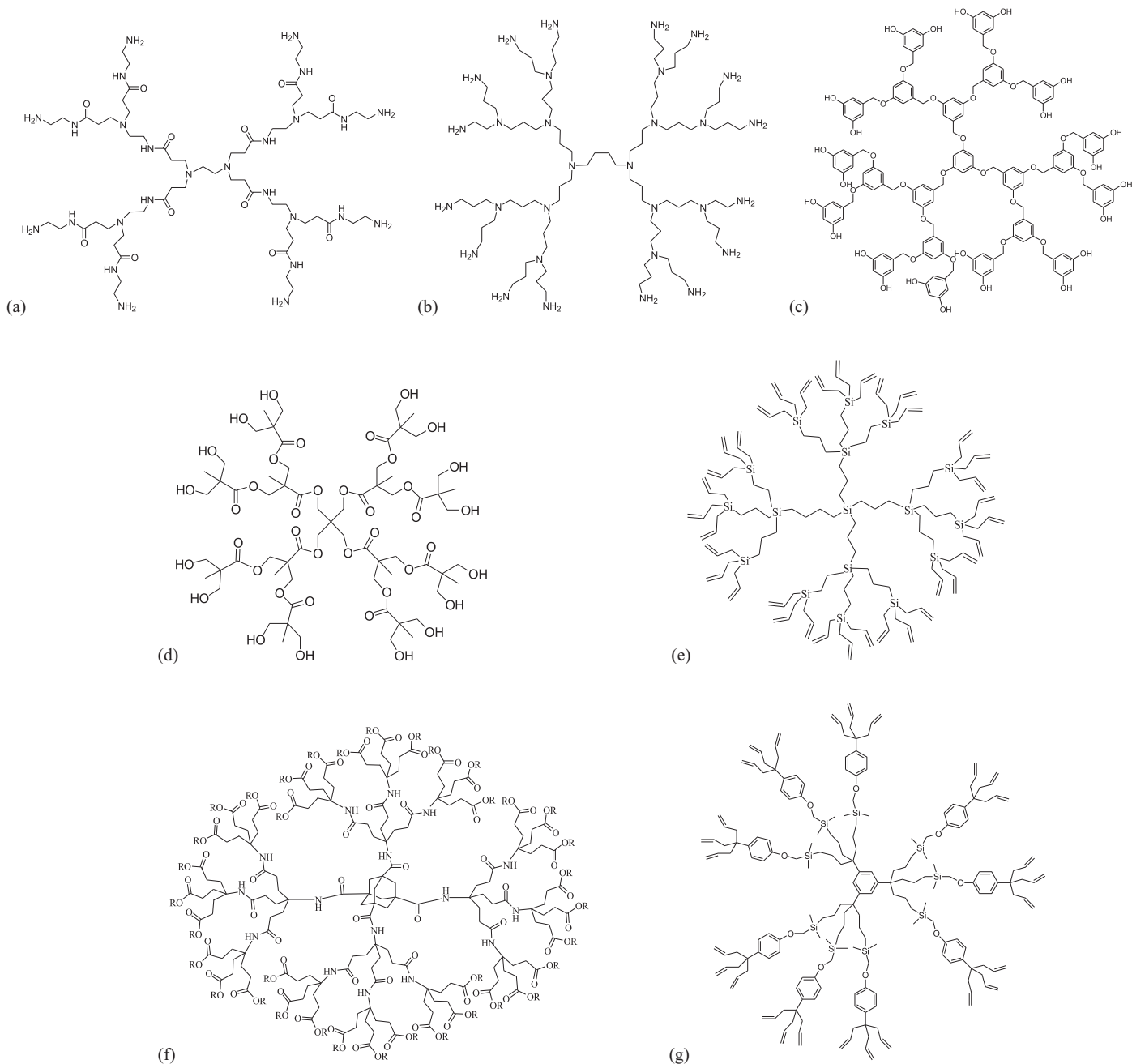
Dendrimers, dendrons, dendronized and dendritic and hyper-branched polymers are a family of nanosized, branched three-dimensional molecular frameworks that have attracted the scientific community since the 1980s [1–7]. Essential and promising applications are in nanomedicine including targeted drug delivery and imaging, materials science with sensors, light harvesting devices and surface engineering and catalysis [8–23]. In the latter field, advances towards green and sustainable chemistry have been a driving force to optimize the use of metal catalysts in terms of efficiency, catalyst recovery and minimization of contamination by metal ions and particles [24–40]. Since the pioneering

work on catalysis of CO/alkene polymerization upon comparing mononuclear and star-shaped hexaphosphine-palladium catalysts was reported in 1992 [41], a great variety of dendritic catalysts have been developed, and corresponding theoretical knowledge and derived technologies in dendritic catalysis have become mature [24–40].

Why is dendritic catalysis so popular? What can dendrimers add to the field of catalysis? Dendritic catalysts exhibit well-defined structures and possess a monodisperse nature which retains the advantage of homogeneous catalysts in terms of showing fast kinetic behavior, easy tenability and rationalization. Dendritic catalysts can easily be removed from the reaction mixture by precipitation, membrane or nanofiltration techniques because of their large size compared with the products, which

instills the advantages of heterogeneous catalysts. Moreover, it is possible to finely tune the catalytic properties of the dendritic catalysts through the adjustment of their structure, size, shape, chemical functionality, and solubility. In a few words, dendrimers have been proposed to bridge the gap between homogeneous and heterogeneous catalysis, and dendritic catalysts have the potential to approach catalysts benefiting from high activity, high selectivity, high stability, and easy separation.

Many reviews have appeared on dendrimer catalysis since the beginning of the 2000s [24–40]. Here we wish to briefly summarize the main concepts of dendrimers in catalysis and essentially review new breakthroughs and trends in the area that have appeared during the last 5 years.

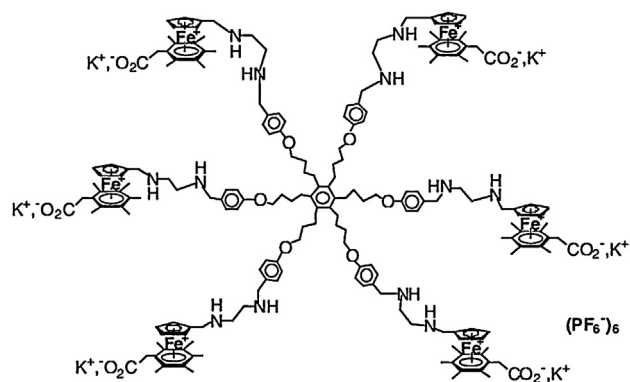


**Fig. 1.** Structures of dendrimers commonly used in catalysis: (a) PAMAM; (b) PPI; (c) polybenzyl ether; (d) polyaliphatic ester; (e) polycarbosilane; (f) polyester amide; and (g) allyl-ended arene-cored dendrimer.

Reprinted with permission from [48] (Fréchet's group).

© 2006 Wiley-VCH.





**Fig. 4.** Astruc's water-soluble star-shaped catalyst for cathodic reduction of nitrates and nitrites to ammonia showing no kinetic drop from the monometallic to the star-shaped catalyst [55].

hydrolytic kinetic resolution (HKR) of terminal epoxides seemingly proceeds using cobalt (salen) complexes as catalysts (Fig. 3) [53]. The catalytic activities of G1 to G3 PAMAM dendrimers with respectively 4, 8 and 16 catalytic residues at the periphery were superior to those of the monomeric and dimeric catalysts, indicating a positive dendrimer effect. This effect was assigned to the dendritic confinement of the Co-salen complexes at the surface of the macromolecule that was claimed to reinforce cooperative catalytic activity. A rather general trend in periphery-functionalized dendritic catalysts which are the majority of metallodendritic catalysts reported, is the bulk provided at the periphery upon increasing the dendrimer generation, restricting access of the substrate to the catalytic metal center. Therefore, a better spatial separation of catalytic sites in the dendrimer should be arranged. This problem has been recognized, and it was suggested that star-shaped structures containing catalysts at the branch termini should not suffer from such steric constraints [54]. Star-shaped hexanuclear catalysts containing six CpFe<sup>I</sup>(arene) complexes (Fig. 4) are efficient redox catalysts for nitrate and nitrite reduction to ammonia in water without kinetic loss compared with monometallic catalysts [55]. This shows here the lack of steric inhibition that is often encountered in dendritic frameworks loaded with catalysts at the branch termini (negative dendritic effect).

The building block (backbone) regions of a dendrimer could provide a localized environment suitable for binding and catalysis (Fig. 2c). The catalytic site concentration of this attachment style is very high, which might result in high reaction rates. An effective approach for the synthesis of this shape of dendritic catalysts is that using ionic bonds in connection with hydrogen bonds to attach the catalyst to the building block of dendrimers [56,57]. Another approach in attaching catalytic sites at dendritic building blocks was provided [58]. Thus phosphine ligands of the catalyst were located at the branching points all along the dendritic construction.

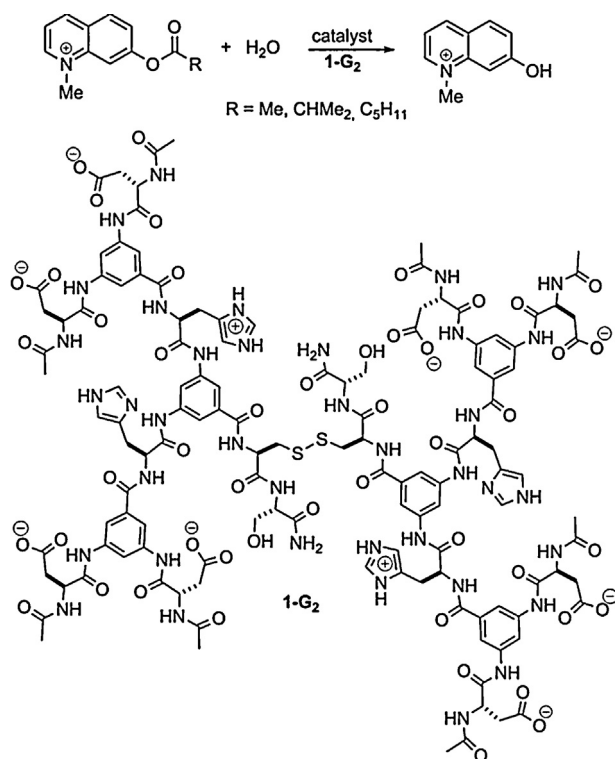
Metal nanoparticles (MNPs) are among the most efficient and selective catalysts [59–67]. They are usually synthesized by reduction of a transition-metal salt, and the generated metal (0) atoms agglomerate; this agglomeration is stopped at a certain point in the presence of various stabilizers such as ligands, polymers, surfactants, ionic liquids or solid supports such as oxides, etc. A problem resides in the stabilization of the nanoparticle (NP) surface without blocking access of substrates to this surface, however, thus a fine balance between stabilization and surface access must be targeted. Localization of a NP inside a dendrimer brings about an elegant solution to this problem. Another important aspect is the control of the size and shape of the NPs that is best accessible upon encapsulation inside dendrimers. Dendrimer-stabilized nanoparticles (DSNs) [68,69] and dendrimer-encapsulated nanoparticles (DENs) [70] can

be used for various types of catalysis as well as molecular dendritic catalysts. Catalysis with DENs was pioneered in 1999 with Gn-OH PAMAM Pd and Pt DENs ( $n = 4–8$ ) for the hydrogenation of allylic alcohol and *N*-isopropylacrylamide in water [71,72]. Another promising area was that of dendrimer-encapsulated nanoparticles in heterogeneous catalysis [73,74]. The powerful Cu<sup>I</sup>-catalyzed “click” reaction between azido and terminal alkyne derivatives (CuAAC) selectively forming disubstituted 1,2,3-triazoles has been used to stabilize transition-metal ions including Pd<sup>II</sup> by the 1,2,3-triazole ligand [75–78] and to form “click”-dendrimer-protected Pd nanoparticles by reduction of the Pd<sup>II</sup> species to PdNP either as DENs or dendrimer-stabilized PdNPs (DSNs). Such PdNPs showed excellent catalytic activities in hydrogenation [79,80] and C–C cross coupling [37,81].

Dendritic catalysts are separated from the reaction medium through precipitation, membrane nanofiltration by taking advantage of the macromolecular and tunable natures of dendrimers. The technological improvements for separation were pioneered by Kragl and Reetz in their seminal study [82–84]. Subsequently, cationic dendrimer or dendron-protected polyoxometallate catalysts were recycled by precipitation upon addition of ether from biphasic CDCl<sub>3</sub>/aqueous mixtures after olefin epoxidation or sulfide oxidation to sulfones and secondary alcohols to ketones. Both families of metallodendrimers and dendron-protected catalysts could be used many times without loss of activity, although the activity of the dendron-protected catalysts decreased upon increasing the dendron generation and bulk [85–87]. Recently, dendritic copper(I) (hexabenzyl) tren complex that were active for “click” reactions between azides and alkynes in toluene or water were recharged at least 10 times through complete precipitation of the product from the reaction medium at  $-18^{\circ}\text{C}$  [88]. Silica gel-supported metallo-dendritic catalysis of olefin hydroformylation with Rh<sup>I</sup> provided another approach for recycling dendritic catalysts upon engineering heterogeneous solid support-bound dendritic catalysts [89]. Subsequent to this seminal work, many studies have been conducted by different groups in which the influence of the generation on catalytic effects, solid support, and backbone structure were investigated.

Asymmetric catalysis is an essential branch of catalysis research. In 1990s, the first example of dendritic asymmetric catalysis was reported [51,90], in which a chiral dendron bearing phosphines at its core was synthesized, thereby establishing the crucial “dendrzyme” concept. A number of reports then followed on asymmetric catalysis by dendritic chiral metal complexes. The first asymmetric rhodium-catalyzed hydrogenation of prochiral olefins in dendrimer catalysis and showed a slightly negative dendritic effect on selectivity upon increasing generation was reported in 1998 [91,92]. A strongly positive dendritic effect in asymmetric catalysis was demonstrated [93] whereby the ee for pyrphos-Pd-functionalized PPI and PAMAM dendrimers-catalyzed allylic amination of 1,3-diphenyl-1-acetoxypropene increased from 9% for the mononuclear reference [(Boc-Pyrphos) PdCl<sub>2</sub>] to 69% for the Pd<sub>64</sub>-PAMAM-dendrimer [94]. Dendritic asymmetric catalysts have been applied to several important organic reactions such as Mannich-type, Diels–Alder, Wittig reaction, Michael addition, asymmetric epoxide ring-opening, asymmetric hydrogenation and asymmetric epoxidation. Recent reviews have emphasized the importance of dendritic asymmetric catalysts [95,96].

Organocatalysis dates back more than 150 years. Since the beginning of the 21st century, dendritic organocatalysis has attracted considerable attention. Until now, most dendrimers (especially for PAMAM and PPI dendrimers) have been modified with organocatalytic moieties for use as support in various organocatalyzed reactions including formation of C–C bonds, cleavage of esters bonds, oxidation and reduction reactions [37]. The hydrolysis of esters using peptidic dendrimers has been examined



**Fig. 5.** Example of a peptide dendrimer used for catalyzing the hydrolysis of esters. Reprinted with permission from [97] (Reymond's group). © 2004 American Chemical Society.

with the view to mimic the efficiency of enzymes. A series of peptide dendrimers having diamino acid or 3,5-diaminobenzoic acid as branching units, bearing histidine, aspartate and serine were used to catalyze the hydrolysis of 7-hydroxy-N-methylquinolinium esters and 8-hydroxypyrene-1,3,6-trisulfonate esters. **1-G<sub>2</sub>** (Fig. 5) is one of these peptide dendrimers that was used for the hydrolysis of quinolinium esters [97]. The number of histidine residues per dendrimers was the crucial factor influencing the catalytic rate constants. Indeed, the G<sub>4</sub> dendrimer was 140 000-fold more efficient than 4-methylimidazole as a reference catalyst for the hydrolysis of the nonanoyl ester of pyrene [98].

### 3. Recent advances and trends

#### 3.1. Metallodendritic catalysts

##### 3.1.1. Suzuki–Miyaura reaction

The first three generations of dendritic bis(dicyclohexylphosphanyl)methylamine-functionalized palladium catalysts (Fig. 6) have been used in the Suzuki coupling reaction [99,100] of halogenoarenes, including chloroarenes with phenylboronic acid [101]. The G<sub>1</sub> dendrimer gave yields comparable to those obtained with the mononuclear complex, but a clear negative effect was observed with an increase of the generation. The dendritic compounds were recovered by precipitation with pentane and reused for three cycles.

Recently, the activity of Pd complexes of the core-functionalized dendriphos ligands has been examined in the Suzuki–Miyaura cross-coupling reaction [102,103]. A series of triarylphosphanes containing dendritically-arranged tetraethylene glycol moieties at the periphery were synthesized (Fig. 7), and the combination of [PdCl<sub>2</sub>(PhCN)<sub>2</sub>] and second generation dendritic derivative **2a<sub>2</sub>** with the TEG chains led to a highly active catalytic system: down to 0.1 mol% catalyst loading yielded 93% conversion,

when nonactivated aryl chloride was employed. Haag designed a hyperbranched water-soluble polyglycerol derivative functionalized with *N*-heterocyclic carbene palladium complexes, and applied it as catalyst for Suzuki cross-coupling reactions in water. Turnover frequencies of up to 2586 h<sup>-1</sup> at 80 °C were observed with the dendritic catalyst along with turnover numbers of up to 59 000, which are among the highest turnover numbers reported for polymer-supported catalysts in neat water. The dendritic catalyst could be reused in five consecutive reactions without loss in activity [104]. A pseudo-homogeneous heterogenized catalyst was synthesized through noncovalently immobilized palladium acetate as a supported ionic liquid catalyst (SILC) in a nanosilica dendrimer PAMDMAM [105]. The supported dendritic catalyst was effective for Suzuki–Miyaura reactions of *ortho*-substituted aryl bromides or aryl triflates without a ligand in 50% aqueous ethanol in air at room temperature. The catalyst could be reused up to five times in 93% average yield after simple centrifugation, and the TON reached 176 000. The efficient use of a “click” dendritic monodentate phosphine ligand in the Pd-catalyzed Suzuki–Miyaura coupling was reported. The dendritic complex was easily removed from the reaction mixture by nanofiltration using ceramic nanofiltration membranes [106].

Mono- and polymetallic palladium complexes containing a 2-pyridyl-1,2,3-triazole (pyta) ligand or a nonbranch-derived (nonapyta) ligand have been synthesized by reaction of palladium acetate with these ligands and used as catalysts for Suzuki–Miyaura, Sonogashira and Heck reactions (Fig. 8) [107]. The unsubstituted monopalladium **1** and nonapalladium complexes **2<sub>9</sub>** were insoluble in all the reaction media; whereas, tri- and tetranuclear palladium complexes (**2<sub>3</sub>** and **2<sub>4</sub>**) were soluble, which allowed conducting catalysis under either homogeneous or heterogeneous conditions. Both types of catalysts showed excellent activity for Suzuki–Miyaura, Sonogashira and Heck reactions. In addition, the recyclable feature of heterogeneous catalysts was verified in the example of Heck reaction.

In many cases, the problem of metal leaching restricted the application of dendritic catalysis in the pharmaceutical industry. The use of phosphorus dendrimers partially addressed the problem. Phosphorus dendrimers (G<sub>0</sub> and G<sub>3</sub>) functionalized with thiazolyl phosphines showed high activity in Pd-catalyzed Suzuki reactions even under mild conditions, and the catalytic systems could be successfully recovered and reused at least five times [108]. In addition, palladium leaching in dendritic catalysis decreased compared with monomeric catalysis. Only trace amounts of metal (<0.55 ppm) were found in the product before purification by column chromatography, and the product met the specification limits for residues of metal catalysts in the pharmaceutical industry [109]. Pyrene-tagged dendritic Pd-phosphine catalysts grafted with magnetic Co/C nanoparticles were prepared and used as catalysts in the Suzuki–Miyaura reactions with high efficiency [110]. Attaching a dendritic ligand onto the NP surface allowed up to five times higher loading (0.5 mmol g<sup>-1</sup> active sites) than the previously reported direct functionalization of catalysts onto the NP [111]. Moreover, the use of a magnetic support made the catalysts more easy to remove from the reaction mixture by simply applying an external magnetic field. It could be reused at least 12 times without loss in activity. Remarkably, Felbinac, which is a commercially available drug of great industrial interest, can be prepared in multiple runs using this catalyst with specification limits for residues of metal catalysts in pharmaceutical industry (<5 ppm Pd) and without tedious purification.

A series of “click”-ferrocenyl dendrimer-encapsulated and stabilized Pd nanoparticle pre-catalysts were synthesized with various generations of 1,2,3-triazolyl dendrimers (G<sub>1</sub>-27, G<sub>2</sub>-81 for DENs, G<sub>0</sub>-9 for DSNs) (Fig. 9). With these PdNPs, catalysis of Suzuki–Miyaura C–C coupling [112] between PhI and PhB(OH)<sub>2</sub>

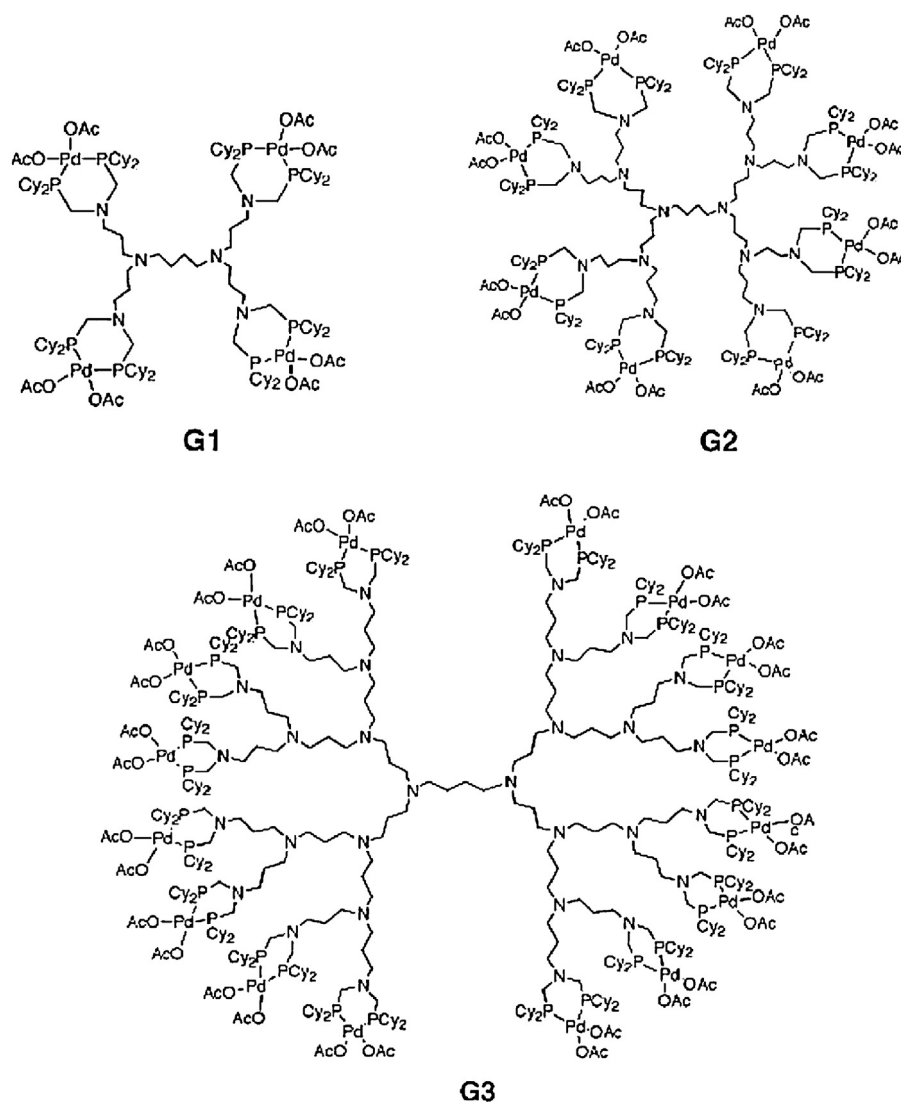


Fig. 6. Dendritic diphosphino Pd(II) complexes.

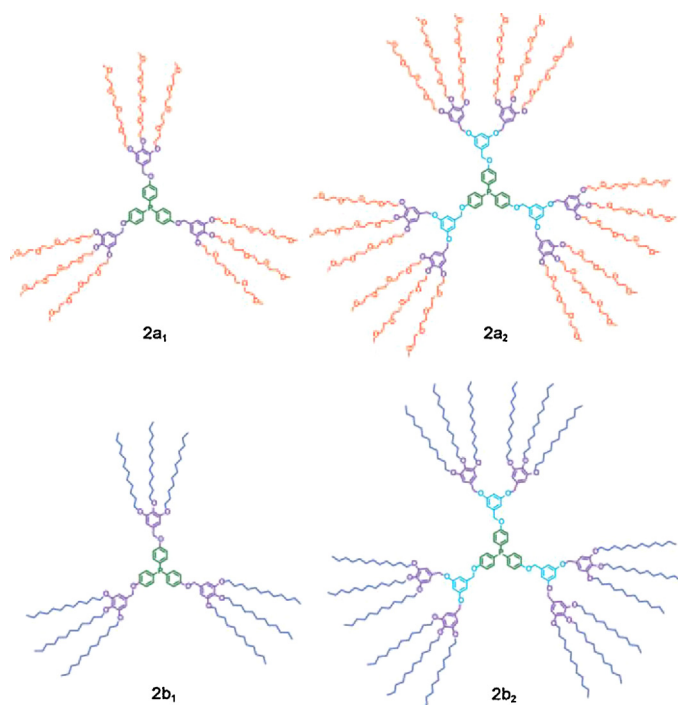
Reprinted with permission from [101] (Astruc's group).  
© 2005 American Chemical Society.

was carried out at room temperature and did not depend on the PdNP size and whether its stabilization is intra- or interdendritic. This indicated that the dendrimer was not involved in the rate-limiting step of the reaction. The dendrimer-stabilized PdNPs worked identically whatever their size, and the TONs increased upon decreasing the amount of catalyst from 1% down to 1 ppm or upon dilution of the reaction solution. Thus, the efficiency of the catalyst was remarkable in homeopathic amounts (54% yield at 25 °C with 1 ppm equivalent of Pd atom, i.e. TON = 540 000). A quantitative yield was not even reached (75% yield) with 1% equivalent Pd atom [81], which, however, confirmed the hypothesis of a “homeopathic” catalytic mechanism. The “homeopathic” mechanism was already observed for the Heck reaction at 150 °C and was rationalized according to a leaching mechanism involving detachment of Pd atoms from the PdNP subsequent to oxidative addition of the organic halide PhI on the PdNP surface [113–117]. This mechanism was established for high-temperature reactions due to decomposition of the Pd catalyst to naked PdNPs, but it was less expected for a room-temperature reaction. The ease of the room-temperature reaction must have been due, however, to the lack of ligation onto the dendrimer-stabilized PdNPs that therefore could easily undergo

oxidative addition of PhI at their surface, which provoked leaching of Pd atoms. These isolated Pd atoms are apparently extraordinarily reactive in solution, because they do not bear ligands other than the very weakly coordinating solvent molecules. The limit in their efficiency is reached when these atoms or small clusters are trapped by their mother NP, if the solution is moderately concentrated. This trapping mechanism that inhibits catalysis is always less efficient as the concentration of catalyst in the solution is lowered. Therefore it is not efficient under extremely diluted solutions, whereas it strongly inhibits catalysis at relatively high concentrations. It is likely that this concept can be extended to other PdNP-catalyzed C–C bond formation reactions (Fig. 10).

### 3.1.2. Mizoroki–Heck reaction

The first example of catalyst recovery and a positive dendritic effect in catalysis with metal dendrimers was reported in 1997 [82], in which poly(propylene imine) dendrimer modified palladium complexes with diphenylphosphanyl methyl end-groups showed significantly higher activity than the mononuclear complex in Heck reaction [118], probably due to its reduced tendency to decompose



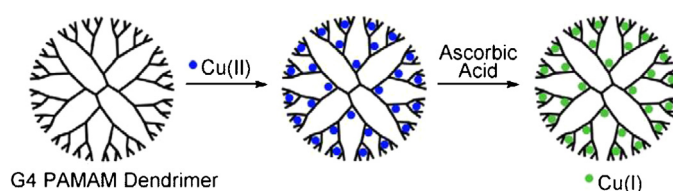
**Fig. 7.** Novel phosphane ligands bearing tetraethylene glycol or *n*-C12 moieties. Reprinted with permission from [103] (Tsuji's group). © 2008 Wiley-VCH.

thermally to metallic Pd. The dendritic catalyst was recovered by precipitation with diethyl ether.

Recently, studies on the efficacies of multivalent vs. monovalent dendritic catalysts through comparative research within or across the dendrimer generations based on C–C bond-forming reactions (especially of Heck reaction) were published [119,120]. A series of partially and fully phosphine–Pd complexes functionalized poly(ether imine) dendrimers catalysts were synthesized, and the comparative analyses showed that an individual catalytic site was far more effective in its catalytic activity when presented in multiple numbers, i.e., in a multivalent dendritic system, than as a single unit within the same generation; and that higher clustering of catalytic moieties is more effective than a lesser number. The study verifies the positive effects of the multivalent presentation of the catalytic moieties.

Amidoamine-based dendrimers with end-grafted 1–5 Pd–Fe units were designed (Fig. 11), and these bimetal complexes exhibited catalytic activity for the Heck cross coupling of iodobenzene with *tert*-butyl acrylate [121]. The comparison of catalytic performance among these dendritic catalysts confirmed a positive cooperative effect. In another example of positive cooperative effect [122], the syntheses of first generation dendritic compounds bearing 1,1-alkane-1,1-diylbis(4-butyl-4,5-dihydro-1*H*-1,2,4-triazol-5-ylidene) palladium(II) dibromide on the periphery were described. The dendritic complex was more active than the corresponding non-dendritic mononuclear species in the Heck reaction, which was indicative of a positive cooperative effect. However in general the catalytic activities of all these complexes were moderate. In contrast, a negative dendritic effect was found when Pd complexes of bidentate phosphines on a polyether dendrons support were used. This observation was explained by the fact that, in the case of bidentate phosphine ligands, the high local density of phosphines dictated by the dendritic architecture was a disadvantage for the Heck reaction [123].

The use of soluble polysiloxanes with linear, star-shaped and hyperbranched architectures having vinyl, 2-butylthioethyl and



**Scheme 1.** Cu(I) loaded PAMAM dendrimer for “click” reaction. Reprinted with permission from [130] (Voelcker's group). © 2011 Elsevier.

2-diphenylphosphinoethyl side groups as supports for palladium(II) catalysts in Heck reactions has been reported [124]. Polysiloxane-supported catalysts did not provide a negative effect on conversion compared with PdCl<sub>2</sub>(PhCN)<sub>2</sub>, but showed good stability and could be reused several times. Linear polymers-supported catalysts exhibited both better catalytic activity and better stability than that of dendritic catalysts.

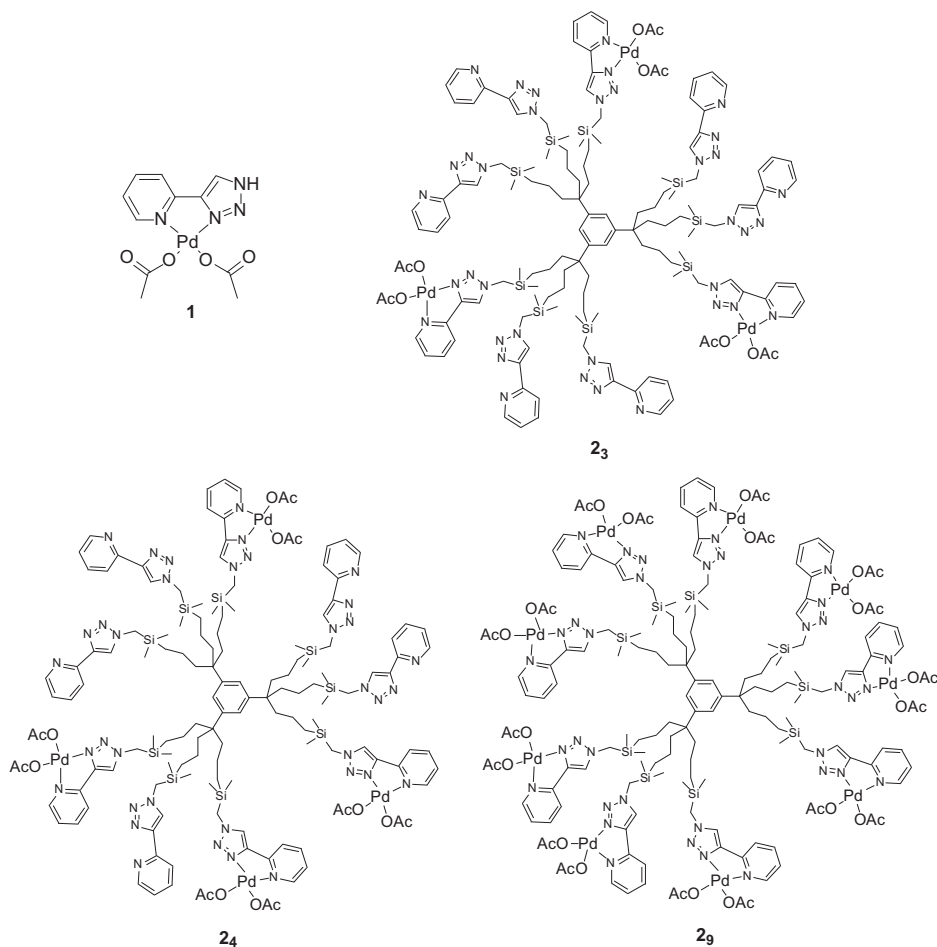
The catalysis by Pd DENs of Heck reactions was carried out with PAMAM and PPI dendrimers by several groups. PPI Pd DENs containing perfluoroether groups catalyzed the Heck reaction between iodobenzene and *n*-butyl acrylate with 100% selectivity at 90 °C, which was superior to yields and selectivities obtained with other Pd NPs. The fluorinated pony-tail functionalized DENs also allowed carrying out PdNP-catalyzed Heck coupling between aryl halides and methacrylate in supercritical CO<sub>2</sub>. Moreover the highly unfavored methyl 2-phenylacrylate was exclusively obtained at 5000 psi and 75 °C, whereas *trans*-cinnamaldehyde was obtained with 97% selectivity otherwise [125]. Although G4–OH DENs were more stable than G2–OH and G3–OH DENs, the lower-generations DENs were also more active catalysts [126]. This observation disclosed a crucial problem in catalysis by DENs, i.e. the correct balance between catalytic efficiency and stability requires careful search for a given dendrimer series, and it is tedious to maintain both advantages of optimized efficiency and stability.

### 3.1.3. Cu-catalyzed alkyne-azide (CuAAC) reaction

The copper-catalyzed alkyne-azide Huisgen-type cycloaddition (CuAAC “click” reaction) [127,128] has appeared as one of the most currently used methods for connecting two fragments together, and has been widely applied in various fields including construction of dendrimers [75,129]. On the other hand, some groups recently, also tried to design efficient dendritic copper complexes for “click” reaction.

The synthesis and catalytic properties of Cu-loaded poly(amidoamine) (PAMAM) dendrimers towards the Cu(I)-catalyzed azide-alkyne cycloaddition (CuAAC) have been described (Scheme 1) [130]. The reactivity was tested on a model reaction between azido propanol and propargyl alcohol in aqueous solution. A significantly faster conversion was found using PAMAM dendrimers as macromolecular Cu(I) ligands compared with traditional small molecular ligand systems, and the macromolecular catalyst could be removed by ultrafiltration.

Copper(I) (hexabenzyl)tren complex **1** and dendritic analogues with 18 or 54 branch termini (Fig. 12) have been synthesized [88,77]. Both parent and dendritic complexes showed outstanding activities for “click” reactions with various substrates in terms of yields and TONs. The metallodendrimers also provided a positive dendritic effect, as shown by comparing kinetics studies of the “click” reaction between phenylacetylene and benzyl azide at 22 °C in toluene using 0.1% catalysts, which was assigned to the dendritic frame bringing about steric protection against the well-known inner-sphere aerobic oxidation of Cu(I) to bis(μ-oxo)-bis-Cu(II). Water-soluble PEG-modified dendritic catalyst exhibited inspiring performance for “click” reactions of water-insoluble substrates in water without co-solvent under ambient conditions. Moreover,



**Fig. 8.** Mono- and polymeric palladium complexes containing 2-pyridyl-1,2,3-triazole (pyta) ligand.

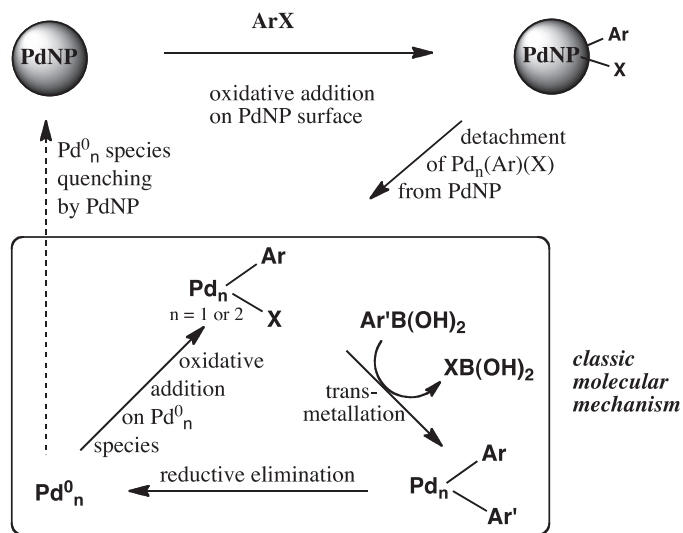
Reprinted with permission from [107] (Astruc's group).  
© 2013 Wiley-VCH.

these copper catalysts were removed from the reaction medium through easy precipitation at  $-18\text{ }^{\circ}\text{C}$  and reused at least three times [88].

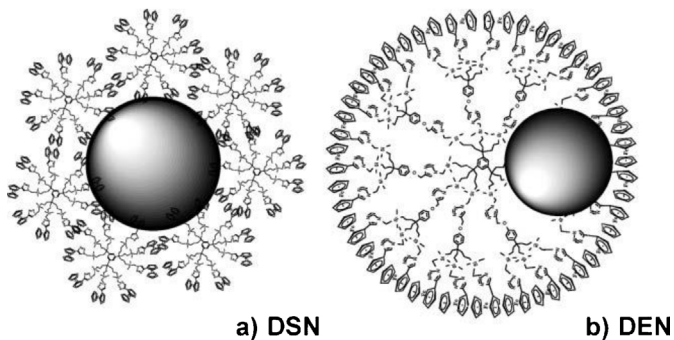
### 3.1.4. Hydrogenation

Both categories of molecular dendritic catalysts and DENs provided excellent performances in hydrogenation [131]. Diphosphine and monophosphine units are ideal bridge between dendritic support and metal for grafting dendritic metal complexes, due to their outstanding capability of coordination, stability, and catalytic performance. Most dendritic catalysts for hydrogenation contain diphosphine or monophosphine [132–134].

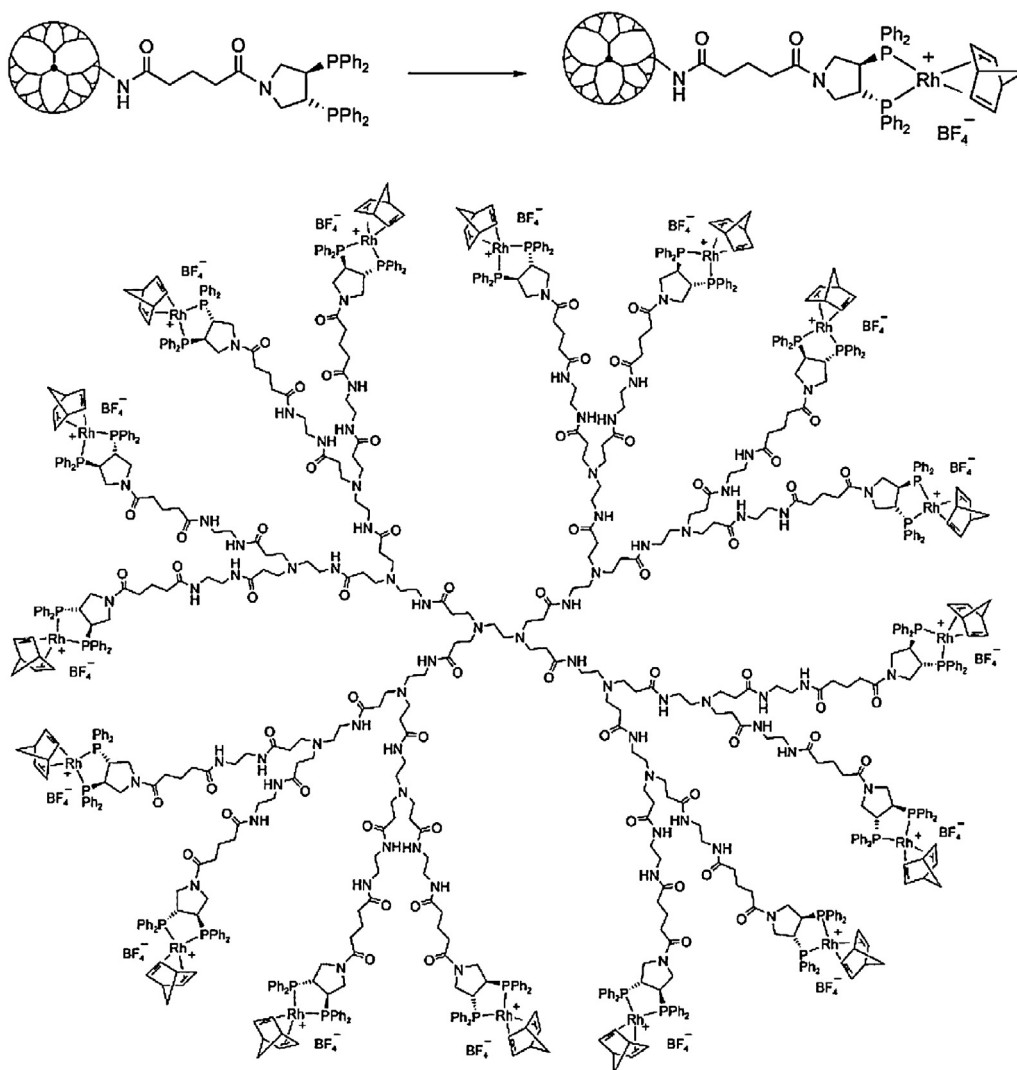
Tripodal-terminated Rh-phosphine dendrimers were efficient catalysts for the hydrogenation of styrene and 1-hexene [135]. In subsequent work, this group immobilized pyrophosphine-Rh(norbornadiene) at the periphery of PPI, PAMAM and



**Fig. 10.** Leaching mechanism in the “homeopathic” catalysis of Suzuki–Miyaura C–C coupling at ambient temperature between PhI and PhB(OH)<sub>2</sub> by “click” ferrocenyl dendrimer-stabilized PdNPs [81].



**Fig. 9.** DSN formed from G0; b) DEN formed from G1. [112].



**Scheme 2.** General synthesis of the pyrphos-Rh(NBD) complexes, and  $\{G_2\}$ -PAMAM-(Glutaroyl-pyrphos-Rh(NBD) BF<sub>4</sub>)<sub>16</sub>.

Reprinted with permission from [136] (Gade's group).  
© 2009 Wiley-VCH.

hyperbranched PEI dendrimers (Scheme 2) [136]. These metallo-dendrimers have been used as catalysts for the hydrogenation of *Z*-methyl  $\alpha$ -acetamidocinnamate. A negative dendritic effect in terms of activity and selectivity was observed with increasing size of the dendrimer supports when the hydrogenation was carried out in methanol, and a stronger negative effect was detected in terms of catalytic activity, stereoselectivity, and recyclability. Moreover, there is no difference in catalytic behavior between hyperbranched polymer-supported and dendrimers-supported Rh complexes in this hydrogenation reaction.

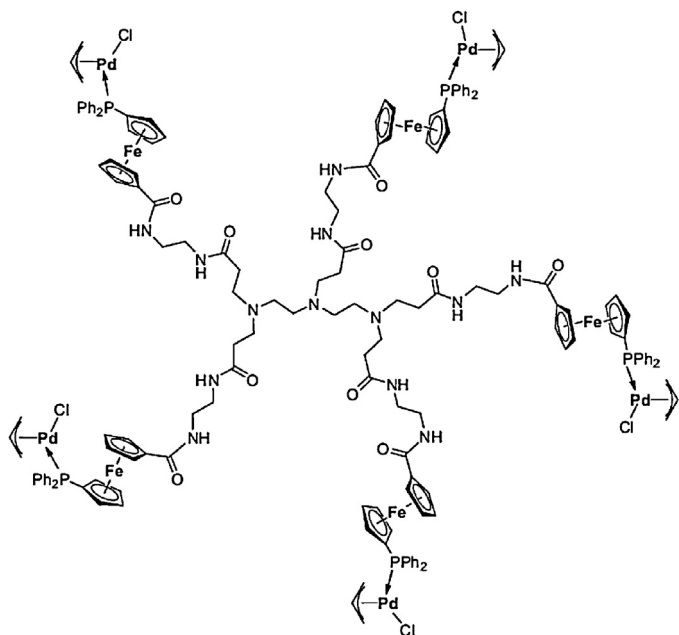
Chiral dendritic monodentate phosphoramidite [137,138] and dendritic BINAP (2,2'-bis(diphenylphosphino)-1,1'-binaphthyl) [139] bearing different dendritic supports were applied as ligands for Rh or Ir-catalyzed asymmetric hydrogenation of  $\alpha$ -dehydroamino acid esters, dimethyl itaconate, quinaldine, and methyl 2-acetamidocinnamate. High enantioselectivities (up to 99% ee) and catalytic activities (up to 4850 h<sup>-1</sup> TOF) were achieved when these catalytic systems of dendritic ligands and metal complexes were employed, and all the catalytic systems provided positive dendritic effects.

The efficiencies of catalytic moieties within and across dendrimer generations for partially and full functionalized poly(alkyl

aryl ether) dendrimers rhodium(I) complexes that were tested in the hydrogenation of styrene [140]. Significant increases of catalytic activities (TONs) with increasing the amount of catalytic residues demonstrated positive effects of the multivalent formulation of the catalytic moieties.

A carbosilane dendrimer functionalized with *P*-stereogenic diphosphine or monophosphines ligands has been designed and their activities in the Rh-catalyzed hydrogenation of dimethylitaconate have been checked [141,142]. A "green" example was reported that the fluorinated dendritic chiral mono-*N*-tosylated 1,2-diphenylethylenediamine (FTSDPEN) was synthesized and applied in the ruthenium(II) complex-catalyzed asymmetric transfer hydrogenation of prochiral ketones in aqueous media with excellent enantioselectivity, and unprecedented recovery and recyclability [143].

Following seminal research on DEN-catalyzed hydrogenation, it was shown that the PAMAM G4-OH Pd<sub>40</sub>NP (Fig. 13) is much more efficient than the G6 and G8 DENs because the latter serve as nanofilters [71,72,144] inhibiting, to some extent, the penetration of the *N*-isopropylacrylamide substrates inside the dendrimer in which the catalytically active NP was located. On the other hand, linear alkenes penetrated more easily, resulting in a much smaller



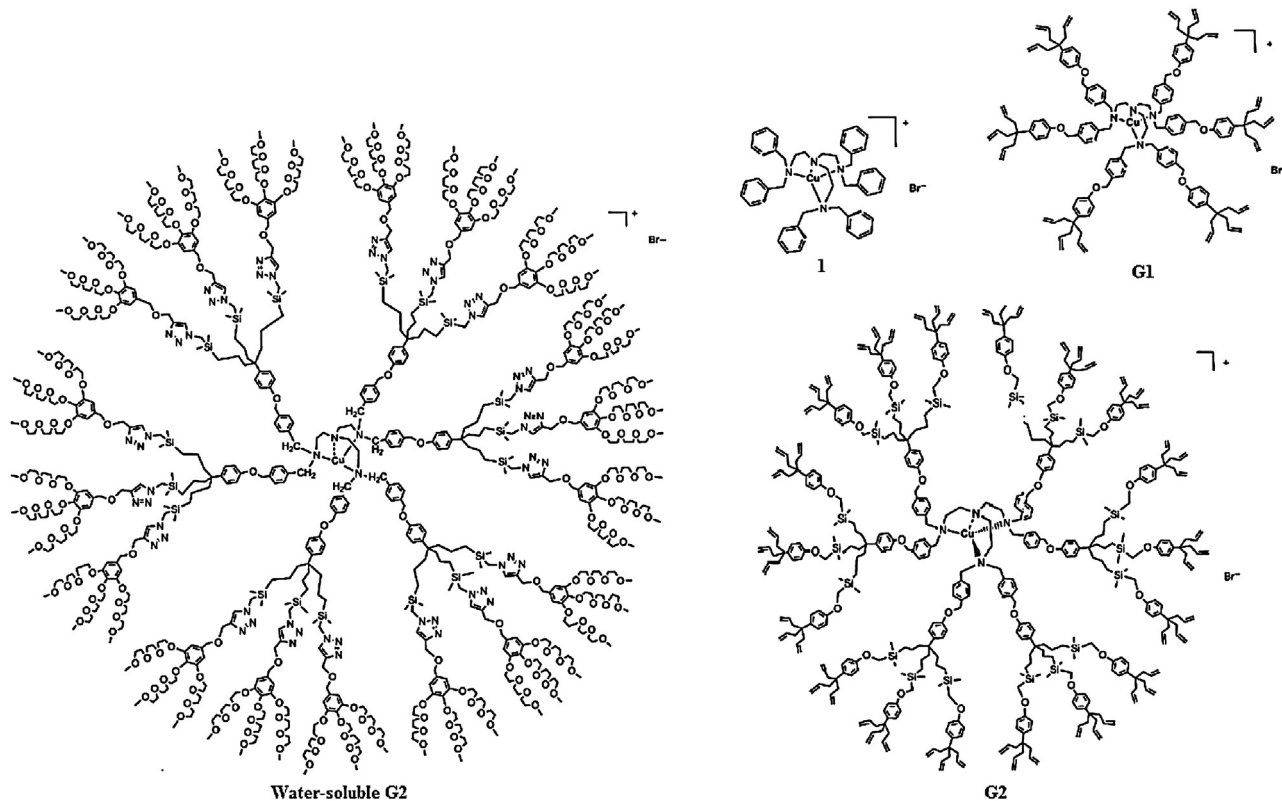
**Fig. 11.** PAMAM-based dendrimers with end-grafted five Pd–Fe units. Reprinted with permission from [121] (Lang's group). © 2010 Elsevier.

decrease in activity. When G4-NH<sub>2</sub> PAMAM dendrimers were functionalized with various epoxide termini having increasing sizes, the hydrogenation catalysis results showed that the DENs functionalized with bulkier epoxides were less efficient catalysts than those having less bulky epoxides [145,146]. Molecular rulers containing

a cyclodextrin stopper and allyl groups spanned by alkyl chains having different sizes were used to estimate the length between the DEN surface and the dendrimer surface, and for G4-OH Pd<sub>40</sub> DENs such a length was estimated to be  $0.7 \pm 0.2$  nm [147,148]. The Yamamoto and Nishihara groups prepared PAMAM G4-OH Rh DENs that catalyzed olefin and nitroarene hydrogenation with a metal-ion/dendrimer ratio of 60 [148]. The G1–3 dihydroxybenzyl-alcohol-based dendrimers stabilized 14–35-nm sized Ag DSNs that catalyzed chloronitrobenzene hydrogenation at 20 bar H<sub>2</sub> and 140 °C [149].

“Click”-ferrocenyl dendrimer-encapsulated and stabilized Pd nanoparticle pre-catalysts (Fig. 9) were used to catalyze hydrogenation reactions. Indeed, selective hydrogenation of dienes to monoenes was achieved readily under ambient conditions for small dienes [80], but large steroidal dienes remained unreacted, in accord with their lack of ability to reach the PdNP surface. The rates (TOFs) and TONs of hydrogenation were all the larger as the PdNPs were smaller, as expected from previous results with polymer-stabilized PdNPs [150–152] according to a mechanism that involves mechanistic steps of the hydrogenation on the PdNP surface.

Heterobimetallic DENs are either alloys DENs (noted M<sup>1</sup>M<sup>2</sup> DENs) or core@shell DENs. TOFs for the hydrogenation of allylic alcohol with Pd-rich heterobimetallic PdPt DENs were significantly higher than those of physical mixtures of the single-metal analogues having the same percentage of the two metals [153–159]. This was attributed to positive synergistic effects [160]. Au@Pt NPs stabilized by Fréchet-type polyarylester dendrons showed higher catalytic activity in hydrogenation of nitrotoluenes to anilines compared with monometallic Pt NPs or a mixture of Pt and Au NPs, which was attributed to the decreased electronic density on the Pt shell arising from the influence of the Au core [161]. Similar effects were invoked for the better activity of heterobimetallic DEN



**Fig. 12.** Copper(I) (hexabenzyl) tren complex **1** and metallodendritic Cu(I) derivative **G1**, **G2**, and water-soluble **G2**.

Reprinted with permission from [88] (Astruc's group). © 2011 Wiley-VCH.

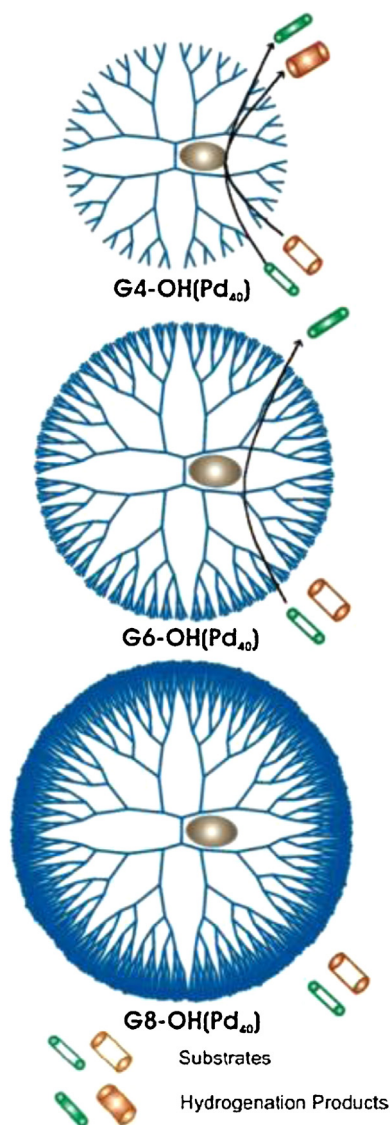


Fig. 13. PAMAM G4, G6 and G8 Pd DENs for selective catalysis.

Reprinted with permission from [72] (Crook's group).  
© 2001 American Chemical Society.

catalysts compared with monometallic DENs hydrogenation of *p*-nitrophenol [153], selective hydrogenation of 1,3-cyclooctadiene [154], hydrodechlorination of 1,2-dichloroethane [155] and CO oxidation [156–159].

### 3.1.5. Carbonylation and hydroformylation reactions

Some remarkable examples involving dendritic catalysts on a solid support such as silica gel have been published (Fig. 14). The dendritic Rh or Pd complexes on solid support showed high activity for carbonylation and hydroformylation reactions [89,162–167]. These systems were easily recovered by simple filtration in air and reused without loss of activity. Recyclable palladium-complexed dendrimers on silica gel were first used as catalysts in intramolecular cyclocarbonylation reactions. From this powerful approach, a series of oxygen-, nitrogen-, or sulfur-containing 12- to 18-membered ring fused heterocycles were synthesized with good yields [168].

### 3.1.6. Oxidation reaction

Polyoxometalates (POMs) [169–171] are a large class of inorganic cage complexes with very interesting properties that render

them attractive for potential applications in a variety of fields including catalysis. The catalytic properties of dendritic POM hybrids were based on electrostatic bonding between POMs (the most frequent one is Venturolo ion  $[\text{PO}_4\{\text{WO}(\text{O}_2)_2\}_4]^{3-}$ ) paired with dendritic cations. Dendritic POMs bearing Venturolo ion exhibited good catalytic activity and recoverability in the oxidation of organic substrates such as alkenes, alcohols, and sulfides [85–87,172–174]. Zirconium-peroxo-based dendritic POMs (Fig. 15) obtained by pairing zirconium-peroxotungstosilicate  $[\text{Zr}_2(\text{O}_2)_2(\text{SiW}_{11}\text{O}_{39})_2]^{12-}$  with ammonium dendrons provided homogeneous dendritic counterparts that also were recoverable and reusable catalysts for the oxidation of sulfides in aqueous/ $\text{CDCl}_3$  biphasic media [175].

Dendritic pyridine derivatives bearing 2,3,4,5-tetra-phenylphenyl substituent-supported palladium complexes suppress the formation of Pd black during aerobic oxidation of alcohols under common conditions [176]. Heterogeneous manganese complexes of polystyrene-supported PAMAM dendrimer showed high stability and catalytic efficiency in oxidation of secondary alcohols, and can be recovered and reused at least six times [177].

### 3.1.7. Polymerization and oligomerization

The well-defined hyperbranched structure of metal dendrimers leads to possibility of site isolation of catalytic residues, which suppress the formation of inactive bis-metal complexes. The dendrimer-substituted *o*-diphenyl-phosphinophenol (Fig. 16, left) is far more active than the parent ligand (Fig. 16, right) for the Ni-catalyzed oligomerization of ethylene in toluene, which was taken into account by the fact that the dendritic architecture suppressed the formation of bis-(P,O)Ni complexes [178]. When the compared analysis was carried out in methanol, a similar catalytic result was obtained, but the process was different from that observed in toluene: both the dendritic ligand and the parent ligand formed bis-(P,O)nickel complexes in methanol according to NMR spectroscopy. However, the dendritic bis-(P,O)Ni complex dissociates to a mono-ligated species under catalytic conditions.

Both a monometallic copper(II) complex and a bimetallic complex assembled with four copper(II) ions and one iron(III) ion bearing a dendritic phenylazomethine (DPAG4, Fig. 17) were used to catalyze the aerobic oxidative polymerization of 2,6-difluorophenol without any base additive [179]. The catalytic efficiency of the bimetallic complex outperforms that of the monometallic copper complex, that is, the participation of the second metal-ion enables facile control of the polymer products with exceptionally high molecular masses and branching. The location of the metal salts in DPAG4 dendrimer was radial, resulting from stepwise complexation as reported in a previous study [180]. The locations of bimetallic entities containing copper and iron in DPAG4 were also investigated. Binary titration experiments showed that iron(III) with stronger affinity than copper(II) for the dendritic ligand preferentially bind to the inner coordination sites of the DPAG4, which was confirmed by UV–vis absorption spectrometry.

### 3.1.8. Arylation and alkylation reactions

Phosphorus dendrimers functionalized with iminopyridine chelating unit (Fig. 18) provided higher yields than with a monomeric ligand for O- and N-arylation and vinylation of phenol and pyrazole [181]. When azabis(oxazoline)-ended phosphorus dendrimers were evaluated as ligands for copper(II)-catalyzed asymmetric benzoylations, a positive dendritic effect in terms of enantioselectivity was observed [182]. The second generation of 2,9-dimethyl-1,10-phenanthroline grafted dendrimer showed similar catalytic activity to that of the monomer in Cu-catalyzed substitution of 4-iodoanisole to give 1,4-dimethoxybenzene [183]. Dendritic poly(propyleneimine) and

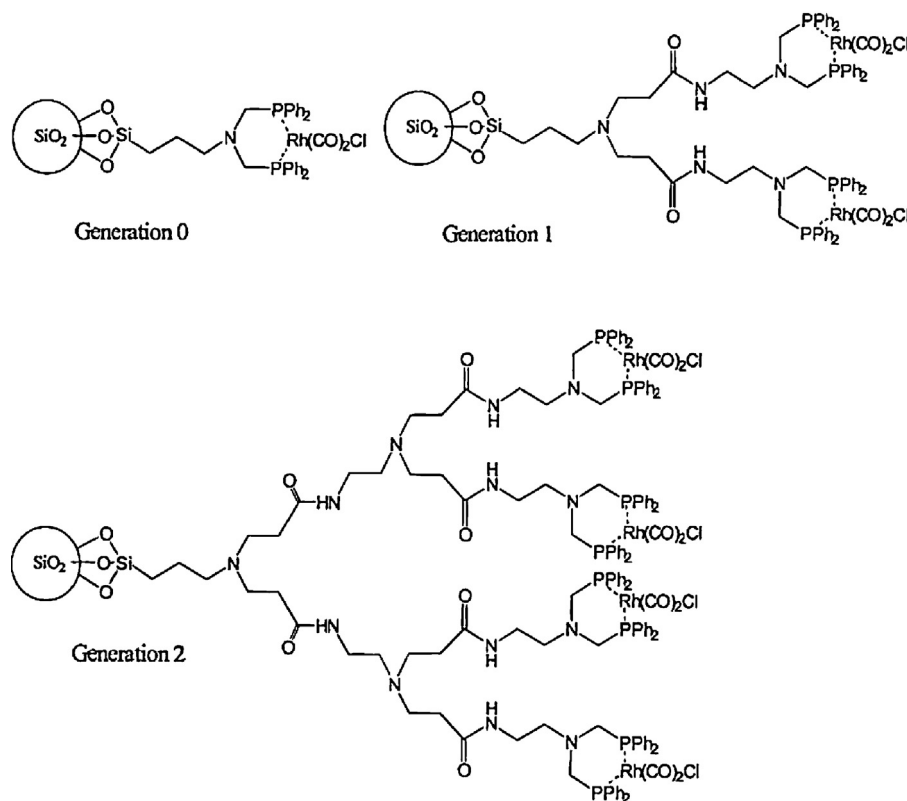


Fig. 14. Rh-PPh<sub>2</sub>-PAMAM-SiO<sub>2</sub> complexes.

Reprinted with permission from [89] (Alper's group).  
© 1999 American Chemical Society.

hyperbranched poly(ethylenimine) with P-containing functional groups were applied as multivalent ligands in the Pd-catalyzed allylic substitution reactions [184]. The G0–G4 phosphorus-based dendrimers decorated with  $\beta$ -diketones were used as ligands for copper in *O*-arylations of 3,5-dimethylphenol by aryl bromides. Although no dendrimer effect was observed, which resulted from the decomposition of the dendrimer under the reaction conditions, it is a very efficient catalytic system for the *O*-arylation reaction [185].

### 3.1.9. Asymmetric synthesis

Examples of asymmetric hydrogenation have already been introduced in the “Hydrogenation” section. Other recent advances in metallodendritic asymmetric synthesis include the Henry reaction, addition of dialkylzinc to aldehyde, asymmetric epoxide ring-opening reaction, Diels–Alder reaction, and three-component condensation.

A series of well-defined chain-end functionalized carbosilane dendrimers having bis- and trisoxazolines distributed at the periphery of their hyperbranched chain ends have been synthesized [186]. Subsequently, dendritic copper complexes that were immobilized in a membrane bag were produced, then “catalysis in tea bag” systems was assessed by studying two benchmark reactions, the  $\alpha$ -hydrazination of a  $\beta$ -keto ester and the Henry reaction of 2-nitrobenzaldehyde with nitromethane (Fig. 19). The bisoxazoline-based catalysts displayed sufficient activity and could be recycled without significant decrease in activity and selectivity. Moreover, the simple operation of dipping the catalyst-filled dialysis bags into reaction vessels containing the substrate was carried out successfully.

A series of dendritic polyglycerol salen ligands have been synthesized [187]. The corresponding dendritic Cr(III) catalysts were

used for asymmetric epoxide ring-opening (ARO) reaction. A negative dendritic effect was shown on the enantioselective of the ARO reaction, which resulted from the orientation of the immobilized catalytic units with respect to one another. To achieve higher enantioselective, pyrrolidine-modified dendritic salen ligands were used and provided improved catalytic activities.

A method for Diels–Alder and three-component condensation reactions using poly(arylether) with a 2,2'-bipyridine core-based dendritic copper catalyst was described [188]. The Diels–Alder reaction of cyclopentadiene with various dienophiles was performed with 10 mol% of the catalyst affording the corresponding adducts in excellent yields; when the dendritic ligand was not used in the reaction, neat copper catalysts could not provide Diels–Alder adducts but promoted the cationic polymerization of cyclopentadiene. This catalyst was also employed for Mannich-type reactions (three-component condensation) of an aldehyde, *o*-anisidine. Using various nucleophiles, better yield was obtained with water as solvent than with dichloromethane, which was attributed to the cohesion effect of organic substrates in water. Moreover, the catalyst was recovered and reused at least five times without losing its activity in all cases.

### 3.1.10. Other reactions

Other recent advances in metallodendritic catalysis focused on thermal decomposition of ammonium perchlorate [189], Ru-catalyzed hydration of phenylacetylene and isomerization of 1-octan-3-ol [190,191], Pd-catalyzed auto-tandem reaction [192,193], Fe-catalyzed alkene epoxidation reactions [194], Cu-catalyzed generation of oxygen radical anions [195], Ru-catalyzed olefin metathesis [196,197], Zn-catalyzed cleavage of the RNA model substrate HPNPP [198,199], Co-catalyzed activation of carbon dioxide [200], co-catalyzed debromination of

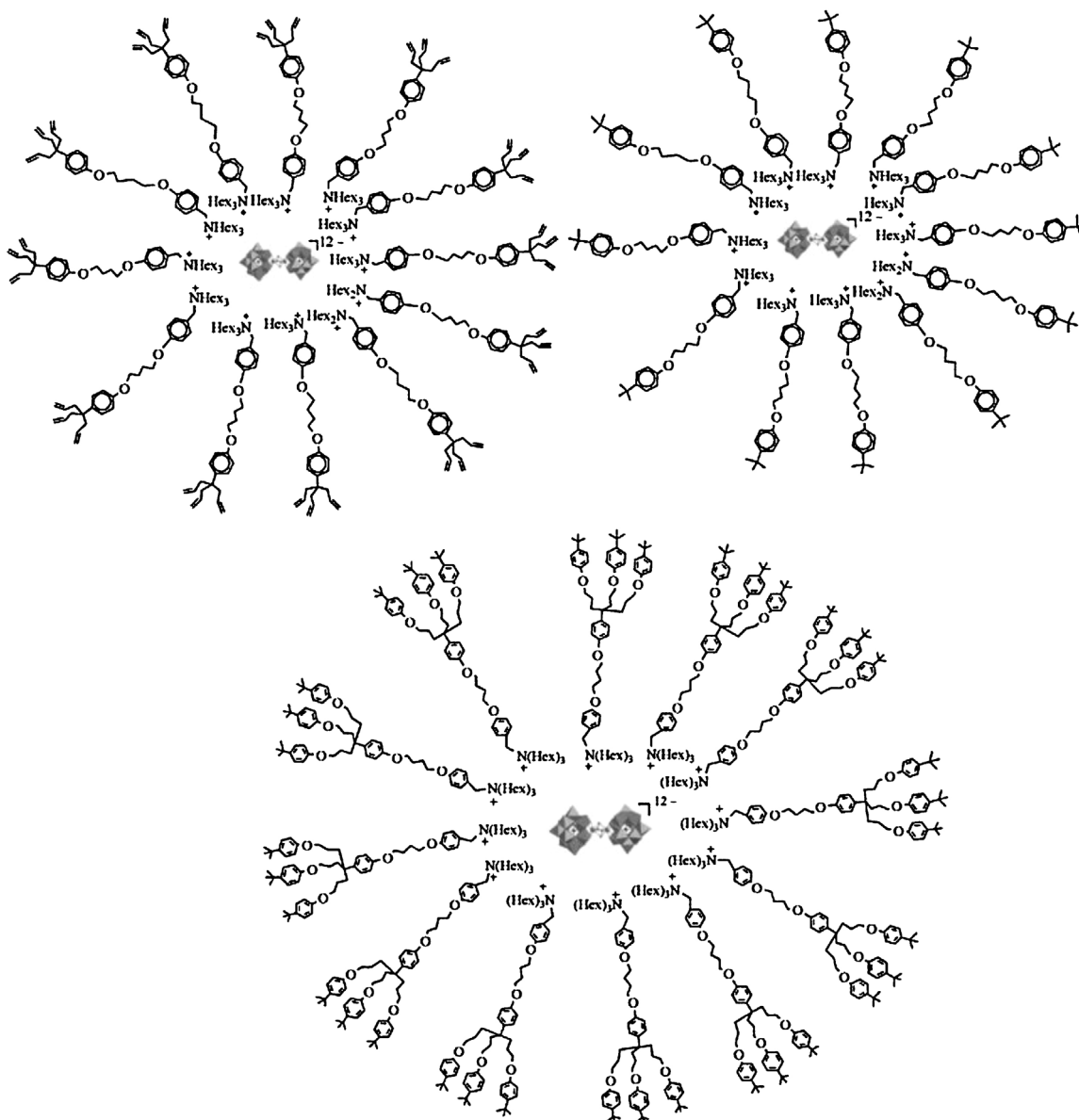


Fig. 15. Zirconium-peroxo-based dendritic POMs.

Reprinted with permission from [175] (Nlate's group).  
© 2010 Wiley-VCH.

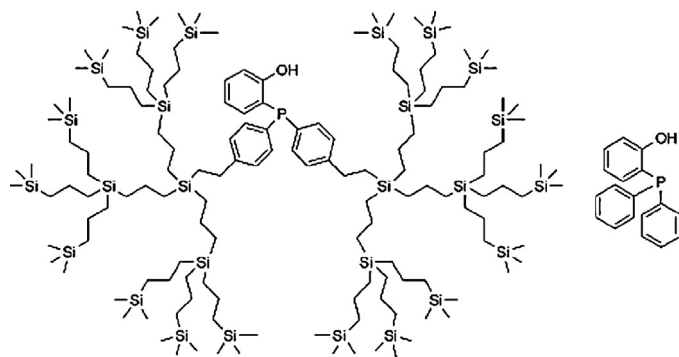
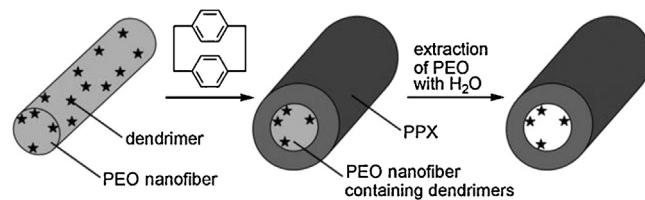


Fig. 16. *o*-Diphenylphosphinophenol ligands.

Reprinted with permission from [178] (Reek and van Leeuwen's group).  
© 2004 American Chemical Society.

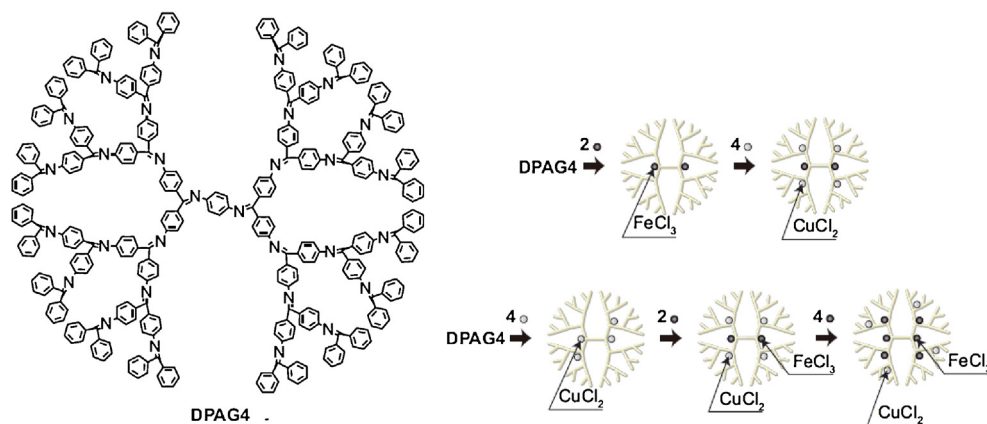
2-phenethylbromide [201], and Rh-catalyzed [2 + 2] cycloaddition reaction reacton [202].

The combination of PTA (1,3,5-triaza-7-phosphaadamantane) [203] and dendrimers might bring about water-soluble organometallic dendritic catalysts. Ruthenium complexes with PTA at the periphery were synthesized and used as catalysts for the hydration of alkynes and the isomerization of allylic alcohols to ketones in aqueous media. Positive dendritic effects on the



Scheme 3. Concept of "bottling" dendritic catalysts in PPX nanotubes.

Reprinted with permission from [221] (Wendorff's group).  
© 2009 Wiley-VCH.

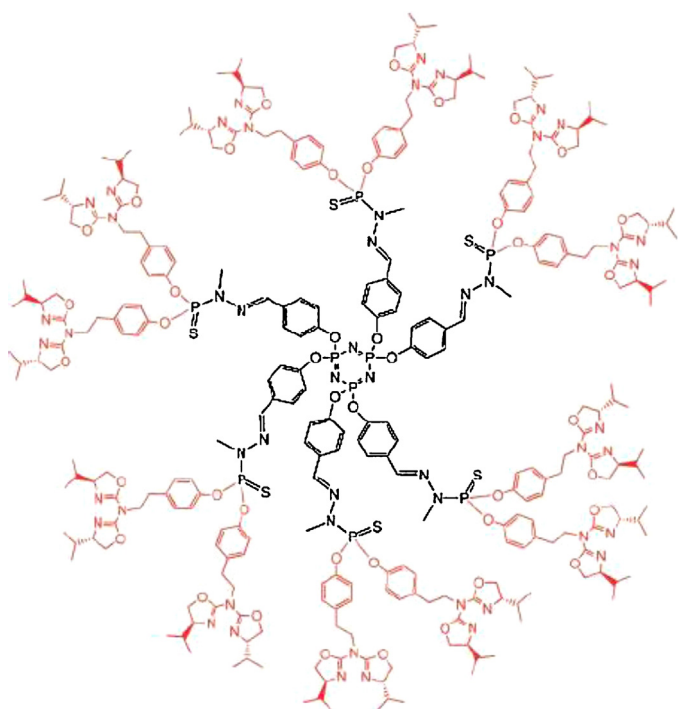


**Fig. 17.** Structures of phenylazomethine dendrimer (DPAG4), and the addition of  $\text{CuCl}_2$  and  $\text{FeCl}_3$  by different methods.

Reprinted with permission from [179] (Yamamoto's group).  
© 2011 John Wiley & Sons, Ltd.

regioselectivity or conversion were observed for both reactions [190]. In addition, the study of the “number of terminal groups vs. dendrimer generation” was investigated for the dendritic ligand **1-G<sub>2</sub>** of the first generation containing 24 PTA groups, **1-G<sub>1</sub>** of the first generation containing 12 PTA groups, and **6-G<sub>2</sub>** of the second generation containing 24 PTA groups (Fig. 20). Through compared analysis of the catalytic efficiencies, the positive influence of the density of catalytic sites on the surface of these dendrimers for the alcohol isomerization reaction in water has been demonstrated [191].

Catalysis of ring-closing metathesis (RCM), cross metathesis (CM) and enyne metathesis (EYM) of hydrophobic substrates was reported in water and air under ambient or mild conditions using low catalytic amounts (0.08 mol%) of a suitably designed “click” dendrimer (Fig. 21) that can be reused many times and



**Fig. 18.** Structure of azabis(oxazoline)-ended dendrimer ligand generation 1.

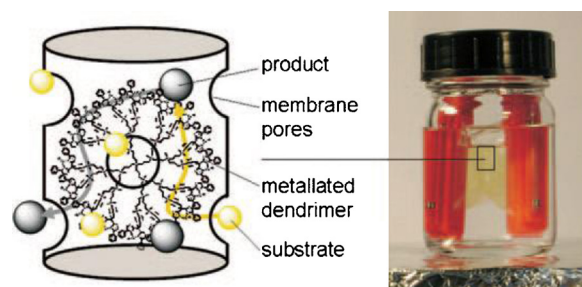
Reprinted with permission from [181] (Majoral's group).  
© 2006 American Chemical Society.

very low amounts of Grubbs' second generation olefin-metathesis catalyst [197,204–206]. The dendrimer plays the protecting role of a nanoreactor towards the catalytically active species, in particular the sensitive ruthenium-methylene intermediate, involved in the metathesis catalytic cycle, preventing catalyst decomposition in the presence of an olefin substrate.

### 3.2. Dendritic organocatalysts

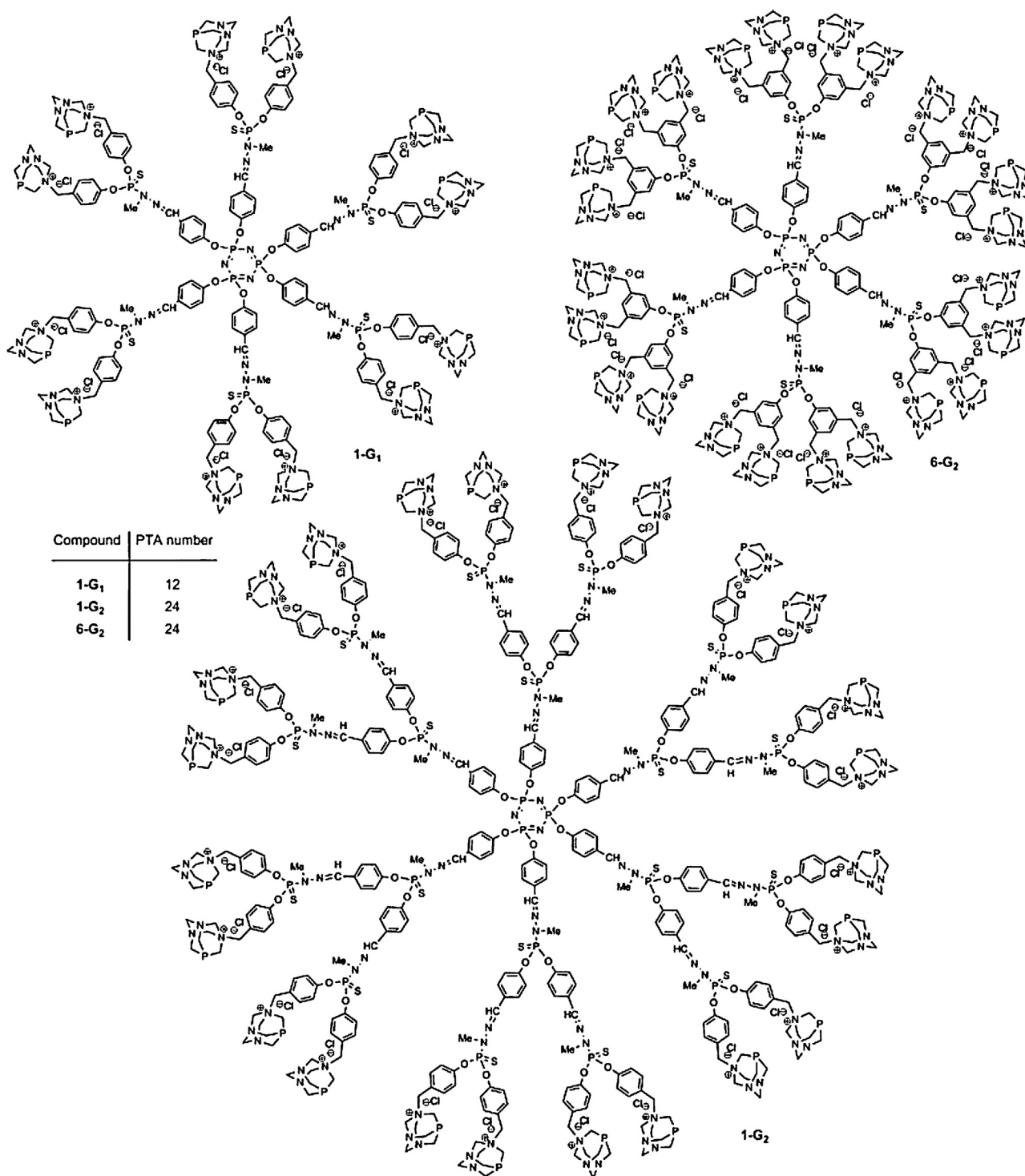
The number of publications on dendritic organocatalysis has dramatically increased during the past few years [207–212]. Michael addition [213–215], hydrolysis reaction [216,217], model aldol reaction [218], epoxidation of enones [219], hydrogenation [220], Knoevenagel reactions [221], transamination [222], aldol reactions [223,224], hydrosilylation [225], superoxide dismutation [226], asymmetric borane reduction of prochiral ketones [227], and ring-opening of epoxides [228] have been reported using dendritic organocatalysts.

For example, a novel method in which  $\text{C}_{16}$  alkyl chains have been attached to the fifth generation of poly(propyleneimine) (PPI) dendrimers was reported [207], and these new dendrimers have been used as efficient tertiary amine catalysts for an intramolecular Michael reaction based on substrate orientation within the internal dendritic nanocavities. The sterically confined nanocavities consisting of regularly arranged amino groups of the dendritic organocatalyst could accommodate the substrate in a reactive conformation for intramolecular cyclization. The recyclable chiral 2-trimethylsilyloxy-methyl-pyrrolidine-functionalized dendritic organocatalyst was synthesized and used in the Michael



**Fig. 19.** An enlarged schematic view of general setup for the recycling using the “catalyst in a tea bag” principle.

Reprinted with permission from [186] (Gade's group).  
© 2009 Wiley-VCH.

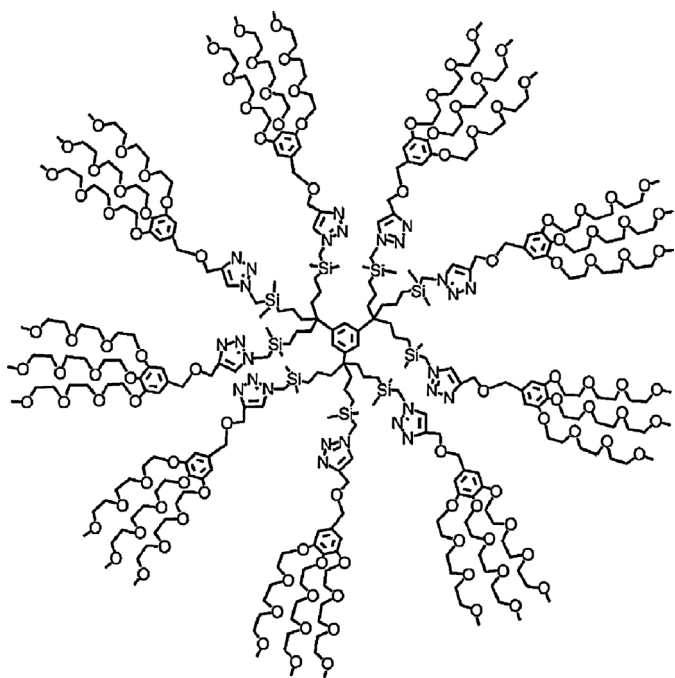


**Fig. 20.** Chemical structure of dendrimers 1-G<sub>1</sub>, 1-G<sub>2</sub>, and 6-G<sub>2</sub>, allowing the comparison between their size and their number of terminal groups. Reprinted with permission from [191] (Caminade's group). © 2012 Elsevier.

addition reaction of various unmodified aldehydes with nitrostyrenes [208]. In this study, the catalyst showed good catalytic activities in terms of yields, enantioselectivities, and diastereoselectivities when aldehydes with different substituents were employed. A series of Wang polystyrene-supported recyclable bifunctional dendritic organocatalysts having various numbers of acidic protons based on chiral diamines have been synthesized [209]. These macromolecules were evaluated as catalysts for asymmetric nitro-Michael addition of acetone to nitroolefins.

Catalytic results showed that the number of H-bond donors of the catalyst was a determinant for the reactivity and enantioselectivity. When the number of acidic protons increases from zero to two, the yield of the product increases 3-fold. However, a better enantioselectivity was achieved with catalysts having one acidic proton.

Poly(*p*-xylylene) (PPX) nanotubes which can be considered as nanoreactors were prepared in 2009 (Scheme 3) [221]. The PPX nanotubes loading PAMAM dendrimers showed activity as



**Fig. 21.** PEG-ended water-soluble dendrimer for Grubbs-catalyzed olefin metathesis of hydrophobic substrates in water [197].

recyclable catalysts in a Knoevenagel reaction. Moreover, the PAMAM dendrimers successfully reacted with acid inside the tube to provide a new catalyst system, in which about 26% of the amines were conjugated with 2,2,6,6-tetramethylpiperidine-*N*-oxyl (TEMPO) moieties. The nanotubes containing TEMPO-conjugated PAMAM derivatives were active as reusable catalysts in the TEMPO/bleach oxidation of benzyl alcohol. The authors believed that it was possible to “bottle” any catalyst into PPX nanotubes through conjugation with PAMAM.

#### 4. Conclusion and outlook

As shown here, dendritic catalysis is a rapidly growing field. Essential new concepts have emerged with various positive and negative dendritic effects. In classical examples, the catalysts were loaded with catalytic species at the periphery. On one hand this brings about a large number of catalytically active species in a small nano-object and on the other hand restriction of substrate access can sometime lead to a negative dendritic effect resulting from bulk limiting reaction rates. In more sophisticated designs, catalysis proceeds in the dendritic interior, thus the dendrimer then plays the role of a nanoreactor, eventually in a biomimetic enzyme-type fashion. Typical examples include nanoparticle catalysis pioneered by Crooks [70,145,146] whereby the dendrimer plays the function of a unimolecular micelle [24,229,230]. The intradendritic ligand design plays a crucial role in this case, and for instance click reactions installing 1,2,3-triazolyl ligands inside the dendrimers turn out to be remarkably successful in this respect [75–78]. Recent enthusiasm toward organocatalysis [207–212] has largely involved dendrimer chemistry that is particularly suited for these “green chemistry” applications.

#### Acknowledgments

Financial support from the Université Bordeaux 1, the Centre National de la Recherche Scientifique and the Chinese Research Council (PhD grant to DW) is gratefully acknowledged.

#### References

- [1] G.R. Newkome, C.N. Moorefield, F. Vögtle, *Dendrimers and Dendrons: Concepts, Synthesis Applications*, Wiley-VCH, Weinheim, 2001.
- [2] J.M.J. Fréchet, D.A. Tomalia, *Dendrimers and Other Dendritic Polymers*, John Wiley & Sons, Ltd, 2001.
- [3] D.A. Tomalia, A.M. Naylor, W.A. Goddard, *Angew. Chem. Int. Ed. Engl.* 29 (1990) 138.
- [4] U. Boas, J.B. Christensen, P.M.H. Heegaard, *Dendrimers in Medicine and Biotechnology: New Molecular Tools*, The Royal Society of Chemistry, Cambridge, UK, 2006.
- [5] F. Vögtle, G. Richardt, N. Werner, *Dendrimer Chemistry*, Wiley-VCH GmbH&Co, Weinheim, 2009.
- [6] A.-M. Caminade, C.-O. Turin, R. Laurent, A. Ouali, B. Delavaux-Nicot, *Dendrimers. Towards Catalytic Material and Biomedical Uses*, Wiley, Chichester, 2011.
- [7] S. Campagna, P. Ceroni, F. Puntoriero, *Designing Dendrimers*, Wiley, Hoboken, NJ, 2012.
- [8] A.W. Bosman, H.M. Janssen, E.W. Meijer, *Chem. Rev.* 99 (1999) 1665.
- [9] G.M. Dykes, *J. Chem. Technol. Biotechnol.* 76 (2001) 903.
- [10] S. Svenson, D.A. Tomalia, *Adv. Drug Deliv. Rev.* 57 (2005) 2106.
- [11] S.E. Stiriba, H. Frey, R. Haag, *Angew. Chem. Int. Ed. Engl.* 41 (2002) 1329.
- [12] U. Boas, P.M.H. Heegaard, *Chem. Soc. Rev.* 33 (2004) 43.
- [13] T.M. Allen, P.R. Cullis, *Science* 303 (2004) 1818.
- [14] C.C. Lee, J.A. MacKay, J.M.J. Fréchet, F.C. Szoka, *Nat. Biotechnol.* 23 (2005) 1517.
- [15] S. Svenson, A.S. Chauhan, *Nanomedicine* 3 (2008) 679.
- [16] Y. Choi, T. Thomas, A. Kotlyar, M.T. Islam, J.R. Baker, *Chem. Biol.* 12 (2005) 35.
- [17] M. Grinstaff, *J. Polym. Sci. A: Polym. Chem.* 46 (2008) 383.
- [18] R. Tekade, P.V. Kumar, N.K. Jain, *Chem. Rev.* 109 (2009) 49.
- [19] T.S. Ahn, A.L. Thompson, P. Bharati, A. Müller, C.J. Bardeen, *J. Phys. Chem.* 110 (2006) 19810.
- [20] V. Balzani, S. Campagna, G. Denti, A. Juris, S. Serroni, M. Venturi, *Acc. Chem. Res.* 31 (1998) 26.
- [21] D. Astruc, E. Boisselier, C. Ornelas, *Chem. Rev.* 110 (2010) 1857.
- [22] N. El Brahmi, S. El Kazzouli, S. Mignani, M. Bousmina, J.P. Majoral, *Tetrahedron* 69 (2013) 3103.
- [23] S. El Kazzouli, N. El Brahmi, S. Mignani, M. Bousmina, M. Zablocka, J.P. Majoral, *Curr. Med. Chem.* 19 (2012) 4995.
- [24] G.R. Newkome, E. He, C.N. Moorefield, *Chem. Rev.* 99 (1999) 1689.
- [25] G.E. Oosterom, J.N.H. Reek, P.C.J. Kamer, P.W.N.M. van Leeuwen, *Angew. Chem. Int. Ed. Engl.* 40 (2001) 1828.
- [26] D. Astruc, F. Chardac, *Chem. Rev.* 101 (2001) 2991.
- [27] R. van Heerbeek, P.C.J. Kamer, P.W.N.M. van Leeuwen, J.N.H. Reek, *Chem. Rev.* 102 (2002) 3717.
- [28] L.J. Twyman, A.S.H. King, I.K. Martin, *Chem. Soc. Rev.* 31 (2002) 69.
- [29] D. Astruc, K. Heuze, S. Gatard, D. Méry, S. Nlate, S. Plault, *Adv. Synth. Catal.* 347 (2005) 329.
- [30] L. Gade (Ed.), *Dendrimer Catalysis*, Springer, Heidelberg, 2006.
- [31] B. Helms, J.M.J. Fréchet, *Adv. Synth. Catal.* 348 (2006) 1125.
- [32] D. Méry, D. Astruc, *Coord. Chem. Rev.* 250 (2006) 1965.
- [33] J.N.H. Reek, S. Arévalo, R. van Heerbeek, P.C.J. Kamer, P.W.N.M. van Leeuwen, *Adv. Catal.* 49 (2006) 71.
- [34] S.-H. Hwang, C.D. Shreiner, C.N. Moorefield, G.R. Newkome, *New J. Chem.* 31 (2007) 1192.
- [35] E. de Jesús, J.C. Flores, *Ind. Eng. Chem. Res.* 47 (2008) 7968.
- [36] F. Martínez-Olíd, J.M. Benito, J.C. Flores, E. de Jesús, *Isr. J. Chem.* 49 (2009) 99.
- [37] D. Astruc, *Tetrahedron Asymm.* 21 (2010) 1041.
- [38] D. Astruc, *Nat. Chem.* 4 (2012) 255.
- [39] A. John, F.M. Nachtigall, L.S. Santos, *Curr. Org. Chem.* 16 (2012) 1776.
- [40] A.-M. Caminade, A. Ouali, M. Keller, J.-P. Majoral, *Chem. Soc. Rev.* 41 (2012) 4113.
- [41] R.A. Kleij, P.W.N.M. van Leeuwen, A.W. van der Made, *Eur. Patent EP0456317*, 1991 (*Chem. Abstr.* 116 (1992) 129870).
- [42] D.A. Tomalia, J.R. Dewald, (Dow Chemical Co.), *US Patent 4,507,466*, 1985.
- [43] E.M.M. de Brabander-van den Berg, E.W. Meijer, *Angew. Chem. Int. Ed. Engl.* 32 (1993) 1308.
- [44] C. Hawker, J.M.J. Fréchet, *Chem. Commun.* (1990) 1010.
- [45] H. Ihre, O.L. Padilla De Jesus, J.M.J. Fréchet, *J. Am. Chem. Soc.* 123 (2001) 5908.
- [46] S.W. Krska, D. Seyferth, *J. Am. Chem. Soc.* 120 (1998) 3604.
- [47] G.R. Newkome, R.K. Behera, C.N. Moorefield, G.R. Baker, *J. Org. Chem.* 56 (1991) 7162.
- [48] J. Ruiz, G. Lafuente, S. Marcen, C. Ornelas, S. Lazare, E. Cloutet, J.-C. Blais, D. Astruc, *J. Am. Chem. Soc.* 125 (2003) 7250.
- [49] C.J. Hawker, J.M.J. Fréchet, *Macromolecules* 23 (1990) 4726.
- [50] K. Yamamoto, T. Imaoka, *Bull. Chem. Soc. Jpn.* 79 (2006) 511.
- [51] H. Brunner, S. Altmann, *Chem. Ber.* 127 (1994) 2285.
- [52] G. Van Koten, D.M. Grove, P. Wijkens, P.W. van Leeuwen, J.C. de Wilde, A.W. van der Made, J.W.C. Knapen, *Nature* 372 (1994) 659.
- [53] R. Breinbauer, E.N. Jacobsen, *Angew. Chem. Int. Ed. Engl.* 39 (2000) 3604.
- [54] S. Rigaut, M.-H. Delville, D. Astruc, *J. Am. Chem. Soc.* 119 (1997) 11132.
- [55] C. Valério, S. Rigaut, J. Ruiz, J.-L. Fillaut, M.-H. Delville, D. Astruc, *Bull. Pol. Acad. Sci.* 46 (1998) 309.
- [56] Y. Niu, R.M. Crooks, in: D. Astruc (Ed.), *Dendrimers and Nanosciences*, vols. 6–8, C.R. Chimie, 2003, p. 1049.
- [57] D. de Groot, B.F.M. de Waal, J.N.H. Reek, A.P.H.J. Shenning, P.C.J. Kamer, E.W. Meijer, P.W.N.M. van Leeuwen, *J. Am. Chem. Soc.* 123 (2001) 8453.

- [58] M. Dasgupta, M.B. Peori, A.K. Kakkar, *Coord. Chem. Rev.* 233–234 (2002) 223.
- [59] L.N. Lewis, *Chem. Rev.* 93 (1993) 2693.
- [60] J.S. Bradley, *Clusters and Colloids*, VCH, Weinheim, 1994.
- [61] H. Bönemann, R. Richards, *Eur. J. Inorg. Chem.* 2001 (2001) 2455.
- [62] A. Roucoux, J. Schulz, H. Patin, *Chem. Rev.* 102 (2002) 3757.
- [63] L.M. Bronstein, H.S. Nalwa (Eds.), *Encyclopedia of Nanoscience and Nanotechnology*, Vol. 7, American Scientific Publishers, Los Angeles, 2004.
- [64] F. Zaera, *Acc. Chem. Res.* 42 (2009) 1152.
- [65] L.M. Bronstein, S.N. Sidorov, P.M. Valetsky, *Russ. Chem. Rev.* 73 (2004) 501.
- [66] D. Astruc, F. Lu, J. Ruiz, *Angew. Chem. Int. Ed. Engl.* 44 (2005) 7852.
- [67] D. Astruc, *Inorg. Chem.* 46 (2007) 1884.
- [68] M. Zhao, L. Sun, R.M. Crooks, *J. Am. Chem. Soc.* 120 (1998) 4877.
- [69] L. Alogh, D.A. Tomalia, *J. Am. Chem. Soc.* 120 (1998) 7355.
- [70] R.M. Crooks, M. Zhao, L. Sun, V. Chechik, L.K. Yeung, *Acc. Chem. Res.* 34 (2001) 181.
- [71] M. Zhao, R.M. Crooks, *Angew. Chem. Int. Ed. Engl.* 38 (1999) 364.
- [72] Y.H. Niu, L.K. Yeung, R.M. Crooks, *J. Am. Chem. Soc.* 123 (2001) 6840.
- [73] B.D. Chandler, J.D. Gilbertson, *Top. Organomet. Chem.* 20 (2006) 97.
- [74] B.D. Chandler, J.D. Gilbertson, in: D. Astruc (Ed.), *Nanoparticles and Catalysis*, Wiley-VCH, Weinheim, 2007, p. 129.
- [75] C. Ornelas, J. Ruiz, E. Cloutet, S. Alves, D. Astruc, *Angew. Chem. Int. Ed. Engl.* 46 (2007) 872.
- [76] C. Ornelas, L. Salmon, J. Ruiz, D. Astruc, *Chem. Eur. J.* 14 (2008) 50.
- [77] N. Candelon, D. Lastécouères, A.K. Diallo, J. Ruiz, D. Astruc, J.-M. Vincent, *Chem. Commun.* (2008) 741.
- [78] S. Badèche, J.-C. Daran, J. Ruiz, D. Astruc, *Inorg. Chem.* 47 (2008) 4903.
- [79] E. Boisselier, C. Ornelas, I. Pianet, J. Ruiz, D. Astruc, *Chem. Eur. J.* 14 (2008) 5577.
- [80] C. Ornelas, L. Salmon, J. Ruiz, D. Astruc, *Chem. Commun.* (2007) 4946.
- [81] A.K. Diallo, C. Ornelas, L. Salmon, J. Ruiz, D. Astruc, *Angew. Chem. Int. Ed. Engl.* 46 (2007) 8644.
- [82] M.-T. Reetz, G. Lohmer, R. Schwickardi, *Angew. Chem. Int. Ed. Engl.* 36 (1997) 1526.
- [83] A.W. Kleij, R.A. Gossege, R.J.M. Klein Gebbink, N. Brinkmann, E.J. Reijerse, U. Kragl, M. Lutz, A.L. Spek, G. van Koten, *J. Am. Chem. Soc.* 122 (2000) 12112.
- [84] U. Kragl, C. Dreisbach, *Angew. Chem. Int. Ed. Engl.* 35 (1996) 642.
- [85] L. Plault, A. Hauseler, S. Nlate, D. Astruc, J. Ruiz, S. Gatar, R. Neumann, *Angew. Chem. Int. Ed. Engl.* 43 (2004) 2924.
- [86] S. Nlate, L. Plault, D. Astruc, *Chem. Eur. J.* 12 (2006) 903.
- [87] S. Nlate, L. Plault, D. Astruc, *New J. Chem.* 31 (2007) 1264.
- [88] L. Liang, J. Ruiz, D. Astruc, *Adv. Synth. Catal.* 353 (2011) 3434.
- [89] S.C. Bourque, F. Maltais, W.J. Xiao, O. Tardif, H. Alper, L.E. Manzer, P. Arya, *J. Am. Chem. Soc.* 121 (1999) 3035.
- [90] H. Brunner, *J. Organomet. Chem.* 500 (1995) 39.
- [91] C. Kölnner, B. Pugin, A. Togni, *J. Am. Chem. Soc.* 120 (1998) 10274.
- [92] C. Kölnner, A. Togni, *Can. J. Chem.* 79 (2001) 1762.
- [93] G.D. Engel, L.H. Gade, *Chem. Eur. J.* 8 (2002) 4319.
- [94] Y. Ribourdouille, G.D. Engel, M. Richard-Plouet, L.H. Gade, *Chem. Commun.* (2003) 1228.
- [95] A.-M. Caminade, P. Servin, R. Laurent, J.-P. Majoral, *Chem. Soc. Rev.* 37 (2008) 56.
- [96] J.K. Kassube, L.H. Gade, *Top. Organomet. Chem.* 20 (2006) 61.
- [97] C. Douat-Casassus, T. Darbre, J.L. Reymond, *J. Am. Chem. Soc.* 126 (2004) 7817.
- [98] E. Delort, T. Darbre, J.L. Reymond, *J. Am. Chem. Soc.* 126 (2004) 15642.
- [99] A. Suzuki, *Chem. Rev.* 95 (1995) 2457.
- [100] A. Suzuki, *J. Organomet. Chem.* 576 (1999) 147.
- [101] J. Lemo, K. Heuzé, D. Astruc, *Org. Lett.* 7 (2005) 2253.
- [102] D.J.M. Snelders, G. van Koten, R.J.M. Klein Gebbink, *J. Am. Chem. Soc.* 131 (2009) 11407.
- [103] T. Fujihara, S. Yoshida, H. Ohta, Y.I. Tsuji, *Angew. Chem. Int. Ed. Engl.* 47 (2008) 8310.
- [104] M. Meise, R. Haag, *ChemSusChem* 1 (2008) 637.
- [105] H. Hagiwara, H. Sasaki, N. Tsubokawa, T. Hoshi, T. Suzuki, T. Tsuda, S. Kuwabata, *Synlett* 13 (2010) 1990.
- [106] M. Janssen, C. Müller, D. Vogt, *Adv. Synth. Catal.* 351 (2009) 313.
- [107] D. Wang, D. Denux, J. Ruiz, D. Astruc, *Adv. Synth. Catal.* 355 (2013) 129.
- [108] M. Keller, A. Hameau, G. Spataro, S. Ladeira, A.-M. Caminade, J.-P. Majoral, A. Ouali, *Green Chem.* 14 (2012) 2807.
- [109] M. Pagliaro, V. Pandarus, R. Ciriminna, F. Bèland, P.D. Cara, *ChemCatChem* 4 (2012) 432.
- [110] M. Keller, V. Collière, O. Reiser, A.-M. Caminade, J.-P. Majoral, A. Ouali, *Angew. Chem. Int. Ed. Engl.* 52 (2013) 3626.
- [111] S. Wittmann, A. Schätz, R.N. Gras, W.J. Stark, O. Reiser, *Angew. Chem. Int. Ed. Engl.* 49 (2010) 1867.
- [112] A. Suzuki, D. Astruc (Eds.), *Modern Arene Chemistry*, Wiley-VCH, Weinheim, 2002, p. 53.
- [113] I.P. Beletskaya, *Chem. Rev.* 100 (2000) 3009.
- [114] J.G. de Vries, *Dalton Trans.* (2006) 421.
- [115] J.G. de Vries, A.H.M. de Vries, *Eur. J. Org. Chem.* 2003 (2003) 799.
- [116] A.H.M. de Vries, F.J. Parlevliet, L. Schmeder-van de Vondervoort, J.H.M. Mommers, H.J.W. Henderickx, M.A.N. Walet, J. de Vries, *Adv. Synth. Catal.* 344 (2002) 996.
- [117] N.T.S. Phan, M. van der Sluis, C.J. Jones, *Adv. Synth. Catal.* 348 (2006) 609.
- [118] S. Bräse, A. de Meijere, in: A. de Meijere, F. Diederich (Eds.), *Metal-Catalyzed Cross-Coupling Reactions*, 1, Second, revised ed., Wiley-VCH, Weinheim, 2004, p. 217.
- [119] G. Jayamurugan, N. Jayaraman, *Adv. Synth. Catal.* 351 (2009) 2379.
- [120] R.S. Bagul, N. Jayaraman, *J. Organomet. Chem.* 701 (2012) 27.
- [121] S. Dietrich, A. Nicolai, H. Lang, *J. Organomet. Chem.* 696 (2011) 739.
- [122] V. Hornillos, J. Guerra, A. de Cózar, P. Prieto, S. Merino, M.A. Maestro, E. Díez-Barra, J. Tejada, *Dalton Trans.* 40 (2011) 4095.
- [123] A. Mansour, T. Kehat, M. Portnoy, *Org. Biomol. Chem.* 6 (2008) 3382.
- [124] M. Cypriak, P. Pospiech, K. Strzelec, K. Wąsikowski, J.W. Sobczak, *J. Mol. Catal. A: Chem.* 319 (2010) 30.
- [125] L.K. Yeung, R.M. Crooks, *Nano Lett.* 1 (2001) 14.
- [126] Y. Li, M.A. El-Sayed, *J. Phys. Chem. B* 105 (2001) 8938.
- [127] V.V. Rostovtsev, L.G. Green, V.V. Fokin, K.B. Sharpless, *Angew. Chem. Int. Ed. Engl.* 41 (2002) 2596.
- [128] M. Meldal, C. Christensen, C.W. Tornøe, *J. Org. Chem.* 67 (2002) 3057.
- [129] L. Liang, D. Astruc, *Coord. Chem. Rev.* 255 (2011) 2933.
- [130] E. Moore, S.J. McInnes, A. Vogt, N.H. Voelcker, *Tetrahedron Lett.* 52 (2011) 2327.
- [131] H. Brunner, in: B. Cornils, W.A. Herrmann (Eds.), *Applied Homogeneous Catalysis with Organometallic Compounds*, vol. 1, second, revised ed., Wiley-VCH, Weinheim, 2002, p. 195.
- [132] A.K. Kakkar, *Macromol. Symp.* 196 (2003) 145.
- [133] B. Yi, H.-P. He, Q.-H. Fan, *J. Mol. Catal. A: Chem.* 315 (2010) 82.
- [134] J. Yu, T.V. RajanBabu, J.R. Parquette, *J. Am. Chem. Soc.* 130 (2008) 7845.
- [135] R.A. Findeis, L.H. Gade, *Eur. J. Org. Chem.* 2003 (2003) 99.
- [136] J.K. Kassube, L.H. Gade, *Adv. Synth. Catal.* 351 (2009) 739.
- [137] W.-J. Tang, Y.-Y. Huang, Y.-M. He, Q.-H. Fan, *Tetrahedron Asymm.* 17 (2006) 536.
- [138] F. Zhang, Y. Li, Z.-W. Li, Y.-M. He, S.-F. Zhu, Q.-H. Fan, Q.-L. Zhou, *Chem. Commun.* (2008) 6048.
- [139] Z.-J. Wang, G.-J. Deng, Y. Li, Y.-M. He, W.-J. Tang, Q.-H. Fan, *Org. Lett.* 9 (2007) 1243.
- [140] B. Natarajan, N. Jayaraman, *J. Organomet. Chem.* 696 (2011) 722.
- [141] L.I. Rodríguez, O. Rossell, M. Seco, G. Muller, *J. Organomet. Chem.* 694 (2009) 1938.
- [142] L.-I. Rodríguez, O. Rossell, M. Seco, G. Muller, *J. Organomet. Chem.* 692 (2007) 851.
- [143] W. Wang, Q. Wang, *Chem. Commun.* 46 (2010) 4616.
- [144] M. Zhao, H. Tokuhisa, R.M. Crooks, *Angew. Chem. Int. Ed. Engl.* 36 (1997) 2596.
- [145] R.W.J. Scott, O.M. Wilson, R.M. Crooks, *J. Phys. Chem. B* 109 (2005) 692.
- [146] V.S. Myers, M.G. Weier, E.V. Carino, D.F. Yancey, S. Pande, R.M. Crooks, *Chem. Sci.* 2 (2011) 1632.
- [147] Y. Niu, R.M. Crooks, *C. R. Chimie* 6 (2003) 1049.
- [148] I. Nakamura, Y. Yamanoi, T. Yonezawa, T. Imaoka, K. Yamamoto, H. Nishihara, *Chem. Commun.* (2008) 5716.
- [149] A. Sutton, G. Franc, A. Kakkar, *J. Polym. Sci. A: Polym. Chem.* 47 (2009) 4482.
- [150] N. Toshima, T. Yonezawa, *New J. Chem.* 22 (1998) 1179.
- [151] N. Toshima, in: E. Pellizzetti (Ed.), *Fine Particles Sciences and Technology – From Micro- to New Particles*, Kluwer, Dordrecht, 1996, p. 371.
- [152] J.-H. He, I. Ichinose, T. Kunitake, A. Nakao, Y. Shiraiishi, N. Toshima, *J. Am. Chem. Soc.* 125 (2003) 11034.
- [153] R.W. Scott, A.K. Datye, R.M. Crooks, *J. Am. Chem. Soc.* 125 (2003) 3708.
- [154] R.W.J. Scott, O.M. Wilson, S.K. Oh, E.A. Kenik, R.M. Crooks, *J. Am. Chem. Soc.* 126 (2004) 15583.
- [155] H. Xie, J.Y. Howe, V. Schwartz, J.R. Monnier, C.T. Williams, H.J. Ploehn, *J. Catal.* 259 (2008) 111.
- [156] B.J. Auten, H. Lang, B.D. Chandler, *Appl. Catal. B: Environ.* 3–4 (2008) 233.
- [157] M.G. Weir, V.S. Myers, A.I. Frenkel, R.M. Crooks, *ChemPhysChem* 11 (2010) 2942.
- [158] B.D. Chandler, C.G. Long, J.D. Gilbertson, C.J. Pursell, G. Vijayaraghavan, K.J. Stevenson, *J. Phys. Chem.* 114 (2010) 11498.
- [159] M. Bernechea, S. Garcia-Rodríguez, P. Terreros, E. de Jesus, F.L.G. Fierro, S. Rojas, *J. Phys. Chem. C* 115 (2011) 1287.
- [160] N. Toshima, T. Yonezawa, K. Kushihashi, *J. Chem. Soc., Faraday Trans.* 89 (1993) 2537.
- [161] W. Zhang, L. Li, Y. Du, X. Wang, P. Yang, *Catal. Lett.* 127 (2009) 429.
- [162] F. Ungvary, *Coord. Chem. Rev.* 167 (1997) 233.
- [163] R.S. Dickson, *Homogeneous Catalysis with Compounds of Rhodium and Iridium*, D. Reidel, Boston, MA, 1985, Chapter 4.
- [164] S.C. Bourque, H. Alper, L.E. Manzer, P. Arya, *J. Am. Chem. Soc.* 122 (2000) 956.
- [165] P. Arya, G. Panda, N.V. Rao, H. Alper, S.C. Bourque, L.E. Manzer, *J. Am. Chem. Soc.* 123 (2001) 2889.
- [166] S.-M. Lu, H. Alper, *J. Am. Chem. Soc.* 125 (2003) 13126.
- [167] S.-M. Lu, H. Alper, *J. Am. Chem. Soc.* 127 (2005) 14776.
- [168] S.-M. Lu, H. Alper, *Chem. Eur. J.* 13 (2007) 5908.
- [169] M.T. Pope, A. Müller, *Angew. Chem. Int. Ed. Engl.* 30 (1991) 34.
- [170] J.T. Rhule, C.L. Hill, D.A. Rud, R.F. Schinazi, *Chem. Rev.* 98 (1998) 327.
- [171] M.T. Pope, A. Müller, *Polyoxometalate Chemistry: From Topology via Self-Assembly to Applications*, Kluwer Academic, Dordrecht, 2001.
- [172] M.V. Vasylyev, D. Astruc, R. Neumann, *Adv. Synth. Catal.* 347 (2005) 39.
- [173] C. Jahier, L. Plault, S. Nlate, *Isr. J. Chem.* 49 (2009) 109.
- [174] C. Jahier, M. Cantuel, N.D. McClenaghan, T. Buffeteau, D. Cavagnat, F. Agbossou, M. Carraro, M. Bonchio, S. Nlate, *Chem. Eur. J.* 15 (2009) 8703.
- [175] C. Jahier, S.S. Mal, U. Kortz, S. Nlate, *Eur. J. Inorg. Chem.* 2010 (2010) 1559.
- [176] T. Iwasawa, M. Tokunaga, Y. Obora, Y. Tsuji, *J. Am. Chem. Soc.* 126 (2004) 6554.
- [177] G.R. Krishnam, K. Sreekumar, *Appl. Catal. A: Gen.* 353 (2009) 80.
- [178] C. Müller, L.J. Ackerman, J.N.H. Reek, P.C.J. Kamer, P.W.N.M. van Leeuwen, *J. Am. Chem. Soc.* 126 (2004) 14960.

- [179] T. Imaoka, Y. Kawana, K. Yamamoto, *Polym. Adv. Technol.* 22 (2011) 1261.
- [180] K. Takahashi, A. Fujii, R. Nakajima, H. Chiba, M. Higuchi, Y. Einaga, K. Yamamoto, *Bull. Chem. Soc. Jpn.* 80 (2007) 1563.
- [181] A. Ouali, R. Laurent, A.-M. Caminade, J.-P. Majoral, M. Taillefer, *J. Am. Chem. Soc.* 128 (2006) 15990.
- [182] A. Gissibl, C. Padié, M. Hager, F. Jaroschik, R. Rasappan, E. Cuevas-Yañez, C.-O. Turrin, A.-M. Caminade, J.-P. Majoral, O. Reiser, *Org. Lett.* 9 (2007) 2895.
- [183] U. Lüning, J.P.W. Eggert, K. Hagemann, *Eur. J. Org. Chem.* 2006 (2006) 2747.
- [184] F. Ribaud, P.W.N.M. van Leeuwen, J.N.H. Reek, *Isr. J. Chem.* 49 (2009) 79.
- [185] M. Keller, M. Ianchuk, S. Ladeira, M. Taillefer, A.M. Caminade, J.P. Majoral, A. Ouali, *Eur. J. Org. Chem.* 2012 (2012) 1056.
- [186] M. Gaab, S. Bellemin-Lapponnaz, L.H. Gade, *Chem. Eur. J.* 15 (2009) 5450.
- [187] J. Keilitz, R. Haag, *Eur. J. Org. Chem.* 2009 (2009) 3272.
- [188] T. Muraki, K.-I. Fujita, M. Kujime, *J. Org. Chem.* 72 (2007) 7863.
- [189] F. Xiao, X. Sun, X. Wu, J. Zhao, Y. Luo, *J. Organomet. Chem.* 713 (2012) 96.
- [190] P. Servin, R. Laurent, L. Gonsalvi, M. Tristany, M. Peruzzini, J.-P. Majoral, A.-M. Caminade, *Dalton Trans.* (2009) 4432.
- [191] P. Servin, R. Laurent, H. Dib, L. Gonsalvi, M. Peruzzini, J.-P. Majoral, A.-M. Caminade, *Tetrahedron Lett.* 53 (2012) 3876.
- [192] N.J.M. Pijnenburg, M. Lutz, M.A. Siegler, A. Spek, G. van Koten, R.J.M.K. Gebbink, *New J. Chem.* 35 (2011) 2356.
- [193] N.J.M. Pijnenburg, H.P. Dijkstra, G. van Koten, R.J.M.K. Gebbink, *Dalton Trans.* 40 (2011) 8896.
- [194] M. Shema-Mizrachi, G.M. Pavan, E. Levin, A. Danani, N.G. Lemco, *J. Am. Chem. Soc.* 133 (2011) 14359.
- [195] C.-L. Kao, Y.-H. Tang, Y.C. Lin, L.-T. Chiu, H.-T. Chen, S.C.N. Hsu, K.-C. Hsieh, C.-Y. Lu, Y.-L. Chen, *Nanomed. Nanotechnol. Biol. Med.* 7 (2011) 273.
- [196] D. Astruc, A.K. Diallo, S. Gatard, L. Liang, C. Ornelas, V. Martinez, D. Méry, J. Ruiz, *Beilstein J. Org. Chem.* 7 (2011) 94.
- [197] A.K. Diallo, E. Boisselier, L. Liang, J. Ruiz, D. Astruc, *Chem. Eur. J.* 16 (2010) 11832.
- [198] M. Martin, F. Manea, R. Fiammengo, L.J. Prins, L. Pasquato, P. Scrimin, *J. Am. Chem. Soc.* 129 (2007) 6982.
- [199] G. Zaupa, L.J. Prins, P. Scrimin, *Bioorg. Med. Chem. Lett.* 19 (2009) 3816.
- [200] T. Imaoka, R. Tanaka, K. Yamamoto, *J. Polym. Sci. A: Polym. Chem.* 44 (2006) 5229.
- [201] K. Tahara, H. Shimakoshi, A. Tanak, Y. Hisaeda, *Dalton Trans.* 39 (2010) 3035.
- [202] L. Garcia, A. Roglans, R. Laurent, J.P. Majoral, A. Pla-Quintana, A.-M. Caminade, *Chem. Commun.* 48 (2012) 9248.
- [203] M.Y. Darensbourg, D. Daigle, *Inorg. Chem.* 14 (1975) 1217.
- [204] R.H. Grubbs (Ed.), *Handbook of Metathesis*, Vol. 1–3, Wiley-VCH, Weinheim, 2002.
- [205] G.C. Vougioukalakis, R.H. Grubbs, *Chem. Rev.* 110 (2010) 1746.
- [206] T.M. Trnka, R.H. Grubbs, *Acc. Chem. Res.* 34 (2001) 18.
- [207] P.I. Dalkó, L. Moisan, *Angew. Chem. Int. Ed. Engl.* 40 (2001) 3726.
- [208] P.R. Schreiner, *Chem. Soc. Rev.* 32 (2003) 289.
- [209] P.I. Dalkó, L. Moisan, *Angew. Chem. Int. Ed. Engl.* 43 (2004) 5138.
- [210] D. Enders, C. Grondal, R.M. Huetti, *Angew. Chem. Int. Ed. Engl.* 46 (2007) 1570.
- [211] D. Enders, O. Niemeyer, A. Henseler, *Chem. Rev.* 107 (2007) 5606.
- [212] A. Dondoni, A. Massi, *Angew. Chem. Int. Ed. Engl.* 47 (2008) 4638.
- [213] Z. Maeno, T. Mitsudome, T. Mizugaki, K. Jitsukawa, K. Kaneda, *Chem. Lett.* 41 (2012) 801.
- [214] Y. Li, X.-Y. Liu, G. Zhao, *Tetrahedron Asymm.* 17 (2006) 2034.
- [215] L. Tuchman-Shukron, M. Portnoy, *Adv. Synth. Catal.* 351 (2009) 541.
- [216] N.A. Uhlich, T. Darbre, J.-L. Reymond, *Org. Biomol. Chem.* 9 (2011) 7071.
- [217] R. Biswas, N. Maillard, J. Kofoed, J.-L. Reymond, *Chem. Commun.* 46 (2010) 8746.
- [218] J.-L. Reymond, T. Darbre, *Org. Biomol. Chem.* 10 (2012) 1483.
- [219] X. Liu, Y. Li, G. Wang, Z. Chai, Y. Wu, G. Zhao, *Tetrahedron Asymm.* 17 (2006) 750.
- [220] Y. Imada, H. Iida, T. Kitagawa, T. Naota, *Chem. Eur. J.* 17 (2011) 5908.
- [221] J.-P. Lindner, C. Röben, A. Studer, M. Stasiak, R. Ronge, A. Greiner, H.-J. Wendorff, *Angew. Chem. Int. Ed. Engl.* 48 (2009) 8874.
- [222] S. Wei, J. Wang, S. Venhuizen, R. Skouta, R. Breslow, *Bioorg. Med. Chem. Lett.* 19 (2009) 5543.
- [223] K. Mitsui, S.A. Hyatt, D.A. Turner, C.M. Hadad, J.R. Parquette, *Chem. Commun.* (2009) 3261.
- [224] C.-M. Lo, H.-F. Chow, *J. Org. Chem.* 74 (2009) 5181.
- [225] J.K. Kassube, H. Wadeh, L.H. Gade, *Adv. Synth. Catal.* 351 (2009) 607.
- [226] G.-F. Liu, M. Filipović, I. Ivanović-Burmazović, F. Beuerle, P. Witte, A. Hirsch, *Angew. Chem. Int. Ed. Engl.* 47 (2008) 3991.
- [227] Y.-N. Niu, Z.-Y. Yan, G.-Q. Li, H.-L. Wei, G.-L. Gao, L.-Y. Wu, Y.-M. Liang, *Tetrahedron Asymm.* 19 (2008) 912.
- [228] G.R. Krishnan, K. Sreekumar, *Polymer* 49 (2008) 5233.
- [229] G.R. Newkome, Z. Yao, G.R. Baker, V.K. Gupta, *J. Org. Chem.* 50 (1985) 2003.
- [230] G.R. Newkome, C. Shreiner, *Chem. Rev.* 110 (2010) 5301.

## Fast-Growing Field of Magnetically Recyclable Nanocatalysts

Dong Wang and Didier Astruc\*

ISM, University of Bordeaux, 351 Cours de la Libération, 33405 Talence Cedex, France



## CONTENTS

1. Introduction	A
1.1. Synthesis and Modification of Magnetic Nanoparticles	A
1.2. Synthesis and Seminal Studies of Magnetic Catalysts	C
1.3. Characterization of Magnetic Catalysts	E
2. Recent Advances and Trends	E
2.1. Magnetically Recyclable Nanocatalysts Based on Transition Metals	E
2.1.1. C–C Coupling: Miyaura–Suzuki, Heck, Sonogashira, and Hiyama Reactions	E
2.1.2. Alkyne–Azide Cycloaddition	I
2.1.3. Hydrogenation of Unsaturated Compounds	K
2.1.4. Reduction of Nitroaromatics	N
2.1.5. Oxidation Reactions	P
2.1.6. Arylation and Alkylation Reactions	R
2.1.7. Epoxidation of Alkenes	S
2.1.8. Multicomponent “One-Pot” Synthesis	T
2.1.9. Fenton-Like Reactions	U
2.1.10. Other Reactions	V
2.2. Magnetically Recyclable Organocatalysts	W
2.3. Magnetically Recyclable Biocatalysts	Z
2.4. Magnetically Recyclable Photocatalysts in the Degradation of Pollutants	AB
3. Conclusions and Outlook	AC
Author Information	AD
Corresponding Author	AD
Notes	AD
Biographies	AD
Acknowledgments	AD
Abbreviations	AD
References	AE
Note Added in Proof	AK

## 1. INTRODUCTION

Catalysis is a key component of “green chemistry”, and one of the urgently needed challenges facing chemists now is the design and use of environmentally benign catalysts.<sup>1–10</sup> A sustainable and “green” catalyst must therefore possess specific features<sup>11</sup> including low preparation cost, high activity, great

selectivity, high stability, efficient recovery, and good recyclability.

Conventional catalysts can be divided into homogeneous and heterogeneous, the former holding advantages such as good activity and selectivity and accessible mechanistic studies leading to catalyst optimization. However, the difficulty of separating homogeneous catalysts from reaction medium consumedly restricts their applications in industry, especially in the drug and pharmaceutical industry owing to the issue of metal contamination in the case of metal-catalyzed synthesis. Heterogenization of active molecules with a solid support fabricating insoluble heterogeneous catalytic systems is an efficient strategy in order to achieve the isolation and separation of catalysts. However, the activities of heterogeneous catalysts are generally lower than those of their homogeneous counterparts, due to the lower dimensionality of the interaction between the components and the catalyst surface.

As semiheterogeneous catalysts, nanocatalysts with a large surface-to-volume ratio, are attractive alternatives to conventional catalysts, substantial enhancements in catalytic activity, selectivity, and stability are realized by tailoring their size, shape, composition, and electronic structure.<sup>12–22</sup> Nanocatalysts are isolated and recovered through filtration or centrifugation methods, whereas the inconvenience and inefficiency of these tedious methods caused by the nano size of the catalyst particles hamper the sustainability and economics of the nanocatalytic strategy.

To overcome these issues, use of magnetic nanoparticles (MNPs) appears to be the most logical solution. Magnetic nanocatalysts are simply and efficiently removed from reaction mixtures with an external magnetic field, and MNPs have emerged as ideal catalysts or supports. This field has indeed been the subject of excellent reviews.<sup>23–28</sup>

Due to this explosive development, new reactions, nanocatalysts, systems, and trends are appearing at a fast rate, and about 400 publications have appeared in the last 2 years. Therefore, in this review, we briefly summarize the basic concepts and seminal studies of magnetically recoverable catalysts; then we highlight the new breakthroughs and trends in the area that have most recently appeared until 2014.

## 1.1. Synthesis and Modification of Magnetic Nanoparticles

The methods of preparation of MNPs play a key role in determining the particle morphology (size, shape, agglomeration, and size distribution), composition, magnetic property, surface chemistry, and catalytic applications. There are several protocols reported in the literature for synthesizing MNPs, such as the coprecipitation method, the micromulsion technique, the sol–gel method, spray and laser pyrolysis, the

Received: March 5, 2014

hydrothermal reaction method, sonolysis, microwave irradiation, biological synthesis, etc.<sup>23,24,29–35</sup> According to particular requirements for MNPs, these methods were operated under optimized conditions (mainly regarding reaction temperature, pH value, concentration, and proportion of starting materials) to synthesize MNPs in the forms of metals (Fe, Co, Ni), alloys (FePt, CoPt), iron oxides (FeO, Fe<sub>2</sub>O<sub>3</sub>, Fe<sub>3</sub>O<sub>4</sub>), or ferrites MFe<sub>2</sub>O<sub>4</sub> (M = Co, Mn, Cu, Zn). These MNPs are directly used as catalysts or as supports for further modification or functionalization with the catalytic species.

Among these MNPs, magnetite (Fe<sub>3</sub>O<sub>4</sub>) has been identified as the ideal and most widely used support in catalysis<sup>36,37</sup> because of its low cost and easy preparation. Magnetite is inert and possesses a very active surface for immobilization or adsorption of catalytic fragments including metal catalysts (Au, Pd, Pt, Cu, Ni, Co, Ir), organocatalysts, and enzymes resulting in formation of remarkably sustainable catalysts. Magnetite has been used in recent years as a versatile catalyst support in a wide range of reactions, such as Suzuki, Heck, Sonogashira, Hiyama, hydrogenation, reduction, oxidation, cycloaddition reactions, asymmetric synthesis, etc. Magnetite has also been directly applied as catalyst in organic transformations. For example, Fe<sub>3</sub>O<sub>4</sub> nanoparticles (NPs) exhibited high catalytic performance for the practical and atom-economic one-pot synthesis of propargylamines via three-component coupling of aliphatic aldehyde, alkyne, and amine. In addition, after completion of the first reaction cycle, Fe<sub>3</sub>O<sub>4</sub> is magnetically separated from the reaction medium with an external magnetic field and reused at least five times without a significant decrease of activity.<sup>38</sup> Other forms of iron oxide, maghemite ( $\gamma$ -Fe<sub>2</sub>O<sub>3</sub>), and spinel ferrites (MFe<sub>2</sub>O<sub>4</sub>) have also received a lot of attention in the field of MNPs catalysis owing to their ferrimagnetism, environmental stability, and other properties.

Aggregation of the naked MNPs is virtually unavoidable because of their small interparticle distances, high surface energy, and the existence of van der Waals forces. To solve this problem, modification of MNPs using suitable stabilizing ligands or coating materials (including small molecules, silica, polymers, carbon, ionic liquids, metal or metal oxide NPs, and their layer-by-layer combinations) has been proved to be the best solution to date. Meanwhile, the modification procedures provide reaction sites or active groups for covalently or noncovalently grafting the active catalytic units onto the coated MNPs to construct magnetically recoverable catalysts.

Dopamine derivatives,<sup>39–41</sup> triethoxysilyl-<sup>42–44</sup> phosphonic acids-functionalized molecules,<sup>45,46</sup> and glutathione<sup>47,48</sup> were frequently applied to stabilize and functionalize MNPs. This process produces grafting sites or reaction sites to bind catalytic species. Dopamine, a natural neurotransmitter that is present in various animals, contains catechol and amine groups. It exhibits an outstanding capacity of coordination to Fe ions of MNPs, the coordination usually being promoted by sonicating the mixture in suspension. The amine groups of dopamine derivatives are versatile chelating reagents (or reactive fragment) to directly coordinate metal catalyst or react with other organic molecules. Triethoxysilyl-functionalized molecules such as commercially available NH<sub>2</sub>-, SH-, and Cl-terminated compounds and their further functionalized derivatives are another type of popular reagents for surface modification of MNPs. The connection of MNPs with these silane reagents is achieved by coupling between the hydroxyl group of MNPs and silane reagents. For instance, the Sato group<sup>44</sup> reported the first example of phase-transfer catalyst (quaternary ammonium and

phosphonium salts)-modified MNPs. In the synthetic process, (3-iodopropyl) trimethoxysilane successively reacted with quaternary ammonium and phosphonium salts, and the homogeneous triethoxysilyl-functionalized phase-transfer catalyst that was obtained was then anchored using MNPs. This semiheterogeneous catalyst showed high performance in terms of activity and stability in the O-alkylation reaction of PhONa with *n*-BuBr in the solvent mixture of toluene and water. Phosphonic acids and glutathione are also bifunctionalized linkers between MNPs and catalytic species.

Silica is the most popular inorganic coating material for MNPs, because it is very easily connected to MNPs. Most MNPs are synthesized in organic solvent using hydrophobic capping reagents, resulting in dispersibility in organic solvents but poor dispersion properties in environmentally benign aqueous media. Silica as coating shell improves the water solubility and biocompatibility of MNPs. The dense silica shell has plenty of Si–OH groups for potential derivatization with various functional units allowing introduction of catalytic molecules to MNPs. Silica shells prevent metal leaching from the core of MNPs under harsh shaking conditions. Coating silica is generally performed through the sol–gel method, microemulsion technique, and deposition of silica deposition from a silicic acid solution. Since the pioneering work on the application of silica-coated MNPs as a recyclable catalyst support was reported by Ying and co-workers,<sup>49</sup> a great variety of catalysts based on silica-coated MNPs have been developed. For example, Jin's group demonstrated that a triethoxysilyl-functionalized Pd complex was easily immobilized on the surface of SiO<sub>2</sub>@Fe<sub>3</sub>O<sub>4</sub> that was prepared by coating Fe<sub>3</sub>O<sub>4</sub> NPs (20 nm in core) with a layer of silica through a sol–gel process. This Pd catalyst was highly active and magnetically recyclable in the Suzuki, Sonogashira, and Stille reactions of unreactive aryl chlorides in aqueous conditions.<sup>50</sup>

Recently, introducing a shell of polymers (or dendrimers) with functional groups to the surface of MNPs has been the subject of increasing attention.<sup>28,35</sup> In catalysis, the catalytic performance of MNPs can be flexibly tuned and considerably affected by the inherent properties of the polymers (or dendrimers), such as solubility, functional groups, molecular weight, degree of cross-linking, hydrophilicity, and hydrophobicity. In general, there are two protocols for the immobilization of MNPs with polymers: in situ polymerization on the surface of MNPs<sup>51,52</sup> and grafting of polymers onto MNPs via coordination, or hydrophobic, or electrostatic interactions.<sup>53,54</sup> For instance, Fe<sub>3</sub>O<sub>4</sub>@PANI NPs with well-defined core–shell nanostructure were fabricated through polymerization of aniline on the surface of the Fe<sub>3</sub>O<sub>4</sub> NPs. After treating Fe<sub>3</sub>O<sub>4</sub>@PANI under acidic or neutral pH conditions, its surface was covered by positive charge, which allowed negatively charged citrate-stabilized AuNPs to be attached to Fe<sub>3</sub>O<sub>4</sub>@PANI through electrostatic attractions.<sup>55</sup> Various commercially available polymers including Pluronic polymer,<sup>56</sup> poly(acrylic acid) (PAA), and polyethylenimine (PEI)<sup>57</sup> have been used as coating materials on the surface of MNPs. Dendrimers, exhibiting well-defined structure and a monodisperse nature, have been identified as ideal capping materials to MNPs for embedding molecular and nanocatalysts. The step-by-step divergent synthesis of dendrimers on the surface,<sup>58</sup> and the grafting of presynthesized dendrimers on the surface are two common protocols to form dendrimer shell of MNPs.<sup>53,59</sup> Alper's group<sup>58</sup> reported for the first time the growth of polyaminoamido (PAMAM) dendrons on silica-

coated MNPs. The stability and solubility (in organic solvents) of  $\text{SiO}_2@\text{Fe}_3\text{O}_4$  NPs were significantly improved after decorating with up to three generations PAMAM dendrons. The successive phosphination and complexation with rhodium toward PAMAM-coated MNPs produced a rhodium complex that was supported on dendronized MNPs. This nanocatalyst displayed excellent activity and selectivity in hydroformylation reactions.

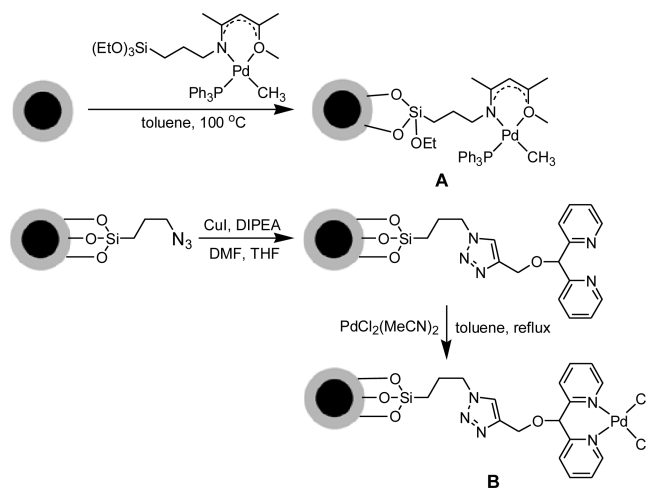
Ionic liquids (ILs) have attracted growing interest owing to their safety, negligible vapor pressure with various polarities, good solubility, capacity as reaction media, and catalytic applications. In the recent reports, ILs-coated MNPs were widely used as catalysts for oxidation, hydrogenation, and condensation reactions.<sup>60–62</sup> They were also used as stabilizers for further immobilization of metal NPs.<sup>63</sup>

Encapsulation of MNPs in various solid supports such as mesoporous materials,<sup>64,65</sup> graphene,<sup>66</sup> carbon nanotubes,<sup>67</sup> and polymers was also efficient for stabilizing MNPs and therefore fabricating magnetic supports. Magnetic mesoporous materials, combining the advantages of mesoporous materials (uniform pore distribution and large surface area) and MNPs, have been used for a variety of applications, especially as supports in catalysis over the past few years. MCM-41 and SBA-15 are the most used mesoporous materials for the support of MNPs. Graphene is a remarkable support for encapsulation of metal NPs, because of its two-dimensional plate-like structure and large specific surface area. Use of graphene not only avoids the aggregation of metal NPs but also enhances their catalytic activity owing to the strong synergistic interaction between the two components. However, in the case of MNPs, the problem of site competition on the surface of graphene between MNPs and the further deposited catalytic species hampers the catalytic application of magnetic graphene as support. In a recent report, Cai's group<sup>66</sup> demonstrated that introduction of a polydopamine shell between MNPs and graphene perfectly solves this problem. Carbon nanotubes (CNTs) exhibit intriguing properties, such as nanoscale dimensions, high specific surface area, mechanical strength, and chemical stability. Implantation of MNPs in CNTs prevents agglomeration and brings the property of magnetic recovery to the support. Among various MNPs,  $\text{Fe}_3\text{O}_4$  is the one most commonly used nanomaterial used in the preparation of magnetic CNTs.<sup>68</sup> Magnetic CNTs are assembled via high-temperature decomposition,<sup>69</sup> polymer wrapping and layer-by-layer assembly,<sup>70</sup> hydrothermal or solvothermal process,<sup>71</sup> and wet chemistry.<sup>72</sup> The in situ hydrothermal or solvothermal process is a fascinating method due to its capacity to easily control the properties of MNPs.

## 1.2. Synthesis and Seminal Studies of Magnetic Catalysts

Grafting transition metal catalysts (including metal complexes and metal NPs), organocatalysts, and enzymes to these MNPs that contain stabilizers, modifying reagents, or supports was achieved through covalent or noncovalent binding processes, providing various magnetic catalysts that have been used in a wide range of reactions.

MNPs-immobilized transition metal catalysts are divided into metal complex catalysts and metal NP catalysts. Metal complex catalysts supported on MNPs have generally been prepared through two procedures: (1) direct reaction of metal complexes with site-surrounded MNPs; (2) coordination of precursors of metal complexes with chelating ligand-modified MNPs. Taking Pd complexes as examples (Figure 1), the presynthesized



**Figure 1.** Synthesis of MNPs-immobilized Pd complexes.

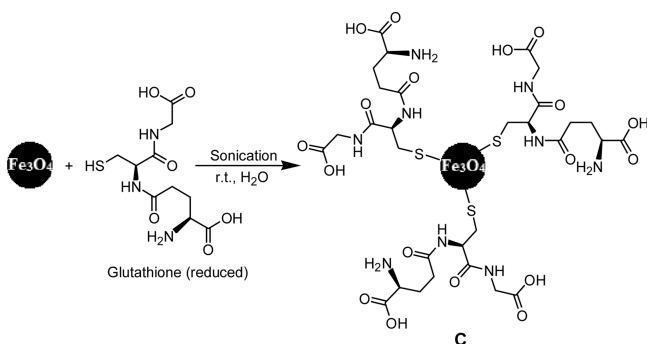
triethoxysilyl-functionalized ( $\beta$ -oxoiminato)(phosphanyl) palladium complex was directly immobilized on the surface of  $\text{SiO}_2@\text{Fe}_3\text{O}_4$  NPs via heterogenization with the Si–OH binding sites of the  $\text{SiO}_2$  shell to give magnetic catalyst A.<sup>50</sup> MNP-supported di(2-pyridyl) methanol was obtained via click reaction between acetylene-terminated di(2-pyridyl) and azide-functionalized MNPs followed by complexation with palladium dichloride with the ligand providing magnetic catalyst B. This catalyst showed excellent catalytic performance in terms of activity and recyclability for Suzuki reactions.<sup>73</sup>

Metal NPs anchored to MNPs have been extensively studied. Immobilization of metal NPs was essentially carried out using a process in which soluble metal precursors first coordinated to surface stabilizers or capping compounds of MNPs. Reduction was then performed, resulting in assembly of metal NPs on MNPs. The size, shape, morphology, and distribution of metal NPs are well tuned by various surface stabilizers or capping compounds under various conditions. Moreover, stabilizer-functionalized MNPs prevent aggregation and leaching of metal NPs. In the vast majority of examples the stabilizers appear to be amine ligands in the form of dopamine, triethoxysilyl amine, amine-containing polymers, or dendrimers (PAMAM). This is due to their excellent nanoparticle (NP) stabilizing properties against aggregation without disturbing their desirable properties. These stabilizers were also recognized to increase the catalytic activity. Pd and Au were the most widely used metals in NPs for MNP catalysis. MNP-immobilized PdNPs and AuNPs played a key role in a variety of catalytic processes including C–C coupling, hydrogenation, oxidation, reduction, and organic synthesis.<sup>26,74,75</sup> Use of MNPs as supports for these noble metals provided great progress regarding the cost, agglomeration, leaching issue, and catalytic efficiency and lifetime.

The catalytic efficiency, selectivity, and recyclability of MNP-immobilized metal NP catalysts are dramatically influenced by the catalytic NP size and shape as well as the MNP support. In general, smaller NPs possess higher catalytic efficiency and selectivity, due to their larger percentage of surface atoms, higher activation energy, and higher sensing response as compared to these of larger particles.<sup>76,77</sup> It has been verified that the shape of NPs, determined by the exposed crystal planes, considerably affects the catalytic performance.<sup>78</sup> The shapes of nanocatalysts are used to favor catalytic sites in specific surface planes. However, it is still a challenge to

construct NPs shapes at will. The catalytic behavior also strongly depends on the choice of MNP support that does not only influence the size and shape of catalytic NPs through varied decorations and components in the synthetic processes of catalytic NPs but also determines the catalytic performance via the interaction with NPs during the catalytic processes.<sup>79</sup> These phenomena enhance the appeal of well-defined MNP-supported metal NP catalysts in a wide variety of organic transformations.

Organocatalysis dates back to more than 150 years ago. Organocatalysts offer several advantages such as high robustness, low toxicity, and straightforward accessibility compared with metallic catalysts.<sup>80</sup> Recently, immobilization of organocatalysts on MNPs was shown to be a highly efficient and environmentally benign approach in organic synthesis. MNPs-anchored organocatalysts were generally prepared by formation of robust chemical bonds between modified MNPs and organocatalyst units. In 2009, the Polshettiwar group<sup>47,48</sup> described the first magnetically recoverable organocatalyst. In this report, glutathione was covalently linked to Fe<sub>3</sub>O<sub>4</sub> NPs via coupling the thiol group with the free hydroxyl groups of the surface of Fe<sub>3</sub>O<sub>4</sub> NPs (Figure 2). The magnetic nano-



**Figure 2.** Synthesis of a magnetic organocatalyst based on glutathione.

organocatalyst **C** based on glutathione was highly active in the Paal–Knorr synthesis of a series of pyrrole heterocycles, aza-Michael reactions, and pyrazole synthesis in aqueous media under microwave conditions. The catalyst can be simply and efficiently collected using a magnetic field and reused at least three reaction cycles without any loss of activity. Afterward, the magnetic glutathione-based organocatalyst was successfully extended to the catalytic homocoupling of arylboronic acids.<sup>81</sup> A number of reports then followed in organic synthesis, particularly in asymmetric synthesis with magnetic organocatalysts.<sup>41,82</sup>

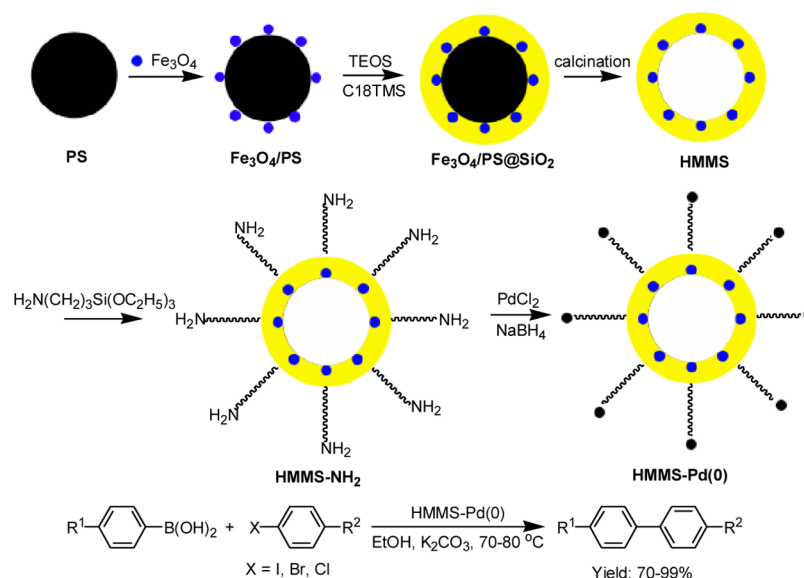
Enzymes have provided a widespread application in the food, textile, chemical, and pharmaceutical industries, due to their crucial properties such as remarkably high activity, regio- and enantioselectivity, specificity, use of mild reaction conditions, and reduced energy consumption. However, complicated and inefficient recovery and purification stages of enzymes restricted their application. Immobilization of enzymes on MNPs (especially on Fe<sub>3</sub>O<sub>4</sub> and  $\gamma$ -Fe<sub>2</sub>O<sub>3</sub> NPs) was a logical solution to overcome these issues.<sup>83,84</sup> The existing immobilization protocols are classified into four categories: (1) adsorption–cross-linking methods; (2) entrapping methods; (3) ionic or covalent coupling methods; (4) other specific biorecognition methods.<sup>85,86</sup> Among them, covalent coupling is the best candidate to achieve this protocol. Several covalent linking chemistries including carbodiimide and maleimide coupling,

disulfide bridges, click chemistry, and thiol–ene chemistry have been widely employed. Silica has been mostly explored as a coating material of MNPs for anchoring biocatalysts, because it is biocompatible, highly stable, and dispersible in aqueous solutions. Since Lilly et al. prepared iron oxide-supported cellulose in 1973,<sup>87</sup> more than 30 kinds of enzymes and biomolecules have been successfully immobilized on MNPs.<sup>88</sup>

Water purification has been studied for decades because of the serious concern of contaminated water (especially those contained organic pollutants) resulting from industrialization and fast development of economy. With the rapid development of photocatalysts,<sup>89,90</sup> magnetically recoverable photocatalysts have been recently extensively used in the field of degradation of pollutants including dyes, herbicides, and related pollutants,<sup>91,92</sup> due to their low toxicity, perfect biocompatibility, and excellent separation properties of MNPs.<sup>93,94</sup> MNP-supported nano-TiO<sub>2</sub> is one of the main and most widely investigated catalysts in the photodegradation of pollutants in water, because nano-TiO<sub>2</sub> is a highly efficient, low-cost, long-term stable, and perfectly biocompatible photocatalyst.<sup>95–100</sup> Moreover, MNPs-supported nano-TiO<sub>2</sub> is easily separated using an external magnetic field and repeatedly used. However, the energy requirement for effective photoexcitation (higher than 3.2 eV) lead to TiO<sub>2</sub>-promoted photodegradation occurring only under UV irradiation. Renewable sunlight irradiation-involved photodegradation of pollutants over TiO<sub>2</sub> is a challenge.<sup>101</sup> Among several strategies to improve the catalytic properties of TiO<sub>2</sub> such as other elements doping, decorating with Lewis acids, dye sensitizing, and coupling with other semiconductors, doping TiO<sub>2</sub> with other elements is a promising strategy to increase its photocatalytic activity. Ao's group<sup>102</sup> synthesized a novel magnetic photocatalyst nitrogen-doped TiO<sub>2</sub>-coated  $\gamma$ -Fe<sub>2</sub>O<sub>3</sub> magnetic activated carbon that showed high photocatalytic activity in degradation of Reactive Brilliant Red X-3B in an aqueous solution under sunlight irradiation. The catalyst also exhibited excellent recyclability; it is magnetically separated using a magnet, and the catalytic activity was preserved for six runs. Magnetic multifunctional metal oxide/graphene composites were recently proved to be promising photocatalysts for degradation of water pollutants including organic dyes, water-borne pathogens, and heavy metal ions.<sup>103,104</sup>

Research on magnetically recyclable nanocatalysts is a fast-growing field. Many seminal studies recently appeared, such as catalytic applications of bimetallic NPs (excluding spinel ferrites), efforts to achieve completely sustainable, “green” and practical organic transformations based on MNPs catalysts, uses of new magnetic multifunctional materials with varied architectures including core-double shell, yolk–shell, hollow and bowl-like structures, and so on.

Bimetallic NPs have a bright future in catalysis due to their enhanced stability, activity, selectivity, and other properties compared to their monometallic counterparts.<sup>105,106</sup> The recently reported magnetically recyclable bimetallic NPs catalysts are divided into two categories: MNPs-immobilized bimetallic NPs (for instance, Fe<sub>3</sub>O<sub>4</sub>@AuPd NPs),<sup>107</sup> and bimetallic NPs containing a magnetic metal (for instance, Ni@Ru, Fe@Au and Ni@Ag).<sup>108–110</sup> These bimetallic NPs display higher activity and selectivity in various organic transformations than those of each monometallic counterpart and physical mixture of monometallic counterparts. Furthermore, these magnetic bimetallic NPs catalysts generally show good recyclability with magnetic separation.



**Figure 3.** Preparation and catalytic applications of HMMS–Pd(0).

Development of sustainable and practical chemistry is a long-term subject. Using MNPs catalysts as platforms, chemists recently made tremendous efforts to achieve rapid and easy immobilization at room temperature in solvent-free conditions at low cost for preparation of highly efficient MNPs with high densities of functional groups, including use of flow reactors. Relevant advancements and progresses have been illustrated in the Recent Advances and Trends section.

Materials with multiple functionalities are presently of great scientific and technological interest. In the field of MNPs catalysis, a series of new multifunctional materials with various structures has been recently designed and used. These materials combine different properties into one particle such as magnetism, high surface area, mechanical strength, thermal stability, and various functional groups. For example, magnetic materials with signal or double-shelled yolk-like structure were constructed as ideal supports of noble metals.<sup>111,112</sup> These yolk–shell composites with a movable core have higher surface area, larger void space, and lower density, which promises higher catalytic efficiency and application as nanoreactors compared to common core–shell composites. Hollow magnetic mesoporous spheres (HMMS) also attracted extensive attention as catalyst carriers, due to their superparamagnetic property, uniform size, large surface area, high catalyst loading, and homogeneous spherical morphologies.<sup>113</sup> Exploration of novel magnetic multifunctional materials in catalysis will never stop.

### 1.3. Characterization of Magnetic Catalysts

After their preparation, the magnetic catalysts have been characterized using a great variety of methods to gain a comprehensive amount of data in order to properly analyze their properties.

The size, shape, and morphologies of magnetic catalysts are determined by transmission electron microscopy (TEM) and/or scanning electron microscopy (SEM). The structure of magnetic catalysts is usually determined by X-ray diffraction (XRD) and/or X-ray photoelectron spectra (XPS). The catalytic amount of magnetic catalysts is measured by elemental analysis (EA) or inductively coupled plasma analysis (ICP). Gas adsorption is a technique that is used for investigation of

the surface area of magnetic catalysts. Fourier transform infrared spectroscopy (FT-IR) is used to monitor and confirm the functionalization of magnetic catalysts. The magnetic property is investigated utilizing the magnetic properties measurement system superconducting quantum interference device (SQUID) or vibrating sample magnetometer (VSM). Thermogravimetric analysis or thermal gravimetric analysis (TGA) is a suitable method to investigate the thermal stability of magnetic catalysts. Photoluminescence (PL) spectroscopy is used for detecting fluorescence property of magnetic catalysts.

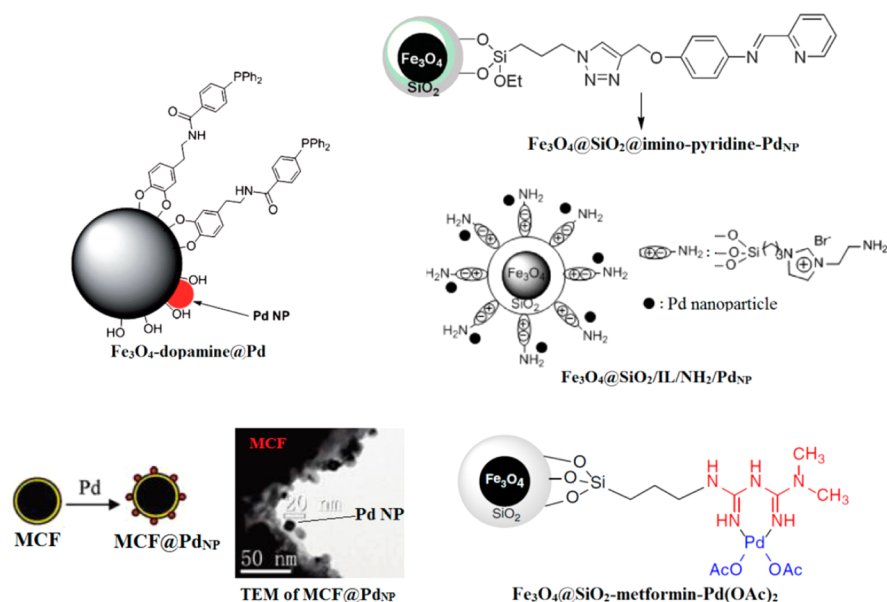
## 2. RECENT ADVANCES AND TRENDS

### 2.1. Magnetically Recyclable Nanocatalysts Based on Transition Metals

**2.1.1. C–C Coupling: Miyaura–Suzuki, Heck, Sonogashira, and Hiyama Reactions.** Cross-coupling reactions to construct C–C bonds are of significant importance in modern chemical transformations. Various catalytic systems based on transition metals as catalysts have emerged. Utilization of MNP-supported transition metal catalysts for construction of C–C bonds via Suzuki, Heck, Sonogashira, and Hiyama reactions has received considerable attention during the past few years.

The Pd-catalyzed Suzuki coupling reaction has been recognized as the most powerful strategy for constructing carbon–carbon bonds. It has been extensively utilized in the synthesis of functional materials, pharmaceuticals, and natural compounds due to its wide substrate scope, mild conditions, high yields, and readily available starting materials.<sup>114–116</sup> The Suzuki reaction probably is the most classic reaction to evaluate the catalytic activities of nanocatalysts consisting in Pd species.

Magnetic mesoporous silica spheres (MMS) currently are very popular supports, among which MCM-41 and SBA-15 are frequently used mesoporous silica materials. Fe<sub>3</sub>O<sub>4</sub>@SiO<sub>2</sub>@mSiO<sub>2</sub> with core-double-shell structure has been prepared by two-step silica-coated processes, two layers of silica shell playing the role of protection (inner shell) and offering large specific surface area (outer shell), respectively.<sup>117</sup> Fe<sub>3</sub>O<sub>4</sub>@SiO<sub>2</sub>@mSiO<sub>2</sub>-immobilized PdNPs have exhibited unprecedented catalytic activity in Suzuki reaction of phenylboronic acid



**Figure 4.** Examples for MNPs-supported Pd catalysts. Reprinted with permission from ref 125. Copyright 2012 Elsevier Ltd. Reprinted with permission from ref 127. Copyright 2011 American Chemical Society. Reprinted with permission from ref 130. Copyright 2013 Wiley-VCH Verlag GmbH & Co. Reprinted with permission from ref 137. Copyright 2012 Elsevier B.V.

with aryl halides, even aryl chloride with up to 93.77% conversion. This success is attributed to productive implantation of PdNPs on/in both of the surface and mesopore channels of attractive silica double shell. Moreover, the catalyst was conveniently recovered upon applying an external magnetic field, and it was recycled six times without any significant loss of catalytic activity.<sup>117</sup> Hollow mesoporous silica spheres (HMS) were not only useful drug carriers but also efficient catalyst carriers, owing to their low density, well-defined structures, and homogeneous spherical morphologies.<sup>113</sup> Compositions of hollow magnetic mesoporous silica spheres (HMMS)-embedded PdNPs were assembled using carboxylic polystyrene (PS) latex<sup>118</sup> or the colloidal carbon spheres of glucose<sup>119</sup> as the precursor of hollow space. PdNPs were implanted in the magnetic heteroaggregates of  $\text{Fe}_3\text{O}_4$  and mesoporous shell, and the implantation step could be carried out either before or after formation of the hollow space (Figure 3). Suzuki reactions were conducted in ethanol in the presence of  $\text{K}_2\text{CO}_3$  with 0.6–0.75 mol % HMMS–Pd as catalyst at 70–80 °C. This catalytic system was broad in substrate scope, efficient even for aryl chlorides,<sup>118</sup> and highly recyclable. The HMMS–Pd catalyst was also a competitive candidate in the hydrogenation of alkene and nitro compounds.

Recently, other magnetic nanocomposites including polymer-coated MNPs,<sup>120–124</sup> ionic liquid-modified MNPs,<sup>125</sup> sulfonated graphene(s-G)-decorated MNPs,<sup>126</sup> and magnetic  $\text{Fe}_3\text{O}_4$ @C (MFC)<sup>127</sup> were also used for stabilization of PdNPs aiming to catalyze Suzuki reactions. Song and co-workers<sup>125</sup> enriched ionic liquid-modified MNPs with amine functional groups and used this nanomaterial as support for the synthesis of  $\text{Fe}_3\text{O}_4$ @ $\text{SiO}_2$ /IL/ $\text{NH}_2$ /Pd<sub>NP</sub> catalyst (Figure 4). The catalyst exhibited excellent activity in the Suzuki reaction of phenylboronic acid with iodobenzene or bromobenzene containing a wide range of substituents using NaOH as base in mixed solvent of ethanol and water at rt. The well-dispersed magnetic nanocatalyst was magnetically separated from the reaction mixture, and its catalytic activity did not deteriorate even after several repeated applications. Sun and his

group<sup>126</sup> assembled  $\text{Fe}_3\text{O}_4$  NPs and PdNPs on s-G and successfully used this semiheterogeneous catalyst in Suzuki reaction. TEM analysis revealed that the PdNPs with a size of 4–5 nm were homogeneously distributed on the  $\text{Fe}_3\text{O}_4$ /s-G pattern. The homogeneously water or water/ethanol-dispersed catalyst was very efficient and maintained similar catalytic performance during several cycles. Diao et al.<sup>127</sup> reported the construction of a magnetically retrievable Pd nanocatalyst that was anchored on magnetic MFC nanocomposites via a precipitation–deposition method. The diameters of MCF and PdNPs were about 360 and 15 nm, respectively (Figure 4). The Suzuki reaction was initially chosen as the model reaction for evaluating the catalytic ability. The MCF@Pd<sub>NP</sub> provided yields in the range 52–100% within 1–3 h when aromatic iodides and bromides were employed in refluxed ethanol. As for challenging chlorobenzene, 95% yield was obtained within 3 h of reaction time in refluxed DMF using 0.308 mol % Pd with the assistance of a small amount of KI. The catalyst was easily handled and removed from the reaction mixture by magnetic separation owing to its good stability and the presence of  $\text{Fe}_3\text{O}_4$ . In addition, MCF@Pd<sub>NP</sub> was also efficient in Heck reactions. Comparing with other magnetic Pd nanocatalysts without phosphine ligands, MCF@Pd<sub>NP</sub> was outstanding.<sup>127</sup>

Synthesis of  $\text{MFe}_2\text{O}_4$  (M = Zn, Co) NPs-supported Pd(0) NPs through ultrasound-assisted coprecipitation in the absence of surface stabilizer or capping agent was reported.<sup>128,129</sup> The solid catalyst  $\text{ZnFe}_2\text{O}_4$ –Pd(0) displayed good performance for the Suzuki reaction; both electron-deficient and electron-rich aromatic iodides and bromides substrates provided high yields of coupling products. The magnetic property allowed one to recover the catalysts magnetically with an external magnet, and no significant loss of activity of  $\text{ZnFe}_2\text{O}_4$ –Pd(0) was detected during five successive cycles.

Phosphine-based ligands proved useful to stabilize PdNPs onto magnetic supports. With the assistance of dopamine–PPh<sub>2</sub> stabilizer that was synthesized by coupling between dopamine and (diphenylphosphino)benzoic acid, PdNPs were successfully loaded on the surface of  $\text{Fe}_3\text{O}_4$  NPs. In the process,

besides phosphine ligands, hydroxyl groups of  $\text{Fe}_3\text{O}_4$  also coordinated to Pd ion, which was depicted by the ratio Pd/dopamine-PPh<sub>2</sub> obtained from analytical data.<sup>130</sup> As suggested by the literature,<sup>131</sup> the formed PdNPs would stay neither on phosphine ligands nor hydroxyl groups but be positioned on the surface of  $\text{Fe}_3\text{O}_4$  (Figure 4), which was further confirmed by analytical data. TEM images of  $\text{Fe}_3\text{O}_4$ -dopamine@Pd showed that the average size of the heteroparticle is around 12 nm. PdNPs with a mean diameter of 2 nm were embedded in the heteroparticles. PdNPs with larger sizes were provided when naked  $\text{Fe}_3\text{O}_4$  was employed. The catalytic behavior of the  $\text{Fe}_3\text{O}_4$ -dopamine@PdNPs was demonstrated in the Suzuki reaction between phenylboronic acid and 4-substituted bromoarenes. When bromoarenes bearing electron-withdrawing groups were employed, high reactivity in terms of selectivity and conversion was found, but for the substrates bearing electron-rich groups the yields significantly decreased. Unfortunately, only 5% yield was obtained in the presence of the challenging chloride derivatives. Investigation of the recyclability of  $\text{Fe}_3\text{O}_4$ -dopamine@PdNPs was conducted by treating 4-bromoanisole with phenylboronic acid. The results showed that the catalyst kept similar catalytic performance after 10 cycles. In addition,  $\text{Fe}_3\text{O}_4$ -dopamine NPs decorated with AuNPs or RhNPs were also assembled, and their catalytic properties were evidenced in the reduction of 4-nitrophenol and hydrogenation of styrene, respectively.

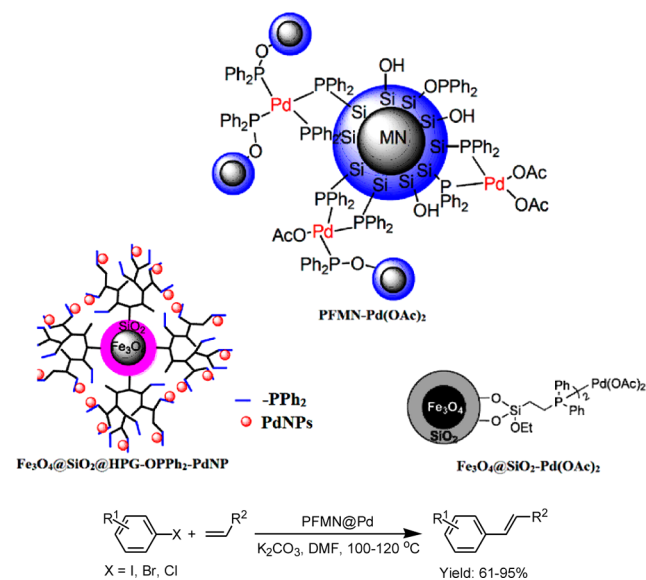
Linkers containing nitrogen were the most frequently used and powerful chelating agents and stabilizers in the synthesis of MNP-supported Pd nanocatalysts.<sup>132</sup> Luo et al.<sup>133</sup> reported the preparation of new imino-pyridine-functionalized MNPs via click chemistry and the corresponding MNP-supported PdNPs  $\text{Fe}_3\text{O}_4$ @ $\text{SiO}_2$ @imino-pyridine-Pd<sub>NP</sub> (Figure 4). This catalyst was then initially evaluated in the Suzuki reaction of 4-bromoacetophenone with phenylboronic acid. Optimized results were obtained with 0.2 mol % catalyst and use of  $\text{K}_2\text{CO}_3$  as a base in aqueous ethanol at 60 °C under air. Under these conditions, electron-withdrawing and electron-donating groups on aryl bromides were tolerated in the reaction, resulting in fairly good to excellent yields and selectivity. However, the catalytic system showed much less activity for the challenging aryl chlorides, even upon extending reaction times and increasing the catalytic amount to 1 mol %. Following the efficiency of  $\text{Fe}_3\text{O}_4$ @ $\text{SiO}_2$ @imino-pyridine-Pd<sub>NP</sub>, the recyclability of the catalyst was investigated in several volume ratios of ethanol/water (1:1, 2:1, 19:1). The amount of water in the reaction medium significantly influenced the catalyst reusability; more water caused the gradual loss of catalytic activity. The best recyclability result was that the reaction could be maintained at 95% yield after six cycles, when 19:1 of ethanol/water was employed as solvent.

MNP-supported Pd complexes provide high performance in the Suzuki reaction, as expected. The chelating fragments mentioned in the literature include triarylphosphine,<sup>134,135</sup> ( $\beta$ -oxoimino)-phosphine,<sup>50</sup> *N*-heterocyclic carbene,<sup>43,136</sup> biguanide,<sup>137</sup> polymer,<sup>138</sup> etc. As described in the literature,<sup>139</sup> the real catalytic species of Pd complexes for Suzuki coupling reactions are Pd(0) NPs that are formed via fast reduction of  $\text{Pd}^{2+}$  ions by the solvent. Complexation of metformin-modified MNPs with  $\text{Pd}(\text{OAc})_2$  was readily achieved, and  $\text{Fe}_3\text{O}_4$ @ $\text{SiO}_2$ -metformin-Pd(OAc)<sub>2</sub> (Figure 4) was further tested as a catalyst in aqueous ethanol.<sup>137</sup> Several aryl bromides containing substituent groups in broad scope were proved suitable partners for the Suzuki reaction reacting with phenylboronic acid. Upon

completion of the reaction, the catalyst was easily collected using an external magnet that was further washed and dried and then subsequently reused in another run with fresh reactants. No significant degradation in catalytic performance was observed in eight successive runs. When inactive chlorobenzene was employed, the reaction proceeded moderately with a 45% yield. In addition, atomic absorption spectroscopy did not detect Pd ions after each reaction. The existence of Pd(0) NPs was confirmed by TEM, and the authors indicated that exposure of  $\text{Fe}_3\text{O}_4$ / $\text{SiO}_2$ -Met-Pd(OAc)<sub>2</sub> to EtOH as cosolvent led to the reduction of  $\text{Pd}^{2+}$  ions to Pd(0) species.

Among these magnetic nanomaterials, NiNPs have attracted great interest in organic synthesis due to their magnetically recoverable property and catalytic activity. NiNPs with a mean diameter of 100 nm and ferromagnetic property were prepared from  $\text{NiCl}_2 \cdot 6\text{H}_2\text{O}$  with the assistance of hydroxypropylmethylcellulose (HPMC). The semiheterogeneous polymer-stabilized NiNPs showed good performance in Suzuki reaction relative to the traditional Ni catalyst, but the recyclability in terms of the number of times and yields was not detailed.<sup>140</sup>

The Heck coupling reaction has been highlighted due to its high efficacy in the synthesis of arylated olefins that are widely utilized in pharmaceuticals, agrochemicals, and cosmetics production. Phosphine-functionalized magnetic nanoparticles (PFMN) have been suggested to be most efficient supports for stabilization of catalytic Pd species in the field of magnetic nanocatalysts in the Heck reactions, because phosphine ligands promote well the immobilization of Pd onto MNPs and control their size, modality, and distribution.<sup>141</sup> Starting from PFMN, the MNPs-anchored palladium(II) complex PFMN-Pd(OAc)<sub>2</sub><sup>142</sup> (Figure 5) with a diameter of 10 nm was readily

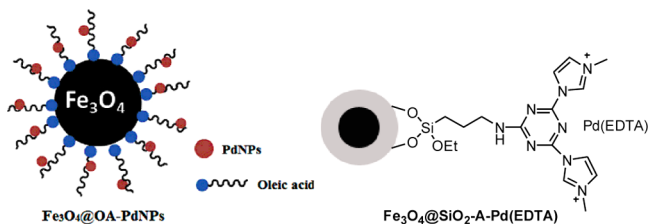


**Figure 5.** Examples for PFMN@Pd used in the Heck reaction. Reprinted with permission from ref 142. Copyright 2013 Elsevier B.V. Reprinted with permission from ref 144. Copyright 2012 Elsevier Ltd.

synthesized and tested initially in the Heck reaction of chlorobenzene with ethyl acrylate using 1 mol % Pd in the presence of  $\text{K}_2\text{CO}_3$  in DMF at 120 °C. The corresponding *trans*-arylated olefin was produced in 93% yield. Investigation of the substrate scope showed that both electron-deficient and electron-rich aryl chlorides proceeded smoothly to furnish the desired products in 88–95% yields.<sup>142</sup> This catalytic system was

remarkably efficient, even by comparison with classic homogeneous catalysts. The leaching of Pd species from the initial catalyst to the reaction medium is a very key issue for evaluation of heterogeneous catalysts. The catalyst PFMN-Pd(OAc)<sub>2</sub> was reused at least four times with sustained selectivity and activity, and ICP analysis revealed that less than 1% of Pd was released from the initial catalyst. In addition, comparative experiments were conducted in the absence of Pd-anchoring phosphine group for synthesis of PFMN-Pd(OAc)<sub>2</sub>, and the phosphine-free catalysts provided much lower yields and recyclability.<sup>142</sup> X-ray photoelectron spectroscopy (XPS) determination indicated that only Pd(II) was found in freshly prepared PFMN-supported Pd catalysts;<sup>142,143</sup> however, the actual catalytic species was zerovalent Pd.<sup>143</sup> Li et al.<sup>144</sup> synthesized hyperbranched polyglycidol (HPG) phosphine-modified MNP that was further employed as support for immobilization of PdNPs. The catalyst Fe<sub>3</sub>O<sub>4</sub>@SiO<sub>2</sub>@HPG-OPPh<sub>2</sub>-PdNP (Figure 5) showed excellent activities in the Heck reaction of a range of aryl iodides and bromides with olefins with yields up to 95%. After almost complete recovery of the catalyst using an external magnetic field, it was used for five additional cycles without loss in catalytic performance. Moreover, the satisfactory catalytic behavior of Fe<sub>3</sub>O<sub>4</sub>@SiO<sub>2</sub>@HPG-OPPh<sub>2</sub>-PdNP was also verified in the Suzuki reaction.

Apart from phosphine-based ligands, other chelating fragments were also efficiently used in Pd-catalyzed Heck reaction. The oleic acid (OA) functionalized Fe<sub>3</sub>O<sub>4</sub> NPs exhibited good immobilization capability for PdNPs; the catalytic property of the assembled nanocatalyst Fe<sub>3</sub>O<sub>4</sub>@OA-PdNPs (Figure 6) was

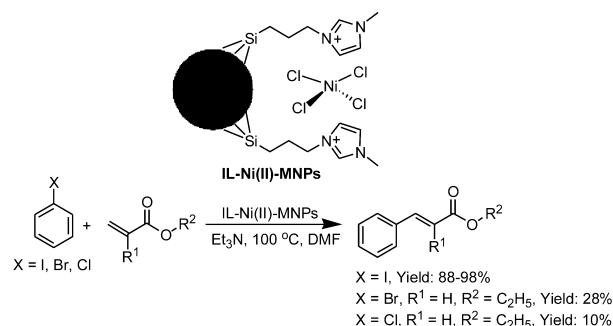


**Figure 6.** Magnetic catalysts Fe<sub>3</sub>O<sub>4</sub>@OA-PdNPs and Fe<sub>3</sub>O<sub>4</sub>@SiO<sub>2</sub>-A-Pd(EDTA) for Heck reactions.<sup>145,146</sup> Reprinted with permissions from ref 145. Copyright 2013 Elsevier.

evaluated in Heck reaction.<sup>145</sup> The cross-coupled product was produced with 98% yield using 10 mg (0.2 mol % [Pd]) Fe<sub>3</sub>O<sub>4</sub>@OA-PdNPs in DMAc at 120 °C in the presence of N(Butyl)<sub>3</sub> and TBAB in the case of bromobenzene and styrene as model substrates. This catalyst showed extraordinary functional group tolerance to aryl halide (Ar-Br, Ar-Cl); a variety of arylated olefins compounds were isolated mostly in good to excellent yields. Investigation of its recyclability indicated that Fe<sub>3</sub>O<sub>4</sub>@OA-PdNPs could be easily collected by an external magnetic attraction. Repeated use for at least four runs retained almost the same activity, with only trace amounts of leaching Pd. Khosropour et al.<sup>146</sup> demonstrated that Fe<sub>3</sub>O<sub>4</sub>@SiO<sub>2</sub> MNPs-anchored dicationic ionic liquid with a 1,3,5-triazine core can be readily constructed and further coordinate with palladium-EDTA, offering a novel MNPs-supported Pd complex (named as Fe<sub>3</sub>O<sub>4</sub>@SiO<sub>2</sub>-A-Pd(EDTA)) (Figure 6). Its catalytic performance was tested by Heck coupling reaction of various aryl halides (Ar-I, Ar-Br) with styrene derivatives bearing a wide range of substituent groups. The corresponding products were synthesized with

80–97% yields and  $1.9 \times 10^3$ – $1.4 \times 10^4$  h<sup>-1</sup> TOFs using 0.003 mol % Pd at 90 °C under silent conditions. When these reactions proceeded under ultrasound irradiation (170 W, 50 °C) instead of silent conditions the yields and TOFs were increased to 88–97% and  $5.1 \times 10^4$ – $2.5 \times 10^5$  h<sup>-1</sup>, respectively. Evaluation of recyclability and stability of Fe<sub>3</sub>O<sub>4</sub>@SiO<sub>2</sub>-A-Pd(EDTA) was conducted under ultrasound irradiation. The catalyst was magnetically removed from the reaction medium and reused for six reaction cycles without obvious decrease in catalytic activity.

Safari et al.<sup>147</sup> prepared magnetic Fe<sub>3</sub>O<sub>4</sub> NPs-supported Ni<sup>2+</sup> containing 1-methyl-3-(3-trimethoxysilylpropyl) imidazolium chloride ionic liquid (IL) catalyst by immobilizing a IL-Ni complex on the surface of MNPs and demonstrated their use as heterogeneous catalysts for the Heck reaction (Figure 7).

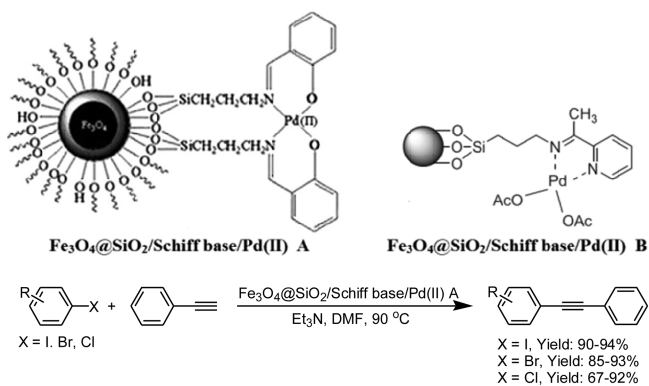


**Figure 7.** Heck reaction with IL-Ni(II)-MNPs.

Excellent yields of coupling products were provided from iodobenzene with olefins at 100 °C in 4 h. However, the coupling of aryl bromide or chloride gave significantly lower yields compared with those obtained with aryl iodides. The catalyst was simply recovered using an external magnetic yield and reused at least five times without loss of catalytic activity in the coupling of iodobenzene with ethyl acrylate. The most prominent advantage of the IL-Ni(II)-functionalized magnetic Fe<sub>3</sub>O<sub>4</sub> NPs catalyst was to avoid the use of expensive Pd.

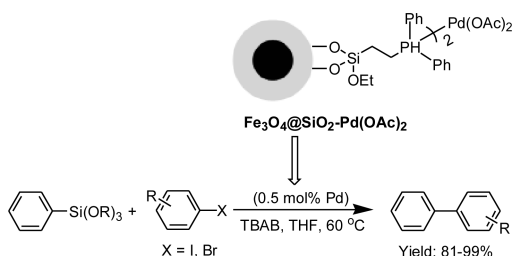
Sonogashira coupling, a common strategy for construction of a C-C bond, has been frequently reported in organic chemistry, especially for synthesis of conjugated compounds. MNPs functionalized with Schiff base ligands have potential application in catalysis due to their excellent complexation ability with metal ions. Recently, MNPs-immobilized Schiff base-Pd (II) catalysts (Figure 8) were synthesized by easy-to-operate methods.<sup>148,149</sup> Their application as efficient catalysts for Sonogashira reactions under heterogeneous phosphine-free and copper-free conditions has been described. Using Fe<sub>3</sub>O<sub>4</sub>@SiO<sub>2</sub>/Schiff base/Pd(II) catalysts, symmetric or asymmetric internal alkynes were produced from the reaction of aryl iodides, bromides, or chlorides with terminal alkynes. These catalysts were magnetically separated from the reaction mixture and recycled for several consecutive runs without appreciable loss of catalytic activity.<sup>148,149</sup>

The literature on catalytic applications of MNPs-supported catalysts is relatively underrepresented in the Hiyama reaction, which is known as a very important cross-coupling transformation of aryltrialkoxysilanes with aryl halides. The latest example of such a process was provided by Wang and co-workers,<sup>150</sup> who reported that the PFMN-immobilized Pd complex Fe<sub>3</sub>O<sub>4</sub>@SiO<sub>2</sub>-Pd(OAc)<sub>2</sub> not only worked well in the Heck reaction<sup>143</sup> but also displayed high activity in the Hiyama



**Figure 8.** Sonogashira reactions with  $\text{Fe}_3\text{O}_4@/\text{SiO}_2/\text{Schiff base}/\text{Pd}(\text{II})$  catalysts.<sup>148,149</sup> Reprinted with permission from ref 148. Copyright 2013 Elsevier B.V. Reprinted with permission from ref 149. Copyright 2010 Elsevier B.V.

reaction (Figure 9). The results of optimized investigations showed that a biaryl compound was isolated in 91% yield when



**Figure 9.** Hiyama reaction with PFMN@Pd catalyst.

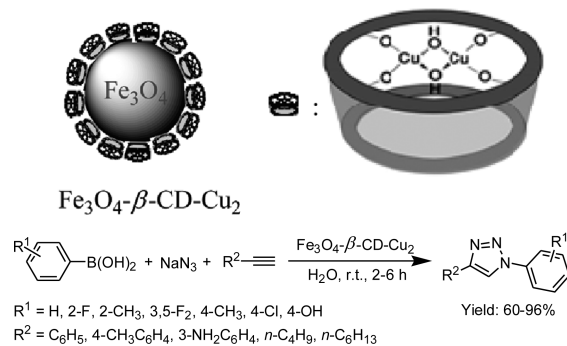
the Hiyama reaction was carried out between 4-iodoanisole and phenyltrimethoxysilane using TBAF as base in the presence of 0.5 mol % Pd in THF at 60 °C. A variety of organic halides reacted with phenyltrimethoxysilane to give the cross-coupling products in good to excellent yields. The authors did not describe the substrate scope of aryltrimethoxysilanes. The recyclability of  $\text{Fe}_3\text{O}_4@/\text{SiO}_2-\text{Pd}(\text{OAc})_2$  was also explored in the coupling of 4-iodoanisole and phenyltrimethoxysilane; the nanocatalyst was recycled at least 10 times with no detectable deactivation. MNPs-supported PdNPs consisting of  $\text{Fe}_3\text{O}_4$  NPs of 25–50 nm in diameter and PdNPs of 5 nm encaged in  $\text{Fe}_3\text{O}_4$  were easily prepared and evaluated in Hiyama reactions of a wide range of aryl bromides and aryl siloxanes.<sup>151</sup> A variety of biaryl subunits were constructed in good to excellent yields with 0.2 mol % of  $\text{Fe}_3\text{O}_4@/\text{PdNP}$  at 90 °C in aqueous solution. In addition, the nanocatalyst exhibited quite the same morphology and catalytic activity even after five cycles.

**2.1.2. Alkyne–Azide Cycloaddition.** 1,2,3-Triazoles, five-membered nitrogen heterocyclic compounds, have tremendous applications in various research fields including synthetic organic, medicinal, materials, and biological chemistry. Therefore, synthesis of 1,2,3-triazoles has been one of the hottest subjects during the past few decades. Among numerous synthetic methods, catalyzed Huisgen cycloaddition of organic azides and alkynes by Cu and Ru catalysts are the most efficient ones and have been widely used to construct the 1,2,3-triazole heterocycles selectively, forming, respectively, 1,4- and 1,5-disubstituted 1,2,3-triazoles.

Copper-catalyzed cycloaddition of alkynes and azides (CuAAC)<sup>152,153</sup> is the most efficient means to incorporate

two functional fragments, and it is undoubtedly to date the most representative example of “click” reaction.<sup>154</sup> Indeed, CuAAC holds several advantages over the thermal Huisgen version including mild reaction conditions, 100% atom economy, exclusive regioselectivity, and broad substrate scope. However, contamination with cytotoxic Cu ion is a long-standing problem that restricts the applications of CuAAC in electronics and biomedicine. To solve this problem, the use of heterogeneous CuAAC catalysts appears to be the most logical solution instead of the other methods including performing CuAAC under continuous flow conditions, chromatographic purification of crude product, or washing crude product with amine (or ammonia). For the heterogenization of CuAAC catalysts, functionalized MNPs have emerged as viable supports.

MNPs-supported Cu catalysts are divided into two sorts that are MNPs-supported Cu complexes and Cu(0) or Cu(I) NPs. MNPs-immobilized binuclear Cu(II)– $\beta$ -cyclodextrin was easily prepared by addition of copper sulfate to a the sodium hydroxide solution of  $\beta$ -cyclodextrin.<sup>155,156</sup> This magnetic catalyst of 10–20 nm in diameter showed high activity in the facile one-pot synthesis of 1,4-disubstituted 1,2,3-triazole through azido reaction/cycloaddition of arylboronic acid, sodium azide, and alkyne in water at rt in air without any additives (Figure 10). The results of investigations of substrate



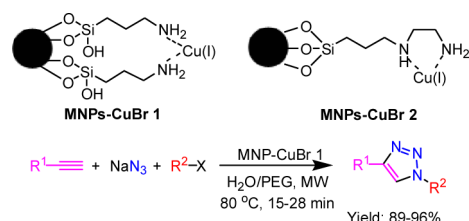
**Figure 10.** One-pot synthesis of 1,2,3-triazoles using  $\text{Fe}_3\text{O}_4-\beta\text{-CD}-\text{Cu}_2$ .<sup>155</sup> Reprinted with permission from ref 155. Copyright 2013 Royal Society of Chemistry.

scope indicated that both different substituted arylboronic acids and alkynes were successfully employed in the catalytic system providing excellent yields.  $\text{Fe}_3\text{O}_4-\beta\text{-CD}-\text{Cu}_2$  was collected by a magnet and successively reused for four reaction cycles without considerable loss in activity.

Díez-González and co-workers<sup>157</sup> prepared nonmagnetic silica flakes and silica NPs- and magnetite/silica NPs-supported copper(I)-*N*-heterocyclic carbene (NHC) catalysts. All three silica materials were used as catalysts in the CuAAC reaction of benzyl azide with phenylacetylene using 1 mol % [Cu] on water at rt and gave quantitative formation of corresponding 1,4-disubstituted 1,2,3-triazoles. The catalysts were then separated from the reaction medium by filtration or using an external magnet, and after washing and drying they were reused for a new reaction cycle. In the fifth cycle, the catalyst supported on silica NPs almost completely lost its activity; the copper-functionalized silica flakes led to moderate yields. On the other hand, the magnetite/silica NPs-supported catalyst retained high activity and selectivity even after a minimum of nine consecutive cycles. Moreover, various 1,4-disubstituted 1,2,3-

triazoles were isolated in good to excellent yields, regardless of the substituent groups on either the alkyne or the azide.

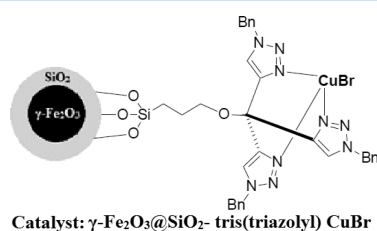
Pincer-type ligands containing two chelating positions are another valuable template for complexation of Cu cation in the synthesis of magnetically separated catalysts for CuAAC.<sup>158,159</sup> Xiong et al. synthesized 3-aminopropyltrimethoxysilane (APTS) and [3-(2-aminoethylamino)propyl]trimethoxysilane (AAPTSS)-modified MNPs that were further treated with CuBr to generate MNPs–CuBr 1 or MNPs–CuBr 2 (Figure 11).<sup>160</sup>



**Figure 11.** MNP–CuBr-catalyzed one-pot synthesis of 1,4-disubstituted 1,2,3-triazoles.

Catalytic applications of these two catalysts were evaluated in the one-pot CuAAC reaction of benzyl chloride and sodium azide with phenylacetylene in mixed reaction medium of water and PEG400 under microwave irradiation conditions. Initial results of the experiment showed that the reactions were performed smoothly using either MNPs–CuBr 1 or MNPs–CuBr 2, and the former exhibited higher activity than the later. MNPs–CuBr 1 was then applied in the investigation of substrate scope using sodium azide and different alkyl halide and alkynes as starting materials, with 1.46 mol % of [Cu]. Most of the 1,4-disubstituted 1,2,3-triazoles were isolated in good to excellent yields with 100% selectivity. The reactivity of 4-bromobutane was lower than that of either benzyl chloride or bromide. The longer chain of the aliphatic halides significantly decelerates the reaction, and disubstituted aliphatic halides such as 1,6-dibromohexane and 1,10-dibromodecane gave very low yields upon reaction with phenylacetylene. The authors indicated that the poor results of aliphatic halides with long chains and disubstituted aliphatic halides were reasonably attributed to their low dielectric constants, poor microwave absorbing properties, and generation of undesired 1,3-diynes. Benzyl bromide showed higher reactivity than benzyl chloride; various functional groups on alkynes were highly tolerated for this catalytic system. In addition, the magnetically collected catalyst MNPs–CuBr 1 was easily recovered and reused for at least seven cycles with a slight decrease of catalytic activity.<sup>160</sup>

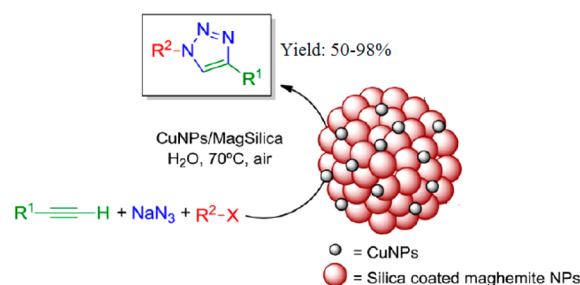
Iron oxide NP-supported tris(triazolyl) CuBr with a diameter of about 25 nm was readily prepared, and its catalytic activity was evaluated in the CuAAC reaction (Figure 12).<sup>161</sup> In initial



**Figure 12.** Click reactions catalyzed by  $\gamma$ -Fe<sub>2</sub>O<sub>3</sub>@SiO<sub>2</sub>-tris(triazolyl) CuBr.<sup>161</sup> Reprinted with permission from ref 161. Copyright 2014 Wiley-VCH Verlag GmbH & Co.

experiments this catalyst with 0.5 mol % loading perfectly promoted the CuAAC reaction of benzyl azide and phenylacetylene in water at rt. After completion of the first run, the catalyst was simply collected and separated using an external magnet from the reaction medium and used for another five catalytic cycles without significant loss of catalytic activity. The amount of leaching copper from the initial catalyst to the reaction media after the first cycle measured by ICP analysis was almost negligible. The scope of the substrates was further examined, and the CuAAC reaction procedure was successfully extended to various organic azides and alkynes and also applied to the one-pot synthesis of triazoles through the cascade reaction of benzyl bromides, alkyne, and sodium azide. Remarkably, for each substrate,  $\gamma$ -Fe<sub>2</sub>O<sub>3</sub>@SiO<sub>2</sub>-tris(triazolyl) CuBr was smoothly used for three catalytic cycles with similar catalytic efficiency or slightly decreased yields. In addition, the catalyst was used in the synthesis of allyl- and TEG-ended 27-branch dendrimers.<sup>161</sup>

MNPs-supported CuNPs have been proved to be useful to catalyze the cycloaddition of azides with alkynes.<sup>162–164</sup> Radivoy and co-workers<sup>165</sup> prepared silica-coated MNPs-supported CuNPs (CuNPs/MagSilica) by fast reduction of CuCl<sub>2</sub> using lithium sand in the presence of 4,4'-di-*tert*-butylbiphenyl. These CuNPs with a narrow size distribution and about 3.0 nm of mean diameter were found to be well dispersed on the magnetic support. CuNPs/MagSilica was used as nanocatalyst in the three-component synthesis of 1,4-disubstituted 1,2,3-triazoles using sodium azide, alkyne, and alkyl halide as reagents (Figure 13). A TOF of 0.012 s<sup>-1</sup> was



**Figure 13.** CuAAC reaction with CuNPs/MagSilica.<sup>165</sup> Reprinted with permission from ref 165. Copyright 2013 Elsevier B.V.

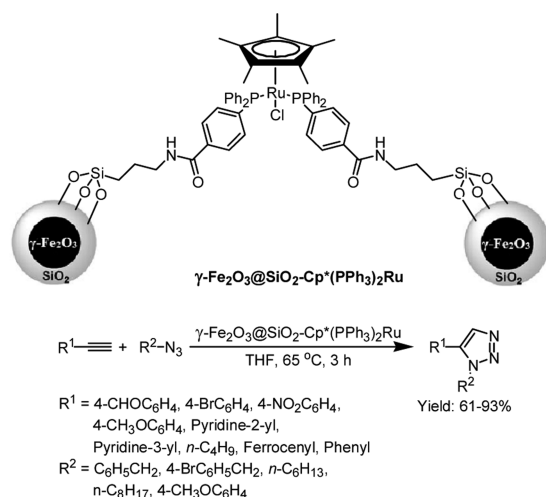
provided when sodium azide, phenylacetylene, and benzyl bromide were employed in water at 70 °C with 4.3% [Cu]. The same methodology was successfully extended to the reactions of benzyl bromide with various aryl alkynes bearing both electron-rich or electron-poor groups and aliphatic alkynes and yielded the corresponding 1,2,3-triazoles in 85–98% yields. Other alkyl azides including 4-methylbenzyl bromide, 2-nitrobenzyl bromide, 4-vinylbenzyl chloride, and *n*-nonyl iodide showed lower reactivities compared with benzyl bromide. The authors did not report the recyclability of CuNPs/MagSilica in these CuAAC reactions.

Magnetic CuFe<sub>2</sub>O<sub>4</sub> NPs consisting of catalytically active copper centers were active for the CuAAC reaction.<sup>162,166</sup> CuFe<sub>2</sub>O<sub>4</sub> was applied as catalyst in the formation of aryl azides from boronic acids under mild conditions. Then on this basis a one-pot approach was developed for the synthesis of 1,4-disubstituted 1,2,3-triazoles using alkyne, sodium azide, and boronic acids as reagents.<sup>167</sup> CuFe<sub>2</sub>O<sub>4</sub> with particle sizes in the range 10–30 nm performed well toward the cascade reaction in terms of yield, selectivity, substrate scope, and recyclability. The

strategy of multicomponent cascade reactions was repeatedly carried out in the synthesis of 1,4-disubstituted 1,2,3-triazoles in the field of MNPs-supported CuAAC reaction. This protocol made the CuAAC reaction consistent with the principles of click chemistry and green chemistry.

MNPs cores have been used as catalysts in some important reactions. A presynthesized graphene-capped  $\gamma\text{-Fe}_2\text{O}_3$  composite was evaluated in one-pot synthesis of 1,4-disubstituted-1,2,3-triazoles through CuAAC reactions of benzyl halide, sodium azide, aryl alkyne in distilled water.<sup>168</sup> A series of 1,4-disubstituted-1,2,3-triazoles was smoothly isolated with 70–93% yields. The comparison test showed that graphene-capped  $\gamma\text{-Fe}_2\text{O}_3$  composite exhibited better catalytic activity than pure  $\gamma\text{-Fe}_2\text{O}_3$ . The enhanced activity caused by the use of graphene was taken into account by its conducting properties and high migration efficiency of electrons<sup>169,170</sup> as well as the avoidance of aggregation of MNPs. In addition, the catalyst was simply collected from the final product by an external magnetic field and reused at least five times without significant loss of catalytic activity.

The  $[\text{Cp}^*\text{Ru}(\text{II})]$  complex-catalyzed cycloaddition of alkynes and azides (RuAAC)<sup>171</sup> is the most remarkable method for synthesis of 1,5-disubstituted 1,2,3-triazoles.  $\gamma\text{-Fe}_2\text{O}_3@ \text{SiO}_2\text{-Cp}^*(\text{PPh}_3)_2\text{Ru}$  was the first magnetically recyclable catalyst for RuAAC reactions (Figure 14).<sup>172</sup> The relatively uniform core–



**Figure 14.** RuAAC reaction with  $\gamma\text{-Fe}_2\text{O}_3@ \text{SiO}_2\text{-Cp}^*(\text{PPh}_3)_2\text{Ru}$ .<sup>172</sup> Reprinted with permission from ref 172. Copyright 2013 Royal Society of Chemistry.

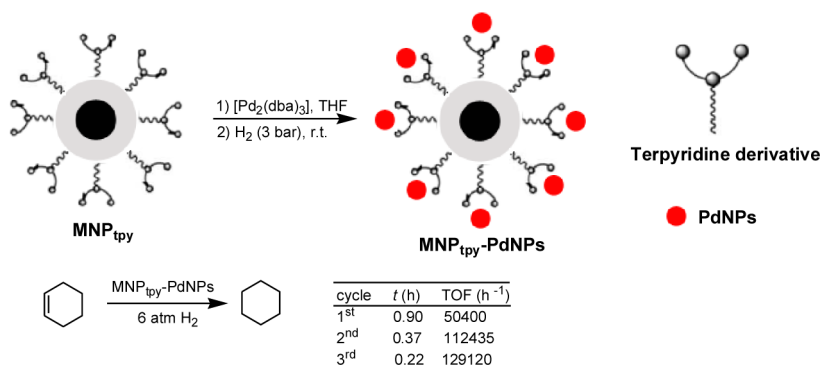
shell NPs with an average size of approximately 30 nm were prepared by immobilization of  $\text{Si}(\text{OMe})_3$ -functionalized  $\text{Cp}^*(\text{PPh}_3)_2\text{Ru}$  complex on the surface of  $\gamma\text{-Fe}_2\text{O}_3@ \text{SiO}_2$  NPs. This catalyst was initially evaluated in the cycloaddition of phenylacetylene and benzyl azide with 2 mol %  $[\text{Ru}]$  in THF at 65 °C. After 3 h, the desired 1,5-disubstituted 1,2,3-triazole was isolated in 91% yield with over 99.9% selectivity, which was revealed by both NMR and GC. After completion of the reaction, the catalyst was magnetically separated from the reaction medium and reused for the next four runs with only a slight decrease in activity and selectivity. Investigation of substrate scope showed that all involved aryl, aliphatic, and ferrocenylacetylene exhibited good reactivities under the above-mentioned conditions. Reactions of aliphatic azides containing a linear chain and benzyl azides bearing different groups proceeded smoothly; aryl azides were also suitable cycloaddition partners. However, the yield of produced 1,5-disubstituted 1,2,3-triazole was somewhat lower.

### 2.1.3. Hydrogenation of Unsaturated Compounds.

Hydrogenation of organic substrates is considered to be one of the most versatile reactions in chemistry, from pharmaceutical science to petrochemistry. Recently, in an effort to develop a more sustainable approach, magnetically retrievable nanocatalysts based on a transition metal were frequently used in the hydrogenation of various unsaturated compounds (including carbonyl compounds) and nitroaromatics. In this section, we focus on demonstrating the recent advance toward unsaturated compounds, and hydrogenation of nitroaromatics will be involved in the next section.

Pd is the most powerful catalyst for hydrogenation of olefins to saturated compounds. Li et al.<sup>173,174</sup> successfully assembled a chitosan magnetite NP-supported Pd catalyst through a facile metal adsorption–reduction procedure in one pot. This catalyst with a Pd content of 0.7 mol % was tested in the hydrogenation of olefins under 1 atm  $\text{H}_2$  in ethanol at rt. Hydrogenation reached completion within 30–60 min. Moreover, the catalyst showed a good recyclability due to strong stabilization of Pd species by the amine groups of chitosan.

Reiser et al. deposited a series of PdNPs with diameters ranging from 2.7 to 30.4 nm onto the surface of  $\text{Co}@ \text{C}$  NPs using  $\text{Pd}_2(\text{dba})_3\cdot\text{CHCl}_3$  as precursor under microwave irradiation.<sup>175</sup> A trend to smaller PdNPs as well as an increased dispersion by decreasing the Pd content in the nanocomposite was observed. The catalytic test for hydrogenation of *trans*-stilbene showed an obvious trend of increasing activity with decreasing Pd NPs sizes, and the smallest PdNPs (2.7 nm) provided the highest TOF value ( $11\,095\text{ h}^{-1}$ ), which was at



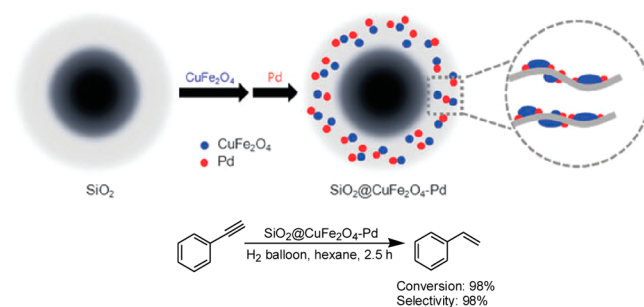
**Figure 15.** Hydrogenation of cyclohexene with  $\text{MNP}_{\text{tpy}}\text{-PdNPs}$ .

least 5 times more than other PdNPs prepared in this report.<sup>175</sup> However, obvious loss of activity was detected upon the recycling process. In addition, in order to achieve high catalytic activity, a larger amount of Co@C NPs support is needed because of the necessity of low palladium loading onto the support. Introduction of stabilizing imidazolium ILs on the surface of Co@C NPs brought a high loading of PdNPs and remarkable recyclability.<sup>176</sup> Magnetic Co@C-IL-immobilized PdNPs with a diameter of 5–15 nm and 34 wt % of Pd content provided a TOF of 50 h<sup>-1</sup> in the hydrogenation of *trans*-stilbene. In this case, 100% conversion was measured in each reaction cycle of the first 12 runs, and simple magnetic separation of catalyst was successfully carried out in the recycling test. It is apparent that the size of catalytic NPs and stabilizers significantly influences the catalytic activity and recyclability of MNP-supported NPs, respectively.

Terpyridine-functionalized Fe<sub>3</sub>O<sub>4</sub>@SiO<sub>2</sub> MNPs (named as MNP<sub>tpy</sub>-PdNPs) were readily prepared and applied as efficient stabilizers to anchor PdNPs that were formed by direct decomposition of [Pd<sub>2</sub>(dba)<sub>3</sub>] on the surface of MNPs (Figure 15).<sup>177</sup> In the preliminary experiments, well-dispersed and uniform PdNPs of about 2.5 nm average size with 180 or 90 ppm Pd content were employed in the hydrogenation of cyclohexene at 75 °C under 6 atm of H<sub>2</sub>. An initial TOF of 50 400 h<sup>-1</sup>, expressed as moles of the substrate transformed per mole of surface Pd atoms per hour, was observed in the first cycle. The TOF obtained in the second cycle was twice that of the first reaction, and an increase was also found from the second run to the third one.<sup>177</sup> This suggests that with the remaining Pd(II) species of the initial catalyst more and more Pd(0) species, the actual catalytic species were gradually formed during the reaction. In order to obtain a significantly high TOF, preactivation of the catalyst was needed in the first cycle; otherwise, the value of TOF decreased to 26 890 h<sup>-1</sup>. Amine-functionalized MNPs-supported PdNPs (named MNP<sub>amine</sub>-PdNPs) were similarly synthesized and compared with MNP<sub>tpy</sub>-PdNPs. MNP<sub>amine</sub>-PdNPs afforded a TOF value of 153 770 h<sup>-1</sup> in the first cycle, and this higher TOF could be attributed to the small mean size (1.8 ± 0.4 nm) of PdNPs.<sup>177</sup> However, a slight decrease in catalytic activity was detected in the second and third reaction cycles; therefore, it appears that the terpyridine ligand is a better stabilizer than the amine ligand; agglomeration of nanoparticles caused decreased activity in the case of MNP<sub>amine</sub>-PdNPs. The morphology and size of the MNP<sub>tpy</sub>-PdNPs did not change in the successive reaction cycles, and ICP analysis revealed that the amount of leaching Pd was negligible (<0.01 ppm). Furthermore, the behavior of the PdNPs as a heterogeneous catalyst was confirmed by a poisoning test with an excess of Hg.<sup>177</sup>

Selective hydrogenation of alkynes to alkenes is delicate because of the further hydrogenation of alkenes to saturated compounds occurring at the same time as a side reaction. Hur et al. reported that CuFe<sub>2</sub>O<sub>4</sub> and PdNPs were sequentially encapsulated in mesoporous silica microsphere to produce magnetic SiO<sub>2</sub>@CuFe<sub>2</sub>O<sub>4</sub>-Pd.<sup>178</sup> For the sake of comparison, other PdNPs such as SiO<sub>2</sub>@Pd, SiO<sub>2</sub>@CoFe<sub>2</sub>O<sub>4</sub>-Pd, and SiO<sub>2</sub>@Fe<sub>3</sub>O<sub>4</sub>-Pd were assembled in the same method as SiO<sub>2</sub>@CuFe<sub>2</sub>O<sub>4</sub>-Pd. Their efficacies for selective hydrogenation of phenylacetylene were tested under balloon pressure of H<sub>2</sub>. The results showed that the nature of solvent deeply affected the reaction rate instead of selectivity. A 0.43 mol% of SiO<sub>2</sub>@CuFe<sub>2</sub>O<sub>4</sub>-Pd achieved high conversion of over 98% in 2.5 h without any additives, with over 98% selectivity toward

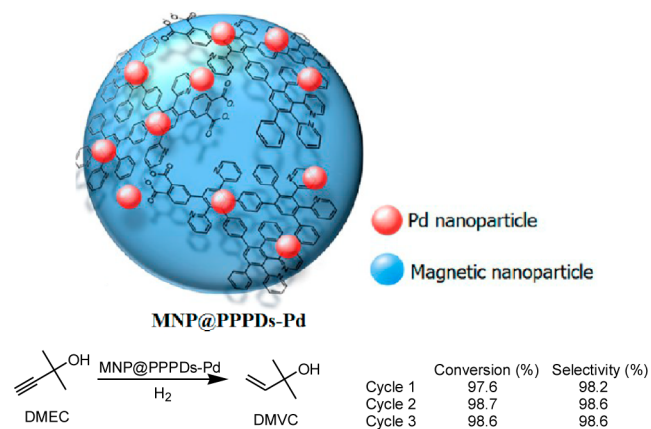
styrene (Figure 16). Under the same conditions, SiO<sub>2</sub>@CoFe<sub>2</sub>O<sub>4</sub>-Pd and SiO<sub>2</sub>@Fe<sub>3</sub>O<sub>4</sub>-Pd provided 18% and 60%



**Figure 16.** Selective hydrogenation of alkynes to alkenes.<sup>178</sup> Reprinted with permission from ref 178. Copyright 2012 Royal Society of Chemistry.

conversion with 99% and 87% selectivity, respectively. SiO<sub>2</sub>@Pd was almost inactive for hydrogenation. Use of the commercial Lindlar catalyst led to ordinary conversion (82%) and selectivity (92%), indicating that SiO<sub>2</sub>@CuFe<sub>2</sub>O<sub>4</sub>-Pd was more selective than the commercial alternative. SiO<sub>2</sub>@CuFe<sub>2</sub>O<sub>4</sub>-Pd also afforded excellent performance for phenylacetylene in terms of conversion and selectivity. The enhanced activity and selectivity of SiO<sub>2</sub>@CuFe<sub>2</sub>O<sub>4</sub>-Pd were attributed to the existence of Pd and CuFe<sub>2</sub>O<sub>4</sub> NPs and the facile coordination between Cu ions and the triple bond.<sup>178</sup>

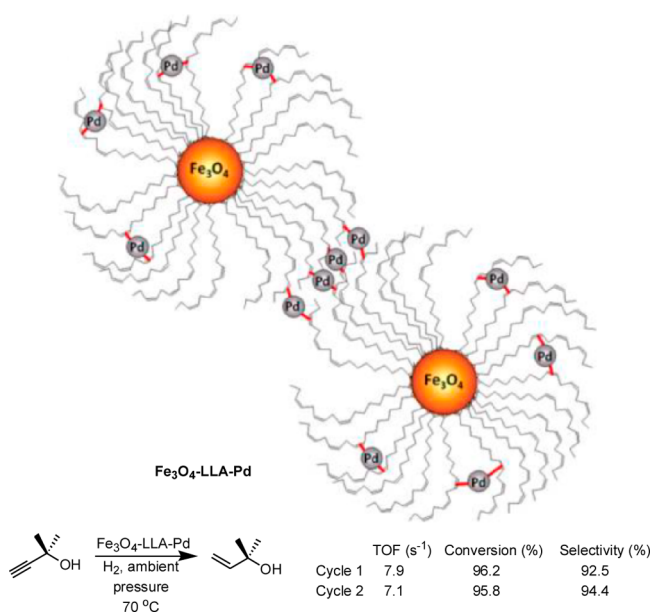
Reduction of alkynol to enol was a popular model reaction of selective hydrogenation.<sup>179</sup> The divergent synthesis of polyphenylenepyridyl dendrons (PPPDs) with anhydride, *o*-dicarboxyl, and *o*-dicarboxylate focal groups was developed by the groups of Bronstein and Shifrina.<sup>180</sup> PdNPs embedded in the second-generation PPPDs-coated magnetic nanocomposites showed high performance in selective hydrogenation of dimethylethynylcarbinol (DMEC) to dimethylvinylcarbinol (DMVC) (Figure 17). DMVC was produced in 98% yield,



**Figure 17.** Selective hydrogenation of DMEC to DMVC catalyzed by MNP@PPPDs-Pd.<sup>180</sup> Reprinted with permission from ref 180. Copyright 2013 American Chemical Society.

with over 98% selectivity, even in the third cycle. The comparison with commercial Lindlar catalysts demonstrated that the reported catalyst MNP@PPPDs-Pd displayed a more attractive activity, selectivity, and recyclability in the selective hydrogenation of DMEC. Bronstein et al.<sup>181</sup> modified original Fe<sub>3</sub>O<sub>4</sub> with a series of acids bearing double bonds or pyridine

fragments. These NPs were further used as a platform to immobilize Pd complexes and to produce magnetically separable Pd catalysts. These catalysts were evaluated in selective hydrogenation of DMEC to DMVC. The best performance in terms of TOFs ( $7.9 \text{ s}^{-1}$ ) and selectivity toward DMVC (92.5%) was achieved upon using PdCl<sub>2</sub> supported on linolenic (LLA)-coated Fe<sub>3</sub>O<sub>4</sub> nanoparticles (named Fe<sub>3</sub>O<sub>4</sub>-LLA-Pd). In the recyclability test, Fe<sub>3</sub>O<sub>4</sub>-LLA-Pd showed an excellent capability to be magnetically collected, a slightly increased selectivity, and only a marginally decreased TOF value in the second reaction cycle. The authors believed that the real catalytic species for the hydrogenation were Pd(II) complexes rather than Pd(0) NPs (Figure 18).



**Figure 18.** Selective hydrogenation of DMEC to DMVC catalyzed by Fe<sub>3</sub>O<sub>4</sub>-LLA-Pd.<sup>181</sup> Reprinted with permission from ref 181. Copyright 2012 American Chemical Society.

Besides Pd, other noble transition metal catalysts including Pt,<sup>182</sup> Ru,<sup>183</sup> bimetallic Ag/Ni,<sup>110</sup> Ir,<sup>184</sup> and Rh<sup>185,186</sup> were shown to have a wide range of catalytic applications in the hydrogenation of unsaturated compounds. MNPs-supported RuNPs were readily prepared through tandem generation of Fe<sub>3</sub>O<sub>4</sub>@SiO<sub>2</sub> and immobilization of RuNPs in one pot. Hydrogenation of acetophenone was successfully achieved with over 99% yield using KOH as base in the presence of a catalytic amount of Fe<sub>3</sub>O<sub>4</sub>@SiO<sub>2</sub>-RuNPs at 100 °C in isopropanol under MW irradiation within 30 min. The scope of carbonyl compounds was then investigated under optimal conditions (Figure 19).<sup>183</sup> Acetophenones containing a wide range of substituents were transformed to the corresponding alcohols with high conversion and selectivity within 30–45 min. Fe<sub>3</sub>O<sub>4</sub>@SiO<sub>2</sub>-RuNPs was magnetically collected and reused at least three times without a decrease of activity. Moreover, only 0.08% of Ru leached from initial catalyst after three reaction cycles. Peng's group<sup>110</sup> found that magnetic core-shell Ag@Ni NPs with a diameter of 14.9 nm were outstanding catalysts for hydrogenation of carbonyl compounds and nitroaromatics under relatively mild conditions. This nanocatalyst allowed easy magnetic separation and excellent recyclability.



**Figure 19.** Hydrogenation of acetophenone and its derivatives with Fe<sub>3</sub>O<sub>4</sub>@SiO<sub>2</sub>-RuNPs.

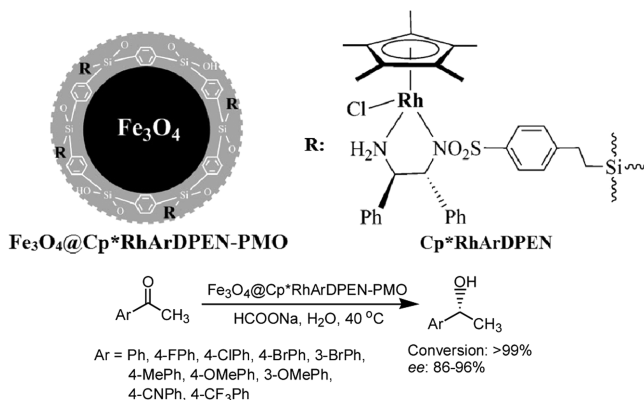
In practical applications, the cost, toxicity, and potential depletion of noble metals have restricted their utilization as catalysts. Thus, in this context FeNPs have emerged as viable alternatives.<sup>187</sup> Breit et al.<sup>188</sup> demonstrated that chemically derived graphene (CDG)-supported FeNPs were a highly efficient catalyst for hydrogenation of various olefins and alkynes. This catalyst was easily recovered using an external magnetic field and reused without any loss in activity. Moores et al.<sup>189</sup> synthesized stabilizer-free iron@iron oxide core-shell NPs (Fe CSNPs) and pioneered their catalytic application in the hydrogenation of alkynes and olefins. The robust nanocatalyst with an average core diameter of  $44 \pm 8.3$  nm and a shell thickness of  $6 \pm 2$  nm catalyzed the hydrogenation of various substrates in ethanol under 40 bar H<sub>2</sub> at 80 °C in the presence of 5 mol % Pd. Within 24 h, styrene was quantitatively converted to ethylbenzene, and 1-decene and 2-norbornene afforded 91% and 96% of hydrogenation yields, respectively. When 1-decyne was employed, decane was produced in 82% yield, meanwhile the incomplete hydrogenation compound 1-decene was isolated in 6% yield.<sup>189</sup> However, Fe CSNPs did not exhibit catalytic activity for carbonyl derivatives. The proposed alkene hydrogenation mechanism involved zerovalent FeNPs core as the real catalytic species. The iron oxide shell provided a substrate access to the surface of the core; the magnetic property was provided by both the shell and the core. Investigation of the recyclability proved that the Fe CSNPs maintained the capability of promoting quantitative transformation of styrene to ethylbenzene in eight successive cycles.<sup>189</sup>

Asymmetric transfer hydrogenation is an important branch of hydrogenation. Recent advances of asymmetric hydrogenation in the field of magnetic catalysis mainly focused on asymmetric hydrogenation of aromatic ketones,<sup>190,191</sup> 2-methylquinoline,<sup>192</sup> and *o*-methylanisole.<sup>193</sup>

CuFe<sub>2</sub>O<sub>4</sub> NPs embedded in mesoporous silica KIT-6 were designed and used as catalyst in the asymmetric hydrogenation of aryl ketone.<sup>191</sup> In the synthetic process, the aggregation problem was solved by an ingenious predrying treatment between the impregnation and the calcination procedures. The desired alcohol product (*S*)-1-phenylethanol was synthesized with 93% ee and 93% yield when the reaction was carried out with 2 mol % KIT-6-supported CuFe<sub>2</sub>O<sub>4</sub> using 0.5 mol % (*S*)-Xyl-Phos as the chiral modifier and PMHS as the reductant in the presence of *t*-BuONa and *t*-BuOH. This catalyst also showed easy recoverability and was utilized in the next reaction cycle after renewing activation under a nitrogen flow overnight at 120 °C.

Transfer hydrogenation reaction, a subsection of hydrogenation, is presently receiving increasing attention. Organorhodium-functionalized MNPs consisting of chiral 4-

((trimethoxysilyl)ethyl)phenylsulfonyl-1,2-diphenylethylene-diamine, 1,4-bis(triethoxysilyl)benzene, Cp<sup>\*</sup>Rh fragment, and Fe<sub>3</sub>O<sub>4</sub> NPs were designed and synthesized.<sup>194</sup> The catalytic behavior of the presented catalyst Fe<sub>3</sub>O<sub>4</sub>@Cp<sup>\*</sup>RhArDPEN-PMO was measured by asymmetric transfer hydrogenation of aromatic ketones (Figure 20). Reactions were conducted over 1



**Figure 20.** Asymmetric transfer hydrogenation reactions catalyzed by Fe<sub>3</sub>O<sub>4</sub>@Cp<sup>\*</sup>RhArDPEN-PMO.<sup>194</sup> Reprinted with permission from ref 194. Copyright 2014 Wiley-VCH Verlag GmbH & Co.

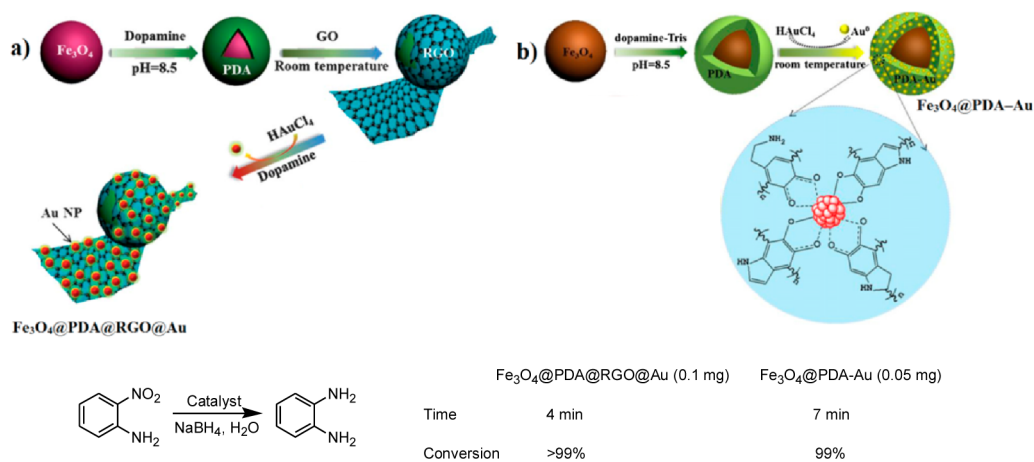
mol % [Rh] in the presence of 50 equiv of HCOONa in aqueous medium, providing the corresponding (*S*) ethanol with quantitative conversion and high enantioselectivity (up to 96% ee). Taking acetophenone as an example, a compared investigation showed that Fe<sub>3</sub>O<sub>4</sub>@Cp<sup>\*</sup>RhArDPEN-PMO provided a higher conversion than its homogeneous counterpart and comparable enantioselectivity.<sup>194</sup> The authors indicated that the high efficiency was attributed to the high hydrophobicity and the confined nature of the catalyst. In addition, after completion of the reaction, Fe<sub>3</sub>O<sub>4</sub>@Cp<sup>\*</sup>RhArDPEN-PMO was easily separable using an external magnetic field and recycled for at least 10 runs without significant loss in activity toward conversion and enantioselectivity.<sup>194</sup>

**2.1.4. Reduction of Nitroaromatics.** Functionalized anilines are key intermediates that are frequently used in the synthesis of pharmaceuticals, dyes, pigments, and pesticides, and reduction of nitroaromatics is the most general strategy yielding anilines. In order to achieve this transformation,

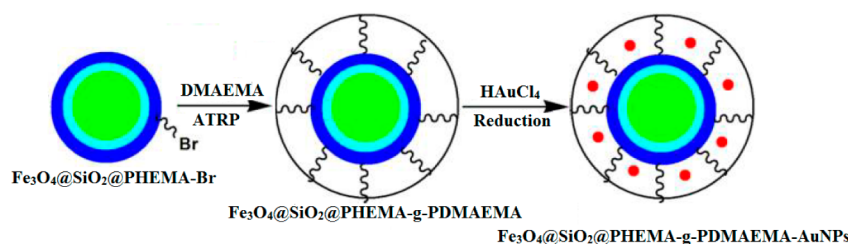
various nanomaterials consisting of transition metals were recently designed and applied as catalysts. Reduction of nitroaromatics (especially for 4-nitrophenol that is the most refractory pollutants) probably is the most popular model reaction for evaluation of the catalytic application of magnetically recoverable catalysts.<sup>195,196</sup> During 2013 only, a variety of MNPs-supported Au, Pd, Ag, Pt, Ni, Fe, and Co catalysts for reduction of aromatic nitro were reported.

UV-vis spectroscopy is usually utilized to monitor the kinetics of nitroaromatic reduction. The reaction time of completed conversion is easily observed, and the linear relationships between ln(*C<sub>t</sub>/C<sub>0</sub>*) and reaction time (the rate constant *k*) are further calculated.

Cai's group synthesized AuNPs supported on graphene-encapsulated magnetic microspheres (named Fe<sub>3</sub>O<sub>4</sub>@PDA@RGO@Au),<sup>66</sup> magnetic yolk-shell microspheres-immobilized AuNPs (SiO<sub>2</sub>@Fe<sub>3</sub>O<sub>4</sub>/C@Au),<sup>111</sup> and AuNPs embedded in polydopamine-coated magnetic microspheres (Fe<sub>3</sub>O<sub>4</sub>@PDA-Au).<sup>197</sup> All three kinds of AuNPs were applied to catalyze nitroaromatic reduction. Synthesis of Fe<sub>3</sub>O<sub>4</sub>@PDA@RGO@Au is shown in Figure 21a.<sup>66</sup> As-prepared polydopamine (PDA)-coated Fe<sub>3</sub>O<sub>4</sub> was treated with graphene oxide (GO), generating graphene oxide (RGO)-encapsulated Fe<sub>3</sub>O<sub>4</sub>@PDA that was further used as a platform to embed AuNPs. The catalytic performance of Fe<sub>3</sub>O<sub>4</sub>@PDA@RGO@Au was tested in *o*-nitroaniline reduction using a fresh NaBH<sub>4</sub> aqueous solution as reductant (Figure 21). Monitoring data of the reaction progress by UV-vis spectroscopy showed that quantitative transformation was achieved within 4 min. The catalyst was simply collected using an external magnet and reused for 10 runs, maintaining excellent conversion with increasing reaction time, which was related to the leaching of Au in each cycle. Unfortunately, about 30% of Au leached from the initial catalyst after 10 reaction runs. The Au content on Fe<sub>3</sub>O<sub>4</sub>@PDA-Au without RGO was about 4.3 wt %, which was much lower than that on Fe<sub>3</sub>O<sub>4</sub>@PDA@RGO@Au (13.58 wt %).<sup>197</sup> Fe<sub>3</sub>O<sub>4</sub>@PDA-Au led to complete transformation of *o*-nitroaniline to diaminoaniline in 7 min, and catalysis was extended to the reduction of other nitroaromatic analogues with excellent conversion within 5–120 min. A vibrating sample magnetometer experiment revealed that Fe<sub>3</sub>O<sub>4</sub>@PDA-Au showed a magnetization of 39.6 emu g<sup>-1</sup>, which allowed easy removal by an external magnetic field. Fe<sub>3</sub>O<sub>4</sub>@PDA-Au



**Figure 21.** Reduction of *o*-nitroaniline catalyzed by Fe<sub>3</sub>O<sub>4</sub>@PDA@RGO@Au<sup>66</sup> or Fe<sub>3</sub>O<sub>4</sub>@PDA-Au.<sup>197</sup> Reprinted with permission from ref 66. Copyright 2012 Royal Society of Chemistry. Reprinted with permission from ref 197. Copyright 2013 Elsevier B.V.



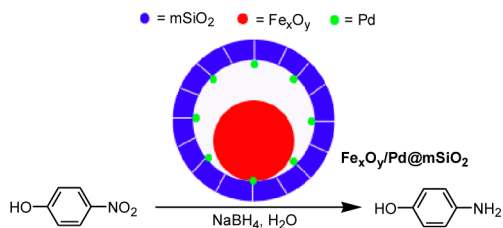
**Figure 22.** Synthetic route to  $\text{Fe}_3\text{O}_4@\text{SiO}_2@\text{PHEMA-g-PDMAEMA-AuNPs}$ .<sup>202</sup> Reprinted with permission from ref 202. Copyright 2013 American Chemical Society.

was repeatedly used for at least 8 cycles, affording similar conversion. The leaching amount of Au was 17% after 8 runs.

Polymer-coated MNPs were also popular supports in the fabrication of magnetically separated nanocatalysts consisting of AuNPs for nitroaromatic reduction. These polymers included polypeptide,<sup>198</sup> polyethylenimine,<sup>199</sup> polydopamine,<sup>197,200</sup> cellulose,<sup>201</sup> and copolymers.<sup>202–204</sup> Bromide-functionalized poly(*N,N'*-methylenebis(acrylamide)-*co*-2-hydroxyethyl methacrylate)-coated  $\text{Fe}_3\text{O}_4@\text{SiO}_2$  microspheres (named  $\text{Fe}_3\text{O}_4@\text{SiO}_2@\text{PHEMA-Br}$ ) reacted with poly(2-dimethylaminoethyl methacrylate) (PDMAEMA) brush to generate a copolymer-modified nanomaterial. AuNPs were then readily encapsulated in the PDMAEMA brush of the nanomaterial through in situ reduction (Figure 22). This hybrid consisting of AuNPs of 3.7 nm size with a narrow polydispersity promoted reduction of 4-nitrophenol to 4-aminophenol quantitatively within 15 min at rt with a rate contrast  $k$  of  $4.5 \times 10^{-3} \text{ s}^{-1}$ . The magnetic character of this system allowed recovery and six times use without significant loss of catalytic activity.<sup>202</sup>

Reduction of nitroaromatics such as 4-nitroaniline and 1,3-dinitrobenzene has been highly efficiently catalyzed by PdNPs supported on various materials including  $\text{NiFe}_2\text{O}_4$ ,<sup>205</sup>  $\text{Fe}_3\text{O}_4$ ,<sup>206,207</sup>  $\text{BaFe}_{12}\text{O}_{19}$ , and  $\text{SrFe}_{12}\text{O}_{19}$ .<sup>208</sup> Pd– $\text{CoFe}_2\text{O}_4$ –graphene composite nanosheets<sup>209</sup> and  $\text{CoFe}_2\text{O}_4$ –polypyrrole–Pd nanofibers<sup>210</sup> with diameters of PdNPs in range of 2–10 and 2–6 nm, respectively, prepared by Wang's group, catalyzed the quantitative reduction of 4-nitrophenol to 4-aminophenol within 7 min. The rate constants  $k$  were  $11.0 \times 10^{-3}$  and  $13.2 \times 10^{-3} \text{ s}^{-1}$  for the first reaction cycles, respectively. The high catalytic activities were attributed to a synergistic effect between PdNPs and  $\text{CoFe}_2\text{O}_4$ –graphene (or  $\text{CoFe}_2\text{O}_4$ –polypyrrole). Unfortunately, a decrease of catalytic activity was observed in the successive reaction cycles due to Pd leaching and catalyst poisoning.

A strategy was proposed to assemble yolk–shell microspheres consisting of a movable silica core, a mesoporous  $\text{SiO}_2$  shell, and PdNPs embedded on the surface of the core.<sup>112</sup> In this material (named  $\text{Fe}_x\text{O}_y/\text{Pd@mSiO}_2$ ) the  $\text{Fe}_x\text{O}_y$  core endowed the nature of superparamagnetism; the outer mesoporous  $\text{SiO}_2$  shell not only protected the core from aggregation and outside harsh conditions but also afforded access for the starting materials toward catalytic applications (Figure 23). For comparison,  $\text{Fe}_3\text{O}_4@\text{C}/\text{Pd}$  composites were also prepared. Both  $\text{Fe}_x\text{O}_y/\text{Pd@mSiO}_2$  and  $\text{Fe}_3\text{O}_4@\text{C}/\text{Pd}$  were evaluated in the reduction of 4-nitrophenol using  $\text{NaBH}_4$  as reducing agent. With the same Pd loading,  $\text{Fe}_3\text{O}_4@\text{C}/\text{Pd}$  led to a higher  $k$  value than that of  $\text{Fe}_x\text{O}_y/\text{Pd@mSiO}_2$ . The result was reasonably attributed to direct exposure of the  $\text{Fe}_3\text{O}_4@\text{C}$  surface to the reaction medium and smaller size of PdNPs of  $\text{Fe}_3\text{O}_4@\text{C}/\text{Pd}$  (10.2 versus 15.6 nm). In addition both catalysts were magnetically separated and reused for at least 10 cycles



**Figure 23.** Reduction of 4-nitrophenol catalyzed by  $\text{Fe}_x\text{O}_y/\text{Pd@mSiO}_2$ .

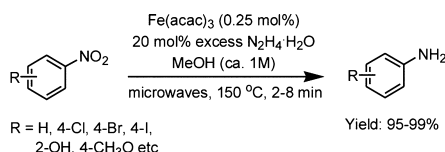
and maintained 100% conversion. However,  $\text{Fe}_x\text{O}_y/\text{Pd@mSiO}_2$  showed a much higher stability than  $\text{Fe}_3\text{O}_4@\text{C}/\text{Pd}$  upon ultrasonic treatment in aqueous solution. Thus, loading NPs on the inner surface of capsules significantly prevented their leaching from the support. In this case, the high stability of  $\text{Fe}_x\text{O}_y/\text{Pd@mSiO}_2$  also benefited from the larger size of PdNPs compared to the mesopores of  $\text{mSiO}_2$  (15.6 versus 2.6 nm).<sup>112</sup>

The layer-by-layer synthesis of double-shell  $\text{Fe}_3\text{O}_4@\text{TiO}_2/\text{Au@Pd@TiO}_2$  microsphere toward the reduction nitroaromatic involved 5 nm size AuNPs and PdNPs.<sup>211,212</sup> This nanomaterial catalyzed quantitative reduction of 4-nitrophenol to 4-aminophenol by  $\text{NaBH}_4$  at rt in 4 min with a TOF value of  $891 \text{ h}^{-1}$ . The calculated rate constant  $k$  value was  $17.7 \times 10^{-3} \text{ s}^{-1}$ , which indicated that  $\text{Fe}_3\text{O}_4@\text{TiO}_2/\text{Au@Pd@TiO}_2$  was a better catalyst than most other  $\text{TiO}_2$ -supported catalysts. This catalyst exhibited remarkable recyclability that could keep with a similar catalytic performance for more than 20 runs.<sup>211,212</sup>

Almost all common stabilizers have been employed in the synthesis of magnetic AgNPs that were competitive candidates in the reduction of nitroaromatics. These magnetically recoverable Ag nanocatalysts included  $\text{Fe}_3\text{O}_4@\text{SiO}_2\text{-Ag}$ ,<sup>213</sup> AgNPs-decorated copolymer-coated MNPs,<sup>214</sup> AgNPs supported on  $\text{Fe}_2\text{O}_3$ -carbons,<sup>215,216</sup> and iron oxide MNPs-supported AgNPs without stabilizer.<sup>217</sup> For instance, Wang et al.<sup>214</sup> reported the preparation of AgNPs loaded on a low-cost magnetic attapulgite nanocomposite grafted cross-linked copolymer (CPSA@MATP) through the adsorption of  $\text{Ag}^+$  with CPSA@MATP and reduction. This CPSA@MATP/AgNPs catalyst system bearing AgNPs with a mean diameter of 20–30 nm was successfully employed in the reduction of 4-nitrophenol, and the reaction was completed within 6 min with a constant  $k$  value of  $17.7 \times 10^{-3} \text{ s}^{-1}$ . The catalyst was simply collected with an external magnet and reused for at least three reaction cycles without a decrease in catalytic performance.

In situ-produced  $\text{Fe}_3\text{O}_4$  NPs from a Fe precursor using hydrazine hydrate as the reducing agent catalyzed the reduction of nitroarenes.<sup>218</sup> The optimized investigation revealed that quantitative transformation was achieved using 20% excess hydrazine hydrate as reducing agent in the presence of 0.25 mol % of  $\text{Fe}(\text{acac})_3$  in 2 min under microwave conditions. Other Fe

precursor such as  $\text{FeCl}_2 \cdot 4\text{H}_2\text{O}$ ,  $\text{FeCl}_3 \cdot 6\text{H}_2\text{O}$ , and  $\text{Fe}(\text{OAc})_2$  also provided full conversion in 2 min, but neither commercially available  $\text{Fe}_3\text{O}_4$  nor zerovalent Fe power promoted the reduction under the above-mentioned conditions. After the reaction cycle, the collected  $\text{Fe}_3\text{O}_4$  was repeatedly used for several runs without loss of activity. Reactions of 20 nitroarenes containing a broad scope of substituent groups proceeded smoothly, and the corresponding anilines were obtained with >95% yields within a few minutes under optimized conditions (Figure 24). This attractive



**Figure 24.** Catalytic reduction of nitroarenes to anilines with hydrazine hydrate using  $\text{Fe}_3\text{O}_4$  NPs generated in situ.

catalytic system was successfully extended to the reduction of aliphatic nitro compounds and azides.<sup>219</sup> As-prepared  $\text{Fe}_3\text{O}_4$  deposited on graphene oxide (GO) sheets was shown to be a highly efficient catalyst for the reduction of nitroarenes with 3.6 equiv of hydrazine hydrate as reducing agent in refluxed ethanol.<sup>220</sup>

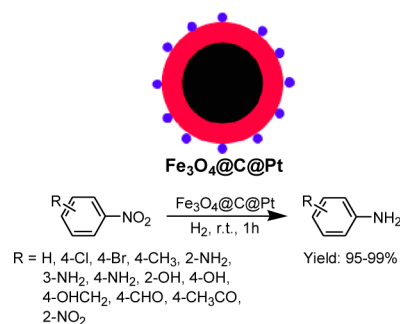
In the synthesis of magnetically recoverable catalysts for the reduction of nitroaromatics, a two-dimensional carbon nanostructure RGO was found to be a versatile support.<sup>109</sup>  $\text{Fe}_x\text{Co}_{100-x}$  NPs loaded on the surface of RGO sheets was prepared through a coreduction process.<sup>221</sup> Three kinds of RGO/ $\text{Fe}_x\text{Co}_{100-x}$  hybrid with different Fe/Co molar ratio were tested as catalysts in the reduction of 4-nitrophenol using  $\text{NaBH}_4$  as reductant, and RGO/ $\text{Fe}_{25}\text{Co}_{75}$  afforded the highest catalytic rate (full conversion was achieved within 8 min), the largest constant  $k$  value ( $9.6 \times 10^{-3} \text{ s}^{-1}$ ), and the largest TOF value ( $2.9 \times 10^{16} \text{ molecules g}^{-1} \text{ s}^{-1}$ ) compared to RGO/ $\text{Fe}_{75}\text{Co}_{25}$  and RGO/ $\text{Fe}_{50}\text{Co}_{50}$ . In addition, RGO/ $\text{Fe}_{25}\text{Co}_{75}$  was reused at least six times with only a slight decrease of activity. The authors indicated that the high efficiency of RGO in the reduction of 4-nitrophenol was attributable to the high adsorption capability of RGO toward 4-nitrophenol via  $\pi$ - $\pi$  stacking interactions, and electron transfer from RGO to catalytic species that resulted in a high concentration of 4-nitrophenol around catalytic species facilitating uptake of electrons by 4-nitrophenol molecules.<sup>221,222</sup>

The spinel-structured ferrites  $\text{CuFe}_2\text{O}_4$  have been used in many applications including efficient catalysis of 4-nitrophenol reduction by excess  $\text{NaBH}_4$  at rt with a constant  $k$  up to  $1.2 \times 10^{-1} \text{ s}^{-1}$ .<sup>223</sup>

MNPs-immobilized NiNPs have been intensively used as catalysts in organic reduction reactions.<sup>224,225</sup> The presence of single poly(ethylene glycol)-10000 (PEG-10000), cetyltrimethylammonium bromide (CTAB), gelatin, and their composites controls the size and morphology of NiNPs, and the catalytic properties in the reduction of 4-nitrophenol were excellent.<sup>226</sup> The obtained NiNPs using composites of CTAB and PEG-10000 as modifier displayed the best catalytic performance with a constant  $k$  value of  $2.7 \times 10^{-3} \text{ s}^{-1}$ . These magnetic NiNPs were magnetically separated with a hand-held magnet and repeatedly used for at least three reaction cycles without loss of activity. In another report, a magnetically separable nanocatalyst consisting of NiNPs 30 nm in size anchored on RGO has been

artificially constructed. The catalyst exhibited good catalytic activity in the reduction of 4-nitrophenol to 4-aminophenol using sodium borohydride as reducing agent. An obvious enhancement of activity was achieved with near-infrared (NIR) irradiation because of the generation of hot spots on the catalyst surface caused by excellent NIR photothermal conversion property of RGO.<sup>227</sup>

$\gamma$ - $\text{Fe}_2\text{O}_3$ -supported PtNPs were fabricated through the metal vapor synthesis (MVS) procedure and applied to the reduction of halonitroaromatics using  $\text{H}_2$  as reductant in the presence of 20 mg of Pt catalyst (containing 1 wt % Pt) at rt.<sup>228</sup> The nanocatalyst showed the best catalytic behavior compared with other Pt-iron oxide systems in the literature in terms of conversion and selectivity to haloaniline derivatives in the reduction reactions of *m*-chloro-, *o*- and *p*-bromo-, and *o*- and *p*-iodonitrobenzenes. In the case of the reduction of *p*-chloro-nitrobenzene, the catalyst was magnetically recycled and reused five times without significant loss of activity. In another report, Ma and co-workers<sup>229</sup> designed the synthesis of PtNPs decorated on carbon-coated MNPs. This  $\text{Fe}_3\text{O}_4@\text{C}@\text{Pt}$  catalyst consisting of PtNPs with a size around 5 nm was used in the reduction of nitroaromatic under  $\text{H}_2$  atmosphere at rt (Figure 25) and showed high efficiency and reusability.



**Figure 25.** Reduction of aromatics catalyzed by  $\text{Fe}_3\text{O}_4@\text{C}@\text{Pt}$ .

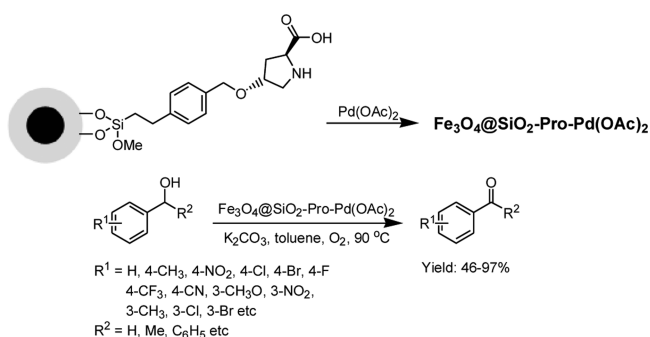
**2.1.5. Oxidation Reactions.** Oxidation reactions are fundamental organic transformation in both academic and industrial synthetic chemistry, but use of traditional stoichiometric or an excess amount of oxidants has caused serious environmental problems. Therefore, transition metal catalysts that are immobilized on modified MNPs have received considerable attention in catalyzing oxidation reactions of organic catalysts by themselves or with cocatalysts due to their high efficiency and recyclability.

Selective oxidation of alcohol is a primary example of oxidation reactions, because the carbonyl products are valuable chemicals both as active intermediates in organic synthesis and as high-value components for fine chemistry.<sup>230</sup> Thus, selective oxidation of alcohols over magnetically retrievable noble-metal-based catalysts is one of the hottest subjects in this research field.

Amino acids (*L*-cysteine,  $\beta$ -alanine, serine, or glycine) modified  $\text{Fe}_3\text{O}_4$  NPs-trapped PdNPs were produced via a simple in situ method.<sup>231</sup> The average diameter sizes of the obtained magnetic hybrid and PdNPs were about 20 and 3 nm, respectively. In the catalytic application of these nanomaterials, oxidation of benzyl alcohol was chosen as model reaction. The reaction was initially carried out at 50 °C in the presence of 30 mg of catalysts under an  $\text{O}_2$  atmosphere and under solvent-free conditions in 1.5 h with 2 mmol of benzyl alcohol. Among the

four different nanocatalysts,  $\text{Fe}_3\text{O}_4/\text{L-cysteine (Cys)-Pd}$  provided the best catalytic results, and benzaldehyde was synthesized with 48% yield and >99% selectivity. The yield was raised to 85% upon increasing the catalytic amount from 30 to 60 mg (containing 6.27 wt % Pd) with the same selectivity. In addition, the catalytic performance was maintained in eight successive reaction cycles. When 80 mg of  $\text{Fe}_3\text{O}_4/\text{Cys-Pd}$  was employed, the yield did not change but the selectivity decreased to 94%. The strategy was extended to oxidation of other aromatic and aliphatic alcohols, yielding aldehydes with 58–85% yields with excellent selectivities.<sup>231</sup>

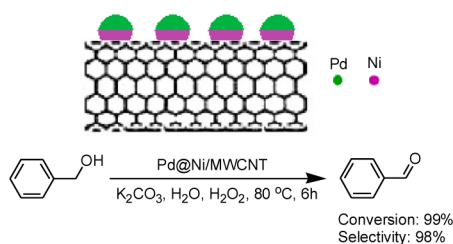
Starting from the functionalized MNPs, the proline moieties were covalently anchored providing proline-modified MNPs, and the magnetic catalyst based on Pd was synthesized via complexation with  $\text{Pd}(\text{OAc})_2$ . This catalyst system catalyzed the aerobic oxidation of alcohols to aldehydes and ketones (Figure 26).<sup>232</sup> Benzyl alcohols bearing both electron-donating



**Figure 26.** Oxidation of alcohols catalyzed by  $\text{Fe}_3\text{O}_4/\text{SiO}_2\text{-Pro-Pd}(\text{OAc})_2$ .

and electron-withdrawing groups were smoothly oxidized over 0.5 mol % of [Pd], producing the corresponding aldehydes in good to excellent yields. When aliphatic alcohols were employed, the yields of isolated products were somewhat lower. In addition, secondary benzylic alcohols were also suitable participants for the oxidation reaction, the desired ketone compounds being obtained in 71–81%. Importantly, catalyst separation was easily achieved using an external magnet with negligible Pd leaching, and the recovered catalyst was recycled for at least eight runs without loss in catalytic performance.

Chen et al. reported the preparation of Pd@Ni bimetallic NPs on multiwalled carbon nanotubes (Pd@Ni/MWCNT) that was shown to be an efficient heterogeneous catalyst for oxidation of benzyl alcohol in  $\text{H}_2\text{O}$  at 80 °C in 6 h using  $\text{H}_2\text{O}_2$  as oxidant in the presence of  $\text{K}_2\text{CO}_3$  (Figure 27).<sup>233</sup> Benzaldehyde was produced with 99% conversion and 98% selectivity, and under the same conditions both Pd/MWCNT



**Figure 27.** Oxidation of benzyl alcohol catalyzed by Pd@Ni/MWCNT.

and Ni/MWCNT afforded lower conversion and selectivity than Pd@Ni/MWCNT. Pd@Ni/MWCNT was magnetically collected and reused four times with steady decline in both conversion and selectivity.<sup>233</sup>

Colloidal AuPd bimetallic NPs were loaded on amino- or thiol-functionalized or bare  $\text{Fe}_3\text{O}_4/\text{SiO}_2$ .<sup>107</sup> These nanocatalysts exhibited some deficiencies in the oxidation of benzyl alcohol with  $\text{O}_2$  as oxidant, such as low catalytic activity, bad stability, and uneasy reusability. To overcome these drawbacks these AuPd NPs were calcined, and the hybrids  $\text{Fe}_3\text{O}_4/\text{SiO}_2\text{-NH}_2\text{-AuPd}(\text{C})$  and  $\text{Fe}_3\text{O}_4/\text{SiO}_2\text{-SH-AuPd}(\text{C})$  showed much better activities, selectivity, and reusability than their precursors.<sup>107</sup>

$\text{Fe}_3\text{O}_4\text{-Co}$  MNPs were explored for oxidation of 1-phenylethanol using excess *tert*-butyl hydroperoxide (TBHP) as the oxidant at 80 °C, and a 92% yield of acetophenone was obtained in 6 h.<sup>234</sup> After completion of the reaction, the highly stable  $\text{Fe}_3\text{O}_4\text{-Co}$  MNPs were collected using an external magnet and reused for 7 runs without obvious loss of catalytic activity. ICP analysis revealed that only 0.09% Co was leached off the initial catalyst after seven reaction cycles. Other alcohol substrates were also successfully oxidized using this catalytic system, providing 18 ketones with 79–94% yields (Figure 28).

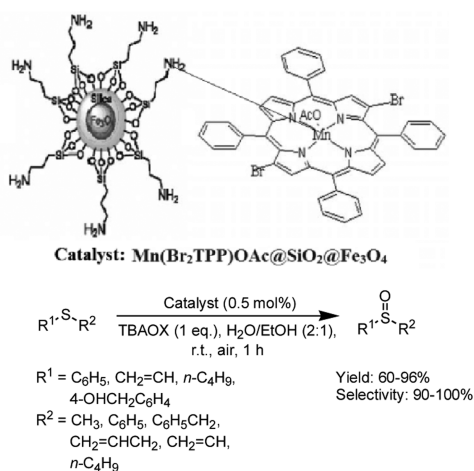


**Figure 28.** Oxidation of alcohols catalyzed by  $\text{Fe}_3\text{O}_4\text{-Co}$  MNPs and TBHP.<sup>234</sup> Reprinted with permission from ref 234. Copyright 2012 Wiley-VCH Verlag GmbH & Co.

Flow chemistry is an emerging area,<sup>235</sup> and combination of continuous flow technology with MNPs is especially attractive, because the use of MNP catalysts overcomes some limitations of continuous flow systems, such as uncontrollable fluid dynamics, limited accessibility of catalytic sites, and uncontrollable swelling.<sup>236</sup> Kappe et al.<sup>237</sup> used mesoporous aluminosilicate-supported iron oxide NPs as catalysts in a flow reactor for catalyzing selective aerobic oxidation of a primary alcohol with TEMPO as a cocatalyst. The model substrate benzyl alcohol was converted into the desired benzaldehyde with up to 42% conversion in a single pass, and continuous recirculation offered full conversion. In addition, the MNPs catalyst showed high stability in the flow process, and no leaching was observed.

Oxidation of sulfides to sulfoxides is a common reaction in the synthesis of pharmaceuticals, fine chemicals, and bioactive molecules. Recently, several magnetically recoverable nanocatalysts were designed and used in the oxidation of sulfides.<sup>238</sup>

The complex  $[\text{Mn}(\text{Br}_2\text{TPP})\text{OAc}]$  anchored on  $\text{Fe}_3\text{O}_4/\text{SiO}_2$  NPs has been synthesized via amine functionality.<sup>239</sup> This thermostable nanocatalyst has a diameter of less than 10 nm and was investigated for oxidation of sulfides. Sulfoxides were efficiently formed in 60–96% yields in 1 h at rt with excellent selectivity when the oxidation reactions proceeded in air in a mixed solvent of water and ethanol with a molar ratio of sulfide/tetra-*n*-butylammonium peroxomonosulfate (TBAOX)/catalyst of 200:200:1 (Figure 29).<sup>239</sup> If the reactions were carried out in pure water with a molar ratio of sulfide/TBAOX/



**Figure 29.** Oxidation of sulfides to sulfoxides catalyzed by Mn(Br<sub>2</sub>TPP)OAc@SiO<sub>2</sub>@Fe<sub>3</sub>O<sub>4</sub>.<sup>239</sup> Reprinted with permission from ref 239. Copyright 2012 Wiley-VCH Verlag GmbH & Co.

catalyst of 200:600:1, the products were sulfone compounds instead of sulfoxides. In addition, the Mn(Br<sub>2</sub>TPP)OAc@SiO<sub>2</sub>@Fe<sub>3</sub>O<sub>4</sub> catalyst also showed good activity in the oxidation of saturated hydrocarbons to ketones.

γ-Fe<sub>2</sub>O<sub>3</sub> was immobilized on graphene through a simple chemical route.<sup>168</sup> The resulting graphene-γ-Fe<sub>2</sub>O<sub>3</sub> MNPs were used as recyclable catalysts for selective oxidation of sulfides to sulfoxides using hydrogen peroxide as the oxidant. Good to excellent yields and selectivity were recorded at 60 °C within a few hours, but meanwhile sulfone compounds were also observed as side products.<sup>168</sup> In the case of the oxidation of methyl phenyl sulfide almost complete conversion (98%) was obtained in the first cycle, and the recyclability of the nanocatalyst was further checked. It was found that the graphene-γ-Fe<sub>2</sub>O<sub>3</sub> MNPs was recovered, recycled, and reused for more than five runs without loss of catalytic activity. The reused catalyst was found unchanged from TEM images and Raman spectra compared with those of the fresh catalyst.

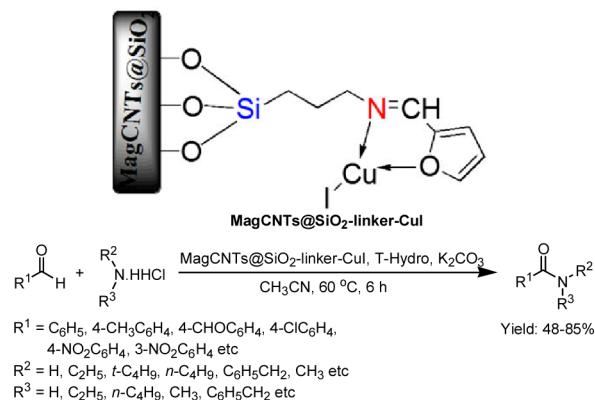
A complex [Mn(phox)<sub>2</sub>(CH<sub>3</sub>OH)<sub>2</sub>]ClO<sub>4</sub> (phox = 2-(2'-hydroxyphenyl)oxazoline)-based composite material with Fe<sub>3</sub>O<sub>4</sub>@SiO<sub>2</sub> was synthesized through aminopropyl linkage, and its catalytic activity was investigated for oxidation of thiols to disulfides using urea–hydrogen peroxide as the oxidant. This heterogeneous magnetic catalyst afforded moderate to good yields, higher selectivity toward disulfides compared with the homogeneous manganese complex, and excellent recyclability.<sup>240</sup>

Oxidative transformations of amines yielding useful nitrone building blocks were intermediate steps in the synthesis of heterocyclic compounds. γ-Fe<sub>2</sub>O<sub>3</sub>@SiO<sub>2</sub> NPs-encapsulated tungstophosphoric acid (γ-Fe<sub>2</sub>O<sub>3</sub>@SiO<sub>2</sub>-H<sub>3</sub>PW<sub>12</sub>O<sub>40</sub>) was synthesized and tested as catalyst for oxidation of secondary amines to nitrones with hydrogen peroxide as the oxidant.<sup>241</sup> Following optimization, oxidation of dibenzylamine at 23 °C in MeOH with 1.1 mol % of catalyst within 2 h afforded the corresponding nitrone in 85% yield, and extension to a variety of secondary amines led to nitrones in moderate to good yields. Moreover, γ-Fe<sub>2</sub>O<sub>3</sub>@SiO<sub>2</sub>-H<sub>3</sub>PW<sub>12</sub>O<sub>40</sub> was magnetically removed and reused at least four times without loss of activity.

Sharma et al. reported the use of 2-acetylpyridine Zn(II) complex-grafted silica@magnetite NPs as catalyst for oxidation of aromatic amines yielding azoxyarenes.<sup>242</sup> In the optimized

investigation using aniline as the test substrate the effects of reaction time and catalytic amount were involved at 80 °C in acetonitrile with H<sub>2</sub>O<sub>2</sub> as oxidant. Encouraged by full conversion and 99% selectivity toward the corresponding azoxyarene, the reaction scope was further studied. The substrates with electron-withdrawing groups provided less conversion and selectivity than electron-rich anilines. The relative steric effect was shown to be negative in terms of conversion and selectivity. The TON values for azoxyarenes in all cases were high; when some substrates were employed, the obtained TOF values were much higher than with the previously reported catalysts. The catalyst was reused up to six consecutive cycles with a steady decline in yield and negligible Zn leaching.<sup>242</sup>

Oxidative amidation of aldehydes with amine salts is a practical and direct method for synthesis of carboxamides. Heydari et al. developed a heterogeneous CuI catalyst supported on silica-coated magnetic carbon nanotubes (MagCNTs@SiO<sub>2</sub>) for oxidative amidation processes (Figure 30).<sup>243</sup> Various carboxamides compounds were effectively



**Figure 30.** Oxidative amidation of aromatic aldehydes with amine hydrochloride salts catalyzed by MagCNTs@SiO<sub>2</sub>-linker-CuI.<sup>243</sup> Reprinted with permission from ref 243. Copyright 2013 John Wiley & Sons, Ltd.

produced in the presence of 0.2 mol % of MagCNTs@SiO<sub>2</sub>-linker-CuI in one pot with moderate to good yields. The stable catalyst was magnetically recovered from the reaction medium, and repeated use in five reaction cycles maintained similar activity. Another report demonstrated that magnetic CuFe<sub>2</sub>O<sub>4</sub> NPs were also an efficient and “green” catalyst for oxidative amidation of aldehydes with amine salts.<sup>244</sup>

Oxidations of cyclohexane<sup>245</sup> and ethylbenzene<sup>246</sup> catalyzed by magnetic nanocatalysts are still challenging subjects, because in general the conversions and selectivities used to be very low. Oxidative degradation of organic pollutants in wastewater through Fenton-like reactions will be discussed in the section Fenton-Like Reactions.

**2.1.6. Arylation and Alkylation Reactions.** *S*-Arylation reactions for construction of carbon–sulfur bonds are a key step in the synthesis of biological molecules and functional materials. Recently, Cu-containing magnetic nanomaterials have emerged as catalysts in *S*-arylation reactions.<sup>247</sup> Uniformly spherical nanocrystalline (from XRD) superparamagnetic CuFe<sub>2</sub>O<sub>4</sub> NPs with a size of 55 ± 5 nm were initially tested as catalysts in the *S*-arylation reaction between thiophenol and 4-iodoacetophenone. The desired 1-(4-(phenylthio)phenyl)ethanone was isolated in 95% yield with 10 mol % of catalyst, 2

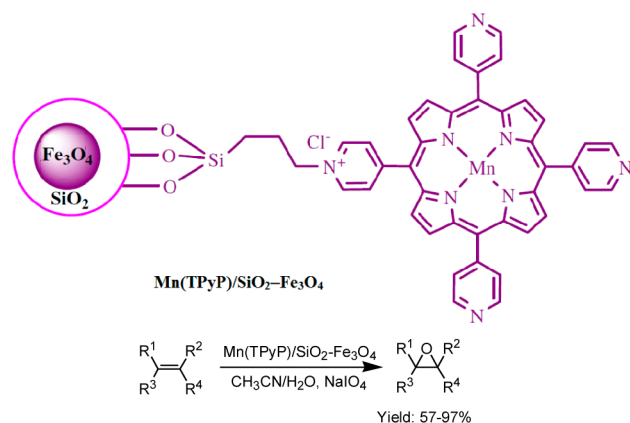


and ethylene glycol using  $\text{AgNO}_3$  and  $\text{FeCl}_3$  precursors and provided excellent catalytic activity and selectivity in epoxidation of styrene with TBHP as oxidant. Both the catalytic activity and the selectivity were much higher than those of unsupported Ag catalyst. Furthermore, the  $\text{AgNP}-\text{Fe}_3\text{O}_4$  nanocatalyst was magnetically removed and reused at least five times keeping the same catalytic performance.<sup>259</sup> In order to demonstrate the effects of MNPs supports on the catalytic performance for epoxidation of alkenes, a series of AgNPs positioned on different ferrites ( $\text{M}_{1-x}\text{Fe}_{2+x}\text{O}_4$ ; M = Co, Ni, Mn, Zn) was prepared via a similar procedure to that for  $\text{AgNP}-\text{Fe}_3\text{O}_4$  nanocomposite.<sup>79</sup> The catalytic investigation showed that all  $\text{AgNP}-\text{M}_{1-x}\text{Fe}_{2+x}\text{O}_4$  nanocatalysts were highly efficient and remarkably recyclable in the epoxidation of styrene; their catalytic activities were influenced by the variation of restriction behavior of ferrite supports for growth of AgNPs, resulting in different relative amounts of crystal planes of AgNPs as well as by the efficiency of ferrite supports in capturing reactive oxygen species.

Inspired by the high activity of tungstic peroxometalates for epoxidation, magnetic material-anchored tungstic peroxometalates catalysts have been designed and developed. Hou's group<sup>260</sup> immobilized an ionic liquid-type peroxotungstate on core-shell  $\text{Fe}_3\text{O}_4-\text{SiO}_2$  NPs by hydrogen bonding or covalent Si-O linkage, assembling  $\text{MNP}-[\text{HDMIM}]_2[\text{W}_2\text{O}_{11}]$  or  $\text{MNP}-[\text{SDMIM}]_2[\text{W}_2\text{O}_{11}]$ , respectively. Both nanocatalysts were shown to be efficient heterogeneous catalysts for epoxidation of a variety of alkenes using  $\text{H}_2\text{O}_2$  as oxidant at 60 °C in  $\text{H}_2\text{O}/\text{CH}_3\text{OH}$ . In cyclooctene epoxidation, the catalysts were readily recovered by simple magnetic decantation and recycled 10 times without significant loss of catalytic activities and selectivities toward epoxide. Another MNPs-supported peroxometalate catalyst  $\text{MNP}-(\text{DSPIM}-\text{PW}_{11})$  prepared through the hydrogen-bonding method exhibited excellent activity and recyclability in cyclooctene epoxidation with  $\text{H}_2\text{O}_2$  under solvent-free conditions (Figure 32). The principles of immobilization by hydrogen bonding should open facile catalyst formation with excellent activities and superior recycling performance.

Using this principle, phosphotungstic acid was immobilized on imidazole-functionalized  $\text{CoFe}_2\text{O}_4$  NPs, and the catalytic potential was evaluated in the epoxidation of various alkenes.<sup>261</sup> When the epoxidations were conducted with 0.1 g of this catalyst (0.98 mmol/g of tungsten content) and 2 equiv of *t*-BuOOH as oxidant in 1,2-dichloroethane at 70 °C within 6 h in 1 mmol-scale reactions the corresponding epoxides were obtained in good to excellent yields and excellent selectivity, and the catalyst displayed constant activity after several consecutive cycles.

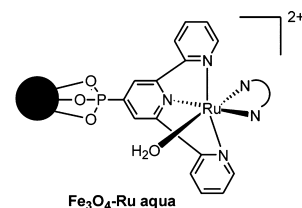
Metalloporphyrin complexes are very active catalysts for epoxidation of alkenes; therefore, the MNPs-supported version has logically emerged.<sup>262</sup> Immobilization of tetra(4-*N*-pyridyl)porphyrinatomanganese(III) acetate  $[\text{Mn}(\text{TPyP})\text{OAc}]$  on  $\text{SiO}_2@\text{Fe}_3\text{O}_4$  MNPs was reported by Tangestaninejad et al.<sup>263</sup> The narrowly distributed  $\text{Mn}(\text{TPyP})/\text{SiO}_2-\text{Fe}_3\text{O}_4$  with an average diameter of around 48 nm provided good catalytic performance, relatively good tolerance, and satisfactory recyclability using  $\text{NaIO}_4$  as oxidant at rt (Figure 33). With regard to catalyst leaching, 0.33%, 0.18%, 0.12% of Mn leached off the initial catalyst in the first three cycles, respectively, and no leaching was detected in the fourth to sixth cycles. In addition, this catalytic system showed activity in alkane hydroxylation.



**Figure 33.** Epoxidation of alkenes catalyzed by  $\text{Mn}(\text{TPyP})/\text{SiO}_2-\text{Fe}_3\text{O}_4$ .<sup>263</sup> Reprinted with permission from ref 263. Copyright 2012 Elsevier Ltd.

Li et al. reported the assembly of magnetic CoNPs within carbon nanotubes (CNTs) by a wet chemical method, and the existence of CoNPs in the interior of CNTs was confirmed by TEM.<sup>264</sup> The catalytic activity of the Co/CNTs in the liquid-phase epoxidation of styrene was studied under an atmospheric pressure of molecular oxygen, epoxidation being complete with 93% of epoxide selectivity within 1 h at 100 °C in DMF. The catalyst was recycled three times without loss of activity,<sup>264</sup> and it was indicated that Co/CNTs were a superior catalyst compared to previously reported catalysts.

Pericàs' group reported the preparation of a magnetically separable molecular ruthenium complex catalyst containing a phosphonated trpy ligand (Figure 34).<sup>265</sup> This nanosystem



**Figure 34.**  $\text{Fe}_3\text{O}_4$ -supported  $[\text{Ru}(\text{trpy-P})(\text{B})(\text{H}_2\text{O})]^{2+}$  ( $\text{Fe}_3\text{O}_4-\text{Ru aqua}$ ).

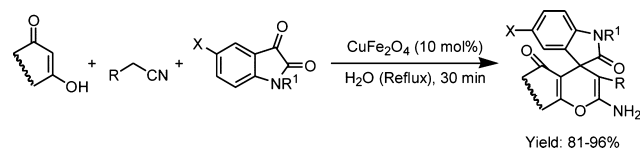
$\text{Fe}_3\text{O}_4-\text{Ru aqua}$  proved to be an excellent catalyst for epoxidation of alkenes. In particular, this nanocatalyst promoted stereoselective synthesis of *cis*-epoxides from reactions of *cis*-olefins, and the  $\text{Fe}_3\text{O}_4$  support in  $\text{Fe}_3\text{O}_4-\text{Ru aqua}$  did not cause any decrease in activity compared to the homogeneous counterpart. In the case of epoxidation of *cis*- $\beta$ -methylstyrene, investigation of the recyclability showed that  $\text{Fe}_3\text{O}_4-\text{Ru aqua}$  was collected using magnetic decantation and exhibited constant activity and slightly decreased selectivity after at least five consecutive cycles.

**2.1.8. Multicomponent "One-Pot" Synthesis.** The multicomponent reaction (MCR) strategy<sup>266,267</sup> displays significant advantages over classical stepwise methods and has been proved to be a powerful method to build diverse and complex molecules, in particular, for the synthesis of biologically active and heterocyclic compounds. MCR offers rapid and convergent construction of molecules from commercially available starting materials without the need of isolation and purification of intermediates, and therefore, it requires less manipulation time, cost, and energy than classic methods. The

combination of MCR with magnetic separation should thus significantly expand green procedures.

In the past two years, magnetically recoverable catalysts have been widely used in multicomponent “one-pot” synthesis of 4*H*-chromene derivatives,<sup>268,269</sup> spirooxindoles,<sup>270</sup> hydantoin derivatives,<sup>271</sup> xanthene derivatives,<sup>272</sup> hexahydroquinoline carboxylates,<sup>273</sup> pyrido[2,3-*d*]pyrimidines,<sup>274</sup> diazepine derivatives,<sup>275</sup> spirohexahydropyrimidines,<sup>276</sup> 1,2,3,5-tetrahydropyrazolo[1,2-*a*][1,2,4]triazole,<sup>277</sup> polysubstituted pyrroles,<sup>278</sup> 4*H*-pyrano[2,3-*c*]pyrazoles,<sup>279</sup> 1,4-dihydropyridine derivatives,<sup>280,281</sup> 4*H*-benzo[*b*]pyrans,<sup>282</sup> 1-amidoalkyl-2-naphthols,<sup>283</sup> spiro-furo-pyridopyrimidine-indulines,<sup>284</sup> and so on.

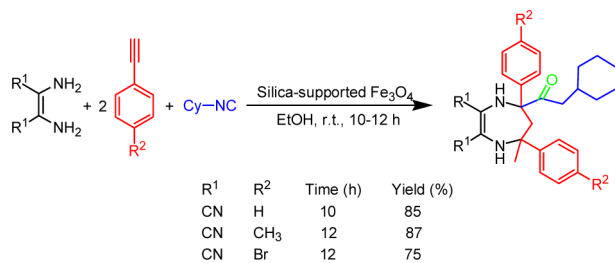
Gharemanzadeh's group<sup>270</sup> reported that CuFe<sub>2</sub>O<sub>4</sub> MNPs displayed high catalytic performance in the synthesis of spirooxindole fused heterocycles using isatins, cyanomethanes, and cyclic 1,3-dicarbonyl derivatives as starting materials in one pot in H<sub>2</sub>O (Figure 35). In the initial investigation, reaction of



**Figure 35.** Synthesis of spirooxindole-fused heterocycles from isatins, active cyanomethanes, and cyclic 1,3-dicarbonyl derivatives catalyzed by CuFe<sub>2</sub>O<sub>4</sub>.

3-hydroxy-1*H*-phenalen-1-one, malononitrile with isatin was carried out in refluxing water in the presence of 10 mol % CuFe<sub>2</sub>O<sub>4</sub> for 30 min, and the desired spirooxindole was isolated in 90% yield. Investigation of the reaction scope using various cyclic 1,3-dicarbonyl compounds, cyanomethanes, and isatins revealed that the CuFe<sub>2</sub>O<sub>4</sub>-catalyzed tandem three-component reactions method tolerated a range of substrates, affording various spirooxindole fused heterocycles in 81–97% yields. The catalytic activity remained unaltered throughout four runs, showing the efficiency and “green” character of this catalyst.

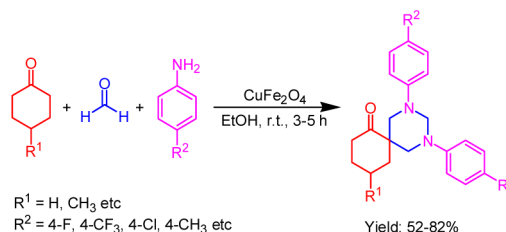
Silica-supported Fe<sub>3</sub>O<sub>4</sub> NPs were applied to promote the reaction of 1,2-diamines, two components of terminal alkynes, and isocyanide in EtOH at rt, yielding diazepines (Figure 36).<sup>275</sup> This two-step procedure was achieved in one pot; first,



**Figure 36.** One-pot multicomponent synthesis of diazepines using 1,2-diamines, terminal alkynes, and isocyanide catalyzed by silica-supported Fe<sub>3</sub>O<sub>4</sub>.

reaction of 1,2-diamines with terminal alkynes proceeded in the presence of silica-supported Fe<sub>3</sub>O<sub>4</sub> for a few hours; then isocyanide was added into the same pot. Three diazepine derivatives containing different substituents were synthesized with 83–92% yields. The magnetically recycled catalyst could be used for at least five times, and isolated yields were similar and remained with no detectable loss.

Dandia's group demonstrated that CuFe<sub>2</sub>O<sub>4</sub> was as a highly efficient and magnetically recoverable catalyst for the one-pot synthesis of spirohexahydropyrimidines from ketones, aromatic amines, and formaldehyde (Figure 37).<sup>276</sup> Reaction of cyclo-

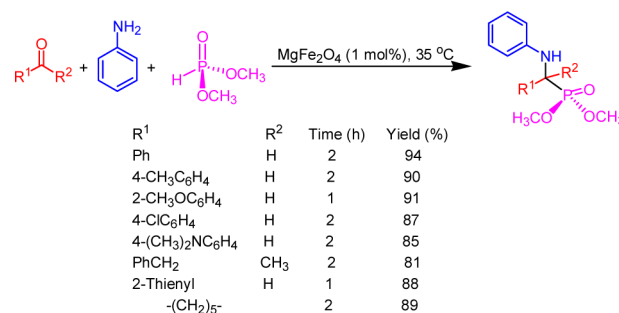


**Figure 37.** Synthesis of spirohexahydropyrimidines from ketones, aromatic amines, and formaldehyde catalyzed by CuFe<sub>2</sub>O<sub>4</sub>.

hexanone, formaldehyde, and 4-fluoroaniline was chosen as the model reaction to optimize the reaction conditions of solvent, reaction times, and catalyst amount, and optimized results (82% yield) were obtained using ethanol and 10 mol % CuFe<sub>2</sub>O<sub>4</sub> within 3 h. The reaction was extended to various aromatic amines, and CuFe<sub>2</sub>O<sub>4</sub> was recovered and reused 5 times with 82%, 81%, 80%, 79%, and 79% yield.

A three-component coupling reaction of aldehyde, alkyne, and amine (A<sup>3</sup>-coupling) catalyzed by graphene-Fe<sub>3</sub>O<sub>4</sub> composite provided a wide range of propargylamines in 65–92% yields. This catalyst exhibited excellent magnetically recoverability, but decreases of 11% in yield were found from the first to the second cycle and from the second to the third cycle.<sup>285</sup>

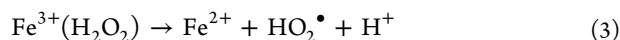
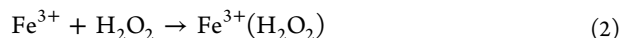
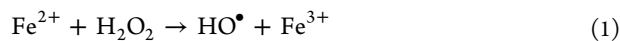
$\alpha$ -Aminophosphonates are essential biologically active compounds. They were synthesized through a three-component coupling reaction involving carbonyl compounds, amines, and dialkyl phosphate using MgFe<sub>2</sub>O<sub>4</sub> as Lewis acid catalyst in good to good to excellent yields in a short time (Figure 38). After completion of the first cycle, MgFe<sub>2</sub>O<sub>4</sub> was removed with an external magnet from the reaction medium and reused for successive 5 runs with the same catalytic activity.<sup>286</sup>



**Figure 38.** One-pot multicomponent synthesis  $\alpha$ -aminophosphonates catalyzed by MgFe<sub>2</sub>O<sub>4</sub>.

**2.1.9. Fenton-Like Reactions.** Among various techniques of water treatment, the Fenton technique (H<sub>2</sub>O<sub>2</sub> + Fe<sup>2+</sup>/Fe<sup>3+</sup>)<sup>287</sup> has proved to be one of the most effective methods for degrading organic pollutants in wastewater. It is an advanced oxidation process (AOP), where the “HO•” radicals (that might be coordinated to iron) usually are the main highly reactive oxidizing species generated from decomposition of hydrogen peroxide in the presence of iron cation. The homogeneous Fenton process has many drawbacks: it requires further

treatment for toxic sludges and other waste products, neutralization of treated solutions before discharge, incomplete pollutant removal, and high-energy requirement. In order to overcome these drawbacks, heterogeneous Fenton-like systems using pure form or dispersed iron oxide particles on a support have been recently developed. Voelker and Kwan<sup>288</sup> provided a reasonable mechanism for production of HO• via iron oxide particles as follows



Iron oxide NPs without support displayed good catalytic performance in the Fenton-like reactions for oxidative degradation of contaminants;<sup>289,290</sup> however, a severe Fe leaching problem restricted their applications. Therefore, various supports or stabilizers including MWCNTs,<sup>68</sup> rGO,<sup>291</sup> citrate,<sup>292</sup> CeO<sub>2</sub>,<sup>293</sup> mesoporous SiO<sub>2</sub>,<sup>294</sup> and hydrogel<sup>295</sup> were widely used for anchoring iron oxide NPs; moreover, the supports enhanced the activity of iron oxide through strong adsorption of pollutants to catalytic sites. In addition, several other strategies have recently been developed to improve the catalytic efficiency of iron oxide NPs, such as microwave assistance,<sup>296</sup> light assistance (photo-Fenton process),<sup>297</sup> and other metal doping processes.<sup>298,299</sup>

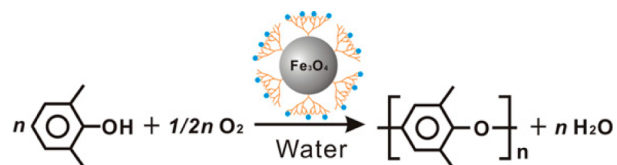
The catalytic property of a magnetic nanoscaled Fe<sub>3</sub>O<sub>4</sub>/CeO<sub>2</sub> composite in the Fenton oxidation of 4-CP was investigated by Wang's group.<sup>293</sup> The Fe<sub>3</sub>O<sub>4</sub>/CeO<sub>2</sub> composite with a size of 5–10 nm was prepared through the impregnation method with CeO<sub>2</sub> NPs and iron precursors and utilized for catalyzing degradation of 4-CP at different pH values, catalytic amounts, 4-CP concentrations, and reaction temperatures in the presence of various H<sub>2</sub>O<sub>2</sub> dosages. When the reaction was conducted at 30 °C and pH 3.0 with 30 mM H<sub>2</sub>O<sub>2</sub>, 2.0 g L<sup>-1</sup> Fe<sub>3</sub>O<sub>4</sub>/CeO<sub>2</sub>, and 0.78 mM 4-CP, a high pseudo-first-order kinetic constant of 0.11 min<sup>-1</sup> was provided. The catalyst was reused in six successive catalytic cycles, and partial dissolution of the NPs on the surface was observed from HRTEM analysis.

SiO<sub>2</sub> microspheres-supported and free  $\gamma$ -Fe<sub>2</sub>O<sub>3</sub> NPs were applied as catalyst in a series of Fenton-like reactions for degradation of methylene blue (MB), methyl orange (MO), or parantrophenol (PNP).<sup>294</sup> Investigation of the MO decomposition revealed that the free  $\gamma$ -Fe<sub>2</sub>O<sub>3</sub> NPs showed higher activity than the supported version, which could be attributed to the facility for the reactants to access to the catalytic sites of free  $\gamma$ -Fe<sub>2</sub>O<sub>3</sub>. However, SiO<sub>2</sub> microspheres-supported  $\gamma$ -Fe<sub>2</sub>O<sub>3</sub> NPs provided a better catalytic performance than the free version for degradation of MB in terms of the initial rates of decolorization ( $v_0$ ) and the decolorization yield (DY), which was explained by the very strong adsorption of MB on the silica surface. Both catalysts afforded moderate mineralization yields (MY) for MO and PNP.<sup>294</sup>

**2.1.10. Other Reactions.** Other recent advances in magnetically recoverable transition metal catalysis focused on Cu-catalyzed oxidative polymerization,<sup>300</sup> Ru-catalyzed succinic acid synthesis from levulinic acid,<sup>301</sup> degradation of contaminants in water,<sup>302–310</sup> esterification,<sup>311</sup> synthesis of  $\beta$ -hydroxy hydroperoxides,<sup>312</sup> synthesis of bis(indolyl)methanes,<sup>313</sup> synthesis of spirooxindoles,<sup>314</sup> Cu-catalyzed oxidative homocoupling of terminal alkynes,<sup>315</sup> dehydrogenation,<sup>316–319</sup> Friedel–Crafts reaction,<sup>320</sup> synthesis of *N*-substituted pyrroles,<sup>321</sup>

alkoxycarbonylation,<sup>322</sup> Pd-catalyzed reductive amination of aldehydes,<sup>323,324</sup> synthesis of diverse *N*-heterocycles,<sup>325,326</sup> oxidative cross-dehydrogenative coupling,<sup>327</sup> Cr-catalyzed hydroxylation of benzene,<sup>328</sup> glycolysis of poly(ethylene terephthalate),<sup>329</sup> synthesis of coumarins via Pechmann reaction,<sup>330</sup> and so on.

Cu(II)–PAMAM dendrimer complexes showed excellent catalytic activity in the aerobic oxidative polymerization of 2,6-dimethylphenol (DMP) to poly(2,6-dimethyl-1,4-phenylene oxide) (PPO).<sup>331</sup> To achieve the recovery of the Cu catalyst, Cu(II) complexes supported on G0–G3 PAMAM-coated Fe<sub>3</sub>O<sub>4</sub> NPs (named Mag-PAMAM-Cu) were prepared and employed as catalysts in the polymerization that was carried out with an aqueous solution of DMP, sodium *n*-dodecyl sulfate, and sodium hydroxide under an oxygen atmosphere at 50 °C. The catalytic activity of the Cu complexes was influenced by the generation number of the PAMAM dendrimer, and Mag-PAMAMG3-Cu gave a superior performance (80.85% PPO yield and 99.8% selectivity toward PPO) than Mag-PAMAMG1-Cu and Mag-PAMAMG2-Cu in the first reaction cycle. Unfortunately, EA and TGA depicted that 25–30% Cu was lost during the reaction or recovery process, which caused an obvious decrease in yields and molecular weight of PPO in the second and third runs. The authors indicated that the main reason for low recovery ratios was the dissociation of Cu(II) with amine groups of PAMAM dendrimers occurring during the recovery after polymerization (Figure 39).<sup>332</sup>



**Figure 39.** Oxidative polymerization of DMP with/Mag–PAMAM–Cu catalyst.<sup>332</sup> Reprinted with permission from ref 332. Copyright 2012 Elsevier Ltd.

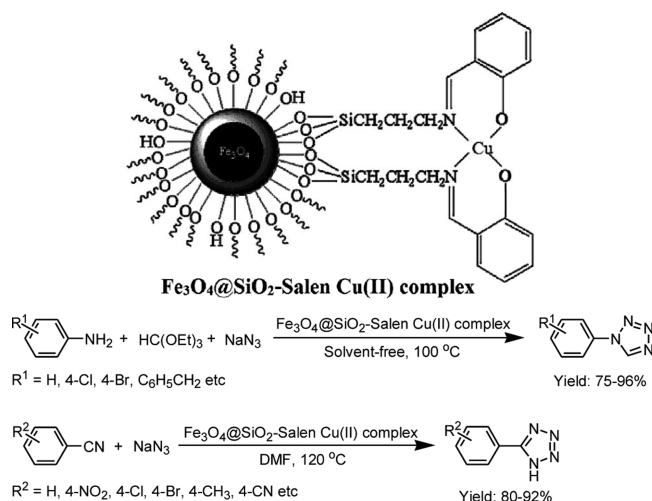
MNPs catalysis is one of the most popular techniques in water treatment. Various contaminations including diclofenac, *p*-chlorophenol, organic dyes, tetrabromobisphenol A (TBBPA), rhodamine B, and acetylsalicylic acid were efficiently degraded in water by MNPs-supported catalysts.

Reduction of pollutants to nontoxic compounds is an effective strategy in water treatment. Zhou et al. demonstrated the preparation of AgNPs embedded in the Fe<sub>3</sub>O<sub>4</sub>@C template NPs with porous carbon shell and their catalytic application in the reduction of organic dye rhodamine B in water. The Fe<sub>3</sub>O<sub>4</sub>@C–Ag hybrid catalyst exhibited highly efficient property and was easily collected and reused without loss of activity.<sup>333</sup> Fe<sub>3</sub>O<sub>4</sub>-immobilized PdNPs provided a remarkable catalytic behavior in bromate reduction to bromide.<sup>334</sup> One hundred percent conversion was achieved within less than 2 h over a range of pH values. The quasi-monodisperse Pd/Fe<sub>3</sub>O<sub>4</sub> catalyst showed good recoverability using an external magnetic field and stability.

A core–satellite structured Au/Pdop/SiO<sub>2</sub>/Fe<sub>3</sub>O<sub>4</sub> composite was synthesized via a simple method and provided high catalytic performance in the catalysis of MB reduction with NaBH<sub>4</sub> as a reducing agent at rt.<sup>335</sup> Full conversion of MB was observed within 30 s over 10 mg of Au/Pdop/SiO<sub>2</sub>/Fe<sub>3</sub>O<sub>4</sub> with a MB concentration of 0.02 mM. MB was completely degraded in 20 min when the concentration was increased to 0.2 mM.

The authors indicated that the high catalytic performance of Au/Pdop/SiO<sub>2</sub>/Fe<sub>3</sub>O<sub>4</sub> is partly attributed to the effective contact between Pdop (polydopamine) and the Au nanocatalysts. The catalyst was magnetically removed from the reaction medium, and a gradual decrease in catalytic efficiency was found in the first 5 runs. Zhang and co-workers<sup>336</sup> applied rGO-supported Fe<sub>3</sub>O<sub>4</sub> (4.8 nm in size) PtNPs (5 nm in size) as a catalyst with high performance in the reduction of MB. The versatile rGO-supported Fe<sub>3</sub>O<sub>4</sub>-Pt composite also efficiently promotes aqueous-phase aerobic oxidation of benzyl alcohol. This kind of rGO-supported Fe<sub>3</sub>O<sub>4</sub>-metal composite is simply synthesized through the solvothermal method and possesses great potential applications in catalysis and other fields.

The Salen Cu(II) complex was connected to the surface of SiO<sub>2</sub>-coated Fe<sub>3</sub>O<sub>4</sub> nanoparticles, and this nanocatalyst was used in the synthesis of 1- and 5-substituted 1*H*-tetrazoles under various conditions (Figure 40).<sup>337</sup> A series of 1-



**Figure 40.** Fe<sub>3</sub>O<sub>4</sub>@SiO<sub>2</sub>-Salen Cu(II)-catalyzed synthesis of 1- and 5-substituted 1*H*-tetrazoles.<sup>337</sup> Reprinted with permission from ref 337. Copyright 2013 Elsevier B.V.

substituted 1*H*-tetrazoles was isolated in good to excellent yields through the reaction of triethyl orthoformate, sodium azide, and several amines at 100 °C under solvent-free conditions over 20 mg of catalyst containing 0.4 mol % Cu(II). Thirteen different 5-substituted 1*H*-tetrazoles in 80–92% yields were synthesized from cycloaddition of sodium azide and nitrile compounds containing a broad scope of substituents at 120 °C in DMF in the presence of 20 mg of Fe<sub>3</sub>O<sub>4</sub>@SiO<sub>2</sub>-Salen Cu(II). Its catalytic recyclability was investigated based on the case of the cyclization of *p*-methoxy aniline, triethyl orthoformate, and sodium azide, and the nanocatalyst was magnetically collected and reused for seven subsequent reaction cycles without deterioration of the catalytic activity. ICP analysis revealed that the leaching amounts of Cu from the initial catalyst were 0.2% and 5.4% after the first and seventh repeated runs, respectively.

Implantation of AgNPs into the mesoporous spheres of HMMS material was achieved via a six-step procedure using colloidal carbon spheres as templates.<sup>338</sup> Condensation of dicarbonyl compounds with amines forming  $\beta$ -enaminones was chosen as a model reaction to evaluate the catalytic property of Ag/HMMS (Figure 41). The reactions proceeded smoothly in methanol at 60 °C within a short time over 31 mg of catalyst,



**Figure 41.** Synthesis of  $\beta$ -enaminones over Ag/hollow magnetic mesoporous spheres (Ag/HMMS).<sup>338</sup> Reprinted with permission from ref 338. Copyright 2013 Elsevier B.V.

providing 84–100% yields.<sup>338</sup> In addition, the good magnetic recoverability and recyclability of the nanocatalysts were verified via a catalytic recycling test.

The Ullmann-type coupling procedure has been shown to be a useful strategy to form carbon–oxygen bonds. Xu et al.<sup>339</sup> found that the stable, easily made, and low-cost magnetic catalyst CuFe<sub>2</sub>O<sub>4</sub> showed high catalytic activity for the Ullmann C–O coupling reaction between phenols and aryl halides. Phenol and iodobenzene were chosen as model substrates, and diphenyl ether was synthesized in 99% yield when the reaction was promoted with 5 mol % CuFe<sub>2</sub>O<sub>4</sub> and 10 mol % diketone ligand 2,2,6,6-tetramethylheptane-3,5-dione in NMP at 135 °C using Cs<sub>2</sub>CO<sub>3</sub> as base. In the investigation of the substrate scope, a series of aryl ethers was obtained in good to excellent yields through reaction of various kinds of phenols with aryl iodides. Aryl bromides, instead of aryl iodides, were also suitable coupling partners of phenols. When 2-chloropyridine was used, the corresponding aryl ether was detected with 65% yield; unfortunately, chlorobenzene only gave traces of product. The reusability of the catalyst showed that CuFe<sub>2</sub>O<sub>4</sub> was magnetically removed from the reaction medium and reused for 6 runs with obvious and steady decrease in yield under 5 mol % catalyst owing to a slight particle aggregation, decomposition of part CuFe<sub>2</sub>O<sub>4</sub> NPs, and progressive loss during the recovery process. A 98% yield was obtained after the fifth reaction cycle over 10 mol % CuFe<sub>2</sub>O<sub>4</sub>. A carbon nanotube-supported  $\alpha$ -Fe<sub>2</sub>O<sub>3</sub>@CuO nanocomposite was another outstanding magnetic catalyst for cross-coupling of aryl halides with phenols to fabricate C–O bonds, and the catalyst was reused up to six reaction cycles without any loss of catalytic activity.<sup>340</sup>

CuFe<sub>2</sub>O<sub>4</sub> MNPs with a particle size in the 10–30 nm range were an efficient catalyst for amination of iodides with ammonia in PEG.<sup>341</sup> Reactions involving various aryl or aliphatic iodides gave the corresponding arylamines in moderate to good yields, but the strategy was not amenable to aryl bromides. The catalyst was magnetically separable and used for at least five cycles with a slight decline in catalytic activity.<sup>341</sup>

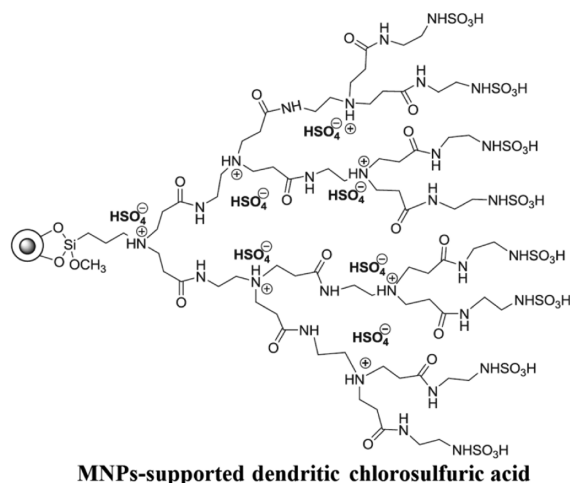
## 2.2. Magnetically Recyclable Organocatalysts

Organocatalysis plays a decisive role in the field of catalysis, and the number of publications on MNPs-supported organocatalysis has dramatically increased during the past 2 years.

Direct asymmetric aldol reactions constructing C–C bonds are a popular strategy in the synthesis of chiral organic compounds. Since List et al. developed the asymmetric aldol reactions catalyzed by L-proline,<sup>342</sup> research on supported L-proline and its derivatives for aldol reactions has rapidly

progressed. Recently, some proline-functionalized magnetic core-shell NPs were designed and used as efficient and recyclable organocatalysts for asymmetric aldol reactions. A novel hybrid consisting of a  $\text{Fe}_3\text{O}_4$  core and polymer brush-like coating with acrylates or methacrylates derived from *trans*-4-hydroxyproline was prepared. The organic nanocatalyst displayed excellent catalytic performance in asymmetric aldol reactions of ketones with aromatic aldehydes and performed very well in the recyclability test.<sup>343</sup> L-4-Hydroxyproline-grafted  $\text{Fe}_3\text{O}_4@/\text{SiO}_2$  MNPs promoted the asymmetric aldol reaction of ketone with aldehyde smoothly with good catalytic activity and selectivity (diastereoselectivity and enantioselectivity). In addition, the catalysts were magnetically separated and reused for at least five cycles without significant loss in activity.<sup>344</sup>  $\text{Fe}_3\text{O}_4@/\text{SiO}_2$  MNPs decorated by L-proline-functionalized imidazolium-based ionic liquid catalyzed the asymmetric aldol reaction that was processed in water without additive.<sup>345</sup> For the reaction between cyclohexanone and 2-nitrobenzaldehyde, 10 mol % of this catalyst provided excellent performance in terms of yield, diastereoselectivity, enantioselectivity, and recyclability, which was attributed to facilitation of the accessibility of the hydrophobic reactants to the active sites in water due to the existence of the ionic liquid moiety and its magnetic nature.

$\alpha$ -Aminophosphonate compounds with a structural analogy to  $\alpha$ -amino acids have been exploited for remarkable applications in modern pharmaceutical chemistry. Acidic organocatalysts including phosphotungstic acid (PTA),<sup>346</sup> dehydroascorbic acid (DHAA),<sup>347</sup> and dendritic chlorosulfuric acid<sup>348</sup> supported on the MNPs were synthesized and applied to the synthesis of  $\alpha$ -aminophosphonates. The Pourjavadi group synthesized a new magnetically separable organocatalyst consisting of chlorosulfuric acid-functionalized PAMAM dendrimers (Figure 42). The immobilized dendritic chlor-



**Figure 42.** Synthesis of  $\alpha$ -aminophosphonates catalyzed by MNPs-supported dendritic chlorosulfuric acid.<sup>348</sup> Reprinted with permission from ref 348. Copyright 2012 Elsevier B.V.

osulfuric acid was shown to be an efficient heterogeneous catalyst for synthesis of  $\alpha$ -aminophosphonates under neat conditions at rt. The catalyst was readily recovered by an external magnetic decantation and recycled for seven reaction cycles without decrease of activity.<sup>348</sup>

Acidic organocatalysts immobilized on MNPs probably are the most common magnetic organocatalysts. Sulfonic

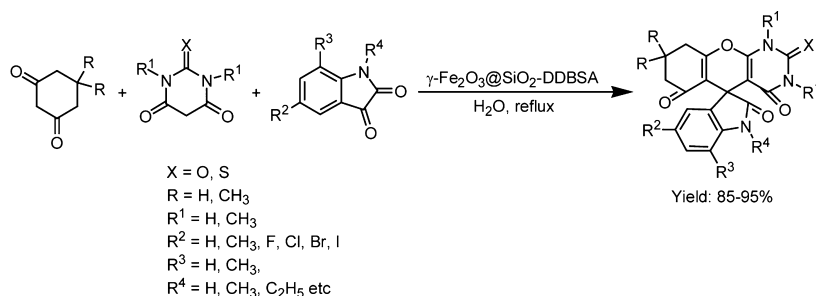
acid,<sup>349–359</sup> polyphosphoric acid,<sup>360</sup> sulfonated-phenylacetic acid,<sup>361</sup> *N*-propylsulfamic acid,<sup>362–364</sup> chlorosulfuric acid,<sup>365</sup> phosphotungstic acid,<sup>366</sup> heteropolyacids,<sup>367</sup> amino acids,<sup>368</sup> sulphamic acid,<sup>369</sup> and dodecyl benzenesulfonic acid<sup>370</sup> were grafted onto MNPs and used as catalysts in esterification, Hantzsch reaction, one-pot synthesis of amidoalkyl naphthols, *N*-formylation reaction, Biginelli reaction, oxidation of sulfides to sulfoxides, synthesis of 2*H*-indazolo[2,1-*b*]phthalazine-triones, synthesis of 2,3-dihydroquinazolin-4(1*H*)-ones, synthesis of 2,4,5-trisubstituted imidazoles, hydrolysis of cellulose, synthesis of 5-ethoxymethylfurfural, synthesis of imidazoles, and synthesis of a library of spirooxindole-pyrimidines in the past 2 years.

For example, Li et al.<sup>349</sup> synthesized nanosize or micosize magnetic catalysts containing an iron oxide core, poly(glycidyl methacrylate) (PGMA) shell, and sulfonic acid groups on the surface. The nanocatalyst with a diameter of 90 nm and high acid capacity was further used for esterification of free fatty acid (16 wt % in waste grease) to fatty acid methyl ester that was synthesized with 96% conversion within 2 h. This catalyst kept high catalytic performance in 10 successive runs. The size of the catalyst was shown to have profound effects on the catalytic property. The microsize catalyst (with a 60–350  $\mu\text{m}$  diameter) provided far less catalytic performance regarding both activity and recyclability than the nanosize version. In comparison, benzenesulfonic acid-functionalized polystyrene-iron oxide (shell-core structure) MNPs and sulfonic acid-grafted silica-iron oxide (shell-core structure) were employed as catalysts for the same esterification reaction. The result showed that the catalyst with polystyrene as shell could not be recycled; the one with sulfonic acid as shell did not perform well concerning catalytic activity and recyclability.

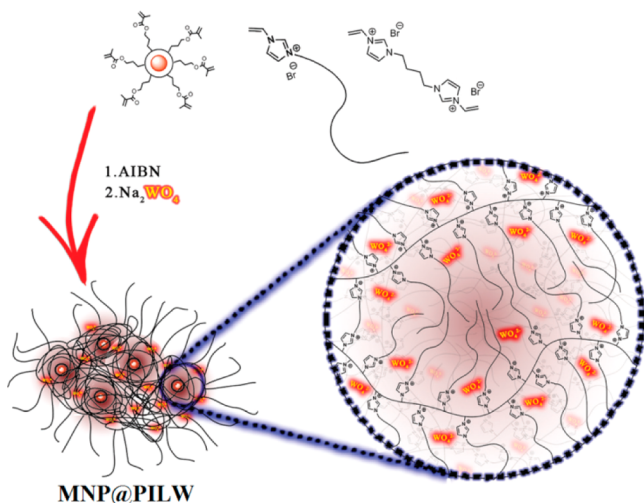
Koukabi et al.<sup>350</sup> reported that a magnetic particle-immobilized solid acid with a high density of sulfonic acid groups was successfully used as catalyst in the Hantzsch reactions of various aromatic, aliphatic, and heteroaromatic aldehydes, acetoacetate derivatives, and ammonium acetate. 1,4-Dihydropyridines were isolated with 90–99% yields after reactions at 90 °C in a short time under solvent-free conditions using 25 mg of catalyst. After completion of the Hantzsch reaction of benzaldehyde, ethyl acetoacetate, and ammonium acetate, the MNPs-supported solid acid catalyst was simply collected by a hand-held magnet and reused five times; the observed yields were 98%, 98%, 98%, 96%, and 96%.

$\gamma$ - $\text{Fe}_2\text{O}_3@/\text{SiO}_2$  NPs-anchored dodecyl benzenesulfonic acid (DDBSA) ( $\gamma$ - $\text{Fe}_2\text{O}_3@/\text{SiO}_2$ -DDBSA) catalyzed the synthesis of spirooxindole-pyrimidine derivatives by three-component condensation reactions of cyclohexane-1,3-diones, barbituric acids, and isatins or acenaphthylene-1,2-dione in water (Figure 43).<sup>370</sup> Dozens of spirooxindole-pyrimidine compounds were synthesized with excellent yields using this catalytic system.  $\gamma$ - $\text{Fe}_2\text{O}_3@/\text{SiO}_2$ -DDBSA was reused for 6 runs without a decline of catalytic activity.

Ionic liquids (ILs) have attracted a great amount of attention in various areas, especially recently in the utilization as catalyst, due to their unique properties of safety, excellent solubility, high ionic conductivity, negligible vapor pressure, and wide liquid range, and MNPs-supported IL types have consequently been utilized in various organic syntheses.<sup>371,372</sup> Pourjavadi's group designed poly(basic ionic liquid)-coated MNPs to catalyze the synthesis of 4*H*-benzo[*b*]pyrans<sup>373</sup> and oxidation reactions.<sup>374</sup> As shown in Figure 44, MNPs were coated by multilayered tungstate-based poly(ionic liquid) cross-linked



**Figure 43.** One-pot, three-component synthesis of a library of spirooxindole–pyrimidines catalyzed by MNPs-supported dodecyl benzenesulfonic acid in aqueous media.



**Figure 44.** Oxidation of alcohols, sulfides, and olefins by  $H_2O_2$  catalyzed by MNP@PILW.<sup>374</sup> Reprinted with permission from ref 374. Copyright 2013 Royal Society of Chemistry.

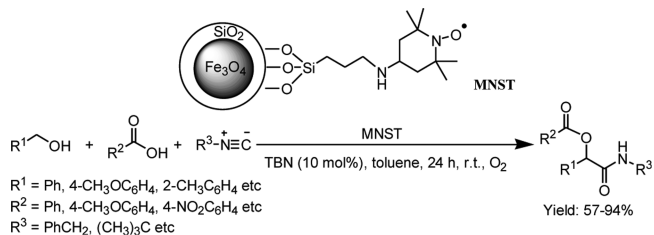
poly(ionic liquid) forming magnetic ionic liquid catalyst MNP@PILW that showed high performance in the selective oxidation of a wide range of alcohols, sulfides, and olefins using  $H_2O_2$  as an oxidant under neat condition or in acetonitrile.<sup>374</sup> The excellent catalytic property was attributed to the hydrophobic surface and the multilayered nature of MNP@PILW. Product separation and catalyst recycling were easily accomplished with the assistance of an external magnet, and the catalyst was recycled several times without loss of catalytic activity.

An ionic liquid immobilized on MNPs was recently used as a magnetically recycled heterogeneous catalyst for multicomponent synthesis of aromatic heterocyclic compounds in one pot.<sup>375</sup>  $Fe_3O_4@SiO_2$  MNPs-supported 3-sulfobutyl-1-(3-propyltriethoxysilane) imidazolium hydrogen sulfate was shown to be an efficient catalyst for the synthesis of benzoxanthenes by a three-component condensation of dimedone with aldehyde and 2-naphthol. A series of benzoxanthenes products was isolated with good to excellent yields from the one-pot reaction at 90 °C under solvent-free conditions within a short time. This “quasi-homogeneous” catalyst also exhibited excellent recyclability during six reaction cycles.<sup>62</sup>

Magnetic organocatalysts have been widely used to catalyze one-pot syntheses. Besides the above-mentioned examples, other reactions focused on the synthesis of pyrazolophthalazinyl spirooxindoles,<sup>376</sup> pyran-annulated heterocyclic compounds,<sup>377</sup>  $\alpha$ -acyloxy carboxamides,<sup>378</sup> chromene derivatives,<sup>379,380</sup> triazolo[1,2-*a*]indazole-triones,<sup>381</sup> 1*H*-pyrazolo-

[1,2-*b*]phthalazine-5,10-dione derivatives<sup>382</sup> over  $Fe_3O_4$ -supported methylene dipyridine,  $Fe_3O_4@SiO_2$ -diazoniabicyclo[2.2.2]octane dichloride (DABCO),  $Fe_3O_4@SiO_2$ -TEMPO, quinuclidine stabilized on  $FeNi_3$  NPs, (3-aminopropyl)-triethoxysilane-modified  $Fe_3O_4$  NPs, aminopropyl coated on magnetic  $Fe_3O_4$  and SBA-15 NPs, etc.

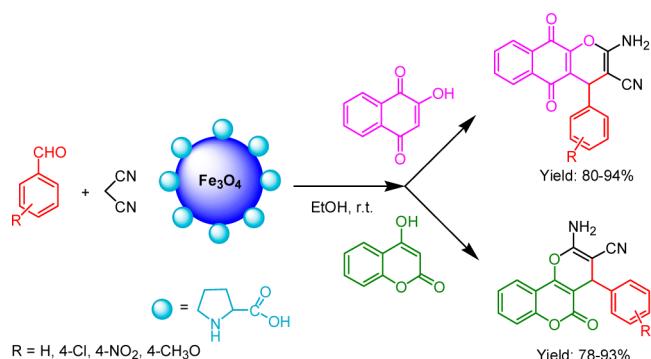
TEMPO (2,2,6,6-tetramethyl-piperidin-1-oxyl) is a remarkable catalyst for oxidation reactions. SBA-15- and MNPs-supported TEMPO have been used to efficiently catalyze the aerobic oxidation of alcohols.<sup>383–385</sup> Karimi and co-workers<sup>378</sup> prepared TEMPO supported on the core–shell  $Fe_3O_4@SiO_2$  MNPs (named MNST) and used this nanomaterial as catalyst in a new domino oxidative Passerini three-component reaction with either primary or secondary alcohols instead of their corresponding aldehydes or ketones (Figure 45). A wide range



**Figure 45.** Oxidative Passerini reaction of alcohols using MNST.

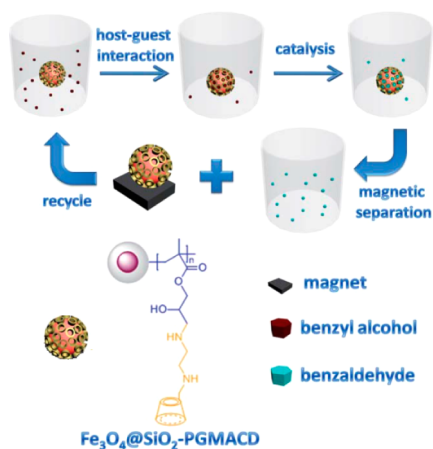
of  $\alpha$ -acyloxy carboxamide compounds were obtained in toluene under a balloon pressure of oxygen at rt in the presence of 10 mol % *tert*-butyl nitrite (TBN) over 1 mol % MNST with moderate to good yields. The test of recyclability was conducted based on the reaction of benzyl alcohol and 4-methoxyphenylacetic acid, and MNST was magnetically removed from the reaction medium; after washing with  $H_2O$  and EtOH it was repeatedly used for 14 consecutive cycles with a slight decline of catalytic activity.

Proline-stabilized  $Fe_3O_4$  NPs were readily constructed in one pot without any supplemental linkers using commercially available Fe precursors and proline.<sup>380</sup> This catalyst with a mean diameter of around 43 nm was examined in the synthesis of chromene derivatives. The synthetic procedure was divided into two steps: condensation of benzaldehyde and malononitrile and ring annulations with 2-hydroxynaphthalene-1,4-dione or 4-hydroxycoumarin (Figure 46).<sup>380</sup> A series of functionalized chromene derivatives was synthesized under ambient conditions in excellent yields. The recyclability investigation revealed that use of a magnet allowed easy recovery of the catalyst that was successively reused for at least four times without loss in activity nor any iron leaching.



**Figure 46.** Synthesis of chromene derivatives using  $\text{Fe}_3\text{O}_4$ -proline MNPs.

As an essential catalyst for production of chemicals,  $\beta$ -cyclodextrin was grafted with MNPs, and this catalyst was then applied to promote the nucleophilic substitution reaction of benzyl halide<sup>386</sup> and selective oxidation of alcohols.<sup>387</sup>  $\text{Fe}_3\text{O}_4@$  $\text{SiO}_2$ -anchored  $\beta$ -cyclodextrin (named  $\text{Fe}_3\text{O}_4@$  $\text{SiO}_2$ -PGMACD) was readily prepared by polymerization on the surfaces of  $\text{Fe}_3\text{O}_4@$  $\text{SiO}_2$  and catalyzed the ring-opening reaction of epoxy groups.  $\text{Fe}_3\text{O}_4@$  $\text{SiO}_2$ -PGMACD showed a high performance in the selective oxidation of alcohols using NaOCl as an oxidant, and its catalytic activity was similar to that of pure  $\beta$ -cyclodextrin.<sup>388</sup> Magnetic separation property and excellent recyclability of  $\text{Fe}_3\text{O}_4@$  $\text{SiO}_2$ -PGMACD were obtained in the oxidation of benzyl alcohol (Figure 47).



**Figure 47.** Schematic representation of the substrate-selective catalysis and recycling of the immobilized catalyst  $\text{Fe}_3\text{O}_4@$  $\text{SiO}_2$ -PGMACD.<sup>388</sup> Reprinted with permission from ref 388. Copyright 2011 Royal Society of Chemistry.

Magnetic nanomaterials make a bridge between homogeneous and heterogeneous catalysts, and their use keeps the remarkable catalytic activity of homogeneous catalysts while providing recycling possibilities through simple magnetic separation. Dendrimers possess the same capability in catalysis.<sup>389–392</sup> Ouali et al.<sup>393</sup> prepared both magnetic nanomaterial- and dendrimer-supported organocatalysts. First, the Jørgensen–Hayashi catalyst [(*S*)- $\alpha,\alpha$ -diphenylprolinol trimethylsilyl ether] was immobilized onto the surface of polymer-coated Co/C nanobeads and at the periphery of phosphorus dendrimers (generations 1–3). Both supported catalysts provided high performance in terms of activities and

selectivities in the Michael additions of various aldehydes with nitroolefins (Figure 48). After completion of the reaction, these catalysts were recovered by magnetic decantation and precipitation with pentane, respectively. A phosphorus dendrimer (generation 3) supported catalyst was reused for at least 4 runs without loss of activity; however, an obvious decrease in activity of Co/C-immobilized catalyst was detected.

Other recent reactions catalyzed by magnetic organocatalysts include asymmetric Friedel–Crafts alkylation of *N*-substituted pyrroles with  $\alpha,\beta$ -unsaturated aldehydes catalyzed by  $\text{Fe}_3\text{O}_4$ -supported MacMillan,<sup>394</sup> regioselective epoxide ring opening with phenol catalyzed by MNPs-immobilized dimethylamino-pyridine,<sup>395</sup> phospho–Michael addition of diethyl phosphate catalyzed by  $\gamma$ - $\text{Fe}_2\text{O}_3$ -pyridine,<sup>396</sup> C–S bond formation catalyzed by mPANI/ $\text{Fe}_3\text{O}_4$  nanocomposite,<sup>397</sup> selective oxidation of sulfide catalyzed by  $\text{Fe}_3\text{O}_4$ -supported DABCO,<sup>398</sup> reduction of methylene blue dye catalyzed by yolk/shell  $\text{Fe}_3\text{O}_4@$ polypyrrole composites,<sup>399</sup> synthesis of phenylpyrido-[4,3-*d*]pyrimidins catalyzed by ( $\text{Fe}_2\text{O}_3$ )–MCM-41–*n*PrNH<sub>2</sub>,<sup>400</sup> acylation catalyzed vitamin B1 supported on  $\gamma$ - $\text{Fe}_2\text{O}_3@$  $\text{SiO}_2$ ,<sup>401</sup> and Knoevenagel condensation catalyzed by polyvinyl amine-coated  $\text{Fe}_3\text{O}_4@$  $\text{SiO}_2$  NPs.<sup>402</sup>

### 2.3. Magnetically Recyclable Biocatalysts

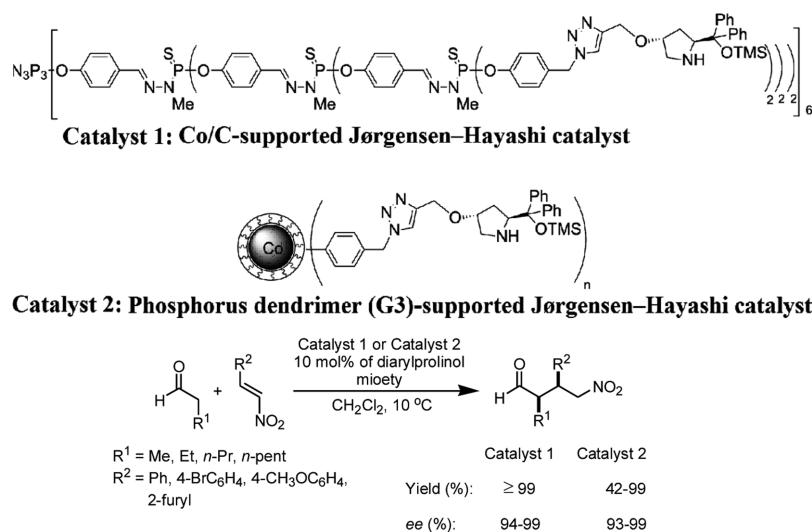
Magnetically recyclable biocatalysts were developed during the past 2 years, and some new immobilization methods of enzymes and new magnetic supports were explored.

Silica-coated MNPs are still the most involved supports for biocatalysts.<sup>403</sup> Zhang et al.<sup>404</sup> demonstrated that  $\alpha$ -amylase supported on amine-functionalized  $\text{SiO}_2@$  $\text{Fe}_3\text{O}_4$  NPs with high loading (235 mg/g) were readily prepared through adsorptive immobilization. The magnetic biocatalyst was evaluated in the hydrolysis of starch that is a polymer of many glucose units. The catalytic activities of immobilized and free  $\alpha$ -amylase were measured by amylase activity units that were defined as the required amount of enzyme to hydrolyze 1 mg of starch in 1 h under appointed conditions. The activity of immobilized  $\alpha$ -amylase was about 80% of that of the nonimmobilized counterpart. However, the presented magnetic  $\alpha$ -amylase was recycled for at least three runs while maintaining similar enzymatic activity. Amine-functionalized  $\text{SiO}_2@$  $\text{Fe}_3\text{O}_4$  NPs were also used to anchor porcine pancrease lipase via covalent immobilization, from which the enhancement of stability (in terms of thermal, pH, and storage) and catalytic activity were observed.<sup>405</sup>

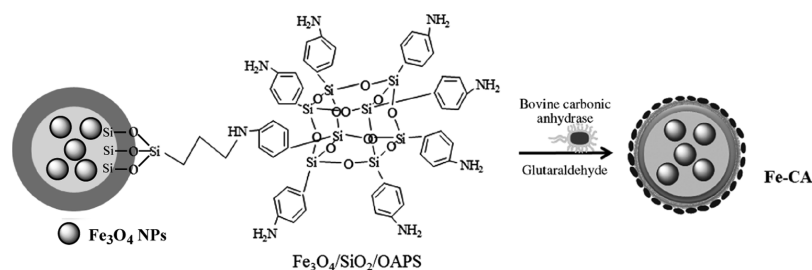
A recent study revealed that carbonic anhydrase (CA) provided excellent enzymatic activity in the catalytic conversion of  $\text{CO}_2$  to bicarbonate.<sup>406</sup> Subsequently, bovine CA was successfully immobilized on (octa(aminophenyl)-silsesquioxane)-modified  $\text{Fe}_3\text{O}_4@$  $\text{SiO}_2$  NPs via covalent bonding (Figure 49).<sup>407</sup> This magnetic biocatalyst with good storage stability displayed satisfactory activity for sequestration of  $\text{CO}_2$  even after 30 reaction cycles using an external magnetic field as a separating tool.

In addition to  $\text{SiO}_2$ -capped iron oxide NPs, other magnetic supports such as alpha chymotrypsin-coated  $\text{Fe}_3\text{O}_4$ ,<sup>408</sup> iron oxide filled magnetic carbon nanotube,<sup>409</sup> a surfactant gum arabic-coated  $\text{Fe}_3\text{O}_4$  NPs,<sup>410</sup> and silica-based  $\beta$ -cyclodextrin<sup>411</sup> were synthesized and used to bind enzymes via covalent<sup>412,413</sup> and noncovalent immobilization<sup>414</sup> to construct magnetically recyclable biocatalysts.

Since the discovery of carbon nanotubes (CNTs) in 1991,<sup>415,416</sup> they have received considerable attention to date



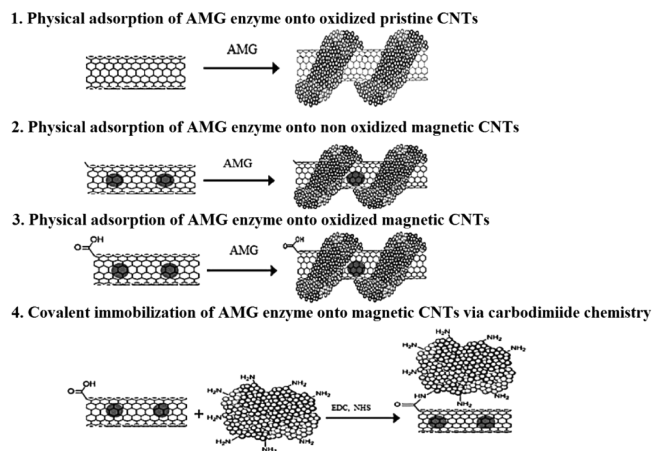
**Figure 48.** Addition of propanal  $\beta$ -nitrostyrene in the presence of dendrimer- and MNPs-supported Jørgensen-Hayashi catalysts.<sup>393</sup> Reprinted with permission from ref 393. Copyright 2013 Wiley-VCH Verlag GmbH & Co.



**Figure 49.** Immobilization of bovine carbonic anhydrase on encapsulated MNPs.<sup>407</sup> Reprinted with permission from ref 407. Copyright 2012 Wiley-VCHVerlagGmbH & Co.

toward various applications, in particular in catalysis because of their high surface area, strong adsorption ability, and great accessibility. CNTs-supported enzymes with high stability have been reported;<sup>417</sup> however, the inconvenient recovery restricted their industrial applications.<sup>418</sup> Use of MNPs-filled CNTs is a promising protocol to solve the issue. Pastorin's group<sup>419</sup> designed and synthesized Amloglucosidase (AMG) supported on CNTs and MNPs-filled CNTs, and immobilization was achieved through physical adsorption and covalent immobilization (Figure 50). The immobilized enzymes disclosed high storage stability in acetate buffer at 4 °C. Their activities were determined upon using starch as the substrate, and lower activity was found compared to free AMG; pristine CNTs provided better activity than magnetic CNTs. Excellent recyclability was observed in all cases of supported AMG. Owing to their magnetic property, magnetic CNTs-supported AMG were easily and efficiently recovered from the reaction medium using a magnet.

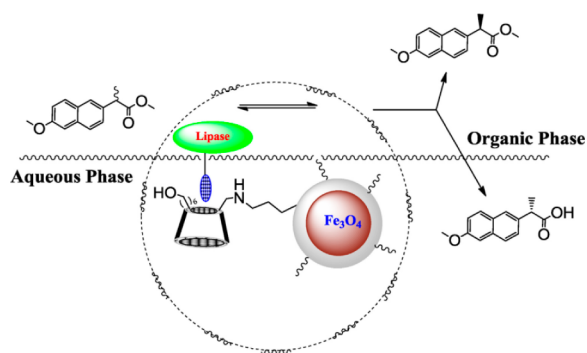
Use of  $\beta$ -cyclodextrin-grafted MNPs as support for immobilization of lipase was reported for the first time by Yilmaz et al.<sup>411</sup> In the synthetic process the presynthesized  $\beta$ -cyclodextrin-grafted  $\text{Fe}_3\text{O}_4$  NPs were readily encapsulated with *Candida rugosa* lipase forming magnetic lipase that was applied as catalyst to the hydrolysis of *p*-nitro-phenylpalmitate and enantioselective hydrolysis of racemic Naproxen methyl ester (Figure 51). These reactions proceeded in an aqueous buffer solution/isooctane reaction system, providing high conversion and enantioselectivity ( $E$  value = 399). For comparison, the enantioselective hydrolysis reaction was also carried out over



**Figure 50.** Immobilization of AMG on CNTs.<sup>419</sup> Reprinted with permission from ref 419. Copyright 2012 American Chemical Society.

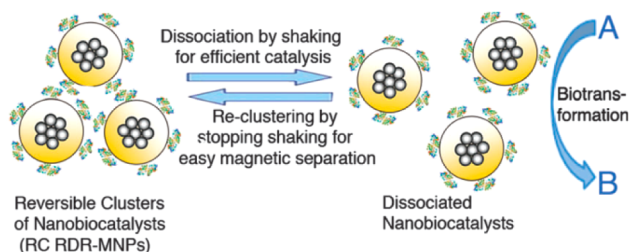
free lipase, and an  $E$  value of 137 was measured, which indicated that immobilization of lipase brought about a remarkable enhancement of enantioselectivity. In addition, the immobilized biocatalyst was magnetically collected and reused.

The size of nanocatalysts is a crucial factor for their catalytic performance. In general, nanocatalysts with smaller diameter exhibit better activity compared to larger versions. In the catalytic application of MNPs-anchored catalysts, a shorter separation time is required especially for biocatalysts, which is



**Figure 51.** Catalysis of enantioselective hydrolysis of rasemic Naproxen methyl ester by  $\beta$ -cyclodextrin-grafted MNPs-supported lipase.<sup>411</sup> Reprinted with permission from ref 411. Copyright 2013 Elsevier B.V.

provided by the use of MNPs of small size. Li et al.<sup>420,421</sup> developed a practical method to reach this challenge. A novel cluster of magnetic nanobiocatalysts based on alcohol dehydrogenase (RDR) was successfully prepared via non-covalent immobilization. The cluster was reversibly formed and dissociated to individual enzyme-modified MNPs under general shaking conditions, and NPs of smaller size were potential biocatalysts with high activity. When shaking was stopped, the individual MNPs reclustered to form easily separated original clusters of magnetic biocatalysts (Figure 52). The reversible

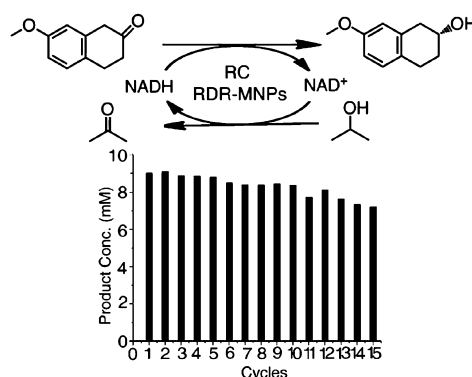


**Figure 52.** Reversible cluster formation of magnetic nanobiocatalysts.<sup>420,421</sup> Reprinted with permission from ref 421. Copyright 2012 Royal Society of Chemistry.

clustering of RDR-MNPs (RC RDR-MNPs) with high enzyme loading afforded the same activity and enantioselectivity as the free enzyme in the bioreduction of 7-methoxy 2-tetralone to produce (*R*)-7-methoxy-2-tetralol.<sup>420,421</sup> The presented biocatalyst was quickly and completely separated with a hand-held magnet and recycled for 15 runs with an acceptable decrease in activity and an enantioselectivity similar to that of the original catalyst (Figure 53).<sup>421</sup>

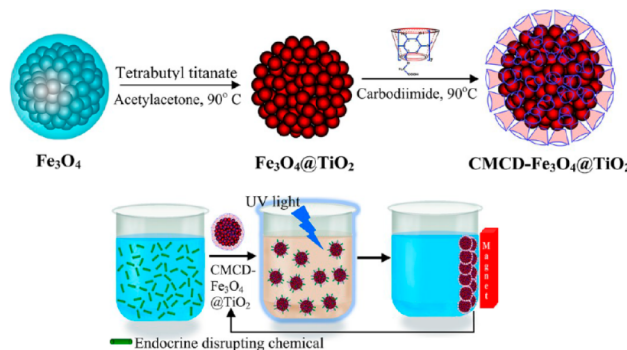
#### 2.4. Magnetically Recyclable Photocatalysts in the Degradation of Pollutants

TiO<sub>2</sub> NPs are the most used catalysts in the photodegradation of pollutants, and a series of novel MNPs-supported TiO<sub>2</sub> NPs was designed and prepared. A core-shell structure of Fe<sub>3</sub>O<sub>4</sub>/SiO<sub>2</sub>/TiO<sub>2</sub> composite was synthesized via the layer-by-layer technique.<sup>422</sup> In the process of immobilizing TiO<sub>2</sub> on presynthesized SiO<sub>2</sub>@Fe<sub>3</sub>O<sub>4</sub> it was found that treatment of silica surface with poly(acrylic acid) led to an enhanced stability of the photocatalyst through formation of a covalent bond between TiO<sub>2</sub> nanocrystals and silica. Moreover, the existence of the SiO<sub>2</sub> shell prevented photodissolution and transfer of electrons-holes from TiO<sub>2</sub> to core particle, and thus, the



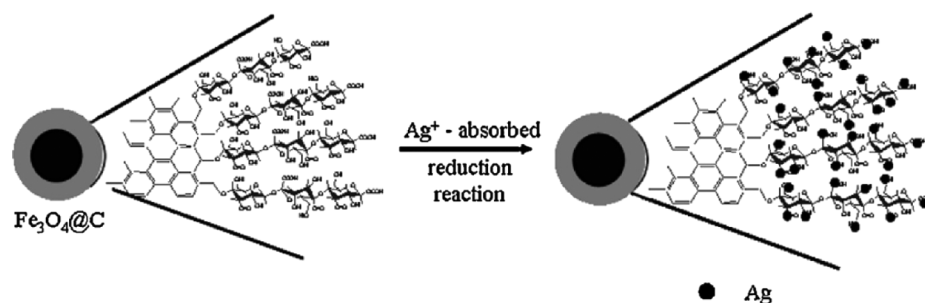
**Figure 53.** Enantioselective reduction of 7-methoxy-2-tetralone catalyzed by RC RDR-MNPs and recycling test.<sup>421</sup> Reprinted with permission from ref 421. Copyright 2012 Royal Society of Chemistry.

photocatalytic activity in the degradation of rhodamine B became promoted under UV illumination.<sup>422</sup> Another supported TiO<sub>2</sub> nanomaterial on SiO<sub>2</sub>@CoFe<sub>2</sub>O<sub>4</sub> showed excellent catalytic activity in the degradation of MB under UV irradiation, and 98.3% of MB was removed within 40 min.<sup>423</sup> Vasudevan et al.<sup>424</sup> demonstrated that cyclodextrin-modified Fe<sub>3</sub>O<sub>4</sub>@TiO<sub>2</sub> NPs (CMCD-Fe<sub>3</sub>O<sub>4</sub>@TiO<sub>2</sub>) were easily prepared and used as photocatalyst in the decomposition of endocrine-disrupting chemicals. The reaction was successfully carried out in water thanks to the aqueous dispersibility of the nanocatalyst containing a cyclodextrin component. During the reaction process, the organic pollutant was captured and destroyed by CMCD-Fe<sub>3</sub>O<sub>4</sub>@TiO<sub>2</sub> under UV irradiation (Figure 54).<sup>424</sup> On the basis of the case of the photo-



**Figure 54.** Synthesis of cyclodextrin-modified Fe<sub>3</sub>O<sub>4</sub>@TiO<sub>2</sub> NPs and their application to the photocatalytic degradation of endocrine-disrupting chemicals in water supplies.<sup>424</sup> Reprinted with permission from ref 424. Copyright 2013 American Chemical Society.

degradation of bisphenol A, after completion of reaction, the catalysts were magnetically separated and reused 10 times with a slight decline of photocatalytic activity. As mentioned in the Introduction, both coupling with other semiconductors and doping with other elements are good ways to improve the photocatalytic property of TiO<sub>2</sub> NPs. In the past 2 years, samarium-doped mesoporous TiO<sub>2</sub> (Sm/MTiO<sub>2</sub>) coated Fe<sub>3</sub>O<sub>4</sub> photocatalysts,<sup>425</sup> magnetic and porous TiO<sub>2</sub>/ZnO/Fe<sub>3</sub>O<sub>4</sub>/PANI,<sup>426</sup> core-shell nano-TiO<sub>2</sub>/Al<sub>2</sub>O<sub>3</sub>/NiFe<sub>2</sub>O<sub>4</sub> hybrid,<sup>427</sup> nano-TiO<sub>2</sub>/C/Fe<sub>x</sub>O<sub>y</sub>,<sup>428</sup> and Fe<sub>3</sub>O<sub>4</sub>@SiO<sub>2</sub>@TiO<sub>2</sub>-Ag composites were prepared and used in degradation of MB, MO, MO, RB 5, and RhB, respectively, either under UV light or in



**Figure 55.** Schematic illustration of the synthetic process to Ag-loaded  $\text{Fe}_3\text{O}_4@\text{C}$  NPs.<sup>433</sup> Reprinted with permission from ref 433. Copyright 2013 Elsevier Ltd.

sunlight, and enhanced catalytic performance was observed in all cases.

A wide range of non- $\text{TiO}_2$ -based metal oxides (including  $\text{CuO}$ ,  $\text{ZnO}$ ,  $\text{MnO}_2$ ,  $\text{Fe}_2\text{O}_3$ ,  $\text{Fe}_3\text{O}_4$ , and  $\text{Al}_2\text{O}_3$ ) and metal sulfides (including  $\text{CdS}$ ,  $\text{CuS}$ ,  $\text{ZnS}$ ,  $\text{MnS}$ ,  $\text{Sb}_2\text{S}_3$ ,  $\text{In}_2\text{S}_3$ , and  $\text{Bi}_2\text{S}_3$ ) also exhibited good visible-light-driven catalytic activity. Several magnetic photocatalysts without  $\text{TiO}_2$  were exploited and studied in degradation of organic pollutants, especially for effluents of textile wastewater. Sahu's group<sup>429</sup> assembled magnetic  $\text{SrFe}_{12}\text{O}_{19}$  and  $\text{SrFe}_{11.4}\text{Al}_{0.6}\text{O}_{19}$  by the microwave combustion method and followed by calcinations at high temperature. Both of them exhibited photocatalytic activity for decomposition of Congo red (CR) under visible and sun lights due to their low band gap. They were efficiently removed from the reaction medium using a magnetic field thanks to the reasonably high values of magnetization. Wang et al.<sup>430</sup> reported that the  $(\text{Cu}-\text{Fe}_2\text{O}_3/\text{Fe})@\text{C}$  hybrid remarkably promoted oxidative photodegradation of MB (>90% of conversion in a short time) under UV-vis light irradiation. The high catalytic property was attributed to the surface-rich electrons of the carbon shell and the capacity of generation of photoelectrons and holes.  $\gamma\text{-Fe}_2\text{O}_3$  NPs with a mean diameter of 35 nm displayed effective activity for the photodegradation of rose bengal (RB) and MB dyes under visible-light irradiation. The catalyst was recovered upon applying an external magnetic field to capture the  $\gamma\text{-Fe}_2\text{O}_3$  NPs.<sup>431</sup> A Ni/ZnO nanomaterial was prepared by reduction of Ni ions via the solvothermal method followed by surface modification. The hexagonal Ni/ZnO nanostructure showed effective photocatalytic activity toward degradation MB molecules under visible-light irradiation and was easily recoverable in the presence of a magnetic field for successive reuses.<sup>432</sup>

Ag nanocrystals with a nearly spherical structure having a mean diameter of 10 nm were immobilized on carbonaceous polysaccharides shell-coated MNPs via direct adsorption of silver ions to core-shell MNPs followed by reduction of the silver ions (Figure 55).<sup>433</sup> Degradation of the pollutant neutral red was chosen as the model reaction for investigation of the photocatalytic activity. Photodegradation proceeded smoothly over this  $\text{Fe}_3\text{O}_4@\text{C}@\text{Ag}$  hybrid NPs under visible light, providing 93.7% of degradation within 30 min. In addition, the magnetic separation of the hybrid NPs was easily achieved using a hand-held magnet.

Graphene as catalyst support efficiently enhances the catalytic effect of these common photocatalysts. Graphene-supported metal oxides ( $\text{TiO}_2$  and  $\text{ZnO}$ ) have been identified as excellent heterogeneous photocatalysts in degradation of pollutants under UV irradiation.<sup>434,435</sup> Wang et al. found that the composites consisting of graphene and  $\text{MFe}_2\text{O}_4$  ( $\text{M} = \text{Zn}$ ,

$\text{Co}$ ,  $\text{Ni}$ ,  $\text{Mn}$ , and  $\text{Cu}$ )<sup>436–439</sup> exhibited good photoactivity in the degradation of dyes and were simply recovered upon applying an external magnetic field. The same group<sup>440</sup> fabricated a magnetically recoverable hybrid  $\text{P25}-\text{CoFe}_2\text{O}_4$ -graphene (P25, a sort of  $\text{TiO}_2$  NPs) via hydrothermal approach in order to combine the advantages of each component in photocatalysis. This nanocomposite was utilized as catalyst in the visible-light-driven photodegradation of various organic dyes.  $\text{P25}-\text{CoFe}_2\text{O}_4$ -graphene was superior to  $\text{CoFe}_2\text{O}_4$ -graphene,  $\text{P25}-\text{CoFe}_2\text{O}_4$ , and  $\text{P25}$ -graphene photocatalysts, the enhancement of activity being caused by the synergistic effect among the individual components. The photocatalyst was collected with a hand-held magnet and reused. On the basis of the report on the fabrication of  $\text{Fe}_{2.25}\text{W}_{0.75}\text{O}_4$  through doping in a  $\text{Fe}_3\text{O}_4$  host matrix,<sup>441</sup> a novel bifunctional RGO-immobilized  $\text{Fe}_{2.25}\text{W}_{0.75}\text{O}_4$  nanomaterial was synthesized through a one-pot hydrothermal method. The composite with excellent thermal stability displayed higher performance than pure  $\text{Fe}_{2.5}\text{W}_{0.75}\text{O}_4$  NPs in the degradation of MO under UV-light irradiation, which was attributed to the enhancing effect of graphene. The hybrid displayed remarkable recyclability with an external magnet thanks to its magnetic property.<sup>442</sup>

### 3. CONCLUSIONS AND OUTLOOK

As shown here, catalysis with magnetically recyclable nanocatalysts is a rapidly growing field in the context of the high demands for development of sustainable and green chemistry. In order to prevent aggregation and achieve grafting catalyst species on presynthesized MNPs, modification and functionalization of MNPs with stabilizing ligands or coating/encapsulating materials (including small molecules, silica, polymers, carbon, ionic liquids, mesoporous materials, graphene, carbon nanotubes) are essential. Further covalent or noncovalent binding processes to transition metal catalysts, organocatalysts, and enzymes efficiently provided various magnetically recoverable catalysts that were used in a wide range of reactions during the past 2 years, such as Suzuki, Heck, Sonogashira, Hiyama, alkyne-azide cycloaddition, hydrogenation, reduction, oxidation, arylation, alkylation, epoxidation of alkenes, multicomponent "one-pot" synthesis, Fenton-like reaction, etc.

Although remarkable progress has been made using magnetically recoverable catalysts in terms of diversity of the reactions, activity, selectivity, and recyclability, both the intrinsic instability of MNPs over a long period of time and the leaching of catalysts under harsh conditions remain the major problems yet to be solved in many reported results. Development of new multifunctionalized materials and useful

methods of immobilizing catalysts units are still required in order to overcome these problems.

Extension of the scope of the field by exploring more magnetically recyclable catalysts for more organic transformations is also called for. For instance, seeking magnetic plasmonic photocatalysts based on AuNPs, AgNPs, and CuNPs for promoting other organic transformations in environmentally friendly and energy sustainable protocol using the application of magnetically recyclable photocatalysts in the degradation of pollutants is a challenging goal.<sup>89,90</sup> Increased use of bimetals (Fe, Co, Mo) to replace expansive “noble” metals should be encouraged for increased sustainable processes. Further work is also required to push these magnetically recyclable catalysts to their use in multikilogram-scale synthesis toward industrial production. Given the fast pace of this area, progress, and perspectives it is most certainly only a matter of time before key industrial applications are realized.

## AUTHOR INFORMATION

### Corresponding Author

\*E-mail: d.astruc@ism.u-bordeaux1.fr.

### Notes

The authors declare no competing financial interest.

### Biographies



Dong Wang studied organic chemistry with Professor Baohua Chen at the University of Lanzhou and received his doctoral degree in 2013. He is presently preparing his Ph.D. in the Nanosciences and Catalysis research group of Professor Didier Astruc at the Université de Bordeaux, where he is working on the synthesis and uses of magnetic nanoparticles-supported nanocatalysts.



Didier Astruc is Professor of Chemistry at the University of Bordeaux and Member of the Institut Universitaire de France. He did his Ph.D.

work in Rennes with R. Dabard and his postdoctoral work at MIT with R. R. Schrock. His present interests are in nanomaterials and their applications in catalysis, sensing, and nanomedicine.

## ACKNOWLEDGMENTS

Financial support from the Université de Bordeaux, the Centre National de la Recherche Scientifique (CNRS), and the Chinese Research Council (Ph.D. grant to D.W.) is gratefully acknowledged.

## ABBREVIATIONS

$\beta$ -CD	$\beta$ -cyclodextrin
AAPTS	[ 3 - ( 2 - aminoethylamino) - p r o p y l ] - trimethoxysilane
AMG	amloglucosidase
APTS	3-aminopropyltrimethoxysilane
CA	carbonic anhydrase
CDG	chemically derived graphene
DHAA	dehydroascorbic acid
CNTs	carbon nanotubes
CTAB	cetyltrimethylammonium bromide
CuAAC	copper-catalyzed cycloaddition of alkynes and azides
DABCO	diazoniabicyclo-[2.2.2]octane dichloride
DDBSA	dodecyl benzene-sulfonic acid
DMEC	dimethylethynylcarbinol
DMP	2,6-dimethylphenol; dimethylvinylcarbinol
DOPA	dopamine hydrochloride
DY	decolorization yield
EA	elemental analysis
<i>E</i> value	enantiomeric ratio for irreversible reactions, $E = \ln[(1 - x)(1 - ee_s)] / \ln[(1 - x)(1 + ee_s)]$ ( $x$ , conversion; $ee_s$ , the enantiomeric excess of the substrate)
Fe CSNPS	iron@iron oxide core-shell nanoparticles
FT-IR	Fourier transform infrared spectroscopy
HMMS	hollow magnetic mesoporous silica spheres

HMS	hollow mesoporous silica spheres	rt	room temperature scanning electron microscopy
HPG	hyperbranched polyglycidol	SEM	scanning electron microscopy
HPMC	hydroxypropylmethylcellulose	SQUID	superconducting quantum interference device
ICP	inductively coupled plasma analysis	TEM	transmission electron microscopy
ILs	ionic liquids	TEMPO	(2,2,6,6-tetramethyl-piperidin-1-oxyl)
GO	graphene oxide	TGA	thermal gravimetric analysis
MagSilica	silica-coated magnetic nanoparticles	VSM	vibrating sample magnetometer
MB	methylene blue	XRD	X-ray diffraction (XRD)
MCF	magnetic Fe <sub>3</sub> O <sub>4</sub> @C	XPS	X-ray photoelectron spectra (XPS)
MCR	multicomponent reaction strategy		
MMS	magnetic mesoporous silica spheres		
MNPs	magnetic nanoparticles		
MO	methyl orange		
MVS	metal vapor synthesis		
MW	microwave		
MWCNT	multiwalled carbon nanotubes		
MY	mineralization yield		
NPs	nanoparticles		
OA	oleic acid		
OAPS	octa(aminophenyl)silsesquioxane		
PAA	poly(acrylic acid)		
PAMAM	polyaminoamido		
PANI	polymer of aniline		
PDA	PDMAEMA, polydopamine		
poly(2-dimethylaminoethyl methacrylate)			
PEA	polyethylenimine		
PEG	poly(ethylene glycol)		
PFMN	phosphine-functionalized magnetic nanoparticles		
PHEMA	poly( <i>N,N'</i> -methylenebis(acrylamide)- <i>co</i> -2-hydroxyethyl methacrylate), poly(glycidyl methacrylate)		
PL	photoluminescence		
PNP	paranitrophenol		
PPO	poly(2,6-dimethyl-1,4-phenylene oxide)		
PS	polystyrene		
PTA	phosphotungstic acid		
RB 5	reactive black 5		
RDR	alcohol dehydrogenase		
RGO	reduced graphene oxide		

## REFERENCES

- (1) Anastas, P. T.; Warner, J. C. *Green Chemistry Theory and Practice*; Oxford University Press: Oxford, 1998.
- (2) Matlack, A. S. *Introduction to Green Chemistry*; Marcel Dekker: New York, 2001.
- (3) Clark, J. H.; Macquarrie, D. J. *Handbook of Green Chemistry and Technology*; Blackwell Publishing: Abingdon, 2002.
- (4) Lancaster, M. *Green Chemistry: An Introductory Text*; RSC: Cambridge, 2002.
- (5) Poliakov, M.; Fitzpatrick, J. M.; Farren, T. R.; Anastas, P. T. *Science* **2002**, *297*, 807.
- (6) Sheldon, R. A. *Chem. Soc. Rev.* **2012**, *41*, 1437.
- (7) Sheldon, R. A. *Chem. Commun.* **2008**, 3352.
- (8) Walsh, P. T.; Li, H.; de Parrodi, C. A. *Chem. Rev.* **2007**, *107*, 2503.
- (9) Nasir Baig, R. B.; Varma, R. S. *Chem. Commun.* **2012**, *48*, 5853.
- (10) Nasir Baig, R. B.; Varma, R. S. *Chem. Soc. Rev.* **2012**, *41*, 1559.
- (11) Gawande, S. B.; Branco, P. S.; Varma, R. S. *ChemSusChem* **2012**, *5*, 65.
- (12) Roduner, E. *Chem. Soc. Rev.* **2006**, *35*, 583.
- (13) Astruc, D.; Lu, F.; Ruiz, J. *Angew. Chem., Int. Ed.* **2005**, *44*, 7852.
- (14) In *Transition-metal Nanoparticles in Catalysis*; Astruc, D., Ed.; Wiley-VCH Verlag GmbH & Co. KGaA: Weinheim, 2008.
- (15) Somorjai, G. A.; Frei, H.; Park, J. Y. *J. Am. Chem. Soc.* **2009**, *131*, 16589.
- (16) Schätz, A.; Reiser, O.; Stark, W. J. *Chem.—Eur. J.* **2010**, *16*, 8950.
- (17) Goesmann, H.; Feldmann, C. *Angew. Chem., Int. Ed.* **2010**, *49*, 1362.
- (18) Arpád, M. *Chem. Rev.* **2011**, *111*, 2251.
- (19) Mondloch, J. E.; Bayram, E.; Finke, R. G. *J. Mol. Catal. A: Chem.* **2012**, *355*, 1.
- (20) Bai, C.; Liu, M. *Nano Today* **2012**, *7*, 258.
- (21) Chng, L. L.; Erathodiyil, N.; Ying, J. Y. *Acc. Chem. Res.* **2013**, *46*, 1825.
- (22) Mitsudome, T.; Kaneda, K. *ChemCatChem* **2013**, *5*, 1681.
- (23) Lu, A.-H.; Salabas, E. L.; Schüth, F. *Angew. Chem., Int. Ed.* **2007**, *46*, 1222.
- (24) Shylesh, S.; Schünemann, V.; Thiel, W. R. *Angew. Chem., Int. Ed.* **2010**, *49*, 3428.
- (25) Zhu, Y.; Stubbs, L. P.; Ho, F.; Liu, R.; Ship, C. P.; Maguire, J. A.; Hosmane, N. S. *ChemCatChem* **2010**, *2*, 365.
- (26) Polshettiwar, V.; Luque, R.; Fihri, A.; Zhu, H.; Bouhrara, M.; Basset, J.-M. *Chem. Rev.* **2011**, *111*, 3036.
- (27) Rossi, L. M.; Garcia, M. A. S.; Vono, L. L. R. *J. Braz. Chem. Soc.* **2012**, *23*, 1959.
- (28) Baig, R. B. N.; Varma, R. S. *Chem. Commun.* **2013**, *49*, 752.

- (29) Zhang, D.; Zhou, C.; Sun, Z.; Wu, L.-Z.; Tung, C.-H.; Zhang, T. *Nanoscale* **2012**, *4*, 6244.
- (30) Hyeon, T. *Chem. Commun.* **2003**, 927.
- (31) Yin, M.; O'Brien, S. *J. Am. Chem. Soc.* **2003**, *125*, 10180.
- (32) Jana, N. R.; Chen, Y.; Peng, X. *Chem. Mater.* **2004**, *16*, 3931.
- (33) Horak, D.; Babic, M.; Mackova, H.; Benes, M. *J. J. Sep. Sci.* **2007**, *30*, 1751.
- (34) Laurent, S.; Forge, D.; Port, M.; Roch, A.; Robic, C.; Vander Elst, L.; Muller, R. N. *Chem. Rev.* **2008**, *108*, 2064.
- (35) Lim, C. W.; Lee, I. S. *Nano Today* **2010**, *5*, 412.
- (36) Gawande, M. B.; Branco, P. S.; Varma, R. S. *Chem. Soc. Rev.* **2013**, *42*, 3371.
- (37) Roy, S.; Pericas, M. A. *Org. Biomol. Chem.* **2009**, *7*, 2669.
- (38) Sreedhar, B.; Kumar, A. S.; Reddy, P. S. *Tetrahedron Lett.* **2010**, *51*, 1891.
- (39) Polshettiwar, V.; Varma, R. S. *Chem.—Eur. J.* **2009**, *15*, 1582.
- (40) Polshettiwar, V.; Varma, R. S. *Org. Biomol. Chem.* **2009**, *7*, 37.
- (41) Gleeson, O.; Tekoriute, R.; Gun'ko, Y. K.; Connon, S. J. *Chem.—Eur. J.* **2009**, *15*, 5669.
- (42) Zheng, Y.; Stevens, P. D.; Gao, Y. *J. Org. Chem.* **2006**, *71*, 537.
- (43) Stevens, P. D.; Li, G.; Fan, J.; Yen, M.; Gao, Y. *Chem. Commun.* **2005**, 4435.
- (44) Kawamura, M.; Sato, K. *Chem. Commun.* **2006**, 4718.
- (45) Hu, A.; Yee, G. T.; Lin, W. *J. Am. Chem. Soc.* **2005**, *127*, 12486.
- (46) Tucker-Schwartz, A.-K.; Garrell, R.-L. *Chem.—Eur. J.* **2010**, *16*, 12718.
- (47) Polshettiwar, V.; Baruwati, B.; Varma, R. S. *Chem. Commun.* **2009**, 1837.
- (48) Polshettiwar, V.; Varma, R. S. *Tetrahedron* **2010**, *66*, 1091.
- (49) Yi, D. K.; Lee, S. S.; Ying, J. Y. *Chem. Mater.* **2006**, *18*, 2459.
- (50) Jin, M.-J.; Lee, D.-H. *Angew. Chem., Int. Ed.* **2010**, *49*, 1119.
- (51) Stevens, P. D.; Fan, J.; Gardimalla, H. M. R.; Yen, M.; Gao, Y. *Org. Lett.* **2005**, *7*, 2085.
- (52) Wang, W.; Xu, Y.; Wang, D. I. C.; Li, Z. *J. Am. Chem. Soc.* **2009**, *131*, 12892.
- (53) Rosario-Amorin, D.; Wang, X.; Gaboyard, M.; Clérac, R.; Nlate, S.; Heuze, K. *Chem.—Eur. J.* **2009**, *15*, 12636.
- (54) Yinghuai, Z.; Kuijin, L.; Huimin, N.; Chuanzhao, L.; Stubbs, L. P.; Siong, C. F.; Mnhua, T.; Peng, S. C. *Adv. Synth. Catal.* **2009**, *351*, 2650.
- (55) Xuan, S.; Wang, Y. J.; Yu, J. C.; Leung, K. C. *Langmuir* **2009**, *25*, 11835.
- (56) Yeo, K. M.; Lee, S. I.; Lee, Y. T.; Chung, Y. K.; Lee, I. S. *Chem. Lett.* **2008**, *37*, 116.
- (57) Wang, Y.; Lee, J. *J. Mol. Catal. A: Chem.* **2007**, *263*, 163.
- (58) Abu-Reziq, R.; Alper, H.; Wang, D.; Post, M. L. *J. Am. Chem. Soc.* **2006**, *128*, 5279.
- (59) Kainz, Q. M.; Schätz, A.; Zöpfl, A.; Stark, W. J.; Reiser, O. *Chem. Mater.* **2011**, *23*, 3606.
- (60) Zheng, X. X.; Luo, S. Z.; Zhang, L.; Cheng, J. P. *Green Chem.* **2009**, *11*, 455.
- (61) Abu-Reziq, R.; Wang, D. S.; Post, M.; Alper, H. *Adv. Synth. Catal.* **2007**, *349*, 2145.
- (62) Zhang, Q.; Su, H.; Luo, J.; Wei, Y. Y. *Green Chem.* **2012**, *14*, 201.
- (63) Jung, J.-Y.; Kim, J.-B.; Taher, A.; Jin, M.-J. *Bull. Korean Chem. Soc.* **2009**, *30*, 3082.
- (64) Lu, A.-H.; Schmidt, W.; Matoussevitch, N.; Bönnemann, H.; Spliethoff, B.; Tesche, B.; Bill, E.; Kiefer, W.; Schüth, F. *Angew. Chem., Int. Ed.* **2004**, *43*, 4303.
- (65) Liu, J.; Qiao, S. Z.; Hu, Q. H.; Lu, G. Q. *Small* **2011**, *7*, 425.
- (66) Zeng, T.; Zhang, X.-L.; Ma, Y.-R.; Niu, H.-Y.; Cai, Y.-Q. *J. Mater. Chem.* **2012**, *22*, 18658.
- (67) Ko, S.; Jang, J. *Angew. Chem., Int. Ed.* **2006**, *45*, 7564.
- (68) Deng, J.; Wen, X.; Wang, Q. *Mater. Res. Bull.* **2012**, *47*, 3369.
- (69) Wang, X. Z.; Zhao, Z. B.; Qu, J. Y.; Wang, Z. Y.; Qiu, J. S. *J. Phys. Chem. Solids* **2010**, *71*, 673.
- (70) Correa-Duarte, M. A.; Grzelczak, M.; Salgueirino-Maceira, V.; Giersig, M.; Liz-Marzan, L. M.; Farle, M.; Sieradzki, K.; Diaz, R. *J. Phys. Chem. B* **2005**, *109*, 19060.
- (71) Wan, J. Q.; Cai, W.; Feng, J. T.; Meng, X. X.; Liu, E. Z. *J. Mater. Chem.* **2007**, *17*, 1188.
- (72) Liu, Y.; Jiang, W.; Wang, Y.; Zhang, X. J.; Song, D.; Li, F. S. *J. Magn. Magn. Mater.* **2009**, *321*, 408.
- (73) Lv, G.; Mai, W.; Jin, R.; Gao, L. *Synlett* **2008**, *9*, 1418.
- (74) Nealon, G. L.; Donnio, B.; Greget, R.; Kappler, J.-P.; Terazzi, E.; Gallani, J.-L. *Nanoscale* **2012**, *4*, 5244.
- (75) Leung, K. C.; Xuan, S.; Zhu, X.; Wang, D.; Chak, C.-P.; Lee, S.-F.; Hob, W. K.-W.; Chung, B. C.-T. *Chem. Soc. Rev.* **2012**, *41*, 1911.
- (76) Goodman, D. W. *Chem. Rev.* **1995**, *95*, 523.
- (77) Campbell, C. T.; Sellers, J. R. V. *Faraday Discuss.* **2013**, *162*, 9.
- (78) Zaera, F. *ChemSusChem* **2013**, *6*, 1797.
- (79) Zhang, D. H.; Li, H. B.; Li, G. D.; Chen, J. S. *Dalton Trans.* **2009**, 10527.
- (80) Dalkó, P. I.; Moisan, L. *Angew. Chem., Int. Ed.* **2004**, *43*, 5138.
- (81) Luque, R.; Babita, B.; Varma, R. S. *Green Chem.* **2010**, *12*, 1540.
- (82) Xu, H.-J.; Wan, X.; Geng, Y.; Xu, X.-L. *Curr. Org. Chem.* **2013**, *17*, 1034.
- (83) Lee, S.-M.; Koo, Y.-M.; Kwak, J. H.; Park, H. G.; Chang, H. N.; Hwang, M.; Park, J.-G.; Kim, J.; Hyeon, T. *Small* **2008**, *4*, 143.
- (84) Netto, C. G. C. M.; Toma, H. E.; Andrade, L. H. J. *Mol. Catal. B: Enzym.* **2013**, *85–86*, 71.
- (85) Medina-Castillo, A. L.; Morales-Sanfrutos, J.; Megia-Fernandez, A.; Fernandez-Sanchez, J. F.; Santoyo-Gonzalez, F.; Fernandez-Gutierrez, A. *J. Polym. Sci., Part A: Polym. Chem.* **2012**, *50*, 3944.
- (86) Huang, J.; Li, X.; Zheng, Y.; Zhang, Y.; Zhao, R.; Gao, X.; Yan, H. *Macromol. Biosci.* **2008**, *8*, 508.
- (87) Robinson, P. J.; Dunnill, P.; Lilly, M. D. *Biotechnol. Bioeng.* **1973**, *15*, 603.
- (88) Yiu, H. H. P.; Keane, M. A. *J. Chem. Technol. Biotechnol.* **2012**, *87*, 583.
- (89) Prier, C. K.; Rankic, D. A.; MacMillan, D. W. C. *Chem. Rev.* **2013**, *113*, 5322.
- (90) Lang, X.; Chen, X.; Zhao, J. *Chem. Soc. Rev.* **2014**, *43*, 473.
- (91) Watson, S.; Beydoun, D.; Amal, R. *J. Photochem. Photobiol., A* **2002**, *148*, 303.
- (92) Kostedt, W. L.; Drwiega, J.; Mazyck, D. W.; Lee, S. W.; Sigmund, W.; Wu, C. Y.; Chadik, P. *Environ. Sci. Technol.* **2005**, *39*, 8052.
- (93) Mahmoudi, M.; Simchi, A.; Imani, M. *J. Phys. Chem. C* **2009**, *113*, 9573.
- (94) Alexiou, C.; Jurgons, R.; Seliger, C.; Iro, H. *J. Nanosci. Nanotechnol.* **2006**, *6*, 2762.
- (95) Tryba, B.; Morawski, A. W.; Inagaki, M. *Appl. Catal. B: Environ.* **2003**, *46*, 203.
- (96) Fujishima, A.; Rao, T. N.; Tryk, D. A. *J. Photochem. Photobiol. C* **2000**, *1*, 1.
- (97) Strini, A.; Cassese, S.; Schiavi, L. *Appl. Catal. B: Environ.* **2005**, *61*, 90.
- (98) Thompson, T. L.; Yates, J. T., Jr. *Chem. Rev.* **2006**, *106*, 4428.
- (99) Lee, S.-Y.; Park, S.-J. *J. Ind. Eng. Chem.* **2013**, *9*, 1761.
- (100) Singh, S.; Mahalingam, H.; Singh, P. K. *Appl. Catal. A: Gen.* **2013**, *462–463*, 178.
- (101) Asahi, R.; Morikawa, T.; Ohwaki, T. *Science* **2001**, *293*, 269.
- (102) Ao, Y.; Xu, J.; Zhang, S.; Fu, D. *J. Phys. Chem. Solids* **2009**, *70*, 1042.
- (103) Upadhyay, R. K.; Soin, N.; Roy, S. S. *RSC Adv.* **2014**, *4*, 3823.
- (104) Yang, M.-Q.; Xu, Y.-J. *Phys. Chem. Chem. Phys.* **2013**, *15*, 19102.
- (105) Xu, D.; Liu, Z.; Yang, H.; Yang, Q.; Zhang, J.; Fang, J.; Zou, S.; Sun, K. *Angew. Chem., Int. Ed.* **2009**, *48*, 4217.
- (106) An, K.; Alayoglu, S.; Ewers, T.; Somorjai, G. A. *J. Colloid Interface Sci.* **2012**, *373*, 1.
- (107) Silva, T. A. G.; Landers, R.; Rossi, L. M. *Catal. Sci. Technol.* **2013**, *3*, 2993.
- (108) Chen, G.; Desinan, S.; Nechache, R.; Rosei, R.; Rosei, F.; Ma, D. *Chem. Commun.* **2011**, *47*, 6308.
- (109) Gupta, V. K.; Atar, N.; Yola, M. L.; Üstündağ, Z.; Uzun, L. *Water Res.* **2014**, *48*, 210.

- (110) Gawande, M. B.; Guo, H.; Rathi, A. K.; Branco, P. S.; Chen, Y.; Varmad, R. S.; Peng, D.-L. *RSC Adv.* **2013**, *3*, 1050.
- (111) Zeng, T.; Zhang, X.; Wang, S.; Ma, Y.; Niu, H.; Cai, Y. *J. Mater. Chem. A* **2013**, *1*, 11641.
- (112) Yao, T.; Cui, T.; Fang, X.; Cui, F.; Wu, J. *Nanoscale* **2013**, *5*, 5896.
- (113) Hu, J.; Chen, M.; Fang, X. S.; Wu, L. M. *Chem. Soc. Rev.* **2011**, *40*, 5472.
- (114) Suzuki, A. *Angew. Chem., Int. Ed.* **2011**, *50*, 6723.
- (115) Li, C.-J. *Chem. Rev.* **1993**, *93*, 2023.
- (116) Miyaura, N.; Suzuki, A. *Chem. Rev.* **1995**, *95*, 2457.
- (117) Li, W.; Zhang, B.; Li, X.; Zhang, H.; Zhang, Q. *Appl. Catal. A: Gen.* **2013**, *459*, 65.
- (118) Wang, P.; Zhang, F.; Long, Y.; Xie, M.; Li, R.; Ma, J. *Catal. Sci. Technol.* **2013**, *3*, 1618.
- (119) Sun, J.; Dong, Z.; Sun, X.; Li, P.; Zhang, F.; Hu, W.; Yang, H.; Wang, H.; Li, R. *J. Mol. Catal. A: Chem.* **2013**, *367*, 46.
- (120) Alonso, A.; Shafir, A.; Macanás, J.; Vallribera, A.; Muñoz, M.; Muraviev, D. N. *Catal. Today* **2012**, *193*, 200.
- (121) Li, S.; Zhang, W.; Sob, M.-H.; Che, C.-M.; Wang, R.; Chen, R. *J. Mol. Catal. A: Chem.* **2012**, *359*, 81.
- (122) Schätz, A.; Long, T. R.; Grass, R. N.; Stark, W. J.; Hanson, P. R.; Reiser, O. *Adv. Funct. Mater.* **2010**, *20*, 4323.
- (123) Zeltner, M.; Schätz, A.; Hefti, M. L.; Stark, W. J. *J. Mater. Chem.* **2011**, *21*, 2991.
- (124) Rosario-Amorin, D.; Gaboyard, M.; Clérac, R.; Vellutini, L.; Nlate, S.; Heuzé, K. *Chem.—Eur. J.* **2012**, *18*, 3305.
- (125) Wang, J.; Xu, B.; Sun, H.; Song, G. *Tetrahedron Lett.* **2013**, *54*, 238.
- (126) Hu, J.; Wang, Y.; Han, M.; Zhou, Y.; Jiang, X.; Sun, P. *Catal. Sci. Technol.* **2012**, *2*, 2332.
- (127) Zhu, M.; Diao, G. J. *Phys. Chem. C* **2011**, *115*, 24743.
- (128) Senapati, K. K.; Roy, S.; Borgohain, C.; Phukan, P. *J. Mol. Catal. A: Chem.* **2012**, *352*, 128.
- (129) Singh, A. S.; Patil, U. B.; Nagarkar, J. M. *Catal. Commun.* **2013**, *35*, 11.
- (130) de Rivera, F. G.; Angurell, I.; Rossell, M. D.; Erni, R.; Llorca, J.; Divins, N. J.; Muller, G.; Seco, M.; Rossell, O. *Chem.—Eur. J.* **2013**, *19*, 11963.
- (131) Costa, N. J. S.; Kiyohara, P. K.; Monteiro, A. L.; Coppel, Y.; Philippot, K.; Rossi, L. M. *J. Catal.* **2010**, *276*, 382.
- (132) Choi, K.-H.; Shokouhimehr, M.; Sung, Y.-E. *Bull. Korean Chem. Soc.* **2013**, *34*, 1477.
- (133) Zhang, Q.; Su, H.; Luo, J.; Wei, Y. *Catal. Sci. Technol.* **2013**, *3*, 235.
- (134) Shylesh, S.; Wang, L.; Thiel, W. R. *Adv. Synth. Catal.* **2010**, *352*, 425.
- (135) Keller, M.; Collière, V.; Reiser, O.; Caminade, A.-M.; Majoral, J.-P.; Ouali, A. *Angew. Chem., Int. Ed.* **2013**, *52*, 3626.
- (136) Yang, H.; Wang, Y.; Qin, Y.; Chong, Y.; Yang, Q.; Li, G.; Zhang, L.; Li, W. *Green Chem.* **2011**, *13*, 1352.
- (137) Beygzadeh, M.; Alizadeh, A.; Khodaei, M. M.; Kordestani, D. *Catal. Commun.* **2013**, *32*, 86.
- (138) Yuan, D.; Zhang, H. *Appl. Catal. A: Gen.* **2014**, *475*, 249.
- (139) Liu, L. F.; Zhang, Y. H.; Xin, B. W. *J. Org. Chem.* **2006**, *71*, 3994.
- (140) Maity, D.; Mollick, M. M. R.; Mondal, D.; Bhowmick, B.; Neogi, S. K.; Banerjee, A.; Chattopadhyay, S.; Bandyopadhyay, S.; Chattopadhyay, D. *Carbohydr. Poly.* **2013**, *98*, 80.
- (141) Yinghuai, Z.; Peng, S. C.; Emi, A.; Zhenshun, S.; Monalisa; Kemp, R. A. *Adv. Synth. Catal.* **2007**, *349*, 1917.
- (142) Khalafi-Nezhad, A.; Panahi, F. *J. Organomet. Chem.* **2013**, *741–742*, 7.
- (143) Li, P.; Wang, L.; Zhang, L.; Wang, G.-W. *Adv. Synth. Catal.* **2012**, *354*, 1307.
- (144) Du, Q.; Zhang, W.; Ma, H.; Zheng, J.; Zhou, B.; Li, Y. *Tetrahedron* **2012**, *68*, 3577.
- (145) Rafiee, E.; Ataei, A.; Nadri, S.; Joshaghani, M.; Eavani, S. *Inorg. Chim. Acta* **2014**, *409*, 302.
- (146) Ghotbinejad, M.; Khosropour, A. R.; Mohammadpoor-Baltork, I.; Moghadam, M.; Tangestaninejad, S.; Mirkhani, V. *RSC Adv.* **2014**, *4*, 8590.
- (147) Safari, J.; Zarnegar, Z. *C. R. Chim.* **2013**, *16*, 821.
- (148) Esmaeilpour, M.; Sardarian, A. R.; Javidi, J. *J. Organomet. Chem.* **2014**, *749*, 233.
- (149) Phan, N. T. S.; Le, H. V. *J. Mol. Catal. A: Chem.* **2011**, *334*, 130.
- (150) Zhang, L.; Li, P.; Li, H.; Wang, L. *Catal. Sci. Technol.* **2012**, *2*, 1859.
- (151) Sreedhar, B.; Kumar, A. S.; Yada, D. *Synlett* **2011**, *8*, 1081.
- (152) Rostovtsev, V. V.; Green, L. G.; Fokin, V. V.; Sharpless, K. B. *Angew. Chem., Int. Ed.* **2002**, *41*, 2596.
- (153) Tornøe, C. W.; Christensen, C.; Meldal, M. *J. Org. Chem.* **2002**, *67*, 3057.
- (154) Kolb, H. C.; Finn, M. G.; Sharpless, K. B. *Angew. Chem., Int. Ed.* **2001**, *40*, 2004.
- (155) Kaboudin, B.; Mostafalua, R.; Yokomatsu, T. *Green Chem.* **2013**, *15*, 2266.
- (156) Kaboudin, B.; Abedia, Y.; Yokomatsu, T. *Org. Biomol. Chem.* **2012**, *10*, 4543.
- (157) Collinson, J.-M.; Wilton-Ely, J. D. E. T.; Díez-González, S. *Chem. Commun.* **2013**, *49*, 11358.
- (158) Baig, R. B. N.; Varma, R. S. *Green Chem.* **2012**, *14*, 625.
- (159) Megia-Fernandez, A.; Ortega-Muñoz, M.; Lopez-Jaramillo, J.; Hernandez-Mateo, F.; Santoyo-Gonzalez, F. *Adv. Synth. Catal.* **2010**, *352*, 3306.
- (160) Xiong, X.; Cai, L. *Catal. Sci. Technol.* **2013**, *3*, 1301.
- (161) Wang, D.; Etienne, L.; Igartua, M. E.; Moya, S.; Astruc, D. *Chem.—Eur. J.* **2014**, DOI: 10.1002/chem.201304536.
- (162) Hudson, R.; Li, C.-J.; Moores, A. *Green Chem.* **2012**, *14*, 622.
- (163) Lee, B. S.; Yi, M.; Chu, S. Y.; Lee, J. Y.; Kwon, H. R.; Lee, K. R.; Kang, D.; Kim, W. S.; Lim, H. B.; Lee, J.; Youn, H.-J.; Chi, D. Y.; Hur, N. H. *Chem. Commun.* **2010**, *46*, 3935.
- (164) Kavács, S.; Zih-Perényi, K.; Révész, Á.; Novák, Z. *Synthesis* **2012**, *44*, 3722.
- (165) Nador, F.; Volpe, M. A.; Alonso, F.; Feldhoff, A.; Kirschning, A.; Radivoy, G. *Appl. Catal. A: Gen.* **2013**, *455*, 39.
- (166) Kumar, B. S. P. A.; Reddy, K. H. V.; Madhav, B.; Ramesh, K.; Nageswar, Y. V. D. *Tetrahedron Lett.* **2012**, *53*, 4595.
- (167) Kumar, A. S.; Reddy, M. A.; Knorn, M.; Reiser, O.; Sreedhar, B. *Eur. J. Org. Chem.* **2013**, *4674*.
- (168) Salam, N.; Sinha, A.; Mondal, P.; Roy, A. S.; Jana, N. R.; Islam, S. M. *RSC Adv.* **2013**, *3*, 18087.
- (169) Ji, Z.; Shen, X.; Zhu, G.; Zhou, H.; Yuan, A. *J. Mater. Chem.* **2012**, *22*, 3471.
- (170) Wu, T.; Zhang, L.; Gao, J.; Liu, Y.; Gao, C.; Yan, J. *J. Mater. Chem. A* **2013**, *1*, 7384.
- (171) Zhang, L.; Chen, X.; Xue, P.; Sun, H. H. Y.; Williams, I. D.; Sharpless, K. B.; Fokin, V. V.; Jia, G. *J. Am. Chem. Soc.* **2005**, *127*, 15998.
- (172) Wang, D.; Salmon, L.; Ruiza, J.; Astruc, D. *Chem. Commun.* **2013**, *49*, 6956.
- (173) Wang, H.-B.; Zhang, Y.-H.; Zhang, Y.-B.; Zhang, F.-W.; Niu, J.-R.; Yang, H.-L.; Li, R.; Ma, J.-T. *Solid State Sci.* **2012**, *14*, 1256.
- (174) Zhou, J.; Dong, Z.; Yang, H.; Shi, Z.; Zhou, X.; Li, R. *Appl. Surf. Sci.* **2013**, *279*, 360.
- (175) Kainz, Q. M.; Linhardt, R.; Grass, R. N.; Vilé, G.; Pérez-Ramírez, J.; Stark, W. J.; Reiser, O. *Adv. Funct. Mater.* **2013**, DOI: 10.1002/adfm.201303277.
- (176) Linhardt, R.; Kainz, Q. M.; Grass, R. N.; Stark, W. J.; Reiser, O. *RSC Adv.* **2014**, *4*, 8541.
- (177) Guerrero, M.; Costa, N. J. S.; Vono, L. L. R.; Rossi, L. M.; Gusevskayad, E. V.; Philippot, K. *J. Mater. Chem. A* **2013**, *1*, 1441.
- (178) Lee, K. H.; Lee, B.; Lee, K. R.; Yi, M. H.; Hur, N. H. *Chem. Commun.* **2012**, *48*, 4414.
- (179) da Silva, F. P.; Rossi, L. M. *Tetrahedron* **2013**, DOI: org/10.1016/j.tet.2013.10.051.

- (180) Kuchkina, N. V.; Yuzik-Klimova, Yu. E.; Sorokina, S. A.; Peregodov, A. S.; Antonov, D. Y.; Gage, S. H.; Boris, B. S.; Nikoshvili, L. Z.; Sulman, E. M.; Morgan, D. G.; Mahmoud, W. E.; Al-Ghamdi, A. A.; Bronstein, L. M.; Shifrina, Z. B. *Macromolecules* **2013**, *46*, 5890.
- (181) Gage, S. H.; Stein, B. D.; Nikoshvili, L. Z.; Matveeva, V. G.; Sulman, M. G.; Sulman, E. M.; Morgan, D. G.; Yuzik-Klimova, E. Y.; Mahmoud, W. E.; Bronstein, L. M. *Langmuir* **2013**, *29*, 466.
- (182) Darwish, M. S. A.; Kunz, U.; Peuker, U. J. *Appl. Polym. Sci.* **2013**, DOI: 10.1002/APP.38864.
- (183) Baig, R. B. N.; Varma, R. S. *ACS Sustainable Chem. Eng.* **2013**, *1*, 805.
- (184) Jacinto, M. J.; Silva, F. P.; Kiyohara, P. K.; Landers, R.; Rossi, L. M. *ChemCatChem* **2012**, *4*, 698.
- (185) Jang, Y.; Kim, S.; Jun, S. W.; Kim, B. H.; Hwang, S.; Song, I. K.; Kim, B. M.; Hyeon, T. *Chem. Commun.* **2011**, *47*, 3601.
- (186) Péllisson, C.-H.; Vono, L. L. R.; Hubert, C.; Denicourt-Nowicki, A.; Rossi, L. M.; Roucoux, A. *Catal. Today* **2012**, *183*, 124.
- (187) Huber, D. L. *Small* **2005**, *1*, 482.
- (188) Stein, M.; Wieland, J.; Steurer, P.; Tölle, F.; Mühlaupt, R.; Breit, B. *Adv. Synth. Catal.* **2011**, *353*, 523.
- (189) Hudson, R.; Rivière, A.; Cirtiu, C. M.; Luska, K. L.; Moores, A. *Chem. Commun.* **2012**, *48*, 3360.
- (190) Hu, A.; Liu, S.; Lin, W. *RSC Adv.* **2012**, *2*, 2576.
- (191) Li, B.; Li, M.; Yao, C.; Shi, Y.; Ye, D.; Wu, J.; Zhao, D. *J. Mater. Chem. A* **2013**, *1*, 6742.
- (192) Wu, L.; He, Y.-M.; Fan, Q.-H. *Adv. Synth. Catal.* **2011**, *353*, 2915.
- (193) González-Gálvez, D.; Nolis, P.; Philippot, K.; Chaudret, B.; van Leeuwen, P. W. N. M. *ACS Catal.* **2012**, *2*, 317.
- (194) Gao, X.; Liu, R.; Zhang, D.; Wu, M.; Cheng, T.; Liu, G. *Chem.—Eur. J.* **2014**, *20*, 1515.
- (195) Li, H.; Liao, J.; Zeng, T. *Catal. Sci. Technol.* **2014**, *4*, 681.
- (196) Martinez, J. J.; Vargasa, L.; Parra, C.; Brijaldob, M. H.; Passos, F. B. J. *Mol. Catal. A: Chem.* **2014**, *383–384*, 31.
- (197) Zeng, T.; Zhang, X.-L.; Niu, H.-Y.; Ma, Y.-R.; Li, W.-H.; Cai, Y.-Q. *Appl. Catal. B: Environ.* **2013**, *134–135*, 26.
- (198) Marcelo, G.; Muñoz-Bonilla, A.; Fernández-García, M. J. *Phys. Chem. C* **2012**, *116*, 24717.
- (199) Zhang, F.; Liu, N.; Zhao, P.; Sun, J.; Wang, P.; Ding, W.; Liu, J.; Jin, J.; Ma, J. *Appl. Surf. Sci.* **2012**, *263*, 471.
- (200) Liu, R.; Guo, Y.; Odusote, G.; Qu, F.; Priestley, F. *ACS Appl. Mater. Interfaces* **2013**, *5*, 9167.
- (201) Xiong, R.; Wang, Y.; Zhang, X.; Lu, C.; Lan, L. *RSC Adv.* **2014**, *4*, 6454.
- (202) Liu, B.; Zhang, D.; Wang, J.; Chen, C.; Yang, X.; Li, C. *J. Phys. Chem. C* **2013**, *117*, 6363.
- (203) Guo, W.; Wang, Q.; Wang, G.; Yang, M.; Dong, W.; Yu, J. *Chem.—Asian J.* **2013**, *8*, 1160.
- (204) Álvarez-Paino, M.; Marcelo, G.; Muñoz-Bonilla, A.; Fernández-García, M. *Macromolecules* **2013**, *46*, 2951.
- (205) Karaoğlu, E.; Özel, U.; Caner, C.; Baykal, A.; Summak, M. M.; Sözeri, H. *Mater. Res. Bull.* **2012**, *47*, 4316.
- (206) Baykal, A.; Karaoğlu, E.; Sözeri, H.; Uysal, E.; Toprak, M. S. *J. Supercond. Novel Magn.* **2013**, *26*, 165.
- (207) Karaoğlu, E.; Summak, M. M.; Baykal, A.; Sözeri, H.; Toprak, M. S. *J. Inorg. Organomet. Polym.* **2013**, *23*, 409.
- (208) Demirelli, M.; Karaoğlu, E.; Baykal, A.; Sözeri, H. *J. Inorg. Organomet. Polym.* **2013**, *23*, 1274.
- (209) Lu, X.; Yang, L.; Bian, X.; Chao, D.; Wang, C. *Part. Part. Syst. Charact.* **2014**, *31*, 245.
- (210) Sun, W.; Lu, X.; Xue, Y.; Tong, Y.; Wang, C. *Macromol. Mater. Eng.* **2013**, DOI: 10.1002/mame.201300171.
- (211) Wang, Q.; Jia, W.; Liu, B.; Dong, A.; Gong, X.; Li, C.; Jing, P.; Li, Y.; Xu, G.; Zhang, J. *J. Mater. Chem. A* **2013**, *1*, 12732.
- (212) Hu, W.; Liu, B.; Wang, Q.; Liu, Y.; Liu, Y.; Jing, P.; Yu, S.; Liu, L.; Zhang, J. *Chem. Commun.* **2013**, *49*, 7596.
- (213) Chi, Y.; Yuan, Q.; Li, Y.; Tu, J.; Zhao, L.; Li, N.; Li, X. *J. Colloid Interface Sci.* **2012**, *383*, 96.
- (214) Mu, B.; Wang, Q.; Wang, A. *J. Mater. Chem. A* **2013**, *1*, 7083.
- (215) Yang, S.; Nie, C.; Liu, H.; Liu, H. *Mater. Lett.* **2013**, *100*, 296.
- (216) Zhu, M.; Wang, C.; Meng, D.; Diao, G. *J. Mater. Chem. A* **2013**, *1*, 2118.
- (217) Chiou, J.-R.; Lai, B.-H.; Hsu, K.-C.; Chen, D.-H. *J. Hazard. Mater.* **2013**, *248–249*, 394.
- (218) Cantillo, D.; Baghbzadeh, M.; Kappe, C. O. *Angew. Chem., Int. Ed.* **2012**, *51*, 10190.
- (219) Cantillo, D.; Moghaddam, M. M.; Kappe, C. O. *J. Org. Chem.* **2013**, *78*, 4530.
- (220) He, G.; Liu, W.; Sun, X.; Chen, Q.; Wang, X.; Chen, H. *Mater. Res. Bull.* **2013**, *48*, 1885.
- (221) Chen, F.; Xi, P.; Ma, C.; Shao, C.; Wang, J.; Wang, S.; Liu, G.; Zeng, Z. *Dalton Trans.* **2013**, *42*, 7936.
- (222) Wang, X.; Liu, D.; Song, S.; Zhang, H. *Chem.—Eur. J.* **2013**, *19*, 5169.
- (223) Feng, J.; Su, L.; Ma, Y.; Ren, C.; Guo, Q.; Chen, X. *Chem. Eng. J.* **2013**, *221*, 16.
- (224) Nabid, M. R.; Bide, Y.; Niknezhad, M. *ChemCatChem* **2014**, *6*, 538.
- (225) Zamani, F.; Kianpour, S. *Catal. Commun.* **2014**, *45*, 1.
- (226) Jiang, Z.; Xie, J.; Jiang, D.; Wei, X.; Chen, M. *CrystEngComm* **2013**, *15*, 560.
- (227) Lai, B. H.; Lin, Y. R.; Chen, D. H. *Chem. Eng. J.* **2013**, *223*, 418.
- (228) Evangelisti, C.; Aronica, L. A.; Botavina, M.; Martra, G.; Battocchio, C.; Polzonetti, G. *J. Mol. Catal. A: Chem.* **2013**, *366*, 288.
- (229) Xie, M.; Zhang, F.; Long, Y.; Ma, J. *RSC Adv.* **2013**, *3*, 10329.
- (230) Liu, B.; Zhang, Z.; Lv, K.; Deng, K.; Duan, H. *Appl. Catal. A: Gen.* **2014**, *472*, 64.
- (231) Zamani, F.; Hosseini, S. M. *Catal. Commun.* **2014**, *43*, 164.
- (232) Zhang, L.; Li, P.; Yang, J.; Wang, M.; Wang, L. *ChemPlusChem* **2014**, *79*, 217.
- (233) Zhang, M.; Sun, Q.; Yan, Z.; Jing, J.; Wei, W.; Jiang, D.; Xie, J.; Chen, M. *Aust. J. Chem.* **2013**, *66*, 564.
- (234) Gawande, M. B.; Rathi, A.; Nogueira, I. D.; Ghumman, C. A. A.; Bundaleski, N.; Teodoro, O. M. N. D.; Branco, P. S. *ChemPlusChem* **2012**, *77*, 865.
- (235) Hodge, P. *Curr. Opin. Chem. Biol.* **2003**, *7*, 362.
- (236) Schätz, A.; Grass, R. N.; Kainz, Q.; Stark, W. J.; Reiser, O. *Chem. Mater.* **2010**, *22*, 305.
- (237) Obermayer, D.; Balu, A. M.; Romero, A. A.; Goessler, W.; Luque, R.; Kappe, C. O. *Green Chem.* **2013**, *15*, 1530.
- (238) Yuan, C.; Liu, H.; Gao, X. *Catal. Lett.* **2014**, *144*, 16.
- (239) Rezaeifard, A.; Jafarpour, M.; Farshid, P.; Naeimi, A. *Eur. J. Inorg. Chem.* **2012**, 5515.
- (240) Bagherzadeh, M.; Hagudoost, M. M.; Moghaddam, F. M.; Foroushani, B. K.; Saryadi, S.; Payab, E. *J. Coord. Chem.* **2013**, *66*, 3025.
- (241) Nikbakht, F.; Heydari, A.; Saberi, D.; Azizi, K. *Tetrahedron Lett.* **2013**, *54*, 6520.
- (242) Sharma, R. K.; Monga, Y. *Appl. Catal., A* **2013**, *454*, 1.
- (243) Saberi, D.; Heydari, A. *Appl. Organometal. Chem.* **2014**, *28*, 101.
- (244) Kumar, A. S.; Thulasiram, B.; Laxmi, S. B.; Rawat, V. S.; Sreedhar, B. *Tetrahedron* **2014**, DOI: org/10.1016/j.tet.2014.01.051.
- (245) Tong, J.; Cai, X.; Wang, H.; Xia, C. *J. Sol-Gel Sci. Technol.* **2013**, *66*, 452.
- (246) Shen, D.-H.; Ji, L.-T.; Liu, Z.-G.; Sheng, W.-B.; Guo, C.-C. *J. Mol. Catal. A: Chem.* **2013**, *379*, 15.
- (247) Panda, N.; Jena, A. K.; Mohapatra, S. *Appl. Catal. A: Gen.* **2012**, *433–434*, 258.
- (248) Baig, R. B. N.; Varma, R. S. *Chem. Commun.* **2012**, *48*, 2582.
- (249) Sharma, R. K.; Monga, Y.; Puri, A.; Gaba, G. *Green Chem.* **2013**, *15*, 2800.
- (250) Zhang, R.; Miao, C.; Shen, Z.; Wang, S.; Xia, C.; Sun, W. *ChemCatChem* **2012**, *4*, 824.
- (251) Parella, R.; Naveen; Babu, S. A. *Catal. Commun.* **2012**, *29*, 118.
- (252) Lee, J.; Chung, J.; Byun, S. M.; Kim, B. M.; Lee, C. *Tetrahedron* **2013**, *69*, S660.

- (253) Bäckvall, J. E. *Modern Oxidation Methods*; Wiley–VCH: Weinheim, 2004.
- (254) Ghorbanloo, M.; Tarasi, R. *Adv. Mater. Res.* **2014**, *829*, 416.
- (255) Williams, F. J.; Bird, D. P. C.; Sykes, E. C. H.; Santra, A. K.; Lambert, R. M. J. *Phys. Chem. B* **2003**, *107*, 3824.
- (256) Zhou, L.; Madix, R. J. *J. Phys. Chem. C* **2008**, *112*, 4725.
- (257) Serafin, J. G.; Liu, A. C.; Seyedmonir, S. R. *J. Mol. Catal. A: Chem.* **1998**, *131*, 157.
- (258) Huang, Z.; Zhang, Y.; Zhao, C.; Qin, J.; Li, H.; Xue, M.; Liu, Y. *Appl. Catal., A* **2006**, *303*, 18.
- (259) Zhang, D. H.; Li, G. D.; Lia, J. X.; Chen, J. S. *Chem. Commun.* **2008**, 3414.
- (260) Qiao, Y.; Li, H.; Hua, L.; Orzechowski, L.; Yan, K.; Feng, B.; Pan, Z.; Theyssen, N.; Leitner, W.; Hou, Z. *ChemPlusChem* **2012**, *77*, 1128.
- (261) Kooti, M.; Afshari, M. *Mater. Res. Bull.* **2012**, *47*, 3473.
- (262) Ucoski, G. M.; Nunes, F. S.; DeFreitas-Silva, G.; Idemori, Y. M.; Nakagaki, S. *Appl. Catal. A: Gen.* **2013**, *459*, 121.
- (263) Saedi, M. S.; Tangestaninejad, S.; Moghadam, M.; Mirkhani, V.; Mohammadpoor-Baltork, I.; Khosropour, A. R. *Polyhedron* **2013**, *49*, 158.
- (264) Shi, Z.-Q.; Dong, Z.-P.; Sun, J.; Zhang, F.-W.; Yang, H.-L.; Zhou, J.-H.; Zhu, X.-H.; Li, R. *Chem. Eng. J.* **2014**, *237*, 81.
- (265) Vaquer, L.; Riente, P.; Sala, X.; Jansat, S.; Benet-Buchholz, J.; Llobet, A.; Pericàs, M. A. *Catal. Sci. Technol.* **2013**, *3*, 706.
- (266) Posner, G. H. *Chem. Rev.* **1986**, *86*, 831.
- (267) Armstrong, R. W.; Combs, A. P.; Tempest, P. A.; Brown, S. D.; Keating, T. A. *Acc. Chem. Res.* **1996**, *29*, 123.
- (268) Safari, J.; Zarnegar, Z.; Heydarian, M. *Bull. Chem. Soc. Jpn.* **2012**, *85*, 1332.
- (269) Pradhan, K.; Paul, S.; Das, A. R. *Catal. Sci. Technol.* **2014**, *4*, 822.
- (270) Bazgir, A.; Hosseini, G.; Ghahremanzadeh, R. *ACS Comb. Sci.* **2013**, *15*, 530.
- (271) Safari, J.; Javadian, L. C. R. *Chim.* **2013**, *16*, 1165.
- (272) Ghasemzadeh, M. A.; Safaei-Ghomi, J.; Zahedi, S. *J. Serb. Chem. Soc.* **2013**, *78*, 769.
- (273) Rostamnia, S.; Nuri, A.; Xin, H.; Pourjavadi, A.; Hosseini, S. H. *Tetrahedron Lett.* **2013**, *54*, 3344.
- (274) Nemati, F.; Saedirad, R. *Chin. Chem. Lett.* **2013**, *24*, 370.
- (275) Maleki, A. *Tetrahedron Lett.* **2013**, *54*, 2055.
- (276) Dandia, A.; Jain, A. K.; Sharma, S. *RSC Adv.* **2013**, *3*, 2924.
- (277) Shaterian, H. R.; Moradi, F. *Rev. Chem. Intermed.* **2013**, DOI: 10.1007/s11164-013-1184-2.
- (278) Paul, S.; Pal, G.; Das, A. R. *RSC Adv.* **2013**, *3*, 8637.
- (279) Azarifar, A.; Nejat-Yami, R.; Kobaisi, M. A.; Azarifar, D. *J. Iran. Chem. Soc.* **2013**, *10*, 439.
- (280) Shafiea, M. R. M.; Ghashanga, M.; Fazlinia, A. *Curr. Nanosci.* **2013**, *9*, 197.
- (281) Nasr-Esfahani, M.; Hoseini, S. J.; Montazerzohori, M.; Mehrabi, R.; Nasrabadi, H. *J. Mol. Catal. A: Chem.* **2014**, *382*, 99.
- (282) Nasser, M. A.; Sadeghzadeh, S. M. *J. Iran. Chem. Soc.* **2013**, *10*, 1047.
- (283) Tayebee, R.; Amini, M. M.; Rostamian, H.; Aliakbari, A. *Dalton Trans.* **2014**, *43*, 1550.
- (284) Naeimi, H.; Rashid, Z.; Zarnani, A. H.; Ghahremanzadeh, R. *New J. Chem.* **2014**, *38*, 348.
- (285) Huo, X.; Liu, J.; Wang, B.; Zhang, H.; Yang, Z.; She, X.; Xia, P. *J. Mater. Chem. A* **2013**, *1*, 651.
- (286) Sheykhani, M.; Mohammadnejad, H.; Akbari, J.; Heydari, A. *Tetrahedron Lett.* **2012**, *53*, 2959.
- (287) Neyens, E.; Baeyens, J. *J. Hazard. Mater.* **2003**, *98*, 33.
- (288) Voelker, B. M.; Kwan, W. P. *Environ. Sci. Technol.* **2003**, *37*, 1150.
- (289) Rusevova, K.; Kopinke, F.-D.; Georgi, A. *J. Hazard. Mater.* **2012**, *241–242*, 433.
- (290) Huang, R.; Fang, Z.; Yan, X.; Cheng, W. *Chem. Eng. J.* **2012**, *197*, 242.
- (291) Liu, W.; Qian, J.; Wang, K.; Xu, H.; Jiang, D.; Liu, Q.; Yang, X.; Li, H. *J. Inorg. Organomet. Polym.* **2013**, *23*, 907.
- (292) Klein, S.; Sommer, A.; Distel, L. V. R.; Neuhuber, W.; Krysch, C. *Biochem. Biophys. Res. Commun.* **2012**, *425*, 393.
- (293) Xu, L.; Wang, J. *Environ. Sci. Technol.* **2012**, *46*, 10145.
- (294) Ferroudj, N.; Nzimoto, J.; Davidson, A.; Talbot, D.; Briot, E.; Dupuis, V.; Bee, A.; Medjram, M. S.; Abramson, S. *Appl. Catal. B: Environ.* **2013**, *136–137*, 9.
- (295) Wang, W.; Liu, Y.; Li, T.; Zhou, M. *Chem. Eng. J.* **2014**, *242*, 1.
- (296) Bai, D.; Yan, P. *Appl. Mech. Mater.* **2014**, *448–453*, 830.
- (297) Lima, M. J.; Leblebici, M. E.; Dias, M. M.; Lopes, J. C. B.; Silva, C. G.; Silva, A. M. T.; Faria, J. L. *Environ. Sci. Pollut. Res.* **2014**, DOI: 10.1007/s11356-014-2515-6.
- (298) Ling, Y.; Long, M.; Hu, P.; Chen, Y.; Huang, J. *J. Hazard. Mater.* **2014**, *264*, 195.
- (299) Luo, M.; Yuan, S.; Tong, M.; Liao, P.; Xie, W.; Xu, X. *Water Res.* **2014**, *48*, 190.
- (300) Wang, H.; Zhang, W.; Shentu, B.; Gu, C.; Weng, Z. *J. Appl. Polym. Sci.* **2012**, *125*, 3730.
- (301) Podolean, I.; Kuncser, V.; Gheorghe, N.; Macovei, D.; Parvulescu, V. I.; Coman, S. M. *Green Chem.* **2013**, *15*, 3077.
- (302) Deng, J.; Shao, Y.; Gao, N.; Tan, C.; Zhou, S.; Hu, X. *J. Hazard. Mater.* **2013**, *262*, 836.
- (303) Taherian, S.; Entezari, M. H.; Ghows, N. *Ultrason. Sonochem.* **2013**, *20*, 1419.
- (304) Amarjargal, A.; Tijing, L. D.; Im, I.-T.; Kim, C. S. *Chem. Eng. J.* **2013**, *226*, 243.
- (305) Lee, P.-Y.; Teng, H.-S.; Yeh, C.-S. *Nanoscale* **2013**, *5*, 7558.
- (306) Su, S.; Guo, W.; Leng, Y.; Yi, C.; Ma, Z. *J. Hazard. Mater.* **2013**, *244–245*, 736.
- (307) Dai, Q.; Wang, J.; Yu, J.; Chen, J.; Chen, J. *Appl. Catal. B: Environ.* **2014**, *144*, 686.
- (308) Xu, J.; Tang, J.; Baig, S. A.; Lv, X.; Xu, X. *J. Hazard. Mater.* **2013**, *244–245*, 628.
- (309) Zhang, X.; Lin, M.; Lin, X.; Zhang, C.; Wei, H.; Zhang, H.; Yang, B. *ACS Appl. Mater. Interfaces* **2014**, *6*, 450.
- (310) Dai, Q.; Wang, J.; Yu, J.; Chen, J.; Chen, J. *Appl. Catal. B: Environ.* **2014**, *144*, 686.
- (311) Li, S.; Zhai, S.-R.; Zhang, J.-M.; Xiao, Z.-Y.; An, Q.-D.; Li, M.-H.; Song, X.-W. *Eur. J. Inorg. Chem.* **2013**, 5428.
- (312) Li, P.-H.; Li, B.-L.; An, Z.-M.; Mo, L.-P.; Cui, Z.-S.; Zhang, Z.-H. *Adv. Synth. Catal.* **2013**, *355*, 2952.
- (313) Tayebee, R.; Amini, M. M.; Abdollahi, N.; Aliakbari, A.; Rabiei, S.; Ramshini, H. *Appl. Catal. A: Gen.* **2013**, *468*, 75.
- (314) Ghahremanzadeh, R.; Rashid, Z.; Zarnani, A. H.; Naeimi, H. *Appl. Catal. A: Gen.* **2013**, *467*, 270.
- (315) Farzaneh, F.; Shafie, Z.; Rashtizadeh, E.; Ghandi, M. *React. Kinet., Mech. Catal.* **2013**, *110*, 119.
- (316) Akbayrak, S.; Kay, M.; Volkan, M.; Özkar, S. *Appl. Catal. B: Environ.* **2014**, *147*, 387.
- (317) Sahiner, N.; Sagbas, S. *J. Power Sources* **2014**, *246*, 55.
- (318) Preethi, V.; Kanmani, S. *Int. J. Hydrogen Energy* **2014**, *39*, 1613.
- (319) Meng, X.; Yang, L.; Cao, N.; Du, C.; Hu, K.; Su, J.; Luo, W.; Cheng, G. *ChemPlusChem* **2014**, *79*, 325.
- (320) Sharma, R. K.; Monga, Y.; Puri, A. *Catal. Commun.* **2013**, *35*, 110.
- (321) Ma, F.-P.; Li, P.-H.; Li, B.-L.; Mo, L.-P.; Liu, N.; Kang, H.-J.; Liu, Y.-N.; Zhang, Z.-H. *Appl. Catal. A: Gen.* **2013**, *457*, 34.
- (322) Prasad, A. S.; Satyanarayana, B. *J. Mol. Catal. A: Chem.* **2013**, *370*, 205.
- (323) Wei, S.; Dong, Z.; Ma, Z.; Sun, J.; Ma, J. *Catal. Commun.* **2013**, *30*, 40.
- (324) Zhou, J.; Dong, Z.; Wang, P.; Shi, Z.; Zhou, X.; Li, R. *J. Mol. Catal. A: Chem.* **2014**, *382*, 15.
- (325) Kidwai, M.; Jain, A.; Bhardwaj, S. *Mol. Diversity* **2012**, *16*, 121.
- (326) Yang, D.; Zhu, X.; Wei, W.; Jiang, M.; Zhang, N.; Ren, D.; You, J.; Wang, H. *Synlett* **2014**, DOI: DOI: 10.1055/s-0033-1340599.
- (327) Hudson, R.; Ishikawa, S.; Li, C.-J.; Moores, A. *Synlett* **2013**, *24*, 1637.

- (328) Zamani, F.; Kianpour, S.; Nekooei, B. *J. Appl. Polym. Sci.* **2014**, DOI: 10.1002/APP.40383.
- (329) Bartolome, L.; Imran, M.; Lee, K. G.; Sangalang, A.; Ahnd, J. K.; Kim, D. H. *Green Chem.* **2014**, *16*, 279.
- (330) Baghbanian, S. M.; Farhang, M. *Synth. Commun.* **2014**, *44*, 697.
- (331) Gu, C.; Xiong, K.; Shentu, B.; Zhang, W.; Weng, Z. *Macromolecules* **2009**, *43*, 1695.
- (332) Wang, H.; Shentu, B.; Zhang, W.; Gu, Z.; Weng, C. *Eur. Polym. J.* **2012**, *48*, 1205.
- (333) Wang, H.; Shen, J.; Li, Y.; Wei, Z.; Cao, G.; Gai, Z.; Hong, K.; Banerjee, P.; Zhou, S. *ACS Appl. Mater. Interfaces* **2013**, *5*, 9446.
- (334) Sun, W.; Li, Q.; Gao, S.; Shang, J. K. *J. Mater. Chem. A* **2013**, *1*, 9215.
- (335) Zhang, M.; Zheng, J.; Zheng, Y.; Xu, J.; He, X.; Chen, L.; Fang, Q. *RSC Adv.* **2013**, *3*, 13818.
- (336) Wu, S.; He, Q.; Zhou, C.; Qi, X.; Huang, X.; Yin, Z.; Yang, Y.; Zhang, H. *Nanoscale* **2012**, *4*, 2478.
- (337) Dehghani, F.; Sardarian, A. R.; Esmaeilpour, M. *J. Organomet. Chem.* **2013**, *743*, 87.
- (338) Sun, J.; Dong, Z.; Li, P.; Zhang, F.; Wei, S.; Shi, Z.; Li, R. *Mater. Chem. Phys.* **2013**, *140*, 1.
- (339) Yang, S.; Wu, C.; Zhou, H.; Yang, Y.; Zhao, Y.; Wang, C.; Yang, W.; Xu, J. *Adv. Synth. Catal.* **2013**, *355*, 53.
- (340) Saberi, D.; Sheykhani, M.; Niknam, K.; Heydari, A. *Catal. Sci. Technol.* **2013**, *3*, 2025.
- (341) Kumar, A. I. S.; Ramani, T.; Sreedhar, B. *Synlett* **2013**, *24*, 938.
- (342) List, B.; Lerner, R. A.; Barbas, C. F. *J. Am. Chem. Soc.* **2000**, *122*, 2395.
- (343) Yacob, Z.; Nan, A.; Liebscher, J. *Adv. Synth. Catal.* **2012**, *354*, 3259.
- (344) Yang, H.; Li, S.; Wang, X.; Zhang, F.; Zhong, X.; Dong, Z.; Ma, J. *J. Mol. Catal. A: Chem.* **2012**, *363–364*, 404.
- (345) Kong, Y.; Tan, R.; Zhao, L.; Yin, D. *Green Chem.* **2013**, *15*, 2422.
- (346) Hamadi, H.; Kooti, M.; Afshari, M.; Ghiasifar, Z.; Adibpour, N. *J. Mol. Catal. A: Chem.* **2013**, *373*, 25.
- (347) Saberi, D.; Cheraghi, S.; Mahdudi, S.; Akbari, J.; Heydari, A. *Tetrahedron Lett.* **2013**, *54*, 6403.
- (348) Pourjavadi, A.; Hosseini, S. H.; Hosseini, S. T.; Aghayemeibody, S. A. *Catal. Commun.* **2012**, *28*, 86.
- (349) Zillillah; Tan, G.; Li, Z. *Green Chem.* **2012**, *14*, 3077.
- (350) Koukabi, N.; Kolvari, E.; Zolfigol, M. A.; Khazaei, A.; Shaghasemi, B. S.; Fasahati, B. *Adv. Synth. Catal.* **2012**, *354*, 2001.
- (351) Safari, J.; Zarnegar, Z. *J. Mol. Catal. A: Chem.* **2013**, *379*, 269.
- (352) Zhang, C.; Wang, H.; Liu, F.; Wang, L.; He, H. *Cellulose* **2013**, *20*, 127.
- (353) Karimi, A. R.; Dalirnasab, Z.; Karimi, M.; Bagherian, F. *Synthesis* **2013**, *45*, 3300.
- (354) Mobaraki, A.; Movassagh, B.; Karimi, B. *Appl. Catal. A: Gen.* **2014**, *472*, 123.
- (355) Mobinikhaledi, A.; Khajeh-Amiri, A. *React. Kinet. Mech. Catal.* **2014**, DOI: 10.1007/s11144-014-0686-2.
- (356) Kolvari, E.; Koukabi, N.; Armandpour, O. *Tetrahedron* **2014**, *70*, 1383.
- (357) Ikenberry, M.; Peña, L.; Wei, D.; Wang, H.; Bossmann, S. H.; Wilke, T.; Wang, D.; Komreddy, V. R.; Rillemad, D. P.; Hohn, K. L. *Green Chem.* **2014**, *16*, 836.
- (358) Zheng, F. C.; Chen, Q. W.; Hu, L.; Yan, N.; Kong, X. K. *Dalton Trans.* **2014**, *43*, 1220.
- (359) Zhang, Z.; Wang, Y.; Fang, Z.; Liu, B. *ChemPlusChem* **2014**, DOI: 10.1002/cplu.201300301.
- (360) Khojastehnezhad, A.; Rahimizadeh, M.; Moeinpour, F.; Eshghi, H.; Bakavoli, M. C. R. *Chim.* **2013**, DOI: doi.org/10.1016/j.jrci.2013.07.013.
- (361) Zamani, F.; Izadi, E. *Catal. Commun.* **2013**, *42*, 104.
- (362) Rostamia, A.; Tahmasbia, B.; Abedib, F.; Shokri, Z. *J. Mol. Catal. A: Chem.* **2013**, *378*, 200.
- (363) Rostami, A.; Tahmasbi, B.; Yari, A. *Bull. Korean Chem. Soc.* **2013**, *34*, 1521.
- (364) Rostami, A.; Tahmasbi, B.; Gholami, H.; Taymorian, H. *Chin. Chem. Lett.* **2013**, *24*, 211.
- (365) Safari, J.; Zarnegar, Z. *Ultrason. Sonochem.* **2013**, *20*, 740.
- (366) Wang, S.; Zhang, Z.; Liu, B.; Li, J. *Catal. Sci. Technol.* **2013**, *3*, 2104.
- (367) Duan, X.; Liu, Y.; Zhao, Q.; Wang, X.; Li, S. *RSC Adv.* **2013**, *3*, 13748.
- (368) Girija, D.; Naik, H. S. B.; Kumar, B. V.; Sudhamani, C. N.; Harish, K. N. *Lett. Org. Chem.* **2013**, *10*, 468.
- (369) Safari, J.; Zarnegar, Z. *J. Chem. Sci.* **2013**, *125*, 835.
- (370) Deng, J.; Mo, L.-P.; Zhao, F.-Y.; Zhang, Z.-H.; Liu, S.-X. *ACS Comb. Sci.* **2012**, *14*, 335.
- (371) Li, P.-H.; Li, B.-L.; Hu, H.-C.; Zhao, X.-N.; Zhang, Z.-H. *Catal. Commun.* **2014**, *46*, 118.
- (372) Safari, J.; Zarnegar, Z. *New J. Chem.* **2014**, *38*, 358.
- (373) Pourjavadi, A.; Hosseini, S. H.; Meibody, S. A. A.; Hosseini, S. T. C. R. *Chim.* **2013**, *16*, 906.
- (374) Pourjavadi, A.; Hosseini, S. H.; Moghaddam, F. M.; Foroushanib, B. K.; Bennett, C. *Green Chem.* **2013**, *15*, 2913.
- (375) Sobhani, S.; Honarmand, M. *Appl. Catal., A* **2013**, *467*, 456.
- (376) Sadeghzadeh, S. M.; Nasser, M. A. *Catal. Today* **2013**, *217*, 80.
- (377) Davarpanah, J.; Kiasat, A. R.; Noorzadeh, S.; Ghahremani, M. *J. Mol. Catal. A: Chem.* **2013**, *376*, 78.
- (378) Karimia, B.; Farhangi, E. *Adv. Synth. Catal.* **2013**, *355*, 508.
- (379) Shaterian, H. R.; Aghakhanizadeh, M. *Catal. Sci. Technol.* **2013**, *3*, 425.
- (380) Azizi, K.; Heydari, A. *RSC Adv.* **2014**, *4*, 6508.
- (381) Sadeghzadeh, S. M. *ChemPlusChem* **2014**, *79*, 278.
- (382) Shaterian, H. R.; Mohammadnia, M. *Res. Chem. Intermed.* **2014**, *40*, 371.
- (383) Tebben, L.; Studer, A. *Angew. Chem., Int. Ed.* **2011**, *50*, 5034.
- (384) Karimi, B.; Farhangi, E. *Chem.—Eur. J.* **2011**, *17*, 6056.
- (385) Zheng, Z.; Wang, J.; Zhang, M.; Xu, L.; Ji, J. *ChemCatChem* **2013**, *5*, 307.
- (386) Kiasat, A. R.; Nazari, S. *J. Inclusion Phenom. Macrocycl. Chem.* **2013**, *76*, 363.
- (387) Zhu, J.; Wang, P.-C.; Lu, M. *J. Braz. Chem. Soc.* **2013**, *24*, 171.
- (388) Kang, Y.; Zhou, L.; Li, X.; Yuan, J. *J. Mater. Chem.* **2011**, *21*, 3704.
- (389) Kang, Y.; Zhou, L.; Li, X.; Yuan, J. *Chem. Rev.* **1999**, *99*, 1689.
- (390) Astruc, D.; Chardac, F. *Chem. Rev.* **2001**, *101*, 2991.
- (391) Wang, D.; Astruc, D. *Coord. Chem. Rev.* **2013**, *257*, 2317.
- (392) Astruc, D.; Heuzé, K.; Gatard, S.; Méry, D.; Nlate, S.; Plault, L. *Adv. Syn. Catal.* **2005**, *347*, 329.
- (393) Keller, M.; Perrier, A.; Linhardt, R.; Travers, L.; Wittmann, S.; Caminade, A.-M.; Majoral, J.-P.; Reiser, O.; Ouali, A. *Adv. Synth. Catal.* **2013**, *355*, 1748.
- (394) Riente, P.; Yadav, J.; Pericàs, M. A. *Org. Lett.* **2012**, *14*, 3668.
- (395) Brunelli, N. A.; Long, W.; Venkatasubbaiah, K.; Jones, C. W. *Top Catal.* **2012**, *55*, 432.
- (396) Sobhani, S.; Bazrafshan, M.; Delluei, A. A.; Parizi, Z. P. *Appl. Catal., A* **2013**, *454*, 145.
- (397) Damodara, D.; Arundhathia, R.; Likhar, P. R. *Catal. Sci. Technol.* **2013**, *3*, 797.
- (398) Rostami, A.; Navasi, Y.; Morad, D.; Ghorbani-Choghamarani, A. *Catal. Commun.* **2014**, *43*, 16.
- (399) Yao, T.; Cui, T.; Fang, X.; Yu, J.; Cui, F.; Wu, J. *Chem. Eng. J.* **2013**, *225*, 230.
- (400) Rostamizadeh, S.; Shadjou, N.; Isapoor, E.; Hasanzadeh, M. J. *Nanosci. Nanotechnol.* **2013**, *13*, 4925.
- (401) Azizi, K.; Heydari, A. *RSC Adv.* **2014**, *4*, 8812.
- (402) Zamani, F.; Izadi, E. *Chin. J. Catal.* **2014**, *35*, 21.
- (403) Sohrabi, N.; Rasouli, N.; Torkzadeh, M. *Chem. Eng. J.* **2014**, *240*, 426.
- (404) Zhang, Q.; Han, X.; Tang, B. *RSC Adv.* **2013**, *3*, 9924.
- (405) Ranjbakhsh, E.; Bordbar, A. K.; Abbasi, M.; Khosropour, A. R.; Shams, E. *Chem. Eng. J.* **2012**, *179*, 272.

- (406) Berg, J. M.; Tymoczko, J. L.; Stryer, L. *Biochemistry*, 6th ed.; W. H. Freeman and Co.: New York, 2007; pp 254.
- (407) Vinoba, M.; Bhagiyalakshmi, M.; Jeong, S. K.; Nam, S. C.; Yoon, Y. *Chem.—Eur. J.* **2012**, *18*, 12028.
- (408) Mukherjee, J.; Gupta, M. N. *Chem. Cent. J.* **2012**, *6*, 133.
- (409) Tan, H.; Feng, W.; Ji, P. *Bioresour. Technol.* **2012**, *155*, 172.
- (410) Iram, M.; Ishfaq, A.; Guo, C.; Liu, H. *Bio. Eng. J.* **2013**, *73*, 72.
- (411) Ozyilmaza, E.; Sayina, S.; Arslanb, M.; Yilmaz, M. *Colloid. Surf. B: Biointerfaces* **2014**, *113*, 182.
- (412) Tudorache, M.; Negoii, A.; Protesescu, L.; Parvulescu, V. I. *Appl. Catal. B: Environ.* **2014**, *145*, 120.
- (413) Verma, M. L.; Chaudhary, R.; Tsuzuki, T.; Barrow, C. J.; Munish, P. *Bioresour. Technol.* **2013**, *135*, 2.
- (414) Nicolás, P.; Lassalle, V.; Ferreira, M. L. *Bioprocess Biosyst. Eng.* **2013**, DOI: 10.1007/s00449-013-1010-7.
- (415) Karajanagi, S. S.; Vertegel, A. A.; Kane, R. S.; Dordick, J. S. *Langmuir* **2004**, *20*, 11594.
- (416) Asuri, P.; Karajanagi, S. S.; Sellitto, E.; Kim, D. Y.; Kane, R. S.; Dordick, J. S. *Biotechnol. Bioeng.* **2006**, *95*, 804.
- (417) Feng, W.; Ji, P. *Biotechnol. Adv.* **2011**, *29*, 889.
- (418) Li, J.; Hong, R.; Luo, G.; Zheng, Y.; Li, H.; Wei, D. *New Carbon Mater.* **2010**, *25*, 192.
- (419) Goh, W. J.; Makam, V. S.; Hu, J.; Kang, L.; Zheng, M.; Yoong, S. L.; C Udalagama, C. N. B.; Pastorn, G. *Langmuir* **2012**, *28*, 16864.
- (420) Ngo, T. P. N.; Li, A.; Tiew, K. W.; Li, Z. *Bioresour. Technol.* **2013**, *145*, 233.
- (421) Ngo, T. P. N.; Zhang, W.; Wang, W.; Li, Z. *Chem. Commun.* **2012**, *48*, 4585.
- (422) Cheng, J. P.; Ma, R.; Li, M.; Wu, J. S.; Liu, F.; Zhang, X. B. *Chem. Eng. J.* **2012**, *210*, 80.
- (423) Harraz, F. A.; Mohamed, R. M.; Rashad, M. M.; Wang, Y. C.; Sigmund, W. *Ceram. Int.* **2014**, *140*, 375.
- (424) Chalasani, R.; Vasudevan, S. *ASC Nano* **2013**, *7*, 4093.
- (425) Shi, Z.; Lai, H.; Yao, S. *Russ. J. Phys. Chem. A* **2012**, *86*, 1326.
- (426) Nabid, M. R.; Sedghi, R.; Gholami, S.; Oskooie, H. A.; Heravi, M. M. *Photochem. Photobiol.* **2013**, *89*, 24.
- (427) Jing, M. X.; Han, C.; Wang, Z.; Shen, X. Q. *J. Nanosci. Nanotechnol.* **2013**, *13*, 4949.
- (428) Lee, H. U.; Lee, G.; Park, J. C.; Lee, Y.-C.; Lee, S. M.; Son, B.; Park, S. Y.; Kim, C.; Lee, S. G.; Lee, S. C.; Nam, B.; Lee, J. W.; Bae, D. R.; Yoon, J.-S.; Lee, J. *Chem. Eng. J.* **2014**, *240*, 91.
- (429) Mohanta, O.; Singhababu, Y. N.; Giri, S. K.; Dadhich, D.; Das, N. N.; Sahu, R. J. *Alloys Compd.* **2013**, *564*, 78.
- (430) Kan, H. Y.; Wang, H. P. *Environ. Sci. Technol.* **2013**, *47*, 7380.
- (431) Dutta, A. K.; Maji, S. K.; Adhikary, B. *Mater. Res. Bull.* **2014**, *49*, 28.
- (432) Senapati, S.; Srivastava, S. K.; Singh, S. B. *Nanoscale* **2012**, *4*, 6604.
- (433) Liang, H.; Niu, H.; Li, P.; Tao, Z.; Mao, C.; Song, J.; Zhang, S. *Mater. Res. Bull.* **2013**, *48*, 2415.
- (434) Chen, C.; Cai, W.-M.; Long, M.-C.; Zhou, B.-X.; Wu, Y.-H.; Wu, D.-Y.; Feng, Y.-J. *ACS Nano* **2010**, *4*, 6425.
- (435) Akhavan, O. *Carbon* **2011**, *49*, 11.
- (436) Fu, Y.-S.; Wan, Y.-H.; Xia, H.; Wang, X. J. *Power Sources* **2012**, *213*, 338.
- (437) Fu, Y.-S.; Xiong, P.; Chen, H.-Q.; Sun, X.-Q.; Wang, X. *Ind. Eng. Chem. Res.* **2012**, *51*, 725.
- (438) Fu, Y.-S.; Chen, Q.; He, M.-Y.; Wan, Y.-H.; Sun, X.-Q.; Xia, H.; Wang, X. *Ind. Eng. Chem. Res.* **2012**, *51*, 11700.
- (439) Fu, Y.; Chen, H.; Sun, X.; Wang, X. *AIChE J.* **2012**, *58*, 3298.
- (440) Sun, J.; Fu, Y.; Xiong, P.; Sun, X.; Xu, B.; Wang, X. *RSC Adv.* **2013**, *3*, 22490.
- (441) Guo, J.; Zhou, X.; Chen, L.; Lu, Y.; Zhang, X.; Hou, W. J. *Nanopart. Res.* **2012**, *14*, 992.
- (442) Guo, J.; Jiang, B.; Zhang, X.; Zhou, X.; Hou, W. J. *Solid State Chem.* **2013**, *205*, 171.
- (443) Paul, S.; Pradhan, K.; Ghosh, S.; De, S. K.; Das, A. R. *Adv. Synth. Catal.* **2014**, *356*, 1301.
- (444) Ghotbnejad, M.; Khosropour, A. R.; Mohammadpoor-Baltork, I.; Moghadam, M.; Tangestaninejad, S.; Mirkhani, V. *J. Mol. Catal. A: Chem.* **2014**, *385*, 78.
- (445) Wang, P.; Liu, H.; Liu, M.; Li, R.; Ma, J. *New J. Chem.* **2014**, *38*, 1138.
- (446) Karimi, B.; Mansouri, F.; Vali, H. *Green Chem.* **2014**, *16*, 2587.
- (447) Nabid, M. R.; Bide, Y.; Ghalavand, N.; Niknezhad, M. *Appl. Organometal. Chem.* **2014**, *28*, 389.
- (448) Shokouhimehr, M.; Kim, T.; Jun, S. W.; Shin, K.; Jang, Y.; Kim, B. H.; Kim, J.; Hyeon, T. *Appl. Catal. A: Gen.* **2014**, *476*, 133.
- (449) An, M.; Cui, J.; Wang, L. J. *Phys. Chem. C* **2014**, *118*, 3062.
- (450) Afshari, M.; Gorjizadeh, M.; Nazari, S.; Naseh, M. J. *Magn. Mater.* **2014**, *363*, 13.
- (451) Yang, D.; An, B.; Wei, W.; Jiang, M.; You, J.; Wang, H. *Tetrahedron* **2014**, *70*, 3630.
- (452) Fernandes, C. I.; Carvalho, M. D.; Ferreira, L. P.; Nunes, C. D.; Vaz, P. D. J. *Organomet. Chem.* **2014**, *760*, 2.
- (453) Sobhani, S.; Falatoooni, Z. M.; Honarmand, M. *RSC Adv.* **2014**, *4*, 15797.
- (454) Srinivas, B. T. V.; Rawat, V. S.; Konda, K.; Sreedhar, B. *Adv. Synth. Catal.* **2014**, *356*, 805.
- (455) Zillillah; Ngu, T. A.; Li, Z. *Green Chem.* **2014**, *16*, 1202.
- (456) Kainz, Q. M.; Reiser, O. *Acc. Chem. Res.* **2014**, *47*, 667.
- (457) Wang, D.; Astruc, D. *Molecules* **2014**, *19*, 4635.

## NOTE ADDED IN PROOF

Major contributions to the field of magnetically recyclable nanocatalysts have appeared since this paper was submitted concerning C–C coupling reactions,<sup>443–446</sup> reduction of nitroaromatics,<sup>447–449</sup> oxidation reactions,<sup>450,451</sup> epoxidation of alkenes,<sup>452</sup> Kabachnik–Fields reaction,<sup>453</sup> synthesis of arylsulfones,<sup>454</sup> esterification and transesterification,<sup>455</sup> and mini-reviews.<sup>456,457</sup>

## **Chapter 2**

### **Iron Oxide Magnetic Nanoparticle-Immobilized Ru Catalysts**

## 2.2 Introduction

Section 2.2 is a micro-review article on magnetically recoverable ruthenium catalysts in organic synthesis. Versatile Ru catalysts supported on MNPs recently provided excellent catalytic performances in a variety of reactions,<sup>1,2</sup> such as hydrogenation with pressures of H<sub>2</sub> gas, transfer hydrogenation, epoxidation, oxidation, hydration, deallylation, olefin metathesis, and azide-alkyne cycloaddition. This review with 79 references highlighted basic concepts and recent trends of MNP-supported Ru complexes and Ru nanoparticles in organic formations. Moreover, the perspectives for further development of MNP-supported Ru catalysts were presented in the review. Some of our own work on the subject is included therein (vide infra).

Section 2.3 demonstrates the synthesis, characterization of a magnetically recyclable Ru complex, and its catalytic application as a regioselective catalyst for alkyne-azide cycloaddition. Ru-catalyzed azide-alkyne cycloaddition (RuAAC), pioneered by the groups of Fokin and Jia,<sup>3,4</sup> is the most efficient strategy for regioselective synthesis of 1,5-disubstituted 1,2,3-triazoles, however, to date there has been no publications on recyclable RuAAC catalysts. In the work, a SiO<sub>2</sub>/γ-Fe<sub>2</sub>O<sub>3</sub> shell-core nanoparticles-anchored pentamethylcyclopentadienyl ruthenium complex was successfully prepared. The catalyst that is presented here gave impressive performances in terms of activity and selectivity towards 1,5-disubstituted 1,2,3-triazoles via cycloaddition of alkynes and organic azides. In addition, it was magnetically recoverable. This work was carried out with the collaboration of Dr. Lionel Salmon who conducted the TEM analyses.

### References:

1. H. Clavier, K. Grela, A. Kirschning, M. Mauduit, S. P. Nolan, *Angew. Chem. Int. Ed.* **2007**, *46*, 6786.
2. J. Li, Y. Zhang, D. Han, Q. Gao, C. Li, *J. Mol. Catal. A Chem.* **2009**, *298*, 31.
3. L. Zhang, X. Chen, P. Xue, H. H. Y. Sun, I. D. Williams, K. B. Sharpless, V. V. Fokin, G. Jia, *J. Am. Chem. Soc.* **2005**, *127*, 15998.
4. B. C. Boren, S. Narayan, L. K. Rasmussen, L. Zhang, H. Zhao, Z. Lin, G. Jia, V. V. Fokin, *J. Am. Chem. Soc.* **2008**, *130*, 8923.

Review

## Magnetically Recoverable Ruthenium Catalysts in Organic Synthesis

Dong Wang and Didier Astruc \*

ISM, UMR CNRS No. 5255, Université Bordeaux, Talence Cedex 33405, France;

E-Mail: wangdong0377@163.com

\* Author to whom correspondence should be addressed; E-Mail: d.astruc@ism.u-bordeaux1.fr;  
Tel.: +33-5-4000-6271.

Received: 24 February 2014; in revised form: 1 April 2014 / Accepted: 10 April 2014 /

Published: 15 April 2014

---

**Abstract:** Magnetically recyclable catalysts with magnetic nanoparticles (MNPs) are becoming a major trend towards sustainable catalysts. In this area, recyclable supported ruthenium complexes and ruthenium nanoparticles occupy a key place and present great advantages compared to classic catalysts. In this micro-review, attention is focused on the fabrication of MNP-supported ruthenium catalysts and their catalytic applications in various organic syntheses.

**Keywords:** magnetic nanoparticles; ruthenium complexes; catalysis; heterogeneous catalysts

---

### 1. Introduction

In recent years, sustainable and practical chemistry using recyclable catalysts has been one of the most fascinating developments in chemistry in both the academic area and industry [1–7]. The heterogenization of highly active catalysts on various organic or inorganic supports is probably the most efficient strategy and has gained significant progress towards the achievement of efficient catalyst recovery.

In a related context, the immobilization of catalytic species on MNPs has received considerable attention and is nowadays undergoing an explosive development [8–12]. This is due to the easy preparation of such catalysts and their functionalization, good stability, large surface-to-volume ratio, and efficient recovery procedure by magnetic attraction. The use of MNPs not only offers high catalytic activity and selectivity benefiting from their nanosize, but also fulfills the demands concerning

convenient catalyst separation. Recently, MNPs have been successfully used to immobilize a wide variety of transition metal catalysts, organocatalysts, and biocatalysts. These catalysts show sustainable, environmentally benign, and economical characters for various reactions including olefin metathesis, cycloaddition, C-C coupling, hydrogenation, oxidation, reduction, *etc.*

Ruthenium complexes are known in a wide range of oxidation states from  $-2$  to  $+8$  and easily accommodate ligands with various coordination geometries, so that they possess unique opportunities as versatile catalysts [13–16]. During the past few years, a series of Ru complexes bearing amine, phosphine, oxygen, carbon and hybrid ligands, have been immobilized on MNPs forming magnetically separable catalysts for a variety of reactions, such as asymmetric hydrogenation of aromatic ketones, stereospecific epoxidation, selective oxidation of alcohols and amines, oxidation of levulinic acid to succinic acid, hydration of nitriles, deallylation, asymmetric transfer hydrogenation, redox isomerization of allylic alcohols, heteroannulation of (*Z*)-enynols, olefin metathesis, and synthesis of 1,5-disubstituted 1,2,3-triazoles via azide-alkyne cycloaddition.

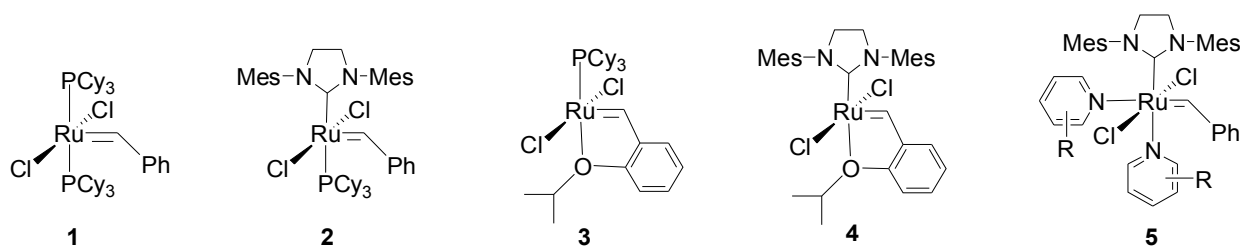
In this review, progress in the field of MNP-supported Ru complexes and Ru nanoparticles in organic synthesis is highlighted. At the end of the review, the advantages of magnetically recoverable Ru catalysts, and some of their perspectives for further development are presented.

## 2. MNP-Supported Ru Catalysts for Organic Synthesis

### 2.1. Olefin Metathesis

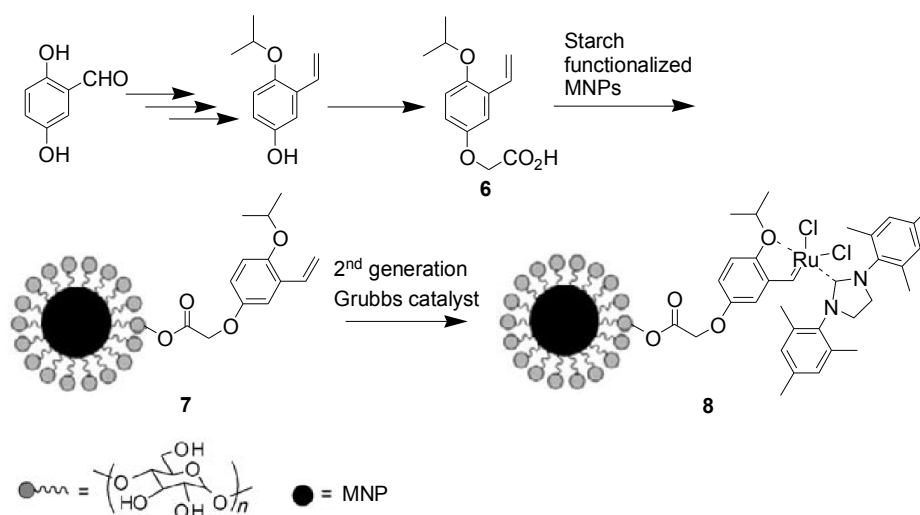
Olefin metathesis has been well recognized as a powerful method of generating C=C bonds in modern chemical transformations, especially in the synthesis of polymers, important petrochemicals, and specialty chemicals [17–28], since it was discovered by American industrial chemists in the 1960s [29–33]. Olefin metathesis includes ring-opening, ring-closing, and cross metathesis reactions. Ru-based Grubbs-type catalysts **1–5** (Scheme 1) [17–19,21,23,30–37] are (together with Schrock-type catalysts) widely used in homogeneously catalyzed olefin metathesis, and show superior catalytic activities and extraordinary functional group tolerance. However, the homogeneous Ru catalysts exhibit some inherent drawbacks including the difficult recovery of the catalysts from reaction medium and metal contamination of the products that restrict their possible applications in the pharmaceutical industry and materials science. To overcome these issues, immobilization of the homogenous metathesis catalysts on various supports such as monoliths [38], silica [39–42], polymers [43–45], and MNPs has been proved to be one of the most logical solutions [46]. Among these supports, MNPs have attracted a great interest in olefin metathesis reactions due to their high stability, nano size, and convenient recovery by using an external magnetic field.

**Scheme 1.** Grubbs-type ruthenium catalysts and derivatives.



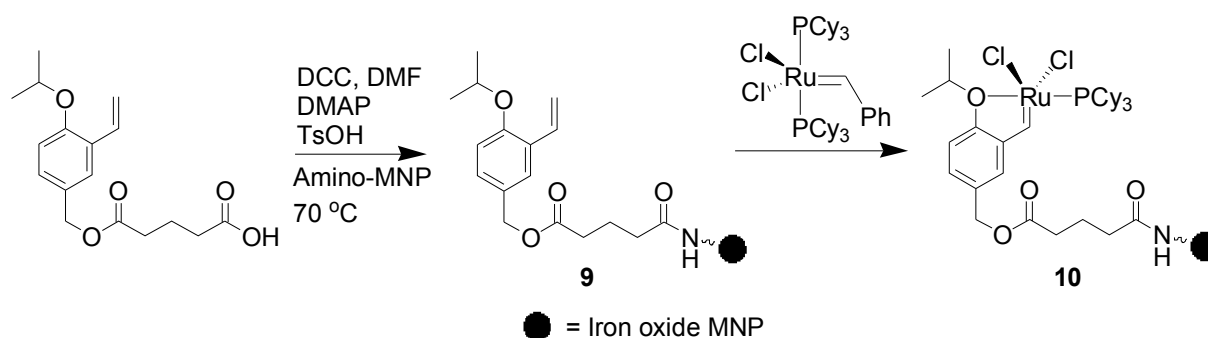
Zhu *et al.* prepared free and MNP-anchored *ortho*-isopropoxystyrene ligand **6** and **7**, successively, and **2** then reacted with **7** producing MNP-immobilized catalyst **8** (Scheme 2) that possesses a mean diameter size of approximately 100 nm, and Ru content of 0.28 mmol/g. Its catalytic activity was evaluated in both self- and cross-metathesis reactions in terms of yield, TON, TOF [47]. In the case of self-metathesis of fatty acid esters (methyl oleate), **8** provided slightly lower activity than **2** under neat conditions. It was recovered from the reaction mixture by attraction of a magnet with less than 3 ppm Ru leaching. In addition, **8** was recycled for at least five times without any significant decrease in activity. The investigation of cross-metathesis of methyl oleate with methyl acrylate revealed that **8** exhibited much higher and similar activity regarding TOF than the unsupported Grubbs-type ruthenium catalysts. It was magnetically collected and re-used for the next two reaction cycles and maintained the same catalytic performance.

**Scheme 2.** Synthesis of the MNP-supported metathesis ruthenium catalyst **8**.



The ruthenium catalyst **10** supported on MNPs was designed and synthesized through the reaction between iron oxide nanoparticles-anchored ligand **9** and Grubbs I catalyst **1** (Scheme 3) [48]. The ring-closing metathesis reactions of a series of substrates were subsequently conducted with **10** (2.5 mol% [Ru]) in  $\text{CH}_2\text{Cl}_2$  at 40 °C. It was found that **10** performed well providing the corresponding cyclic olefins with excellent yields and was recycled up to 22 times without considerable loss in catalytic efficiency.

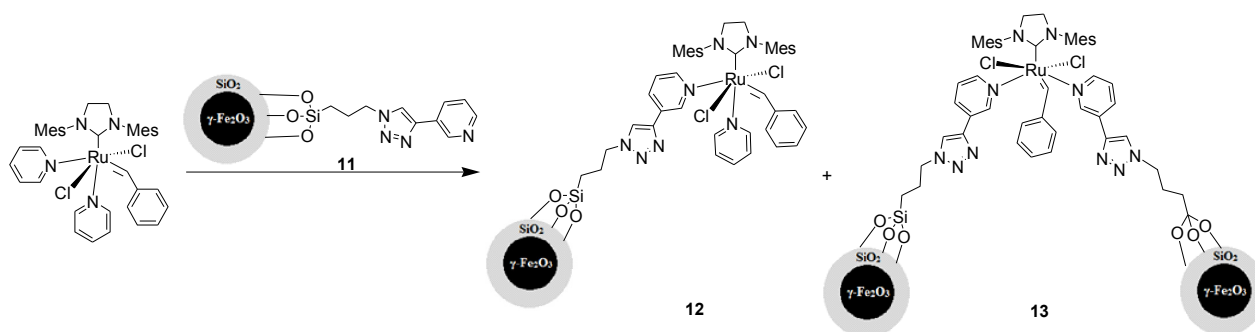
**Scheme 3.** Synthesis of MNP-supported metathesis ruthenium catalyst **10**.



The Grubbs-III catalyst **5** is highly active for cross metathesis and ring-opening-metathesis polymerization [36,37]. Kirschning's group [45] demonstrated that **5** was easily immobilized through ligand exchange using polyvinyl pyridine (PVP). The resulting Ru-doped PVP smoothly catalyzed ring-closing metathesis and cross-metathesis reactions at relatively high temperature. The supported catalyst was recyclable in the case of ring-closing metathesis, but an obvious loss of activity was revealed. Emrick *et al.* [49] prepared PEG-functionalized Grubbs III catalyst **5** via ligand exchange, and the catalyst that was obtained was water soluble and effective for ring-opening-metathesis polymerization of norbornene derivatives. Encouraged by the straightforward procedure for immobilization of Grubbs III catalyst, we explored the possibility of anchoring Grubbs III catalyst **5** on MNPs in order to improve the recovery.

As shown in Scheme 4, the pre-prepared MNP-supported “click” pyridine ligand **11** (in ten-fold excess) was coordinated to the Ru center of **5** to construct a MNP-enriched Grubbs III catalyst, and the immobilization was confirmed by FT-IR analysis. The supported catalyst should be a mixture resulting from mono- and disubstitution of pyridine ligands by the MNP-derived pyridines in Grubbs-III catalysts (**12**) and (**13**) respectively. The catalytic behavior of this mixture of catalysts was checked for cross metathesis, ring-closing metathesis, and ring-opening metathesis polymerization of olefins. The results showed that only trace of the desired product of cross metathesis reaction between but-3-enitrile and 1-octadecene was obtained, with 2.5 mol% [Ru] at 40 °C. The ring-closing metathesis reaction of 2,2-diallylmalonic acid diethyl ester did not occur at room temperature in the presence of 2.5 mol% [Ru]. When the temperature was raised to 110 °C, a 34% of yield was obtained, and the catalyst was magnetically recoverable, but deactivated by the third run. In addition, the investigation of ring-opening metathesis polymerization reaction of a norbornene derivative (*cis*-5-norbornene-*exo*-2,3-dicarboxylic anhydride) with the monomer/[Ru] ratio of 13:1, demonstrated that the corresponding polymer was isolated with 80% monomer conversion in 15 h. In conclusion, the catalytic performances of the MNP-supported Grubbs III catalyst for all three metathesis reactions were worse than those of the unsupported Grubbs III catalyst [36,37]. The low catalytic efficiency was attributed to the instability of the coordination between the MNP-immobilized pyridine ligand and Ru, the bulky linker between MNPs and pyridine, and eventually the less efficient substituent group on pyridine concerning metathesis activity [36].

**Scheme 4.** Synthesis of  $\gamma\text{-Fe}_2\text{O}_3@\text{SiO}_2$  immobilized third generation Grubbs catalysts **12** and **13**.

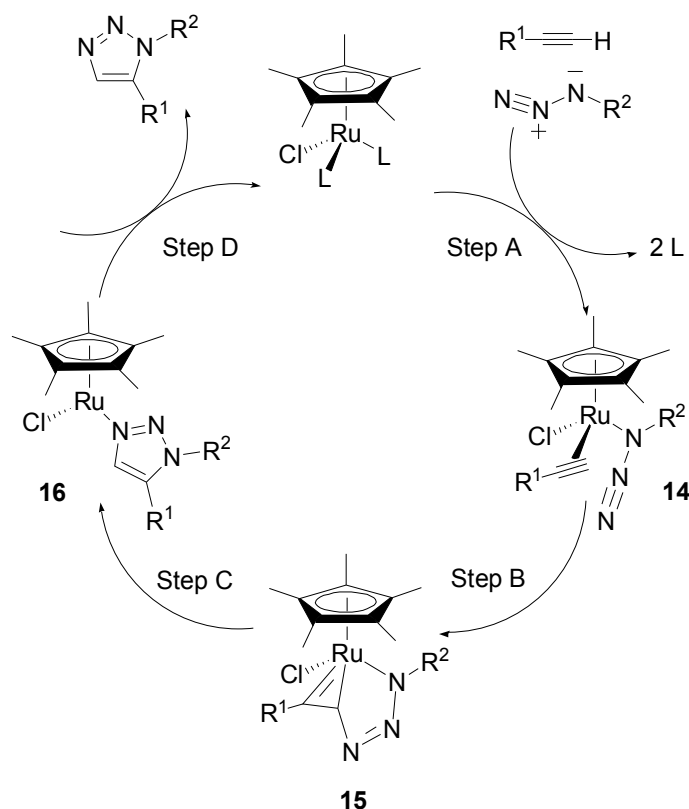


## 2.2. Azide-Alkyne Cycloaddition

The five-membered nitrogen heterocyclic 1,2,3-triazoles have attracted considerable attention in all fields of chemistry, ranging from synthetic organic/inorganic chemistry to pharmaceutical science. Among the numerous methods for 1,2,3-triazole synthesis, azide-alkyne cycloadditions involving Cu [50,51] and Ru [52] catalysis are most efficient ones and they have been widely used for the construction of 1,4- and 1,5-disubstituted 1,2,3-triazoles, respectively.

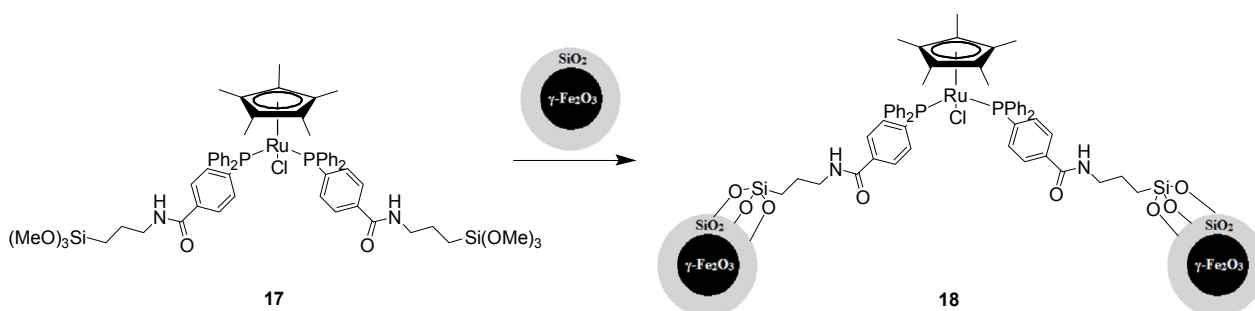
Some Cp\*Ru(II) complexes [52–55] and the cluster (Cp\*Ru)<sub>n</sub> in DMF under microwaves [54] are excellent metal catalysts to regioselectively assemble 1,5-disubstituted 1,2,3-triazoles. As schematically outlined in Scheme 5, the coordination of the starting materials onto the Ru center (step A) produces the Ru intermediate **14** that most certainly undergoes oxidative coupling of the azide and alkyne to give the 6-membered ruthenacycle **15** (step B), which controls the regioselectivity. The next formation of the C-N bond would then occur by reductive elimination yielding the 1,5-disubstituted 1,2,3-triazole, possibly via the coordinated heterocycle **16** (step C). Fokin's group has reported DFT calculations supporting these mechanistic details [52]. Disubstituted alkynes work as well as terminal alkynes in this RuAAC “click” reaction, whereas only terminal alkynes give the 1,4-disubstituted 1,2,3 triazoles upon Cu-catalysis (CuAAC), because of the required terminal alkyne deprotonation giving a Cu-alkynyl species as an initial step of the latter reaction. The recovery of the Ru catalyst, however, remains a long-standing problem. Viewing economy and environmental benefit, it is essential to develop investigations of the suppression of heterogeneous Ru contamination by Ru(II) complexes upon Ru separation following the synthesis of 1,2,3-triazoles.

**Scheme 5.** Proposed mechanism for Cp\*Ru(II) catalyzed azide-alkyne cycloaddition.

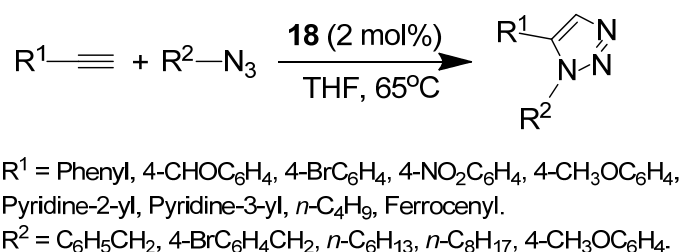


Our group has reported the first example of MNP-supported  $\text{Cp}^*(\text{PPh}_3)_2\text{Ru}(\text{II})$  catalyst for azide-alkyne cycloaddition (AAC) [56]. The  $\text{Si}(\text{OMe})_3$ -functionalized  $\text{Cp}^*(\text{PPh}_3)_2\text{Ru}$  complex **17** was obtained via coordination of  $\text{Si}(\text{OMe})_3$ -functionalized  $\text{PPh}_3$  with the  $(\text{Cp}^*\text{RuCl}_2)_n$  cluster. Subsequently, core-shell  $\gamma\text{-Fe}_2\text{O}_3@/\text{SiO}_2$  nanoparticles with an average size of 30 nm were successfully enriched with **17** by coupling reaction as shown in Scheme 6. This catalyst **18** was initially evaluated in AAC using phenylacetylene and benzyl azide as model substrates with 2 mol% [Ru] in THF. The corresponding 1,5-disubstituted 1,2,3-triazole was synthesized in 91% yield and over 99.9% selectivity within 3 h. Then, the catalyst **18** was easily removed from the reaction medium by magnetic attraction and recycled at least five times with a gradual slight loss of activity (down to 77%), and a slight decrease in selectivity for the 1,5-disubstituted 1,2,3-triazole product. The substrate scope was then investigated using aryl, aliphatic, and ferrocenyl acetylenes that exhibited good reactivities with benzyl azide in the presence of **18**. The aliphatic azides and benzyl azides bearing a Br substituent are also suitable cycloaddition partners; when aryl azide (*p*-methoxyphenyl azide) was employed, the yield of 1,5-disubstituted 1,2,3-triazole was somewhat lower (Scheme 7). The catalyst **18** was also active with internal alkynes such as 1,2-diphenylethyne, and the 1,4,5-trisubstituted 1,2,3-triazole product was obtained in 77% yield.

**Scheme 6.** Synthesis of  $\text{Cp}^*(\text{PPh}_3)_2\text{Ru}/\text{SiO}_2/\gamma\text{-Fe}_2\text{O}_3$  **18**.



**Scheme 7.** RuAAC reactions in the presence of the magnetic catalyst  $\text{Cp}^*(\text{PPh}_3)_2\text{Ru}/\text{SiO}_2/\gamma\text{-Fe}_2\text{O}_3$  **18**.



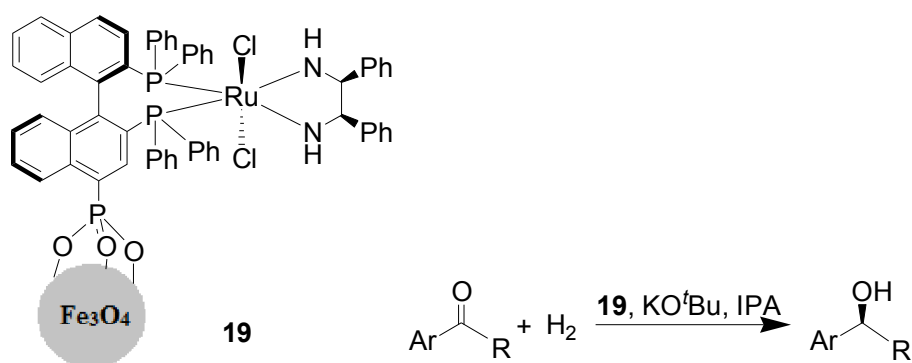
### 2.3. Hydrogenation

Hydrogenation reactions, in particular asymmetric hydrogenations, have been widely studied, because they are among the most versatile reactions in all fields of chemistry from pharmaceutical science to petrochemistry. Recently, MNP-immobilized Ru complexes were shown to be efficient catalysts for asymmetric or symmetric hydrogenation of unsaturated compounds.

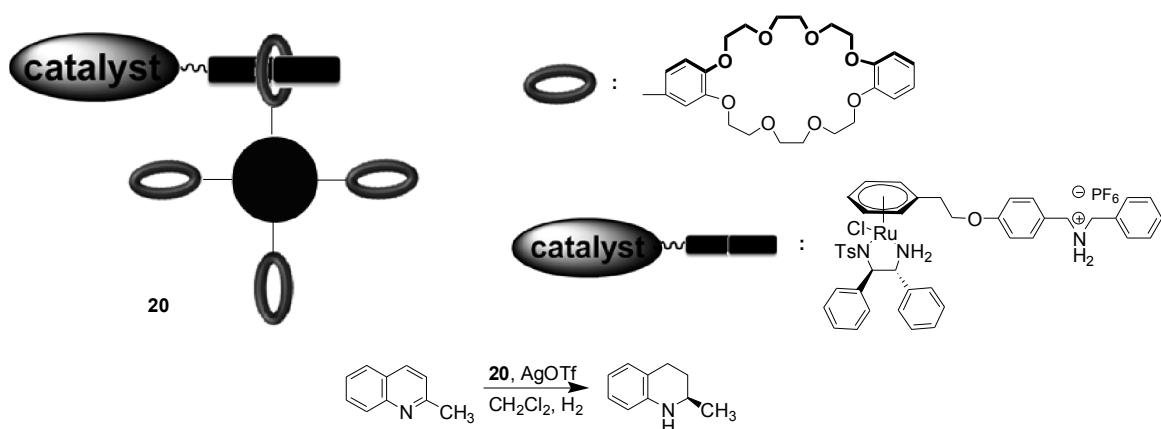
$\text{Fe}_3\text{O}_4$  nanoparticles were readily prepared by the coprecipitation method, and these MNPs were then successfully used for the immobilization of the as-synthesized  $\text{Ru}(\text{BINAP-PO}_3\text{H}_2)(\text{DPEN})\text{Cl}_2$  complex,

forming MNP-anchored chiral Ru catalyst **19**. This heterogeneous catalyst afforded high catalytic activity and enantioselectivity in the asymmetric hydrogenation of aromatic ketones in the presence of KO<sup>t</sup>Bu under 700 psi of hydrogen pressure (Scheme 8) [57]. A series of secondary alcohols were generated through hydrogenation of their corresponding aromatic ketones over 0.1 mol% of **19**, with 100% conversion and remarkably high *e.e.* values compared with its homogeneous counterpart Ru(BINAP-PO<sub>3</sub>H<sub>2</sub>)(DPEN)Cl<sub>2</sub>. Furthermore, after completion of the reactions, the heterogeneous catalyst was magnetically recovered and reused for 14 times without noticeable loss in both conversion and *e.e.* value. In this report, the synthesis of other Fe<sub>3</sub>O<sub>4</sub> nanoparticles was also reported to involve the use of thermal decomposition, and the supported Ru complex showed lower durability (being only reused for four cycle runs) in comparison with the above-mentioned catalyst **19**.

**Scheme 8.** Asymmetric hydrogenation of aromatic ketones in the presence of the MNP-supported chiral Ru catalyst **19**.



**Scheme 9.** Asymmetric hydrogenation of 2-methylquinoline in the presence of **20**.

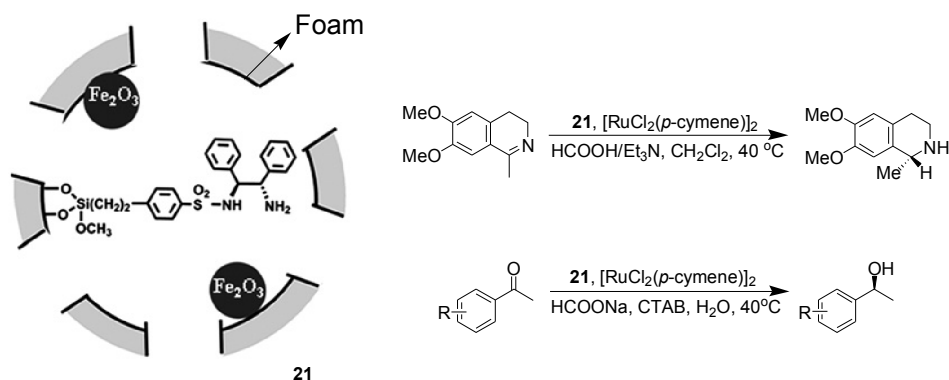


Fan's group [58] reported a novel magnetically separable Ru catalyst **20** containing a host-guest assembly, in which dibenzo[24]crown-8-modified Fe<sub>3</sub>O<sub>4</sub> nanoparticles was used as a host, and a dialkylammonium salt tag connected with (η<sup>6</sup>-arene)[*N*-(*para*-toluenesulfonyl)-1,2-diphenylethylenediamine]ruthenium trifluoromethanesulfonate [Ru(OTf)(TsDPEN)(η<sup>6</sup>-arene)] was regarded as a guest (Scheme 9). The catalytic performance of **20** was evaluated in the asymmetric hydrogenation of 2-methylquinoline, and the reaction was carried out using 2 mol% of **20** in the presence of AgOTf under 50 atm H<sub>2</sub> at 150 °C in CH<sub>2</sub>Cl<sub>2</sub>. The corresponding hydrogenated compound was produced with full conversion and 89% of *e.e.* value. On the basis of the formation of a pseudorotaxane complex

between the host and the guest, the Ru catalyst was easily collected from the reaction medium by using an external magnetic decantation, and reused for at least 5 runs without significant decrease in activity and enantioselectivity.

Transfer hydrogenation is considered to be one of the most important branches of hydrogenation, and it has received more and more attention, because of the easy availability of reductants, its high performance, operational simplicity, and low cost [59,60]. In this field, Ru-TsDPEN (TsDPEN = *N*-(*p*-toluenesulfonyl)-1,2-diphenylethylenediamine) is perhaps the most popular chiral catalyst, with the use of 2-propanol, HCOOH–Et<sub>3</sub>N mixture and aqueous HCOONa as hydrogen donors. Recently, a magnetic siliceous mesocellular foam material-encapsulated Ru-TsDPEN derived catalyst was developed. Starting from siliceous mesocellular foam, the functionalization with  $\gamma$ -Fe<sub>2</sub>O<sub>3</sub> and TsDPEN provided the magnetic siliceous mesocellular foam-caged TsDPEN ligand **21** (Scheme 10). The catalytic property of **21**-[RuCl<sub>2</sub>(*p*-cymene)]<sub>2</sub> was initially tested in the asymmetric hydrogenation of substituted dihydroisoquinoline using HCOOH–Et<sub>3</sub>N azeotrope (molar ratio 2.5/1, pH 3.1) as hydrogen donor. The reaction gave 98% yield and 94% *e.e.* values, which were comparable with the result of the use of homogeneous Ru-TsDPEN. The catalyst was then successfully extended to the asymmetric hydrogenation of aromatic ketones with HCOONa–H<sub>2</sub>O as hydrogen donor. Various secondary alcohols were produced with 99% conversions and 89%–97% *e.e.* values. Moreover, this combination of **21** and [RuCl<sub>2</sub>(*p*-cymene)]<sub>2</sub> allowed the Ru catalyst to be simply recovered with an external magnet and reused consecutively for at least nine runs, while maintaining nearly the same activity and enantioselectivity [61].

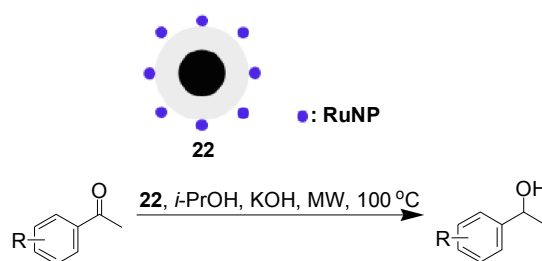
**Scheme 10.** Asymmetric hydrogenation of aromatic ketones using catalyst Ru-**21**.



Varma *et al.* [62,63] demonstrated that MNP-supported RuNPs were competitive candidates for the catalysis of transfer hydrogenation of carbonyl compounds. RuNPs supported on NiFe<sub>2</sub>O<sub>4</sub> were readily prepared and utilized for transfer hydrogenation of a range of carbonyl compounds with isopropyl alcohol as hydrogen donor under microwave irradiation conditions. The desired hydrogenated compounds were isolated in 90%–98% yields. The supported catalyst showed good recyclability. After magnetic collection, it was recycled for another four runs, and its activity remained high [62]. In another report, the same group achieved the assembly of RuNPs on Fe<sub>3</sub>O<sub>4</sub>@SiO<sub>2</sub> nanoparticles from Fe<sup>2+</sup>, Fe<sup>3+</sup> and Ru<sup>3+</sup> precursors in one-pot. The transfer hydrogenation of acetophenone was conducted using isopropanol as a solvent and KOH as base using the obtained hybrid nanocatalyst **22** as catalyst under microwaves irradiation. Within 30 min, acetophenone was quantitatively converted to the

corresponding alcohol. A wide range of secondary alcohols were synthesized in good to excellent yields under the same conditions (Scheme 11) [63]. In the case of the transfer hydrogenation of acetophenone, after the completion of the first reaction, catalyst **22** was collected magnetically and successfully recycled for at least 3 times with the same yield. ICP-AES and TEM analyses revealed that no Ru metal was detected in the reaction medium after completion of the reaction, and the catalyst nearly remained with the same size and morphology during the first three reaction cycles.

**Scheme 11.** Magnetic silica-supported RuNPs: An efficient catalyst for transfer hydrogenation of carbonyl compounds.

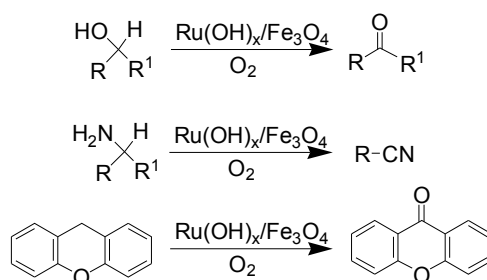


#### 2.4. Oxidation

Oxidation is of paramount importance in both academic and industrial synthetic chemistry. MNP-immobilized Ru catalysts have received considerable attention for the oxidation of alcohols, amines, levulinic acid, and special alkylarene (xanthenes).

Ruthenium hydroxide supported on  $\text{Fe}_3\text{O}_4$  nanoparticles ( $\text{Ru(OH)}_x/\text{Fe}_3\text{O}_4$ ) was easily prepared and exhibited high catalytic performances in aerobic oxidation of alcohols, amines, and xanthene (Scheme 12) [64,65]. The oxidation of various alcohols was efficiently conducted with 3.8 mol% of [Ru] under 1 atm of molecular oxygen, and the corresponding aldehydes and ketones were provided in excellent yields and almost 100% selectivity [64]. The catalytic system was then successfully extended to the oxidation of amines to form nitriles, and high yields were generally detected. However, small amounts of *N*-alkylimines were also observed as byproducts in the process. In addition, xanthene was also quantitatively oxidized to 9-xanthenone with >99% yield under the same conditions [64]. The recyclability test revealed that almost all the  $\text{Ru(OH)}_x/\text{Fe}_3\text{O}_4$  catalyst was removed from the reaction medium in each case and continuously used for other reaction cycles.

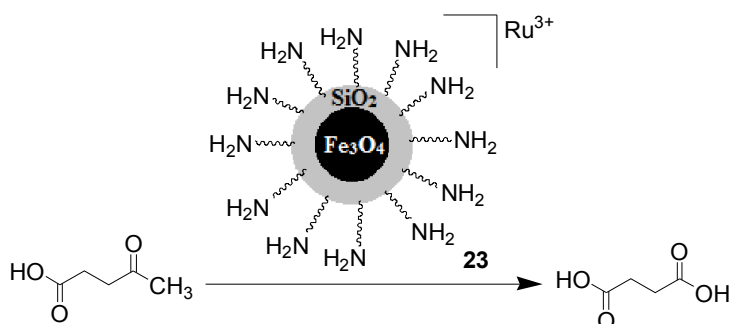
**Scheme 12.** Oxidation of alcohols and amines over  $\text{Ru(OH)}_x/\text{Fe}_3\text{O}_4$  nanoparticles.



Coman and coworkers [66] reported that the oxidation of levulinic acid to succinic acid was efficiently promoted by Ru(III)/functionalized silica-coated magnetic nanoparticles **23** (Scheme 13).

This catalyst was easily prepared through three-step synthesis including silica protection of  $\text{Fe}_3\text{O}_4$  nanoparticles, functionalization with aminopropyl groups, and coordination with  $\text{RuCl}_3$ . The catalytic performance of **23** strongly depends on the pressure of oxygen, reaction temperature and solvent. The reaction reached 53.8% conversion and 96% selectivity towards succinic acid under 10 bar of oxygen at 150 °C in water within 6 h (Scheme 13). The use of lower pressure of oxygen, lower reaction temperature and other solvents decreased the conversion of levulinic acid, however. Furthermore, this heterogeneous catalyst was consecutively reused at least four times, with conversion ranging from 53.5% to 58%, and selectivity ranging from 93.4% to 98.5%. ICP analysis showed that only negligible amounts of Ru leached from the initial catalyst, which indicated the high stability of the catalyst **23**. The authors mentioned that the actual catalytic species for the oxidation is perhaps  $[\text{Ru}(\text{H}_2\text{O})_5\text{OH}]^{2+}$  that was generated by the reaction of Ru species with  $\text{H}_2\text{O}$ , but no evidence was offered to confirm this proposition.

**Scheme 13.** Ru-based magnetic nanoparticles (MNP) for succinic acid synthesis from levulinic acid.



A Ru(III)/amine-functionalized  $\text{Fe}_3\text{O}_4@\text{SiO}_2$  nanocatalyst with a mean diameter of 60 nm was evaluated in the oxidation of alcohols, and it was shown that a series of carbonyl compounds were obtained with excellent conversions and over 99% selectivity, in the presence of 3 atm oxygen at 100 °C with 4 mol% [Ru]. Interestingly, the magnetic Ru(0) NPs that were generated by reduction of the present magnetic Ru(III) catalyst were able to catalyze the hydrogenation of cyclohexene giving full conversion and TOF of  $420 \text{ h}^{-1}$ , under 6 atm hydrogen at 75 °C [67]. In both cases of oxidation and hydrogenation, the amounts of leaching Ru were negligible, which was attributed to the powerful coordination ability of amino group to Ru. This report strongly demonstrates the versatility of Ru catalysts.

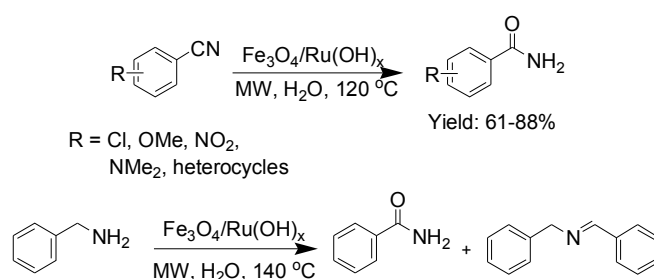
## 2.5. Nitrile Hydration

Functionalized amides are key intermediates that are frequently used in various chemical fields, and nitrile hydration is the one of the most important technologies for the large-scale synthesis of amides. In order to achieve this transformation, MNPs-anchored Ru complexes were recently designed and applied as catalysts.

Amine-modified MNPs were synthesized through sonicating  $\text{Fe}_3\text{O}_4$  nanoparticles with dopamine. The obtained functionalized MNPs then coordinated  $\text{RuCl}_3$  at a basic pH, constructing the hybrid nanoparticles decorated with  $\text{Ru}(\text{OH})_x$ . This nanomaterial was explored as a catalyst for the hydration of nitriles in aqueous medium under microwave irradiation [68]. In the initial experiment, hydration of benzonitrile was chosen as a model reaction, and the desired amide was produced in 85% yield

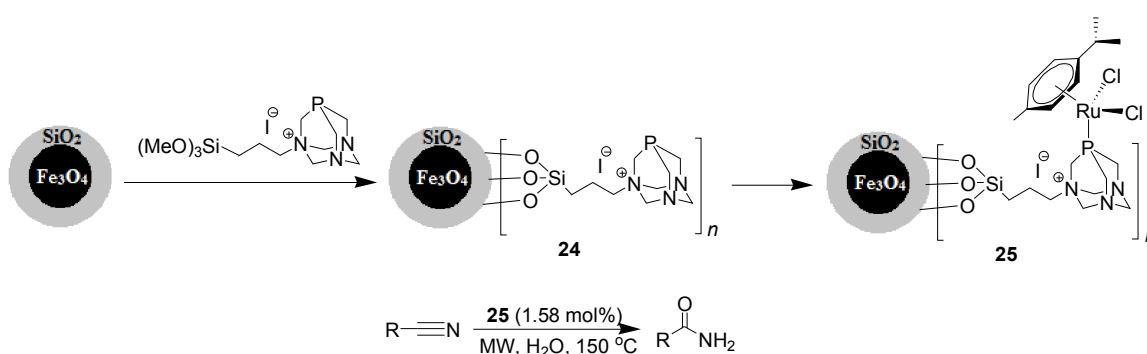
after 30 min of microwave irradiation at 130 °C in water. Furthermore, with this model reaction, the magnetic Ru catalyst was efficiently recovered by using a handheld magnet and reused for at least 3 reaction cycles without obvious loss of activity. Using the same catalytic system, 14 amides were synthesized in 61%–88% yields (Scheme 14). The scope of this strategy was also tested for the oxidation of benzyl amine, and a mixture of corresponding amide and benzylidenebenzylamine were generated (Scheme 14). The percentage of benzylidenebenzylamine in the mixture increased up to 78% upon prolonging the time of microwave irradiation. A subsequent report from the same group [69] demonstrated that Ru(OH)<sub>x</sub> supported on Fe<sub>3</sub>O<sub>4</sub> nanoparticles was readily prepared from Fe<sup>2+</sup>, Fe<sup>3+</sup>, and Ru<sup>3+</sup> precursors in one-pot, and showed a highly efficient activity and selectivity in the hydration of nitrile.

**Scheme 14.** Hydration of nitrile using Fe<sub>3</sub>O<sub>4</sub>/Ru(OH)<sub>x</sub>.



Ruthenium(II)-arene derivatives bearing the phosphane 1,3,5-triaza-7-phosphatricyclo[3.3.1.1]decane (abbreviated as RAPTA) is a classical organometallic compound with versatile applications in catalysis [70–72]. The groups of Basset and Polshettiwar [73] firstly reported the immobilization of RAPTA on MNPs. The synthetic procedure involves the preparation of MNPs-anchored PTA ligand **24** upon reaction of SiO<sub>2</sub>-coated Fe<sub>3</sub>O<sub>4</sub> with trimethoxysilane-functionalized PTA ligand. Further reaction of **24** with a slight excess of the commercially available Ru precursor [RuCl(μ-Cl)(η<sup>6</sup>-*p*-cymene)<sub>2</sub>] provided the magnetic Fe<sub>3</sub>O<sub>4</sub>-RAPTA nanoparticles **25** that was subsequently evaluated in the hydration of nitriles (Scheme 15). Under microwaves irradiation, 55 amides bearing a broad scope of substituting groups were efficiently isolated using 1.58 mol% of [Ru] within short time, with excellent GC yields. Aiming to seek the possibility of practical application, the recyclability of **25** was examined based on the hydration of both benzonitrile and 2-phenoxyacetonitrile. The catalyst **25** was simply separated using an external magnetic field, and continuously used for 4 and 5 times with slight decrease in yield.

**Scheme 15.** Hydration of nitriles catalyzed by the Ru complex-functionalized MNP **25**.

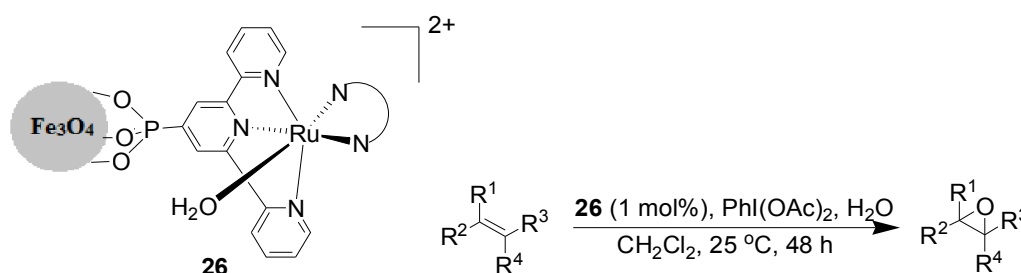


All the above-mentioned processes of hydration of nitriles to amides over MNPs-supported Ru catalysts are truly green and sustainable due to the use of environmentally friendly water as the reaction medium, the use of alternative microwave energy source, and their excellent recyclability.

## 2.6. Other Reactions

Other organic transformations catalyzed by MNP-immobilized Ru catalysts include redox isomerization of allylic alcohols, heteroannulation of (*Z*)-enynols, deallylation, trimethylsilylation of alcohols and phenols, and hydrolysis reactions. The highly active and selective homogeneous epoxidation catalyst  $[\text{Ru}(\text{trpy-P})(\text{B})(\text{H}_2\text{O})]^{2+}$  (trpy-P is diethyl [2,2':6',2'-terpyridin]-4'-ylphosphonate, B = bpm) was immobilized on  $\text{Fe}_3\text{O}_4$  nanoparticles. The resultant heterogeneous catalyst **26** displayed practically the same behavior as its homogeneous counterpart in the epoxidation of alkenes (Scheme 16) [74]. A series of epoxides were synthesized in moderate to good both yields and selectivity towards *cis*-epoxides. The catalyst **26** exhibited an outstanding recyclability and could keep with a similar catalytic performance in terms of activity and selectivity for more than 5 runs.

**Scheme 16.** Epoxidation of selected alkenes catalyzed by molecular ruthenium complexes anchored on MNPs.

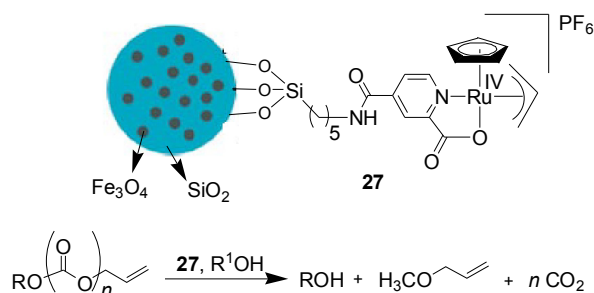


The preparation and catalytic application of the complex  $[\text{CpRu}(\eta^3\text{-C}_3\text{H}_5)(2\text{-pyridinecarboxylato})]\text{PF}_6$  supported on micro-size spherical  $\text{Fe}_3\text{O}_4@\text{SiO}_2$  particles were reported by Kitamura's group [75]. The as-synthesized magnetic catalyst **27** with good dispersibility powerfully promoted the cleavage of allyl esters in alcoholic solvents in the absence of any extra additives (Scheme 17). Multiple recycling experiments for the cleavage of allyl esters involving magnetic decantation of the catalyst were carried out using **27** with slight loss of activity. Below 0.2% of Ru leaching was detected in each reaction cycle. The results presented here should further enhance the utility of this heterogeneous catalyst in protecting group chemistry.

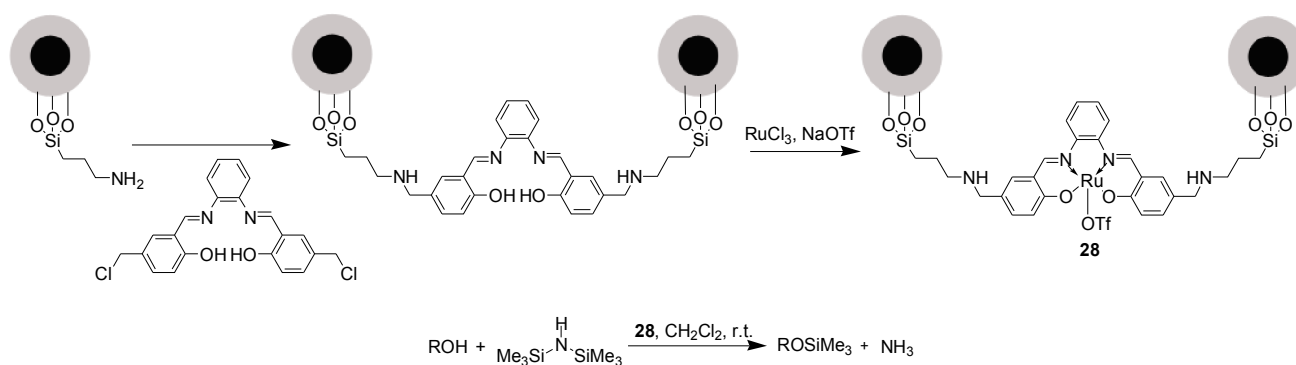
Starting from  $\text{NH}_2$ -modified MNPs, the MNPs-supported complex  $[\text{Ru}^{\text{III}}(\text{Salophen})\text{OTf}]$ , **28**, was assembled via the successive reactions of  $\text{NH}_2$ -modified MNPs with  $\text{H}_2\text{Salophen}$ ,  $\text{RuCl}_3$  and  $\text{NaOTf}$  (Scheme 18) [76]. This catalyst **28** exhibited remarkable catalytic performances for the trimethylsilylation of primary and secondary alcohols as well as phenols with hexamethyldisilazane (HMDS). Benzylic alcohols bearing both electron-donating and electron-withdrawing groups smoothly reacted with HMDS over 4 mol% of  $[\text{Ru}]$ , producing the corresponding TMS ethers in 96%–100% yields in a short time at room temperature. Linear, secondary, tertiary alcohols, and phenols were also suitable participants for the trimethylsilylation, the desired TMS ethers being provided in high yields. However, the reaction times were longer in comparison with those involving benzylic alcohols. Importantly,

catalyst separation was easily achieved using an external magnet without any Ru leaching, and the recovered catalyst was recycled for at least 5 runs without loss in catalytic performance.

**Scheme 17.** Cleavage of allyl esters catalyzed by the magnetically recoverable complex  $[\text{CpRu}(\eta^3\text{-C}_3\text{H}_5)(2\text{-pyridinecarboxylato})]\text{PF}_6$ .



**Scheme 18.** Trimethylsilylation of alcohols and phenols with HMDS catalyzed by **28**.



Bimetallic transition metal core-shell nanoparticles (NPs) have a bright future in catalysis due to their enhanced stability, activity, and other properties compared to their monometallic counterparts [77,78]. Ma *et al.* [79] pioneered the synthesis of bifunctional catalytic and magnetic Ni@Ru core-shell NPs through the seeded-growth method; meanwhile monometallic NiNPs, RuNPs were prepared. All the as-synthesized NPs as well as a physical mixture of NiNPs and RuNPs were used as catalysts in the hydrolysis of ammonia-borane (AB). NiNPs were found to be inactive for this transformation; both monometallic Ru and the physical mixture were active, but with similar level of activity. Interestingly, Ni@Ru NPs with the same amount of [Ru] as in the monometallic Ru and in the physical mixture exhibited remarkably enhanced catalytic performances, which was attributed to the much smaller size of RuNPs in Ni@Ru NPs than in monometallic RuNPs (2.5 nm vs. 8 nm), the increased stability of the deposited RuNPs, and the interaction between NiNPs and RuNPs on the electronic structure of the active metal in Ni@Ru NPs. Importantly, the recyclability test revealed that the Ni@Ru NPs catalyst was able to be magnetically collected and used for 3 more cycles with slight decrease in activity.

### 3. Conclusions and Perspectives

MNPs represent a bridge between homogeneous and heterogeneous catalysis, and are a family of prospective materials with a bright future. To date, MNP-supported ruthenium catalysts have been readily prepared and efficiently used as catalysts in olefin metathesis, azide-alkyne cycloaddition,

hydrogenation, oxidation, nitrile hydration, and several other reactions. The use of MNPs shows many advantages such as convenient separation, efficient recovery, and similar or higher activity compared to their homogeneous counterparts. These strategies for immobilizing Ru complexes on MNPs open a broad field of application of Ru complexes toward “green” chemistry.

Although remarkable progress has been made, only selected Ru complexes were involved in these reactions until now, and not all catalysts have provided satisfactory results. We believe that a fast-increasing number of multi-functionalized MNPs and useful methods will be probed, developed and used for the immobilization of various Ru complexes in various catalytic reactions. Further work is also required to extend these sustainable catalysts towards use in industrial production.

## Acknowledgments

Financial support from the Université de Bordeaux, the Centre National de la Recherche Scientifique and the Chinese Research Council (PhD grant to DW) is gratefully acknowledged.

## Conflicts of Interest

The authors declare no conflict of interest.

## References

1. Anastas, P.T.; Warner, J.C. *Green Chemistry Theory and Practice*; Oxford University Press: Oxford, UK, 1998.
2. Matlack, A.S. *Introduction to Green Chemistry*; Marcel Dekker: New York, NY, USA, 2001.
3. Clark, J.H.; Macquarrie, D.J. *Handbook of Green Chemistry and Technology*; Blackwell Publishing: Abingdon, UK, 2002.
4. Lu, F.; Ruiz, J.; Astruc, D. Palladium-dodecanethiolate nanoparticles as stable and recyclable catalysts for the Suzuki-Miyaura reaction of aryl halides under ambient conditions. *Tetrahedron Lett.* **2004**, *45*, 9443–9445.
5. Astruc, D.; Lu, F.; Ruiz, J. Nanoparticles as Recyclable Catalysts: The Frontier between Homogeneous and Heterogeneous Catalysis. *Angew. Chem. Int. Ed.* **2005**, *44*, 7852–7872.
6. *Transition-Metal Nanoparticles in Catalysis*; Astruc, D., Ed.; Wiley-VCH Verlag GmbH & Co. KGaA: Weinheim, Germany, 2008.
7. Wang, D.; Astruc, D. Dendritic catalysis—Basic concepts and recent trends. *Coord. Chem. Rev.* **2013**, *257*, 2317–2334.
8. Lu, A.-H.; Salabas, E.L.; Schüth, F. Magnetic Nanoparticles: Synthesis, Protection, Functionalization, and Application. *Angew. Chem. Int. Ed.* **2007**, *46*, 1222–1244.
9. Shylesh, S.; Schünemann, V.; Thiel, W.R. Magnetically Separable Nanocatalysts: Bridges between Homogeneous and Heterogeneous Catalysis. *Angew. Chem. Int. Ed.* **2010**, *49*, 3428–3459.
10. Zhu, Y.; Stubbs, L.P.; Ho, F.; Liu, R.; Ship, C.P.; Maguire, J.A.; Hosmane, N.S. Magnetic Nanocomposites: A New Perspective in Catalysis. *Chem. Cat. Chem.* **2010**, *2*, 365–374.
11. Polshettiwar, V.; Luque, R.; Fihri, A.; Zhu, H.; Bouhrara, M.; Basset, J.-M. Magnetically Recoverable Nanocatalysts. *Chem. Rev.* **2011**, *111*, 3036–3075.

12. Baig, R.B.N.; Varma, R.S. Magnetically retrievable catalysts for organic synthesis. *Chem. Commun.* **2013**, *49*, 752–770.
13. Trost, B.M.; Toste, F.D.; Pinkerton, A.B. Non-Metathesis Ruthenium-Catalyzed C-C Bond Formation. *Chem. Rev.* **2001**, *101*, 2067–2096.
14. Trost, B.M.; Frederiksen, M.U.; Rudd, M.T. Ruthenium-Catalyzed Reactions—A Treasure Trove of Atom-Economic Transformations. *Angew. Chem. Int. Ed.* **2005**, *44*, 6630–6666.
15. Arockiam, P.B.; Bruneau, C.; Dixneuf, P.H. Ruthenium(II)-Catalyzed C–H Bond Activation and Functionalization. *Chem. Rev.* **2012**, *112*, 5879–5918.
16. Dragutan, V.; Dragutan, I.; Delaude, L.; Demonceau, A. NHC–Ru complexes—Friendly catalytic tools for manifold chemical transformations. *Coord. Chem. Rev.* **2007**, *251*, 765–794.
17. *Handbook of Metathesis*; Grubbs, R.H., Ed.; Wiley-VCH: Weinheim, Germany, 2003; Volume 1.
18. *Handbook of Metathesis*; Grubbs, R.H., Ed.; Wiley-VCH: Weinheim, Germany, 2003; Volume 2.
19. *Handbook of Metathesis*; Grubbs, R.H., Ed.; Wiley-VCH: Weinheim, Germany, 2003; Volume 3.
20. Chauvin, Y. Olefin Metathesis: The Early Days. *Angew. Chem. Int. Ed.* **2006**, *45*, 3741–3747.
21. Grubbs, R.H. Olefin-Metathesis Catalysts for the Preparation of Molecules and Materials. *Angew. Chem. Int. Ed.* **2006**, *45*, 3760–3765.
22. Schrock, R.R.; Hoveyda, A.H. Molybdenum and Tungsten Imido Alkylidene Complexes as Efficient Olefin-Metathesis Catalysts. *Angew. Chem. Int. Ed.* **2006**, *45*, 3832–3844.
23. *Metathesis- Theory and Practice*; Grela, K., Ed.; Wiley: Hoboken, NJ, USA, 2014.
24. Van Otterlo, W.A.L.; de Koning, C.B. Metathesis in the Synthesis of Aromatic Compounds. *Chem. Rev.* **2009**, *109*, 3743–3782.
25. Buchmeiser, M.R. Polymer-Supported Well-Defined Metathesis Catalysts. *Chem. Rev.* **2009**, *109*, 303–321.
26. Vougioukalakis, G.C.; Grubbs, R.H. Ruthenium-Based Heterocyclic Carbene-Coordinated Olefin Metathesis Catalysts. *Chem. Rev.* **2010**, *110*, 1746–1787.
27. Kress, S.; Blechert, S. Asymmetric catalysts for stereocontrolled olefin metathesis reactions. *Chem. Soc. Rev.* **2012**, *41*, 4389–4408.
28. Deraedt, C.; D’Halluin, M.; Astruc, D. Metathesis Reactions: Recent Trends and Challenges. *Eur. J. Inorg. Chem.* **2013**, *2013*, 4881–4908.
29. Banks, R.L.; Bailey, G.C. Olefin disproportionation: A new catalytic process. *Ind. Eng. Chem. Prod. Res. Dev.* **1964**, *3*, 170–173.
30. Nguyen, S.T.; Johnson, L.K.; Grubbs, R.H.; Ziller, J.W. Ring-Opening Metathesis Polymerization (ROMP) of Norbornene by a Group VIII Carbon Complex in Protic Media. *J. Am. Chem. Soc.* **1992**, *114*, 3974–3975.
31. Schwab, P.; France, M.B.; Ziller, J.W.; Grubbs, R.H. A Series of Well-Defined Metathesis Catalysts—Synthesis of  $[\text{RuCl}_2(=\text{CHR}')(\text{PR}_3)_2]$  and Its Reactions. *Angew. Chem. Int. Ed. Engl.* **1995**, *34*, 2039–2041.
32. Wu, Z.; Nguyen, S.T.; Grubbs, R.H.; Ziller, J.W. Reactions of Ruthenium Carbenes of the Type  $(\text{PPh}_3)_2(\text{X})_2\text{Ru}=\text{CH}-\text{CH}=\text{CPh}_2$  (X = Cl and  $\text{CF}_3\text{COO}$ ) with Strained Acyclic Olefins and Functionalized Olefins. *J. Am. Chem. Soc.* **1995**, *117*, 5503–5511.

33. Scholl, M.; Ding, S.; Lee, C.W.; Grubbs, R.H. Synthesis and Activity of a New Generation of Ruthenium-Based Olefin Metathesis Catalysts Coordinated with 1,3-Dimesityl-4,5-dihydroimidazol-2-ylidene Ligands. *Org. Lett.* **1999**, *1*, 953–956.
34. Kingsbury, J.S.; Harrity, J.P.A.; Bonitatebus, P.J.; Hoveyda, A.H. A Recyclable Ru-Based Metathesis Catalyst. *J. Am. Chem. Soc.* **1999**, *121*, 791–799.
35. Garber, S.B.; Kingsbury, J.S.; Gray, B.L.; Hoveyda, A.H. Efficient and Recyclable Monomeric and Dendritic Ru-Based Metathesis Catalysts. *J. Am. Chem. Soc.* **2000**, *122*, 8168–8179.
36. Love, J.A.; Morgan, J.P.; Trnka, T.M.; Grubbs, R.H. A Practical and Highly Active Ruthenium-Based Catalyst that Effects the Cross Metathesis of Acrylonitrile. *Angew. Chem. Int. Ed.* **2002**, *41*, 4035–4037.
37. Choi, T.L.; Grubbs, R.H. Controlled Living Ring-Opening-Metathesis Polymerization by a Fast-Initiating Ruthenium Catalyst. *Angew. Chem. Int. Ed.* **2003**, *42*, 1743–1746.
38. Mayr, M.; Wang, D.; Kröll, R.; Schuler, N.; Prühs, S.; Fürstner, A.; Buchmeiser, M.R. Monolithic Disk-Supported Metathesis Catalysts for Use in Combinatorial Chemistry. *Adv. Synth. Catal.* **2005**, *347*, 484–492.
39. Michalek, F.; Mädge, D.; Rühle, J.; Bannwarth, W. The activity of covalently immobilized Grubbs–Hoveyda type catalyst is highly dependent on the nature of the support material. *J. Organomet. Chem.* **2006**, *691*, 5172–5180.
40. Mayr, M.; Buchmeiser, M.R.; Wurst, K. Synthesis of a Silica-Based Heterogeneous Second Generation Grubbs Catalyst. *Adv. Synth. Catal.* **2002**, *344*, 712–719.
41. Allen, D.P.; Wingerden, M.M.V.; Grubbs, R.H. Well-Defined Silica-Supported Olefin Metathesis Catalysts. *Org. Lett.* **2009**, *11*, 1261–1264.
42. Monge-Marcet, A.; Pleixats, R.; Cattoën, X.; Man, M.W.C. Sol–gel immobilized Hoveyda–Grubbs complex through the NHC ligand: A recyclable metathesis catalyst. *J. Mol. Catal. A* **2012**, *357*, 59–66.
43. Yao, Q. A Soluble Polymer-Bound Ruthenium Carbon Complex: A Robust and Reusable Catalyst for Ring-Closing Olefin Metathesis. *Angew. Chem. Int. Ed.* **2000**, *39*, 3896–3898.
44. Yao, Q.; Motta, A.R. Immobilization of the Grubbs second-generation ruthenium-carbene complex on poly(ethylene glycol): A highly reactive and recyclable catalyst for ring-closing and cross-metathesis. *Tetrahedron Lett.* **2004**, *45*, 2447–2451.
45. Mennecke, K.; Grela, K.; Kunz, U.; Kirschning, A. Immobilisation of the Grubbs III Olefin Metathesis Catalyst with Polyvinyl Pyridine (PVP). *Syn. Lett.* **2005**, *19*, 2948–2952.
46. Clavier, H.; Grela, K.; Kirschning, A.; Mauduit, M.; Nolan, S.P. Sustainable Concepts in Olefin Metathesis. *Angew. Chem. Int. Ed.* **2007**, *46*, 6786–6801.
47. Zhu, Y.; Loo, K.; Ng, H.; Li, C.; Stubbs, L.P.; Chia, F.S.; Tan, M.; Peng, S.C. Magnetic Nanoparticles Supported Second Generation Hoveyda-Grubbs Catalyst for Metathesis of Unsaturated Fatty Acid Esters. *Adv. Synth. Catal.* **2009**, *351*, 2650–2656.
48. Che, C.; Li, W.; Lin, S.; Chen, J.; Zheng, J.; Wu, J.-C.; Zheng, Q.; Zhang, G.; Yang, Z.; Jiang, B. Magnetic nanoparticle-supported Hoveyda-Grubbs catalysts for ring-closing metathesis reactions. *Chem. Commun.* **2009**, 5990–5992.

49. Samanta, D.; Kratz, K.; Zhang, X.; Emrick, T. A Synthesis of PEG- and Phosphorylcholine-Substituted Pyridines To Afford Water-Soluble Ruthenium Benzylidene Metathesis Catalysts. *Macromolecules* **2008**, *41*, 530–532.
50. Rostovtsev, V.V.; Green, L.G.; Fokin, V.V.; Sharpless, K.B. A Stepwise Huisgen Cycloaddition Process: Copper(I) Catalyzed Regioselective “Ligation” of Azides and Terminal Alkynes. *Angew. Chem. Int. Ed.* **2002**, *41*, 2596–2599.
51. Tornøe, C.W.; Christensen, C.; Meldal, M. Petidotriazoles on Solid Phase: [1,2,3]-Triazoles by Regiospecific Copper(I)-Catalyzed 1,3-Dipolar Cycloadditions of Terminal Alkynes to Azides. *J. Org. Chem.* **2002**, *67*, 3057–3064.
52. Zhang, L.; Chen, X.; Xue, P.; Sun, H.H.Y.; Williams, I.D.; Sharpless, K.B.; Fokin, V.V.; Jia, G. Ruthenium-Catalyzed Cycloaddition of Alkynes and Organic Azide. *J. Am. Chem. Soc.* **2005**, *127*, 15998–15999.
53. Boren, B.C.; Narayan, S.; Rasmussen, L.K.; Zhang, L.; Zhao, H.; Lin, Z.; Jia, G.; Fokin, V.V. Ruthenium-Catalyzed Azide-Alkyne Cycloaddition: Scope and Mechanism. *J. Am. Chem. Soc.* **2008**, *130*, 8923–8930.
54. Rasmussen, L.K.; Boren, B.C.; Fokin, V.V. Ruthenium-Catalyzed Cycloaddition of Aryl Azides and Alkynes. *Org. Lett.* **2007**, *9*, 5337–5339.
55. Johansson, J.R.; Lincoln, P.; Nordén, B.; Kann, N. Sequential One-Pot Ruthenium-Catalyzed Azide-Alkyne Cycloaddition from Primary Alkyl Halides and Sodium Azide. *J. Org. Chem.* **2011**, *76*, 2355–2359.
56. Wang, D.; Salmon, L.; Ruiz, J.; Astruc, D. A recyclable ruthenium(II) complex supported on magnetic nanoparticles: A regioselective catalyst for alkyne–azide cycloaddition. *Chem. Commun.* **2013**, *49*, 6956–6958.
57. Hu, A.; Yee, G.T.; Lin, W.; Nicolaou, K.C.; Edmonds, D.J.; Bulger, P.G. Magnetically Recoverable Chiral Catalysts Immobilized on Magnetite Nanoparticles for Asymmetric Hydrogenation of Aromatic Ketones. *J. Am. Chem. Soc.* **2005**, *127*, 12486–12487.
58. Wu, L.; He, Y.-M.; Fan, Q.-H. Controlled Reversible Anchoring of  $\eta^6$ -Arene/TsDPENRuthenium(II) Complex onto Magnetic Nanoparticles: A New Strategy for Catalyst Separation and Recycling. *Adv. Synth. Catal.* **2011**, *353*, 2915–2919.
59. Hashiguchi, S.; Fujii, A.; Takehara, J.; Ikariya, T.; Noyori, R. Asymmetric Transfer Hydrogenation of Aromatic Ketones Catalyzed by Chiral Ruthenium(II) Complexes. *J. Am. Chem. Soc.* **1995**, *117*, 7562–7563.
60. Uematsu, N.; Fujii, A.; Hashiguchi, S.; Ikariya, T.; Noyori, R. Asymmetric Transfer Hydrogenation of Imines. *J. Am. Chem. Soc.* **1996**, *118*, 4916–4917.
61. Li, J.; Zhang, Y.; Han, D.; Gao, Q.; Li, C. Asymmetric transfer hydrogenation using recoverable ruthenium catalyst immobilized into magnetic mesoporous silica. *J. Mol. Catal. A Chem.* **2009**, *298*, 31–35.
62. Baruwati, B.; Polshettiwar, V.; Varma, R.S. Magnetically recoverable supported ruthenium catalyst for hydrogenation of alkynes and transfer hydrogenation of carbonyl compounds. *Tetrahedron Lett.* **2009**, *50*, 1215–1218.

63. Baig, R.B.N.; Varma, R.S. Magnetic Silica-Supported Ruthenium Nanoparticles: An Efficient Catalyst for Transfer Hydrogenation of Carbonyl Compounds. *ACS Sustain. Chem. Eng.* **2013**, *1*, 805–809.
64. Kotani, M.; Koike, T.; Yamaguchi, K.; Mizuno, N. Ruthenium hydroxide on magnetite as a magnetically separable heterogeneous catalyst for liquid-phase oxidation and reduction. *Green Chem.* **2006**, *8*, 735–741.
65. Costa, V.V.; Jacinto, M.J.; Rossi, L.M.; Landers, R.; Gusevskaya, E.V. Aerobic oxidation of monoterpenic alcohols catalyzed by ruthenium hydroxide supported on silica-coated magnetic nanoparticles. *J. Catal.* **2011**, *282*, 209–214.
66. Podolean, I.; Kuncser, V.; Gheorghe, N.; Macovei, D.; Parvulescu, V.I.; Coman, S.M. Ru-based magnetic nanoparticles (MNP) for succinic acid synthesis from levulinic acid. *Green Chem.* **2013**, *15*, 3077–3082.
67. Jacinto, M.J.; Santos, O.H.C.F.; Jardim, R.F.; Landers, R.; Rossi, L.M. Preparation of recoverable Ru catalysts for liquid-phase oxidation and hydrogenation reactions. *Appl. Catal. A* **2009**, *360*, 177–182.
68. Polshettiwar, V.; Varma, R.S. Nanoparticle-Supported and Magnetically Recoverable Ruthenium Hydroxide Catalyst: Efficient Hydration of Nitriles to Amides in Aqueous Medium. *Chem. Eur. J.* **2009**, *15*, 1582–1586.
69. Baig, R.B.N.; Varma, R.S. A facile one-pot synthesis of ruthenium hydroxide nanoparticles on magnetic silica: Aqueous hydration of nitriles to amides. *Chem. Commun.* **2012**, *48*, 6220–6222.
70. Sclaro, C.; Bergamo, A.; Brescacin, L.; Delfino, R.; Cocchietto, M.; Laurency, G.; Geldbach, T.J.; Sava, G.; Dyson, P.J. *In Vitro* and *in Vivo* Evaluation of Ruthenium(II)-Arene PTA Complexes. *J. Med. Chem.* **2005**, *48*, 4161–4171.
71. Phillips, A.D.; Gonsalvi, L.; Romerosa, A.; Vizza, F.; Peruzzini, M. Coordination chemistry of 1,3,5-triaza-7-phosphaadamantane (PTA) Transition metal complexes and related catalytic, medicinal and photoluminescent applications. *Coord. Chem. Rev.* **2004**, *248*, 955–993.
72. Hartinger, C.G.; Dyson, P.J. Bioorganometallic chemistry—from teaching paradigms to medicinal applications. *Chem. Soc. Rev.* **2009**, *38*, 391–401.
73. García-Garrido, S.E.; Francos, J.; Cadierno, V.; Basset, J.-M.; Polshettiwar, V. Chemistry by Nanocatalysis: First Example of a Solid-Supported RAPTA Complex for Organic Reactions in Aqueous Medium. *Chem. Sus. Chem.* **2011**, *4*, 104–111.
74. Vaquer, L.; Riente, P.; Sala, X.; Jansat, S.; Benet-Buchholz, J.; Llobet, A.; Pericàs, M.A. Molecular ruthenium complexes anchored on magnetic nanoparticles that act as powerful and magnetically recyclable stereospecific epoxidation catalysts. *Catal. Sci. Technol.* **2013**, *3*, 706–714.
75. Hirakawa, T.; Tanaka, S.; Usuki, N.; Kanzaki, H.; Kishimoto, M.; Kitamura, M. A Magnetically Separable Heterogeneous Deallylation Catalyst: [CpRu( $\eta^3$ -C<sub>3</sub>H<sub>5</sub>)(2-pyridinecarboxylato)]PF<sub>6</sub> Complex Supported on a Ferromagnetic Microsize Particle Fe<sub>3</sub>O<sub>4</sub>@SiO<sub>2</sub>. *Eur. J. Org. Chem.* **2009**, *2009*, 789–792.
76. Torki, M.; Tangestaninejad, S.; Mirkhani, V.; Moghadam, M.; Mohammadpoor-Baltork, I. Ru<sup>III</sup>(OTf)SalophenCH<sub>2</sub>–NHSiO<sub>2</sub>–Fe: An efficient and magnetically recoverable catalyst for

trimethylsilylation of alcohols and phenols with hexamethyldisilazane. *Appl. Organomet. Chem.* **2014**, *28*, 304–309.

77. Xu, D.; Liu, Z.; Yang, H.; Yang, Q.; Zhang, J.; Fang, J.; Zou S.; Sun, K. Solution-Based Evolution and Enhanced Methanol Oxidation Activity of Monodisperse Platinum-Copper Nanocubes. *Angew. Chem. Int. Ed.* **2009**, *48*, 4217–4221.
78. Singh, S.K.; Xu, Q. Bioimaging of targeting cancers using aptamer-conjugated carbon nanodots. *Chem. Commun.* **2010**, *46*, 6543–6545.
79. Chen, G.; Desinan, S.; Nechache, R.; Rosei, R.; Rosei, F.; Ma, D. Bifunctional catalytic/magnetic Ni@Ru core-shell nanoparticles. *Chem. Commun.* **2011**, *47*, 6308–6310.

*Sample Availability:* Samples of the compounds **11**, **12**, **13**, **17**, **18** are available from the authors.

© 2014 by the authors; licensee MDPI, Basel, Switzerland. This article is an open access article distributed under the terms and conditions of the Creative Commons Attribution license (<http://creativecommons.org/licenses/by/3.0/>).

# A recyclable ruthenium(II) complex supported on magnetic nanoparticles: a regioselective catalyst for alkyne–azide cycloaddition†

Dong Wang,<sup>a</sup> Lionel Salmon,<sup>b</sup> Jaime Ruiz<sup>a</sup> and Didier Astruc<sup>\*a</sup>

Cite this: *Chem. Commun.*, 2013, **49**, 6956

Received 24th April 2013,  
Accepted 13th June 2013

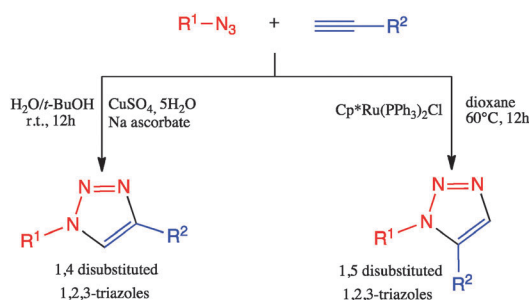
DOI: 10.1039/c3cc43048k

www.rsc.org/chemcomm

**A magnetically separable ruthenium catalyst was synthesized through immobilizing a pentamethylcyclopentadienyl ruthenium complex on iron oxide nanoparticles. The catalyst is highly active and selective for the synthesis of 1,5-disubstituted 1,2,3-triazoles via cycloaddition of alkynes and organic azides and can be recycled at least 5 times.**

1,2,3-Triazoles are five-membered nitrogen heterocyclic compounds that have been widely used in various research fields including synthetic organic,<sup>1</sup> medicinal,<sup>2</sup> materials,<sup>3</sup> and biological chemistry.<sup>4</sup> Among numerous methods, catalyzed Huisgen cycloaddition of alkynes and organic azides by complexes of Cu(I) (CuAAC)<sup>5</sup> and [Cp\*Ru(II)] (RuAAC)<sup>6</sup> are the two most efficient ones that have been used to assemble the 1,2,3-triazole ring, respectively, forming 1,4- and 1,5-disubstituted 1,2,3-triazoles selectively (Scheme 1).

Since the latter method (RuAAC) was pioneered by the groups of Fokin and Jia,<sup>6a</sup> some [Cp\*Ru] complexes<sup>6</sup> have been successfully applied for the catalysis of RuAAC reactions, such as Cp\*RuCl(PPh<sub>3</sub>)<sub>2</sub>, Cp\*RuCl(NBD), Cp\*RuCl(COD), and [Cp\*RuCl]<sub>4</sub>. However, to date only a handful of reports have been published in the field of RuAAC, and there has been no publication on recyclable RuAAC catalysts.



**Scheme 1** Regioselective copper vs. ruthenium-catalyzed alkyne–azide cycloaddition reactions (CuAAC and RuAAC).

<sup>a</sup> ISM, Univ. Bordeaux, 351 Cours de la Libération, 33405 Talence Cedex, France.  
E-mail: d.astruc@ism.u-bordeaux1.fr

<sup>b</sup> LCC, CNRS, 205 Route de Narbonne, 31077 Toulouse Cedex, France

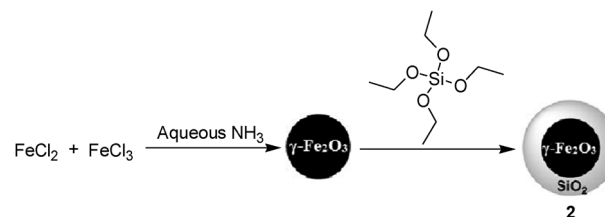
† Electronic supplementary information (ESI) available. See DOI: 10.1039/c3cc43048k

The immobilization of homogeneous catalysts to facilitate their separation and recycling is a task of great economic and environmental importance in catalysis science. Various inorganic and organic supports have been explored, such as inorganic solids,<sup>7</sup> polymers,<sup>8</sup> fluorinated tags,<sup>9</sup> and ionic liquids.<sup>10</sup>

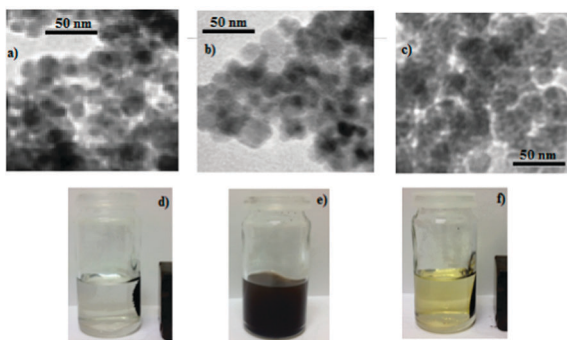
Magnetic nanoparticles (MNPs) have recently emerged as ideal catalyst supports due to their large surface area, straightforward and relatively low preparation cost, low toxicity, good stability, as well as facile separation by magnetic forces.<sup>11</sup> The catalysts supported on magnetic nanoparticles combine these advantages of heterogeneous catalysts (easy recovery and regeneration) and nanocatalysts (such as a large surface-to-volume ratio relative to bulk materials, excellent activity, great selectivity, and high stability), and overcome the aggregation problem of metallic nanoparticles. Moreover, their property of magnetic separability eliminates the requirement of catalyst filtration after completion of the reaction.

Herein, we report simple and efficient synthesis of an iron-oxide magnetic nanoparticle-supported pentamethylcyclopentadienyl ruthenium(II) catalyst and its application in Huisgen cycloaddition of alkynes and organic azides for the fully selective construction of 1,5-disubstituted 1,2,3-triazoles.

The primary step of this objective was achieved by the synthesis of magnetic nanoparticles (Scheme 2). Monodisperse silica-coated  $\gamma$ -Fe<sub>2</sub>O<sub>3</sub> nanoparticles (SiO<sub>2</sub>/ $\gamma$ -Fe<sub>2</sub>O<sub>3</sub>) **2** were derived by coating  $\gamma$ -Fe<sub>2</sub>O<sub>3</sub> core **1** (which was obtained by a co-precipitation method) with a silica layer. In this process, tetraethoxysilane (TEOS) and aqueous NH<sub>3</sub> were used as a silica source and a hydrolyzing agent, respectively.<sup>12</sup> Transmission electron microscopy (TEM) images of **2** showed the core-shell structure and the silica coating that has a



**Scheme 2** Synthesis of SiO<sub>2</sub>/ $\gamma$ -Fe<sub>2</sub>O<sub>3</sub> nanoparticles.

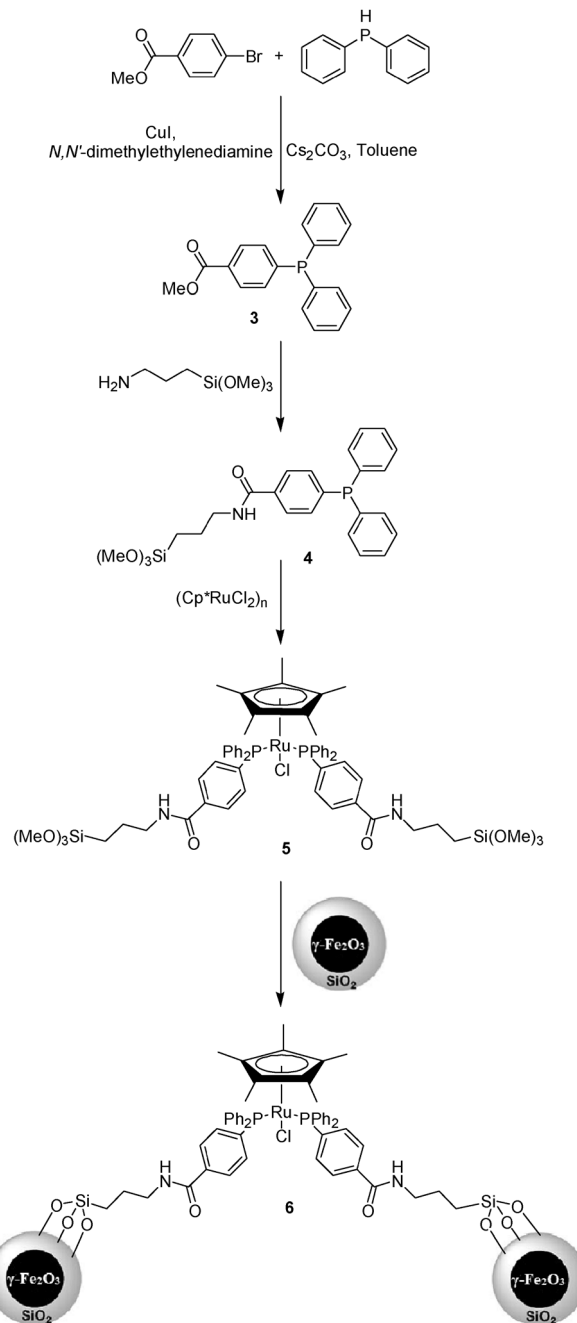


**Fig. 1** (a) TEM image of  $\text{SiO}_2/\gamma\text{-Fe}_2\text{O}_3$ ; (b) TEM image of  $\text{Cp}^*\text{Ru}/\text{SiO}_2/\gamma\text{-Fe}_2\text{O}_3$  before reaction; (c) TEM image of  $\text{Cp}^*\text{Ru}/\text{SiO}_2/\gamma\text{-Fe}_2\text{O}_3$  after 5 reaction cycles; (d)  $\text{Cp}^*\text{Ru}/\text{SiO}_2/\gamma\text{-Fe}_2\text{O}_3$  in THF using a small magnet; (e)  $\text{Cp}^*\text{Ru}/\text{SiO}_2/\gamma\text{-Fe}_2\text{O}_3$  dispersion in a reaction medium; (f) catalyst separation using a small magnet.

uniform thickness of 9 nm (Fig. 1a). The dense silica shell has plenty of Si–OH units for potential derivatization with different functional groups, and also prevents leaching of iron from the core under harsh shaking conditions. The silylated  $\text{Cp}^*\text{Ru}(\text{II})$  complex **5** was obtained through coordination between the cluster  $(\text{Cp}^*\text{RuCl}_2)_n$  and  $\text{Si}(\text{OMe})_3$ -functionalized triarylphosphine **4**.<sup>13,14</sup> Then **5** was successfully immobilized on the surface of robust  $\text{SiO}_2/\gamma\text{-Fe}_2\text{O}_3$  via the heterogenization with the Si–OH binding sites of **2**. The TEM images of the targeted magnetic nanoparticle catalyst ( $\text{Cp}^*\text{Ru}/\text{SiO}_2/\gamma\text{-Fe}_2\text{O}_3$ ) **6** depicted relatively uniform core–shell nanoparticles with an average size of approximately 30 nm (Fig. 1b). The loading of the ruthenium complex in **6** was calculated by determination of the nitrogen content (C, H, N elemental analysis), and the result showed that it was approximately  $0.16 \text{ mmol g}^{-1}$  (Scheme 3).

The catalytic application of magnetically recyclable catalyst **6** in cycloaddition of alkynes and organic azides was further investigated (Table 1). Phenylacetylene and benzyl azide were chosen as the model substrates, and the cycloaddition was conducted at  $65^\circ\text{C}$  under a nitrogen atmosphere for 3 h in the presence of 2 mol% of **6**. As shown in Table 1, the corresponding 1,5-disubstituted 1,2,3-triazole **7a** was produced in 91% yield with almost 100% selectivity (99.96% selectivity, which was determined using both GC and NMR). The catalyst **6** showed excellent magnetic properties, stability (Fig. 1d) and dispersion (Fig. 1e) in the reaction medium, and can be easily collected using external magnets after completion of the reactions (Fig. 1f), which minimizes the loss of catalytically active particles and oxidation of sensitive ruthenium complexes during separation. The catalyst **6** could be reused five times by simple magnetic separation with only a minimum decrease in catalytic activity and selectivity (Table 1). Moreover, the morphology and size of the nanoparticles do not change much even after five cycles.

Encouraged by the efficiency of the reaction protocol described above, the scope of the reaction was examined. Firstly, various terminal alkynes were investigated in reactions with benzyl azides. Alkynes containing electron-withdrawing or electron-releasing groups were suitable cycloaddition partners (Fig. 2). The reactions of heteroatom-containing alkynes also proceeded smoothly. The aliphatic alkyne 1-hexyne and ferrocenylacetylene were suitable substrates producing triazoles in 84% and 93% yield (**7h**, **7i**), respectively. The organic azide substrates were further investigated, and the results indicated that both benzyl and alkyl azides reacted

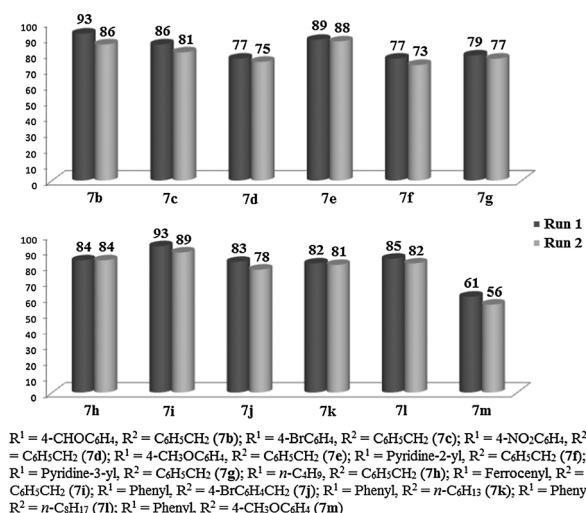
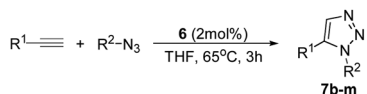


**Scheme 3** Synthesis of  $\text{Cp}^*(\text{PPh}_3)_2\text{Ru}/\text{SiO}_2/\gamma\text{-Fe}_2\text{O}_3$ .

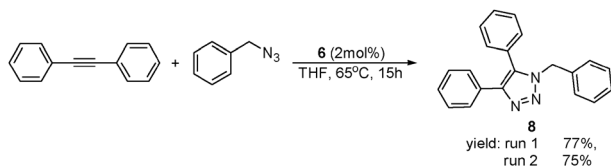
**Table 1** Reusability test for the magnetic catalyst **6** in cycloaddition of phenylacetylene and benzyl azides<sup>a</sup>

Run	1	2	3	4	5
Yield <sup>b</sup> (%)	91	87	83	86	77
Selectivity <sup>c</sup> (%)	99.9	99.5	99.4	98.3	98.3

<sup>a</sup> The reaction was carried out using phenylacetylene (0.5 mmol) and benzyl azide (0.5 mmol) in the presence of **6** (63 mg) at  $65^\circ\text{C}$  under a nitrogen atmosphere. <sup>b</sup> Isolated yields after column chromatography. <sup>c</sup> Determination using GC or/and NMR.



**Fig. 2** RuAAC reactions in the presence of the magnetic catalyst **6**. The bar graph shows the yields determined by isolation after column chromatography.



**Scheme 4** Cp<sup>\*</sup>Ru/SiO<sub>2</sub>/γ-Fe<sub>2</sub>O<sub>3</sub>-catalyzed synthesis of 1,4,5-trisubstituted triazole from internal alkynes.

successfully, whereas with aryl azides the yield was somewhat lower (**7m**). In addition, **6** was active with internal alkynes as well, and 1,4,5-trisubstituted 1,2,3-triazole **8** was obtained in 77% yield upon cycloaddition of 1,2-diphenylethyne with benzyl azides (Scheme 4). This aspect is all the more valuable as internal alkynes are unreactive toward the click reaction catalyzed by Cu(I). The reusability of **6** was also verified with all substrates as shown in Table 1 and Fig. 2. In addition, we found that the catalytic system was successfully and reproducibly applied up to 10 mmol-scale synthesis (Scheme S1, ESI<sup>†</sup>), allowing the isolation of 1.86 g (79% yield) of **7a**.

In conclusion, we have shown here the successful preparation and immobilization of a silylated Cp<sup>\*</sup>Ru(II) complex on the surface of SiO<sub>2</sub>/γ-Fe<sub>2</sub>O<sub>3</sub> nanoparticles. Using a magnetic support enables the recovery of the catalyst by simply applying an external magnetic field, which avoids the need for precipitation or filtration steps. The magnetic catalyst **6** that was prepared showed high catalytic activity and selectivity in the cycloaddition of alkynes and organic azides for constructing 1,5-disubstituted 1,2,3-triazoles. Moreover, the catalyst could be recovered and reused at least five times with only a slight decrease in catalytic activity and selectivity, and it is therefore the first recyclable catalyst for the RuAAC reaction.

In addition, given the considerable uses of the Cp<sup>\*</sup>Ru(II) catalysts in organic synthesis, the principles and results presented here should open a field of applications in “green” chemistry involving the recycling of such catalysts.

Financial support from the China Scholarship Council (CSC) (PhD grant to DW), the Universities Bordeaux 1 and Toulouse III, and the Centre National de la Recherche Scientifique (CNRS) is gratefully acknowledged.

## References

- (a) S. Wacharasindhu, S. Bardhan, Z.-K. Wan, K. Tabei and T. S. Mansour, *J. Am. Chem. Soc.*, 2009, **131**, 4174; (b) Y. X. Liu, W. M. Yan, Y. F. Chen, J. L. Petersen and X. D. Shi, *Org. Lett.*, 2008, **10**, 5389; (c) A. R. Katritzky, S. Bobrov, K. Kostyantyn, Y. Ji and P. J. Steel, *J. Org. Chem.*, 2003, **68**, 5713.
- (a) R. Manetsch, A. Krasiski, Z. Radi, J. Rauschel, P. Taylor, K. B. Sharpless and H. C. Kolb, *J. Am. Chem. Soc.*, 2004, **126**, 12809; (b) M. Whiting, J. Muldoon, Y. C. Lin, S. M. Silverman, W. Lindstrom, A. J. Olson, H. C. Kolb, M. G. Finn, K. B. Sharpless, J. H. Elder and V. V. Fokin, *Angew. Chem., Int. Ed.*, 2006, **45**, 1435; (c) J. Wang, G. Sui, V. P. Mocharla, R. J. Lin, M. E. Phelps, H. C. Kolb and H.-R. Tseng, *Angew. Chem., Int. Ed.*, 2006, **45**, 5276.
- (a) H. Nandivada, X. W. Jiang and J. Lahann, *Adv. Mater.*, 2007, **19**, 2197; (b) C. F. Ye, G. L. Gard, R. W. Winter, R. G. Syvret, B. Twamley and J. M. Shreeve, *Org. Lett.*, 2007, **9**, 3841; (c) P. Wu, A. K. Feldman, A. K. Nugent, C. J. Hawker, A. Scheel, B. Voit, J. Pyun, J. M. J. Fréchet, K. B. Sharpless and V. V. Fokin, *Angew. Chem., Int. Ed.*, 2004, **43**, 3928.
- (a) D. R. Buckle and C. J. M. Rockell, *J. Chem. Soc., Perkin Trans. 1*, 1982, 627; (b) M. J. Genin, D. A. Allwine, D. J. Anderson, M. R. Barbachyn, D. E. Emmert, S. A. Garmon, D. R. Graber, K. C. Grega, J. B. Hester, D. K. Hutchinson, J. Morris, R. J. Reischer, C. W. Ford, G. E. Zurenko, J. C. Hamel, R. D. Schaadt, D. Stapert and B. H. Yagi, *J. Med. Chem.*, 2000, **43**, 953.
- (a) V. V. Rostovtsev, L. G. Green, V. V. Fokin and K. B. Sharpless, *Angew. Chem., Int. Ed.*, 2002, **41**, 2596; (b) C. W. Tonoe, C. Christensen and M. Medal, *J. Org. Chem.*, 2002, **67**, 3057; (c) M. Meldal and C. W. Tornoe, *Chem. Rev.*, 2010, **39**, 1338; (d) J. E. Hein and V. V. Fokin, *Chem. Soc. Rev.*, 2010, **39**, 1302; (e) L. Liang and D. Astruc, *Coord. Chem. Rev.*, 2011, **255**, 2933.
- (a) L. Zhang, X. Chen, P. Xue, H. H. Y. Sun, I. D. Williams, K. B. Sharpless, V. V. Fokin and G. Jia, *J. Am. Chem. Soc.*, 2005, **127**, 15998; (b) B. C. Boren, S. Narayan, L. K. Rasmussen, L. Zhang, H. Zhao, Z. Lin, G. Jia and V. V. Fokin, *J. Am. Chem. Soc.*, 2008, **130**, 8923; (c) L. K. Rasmussen, B. C. Boren and V. V. Fokin, *Org. Lett.*, 2007, **9**, 5337; (d) J. R. Johansson, P. Lincoln, B. Nordén and N. Kann, *J. Org. Chem.*, 2011, **76**, 2355.
- (a) T. Fey, H. Fischer, S. Bachmann, K. Albert and C. Bolm, *J. Org. Chem.*, 2001, **66**, 8154; (b) P. N. Liu, P. M. Gu, F. Wang and Y. Q. Tu, *Org. Lett.*, 2004, **6**, 169; (c) Y. Gu, C. Ogawa, J. Kobayashi, Y. Mori and S. Kobayashi, *Angew. Chem., Int. Ed.*, 2006, **45**, 7217; (d) J. Lim, S. S. Lee, S. N. Riduan and J. Y. Ying, *Adv. Synth. Catal.*, 2007, **349**, 1066.
- (a) M. Gilhespy, M. Lok and X. Baucherel, *Chem. Commun.*, 2005, 1085; (b) T. Sekiguti, Y. Iizuka, S. Takizawa, D. Jayaprakash, T. Arai and H. Sasai, *Org. Lett.*, 2003, **5**, 2647; (c) S. Lu and M. H. Alper, *J. Am. Chem. Soc.*, 2003, **125**, 13126.
- (a) W. Zhang, *Chem. Rev.*, 2004, **104**, 2531; (b) M. Wende and J. A. Gladysz, *J. Am. Chem. Soc.*, 2003, **125**, 5861; (c) R. C. da Costa and J. A. Gladysz, *Adv. Synth. Catal.*, 2007, **349**, 243.
- (a) T. J. Geldbach and P. J. Dyson, *J. Am. Chem. Soc.*, 2004, **126**, 8114; (b) M. Lombardo, F. Pasi, S. Easwar and C. Trombini, *Adv. Synth. Catal.*, 2007, **349**, 2061; (c) S. Luo, X. Mi, L. Zhang, S. Liu, H. Xu and J. P. Cheng, *Angew. Chem., Int. Ed.*, 2006, **45**, 3093.
- (a) V. Polshettiwar, R. Luque, A. Fihri, H. Zhu, M. Bouhrara and J.-M. Basset, *Chem. Rev.*, 2011, **111**, 3036; (b) A. Fihri, M. Bouhrara, B. Nekouishahari, J.-M. Basset and V. Polshettiwar, *Chem. Soc. Rev.*, 2011, **40**, 5181; (c) R. B. Bedford, M. Betham, D. W. Bruce, S. A. Davis, R. M. Frost and M. Hird, *Chem. Commun.*, 2006, 1398; (d) D. Astruc, F. Lu and J. Ruiz, *Angew. Chem., Int. Ed.*, 2005, **44**, 7852; (e) T. J. Yoon, W. Lee, Y. S. Oh and J. K. Lee, *New J. Chem.*, 2003, **27**, 227; (f) T. J. Yoon, J. I. Kim and J. K. Lee, *Inorg. Chim. Acta*, 2003, **345**, 228; (g) B. Berkovski, in *Magnetic Fluids and Applications Handbook*, ed. B. Berkovski and V. Bashstovoy, Begell House, Inc., New York, Wallingford, 1996, pp. 1–250.
- S. Shylesh, L. Wang and W. R. Thiel, *Adv. Synth. Catal.*, 2010, **352**, 425.
- D. Gelman, L. Jiang and S. L. Buchwald, *Org. Lett.*, 2003, **5**, 2315.
- L. Wang, A. Reis, A. Seifert, T. Philippi, S. Ernst, M. Jia and W. R. Thiel, *Dalton Trans.*, 2009, 3315.

## **Chapter 3**

### **Magnetic Nanoparticle-Immobilized Tris(triazolyl) Cu(I) Catalyst for the Copper-catalyzed Alkyne Azide (CuAAC) "Click" Reaction**

### 3.1 Introduction

The copper-catalyzed alkyne-azide Huisgen-type cycloaddition (“click” reaction) yielding 1,4-disubstituted 1,2,3-triazoles has received a lot of attentions and driven various applications in biological science, synthetic organic chemistry, medicinal chemistry and material chemistry, since it was discovered by the groups of Sharpless and Meldal in 2002.<sup>1,2</sup> In the previous work of our group, the Cu(I) complexes with (hexabenzyl)tren, and dendritic analogues with 18- or 54- branch termini were first prepared.<sup>3</sup> These Cu (hexabenzyl)tren catalysts are remarkably powerful for “click” reaction in organic solvent and in water, in addition, the these metallodendrimers showed a rare positive dendritic effect. In 2011, our group also published a comprehensive article entitled “*The Copper(I)-catalyzed Alkyne-Azide Cycloaddition (CuAAC) “Click” Reaction and its Applications. An Overview*” for reviewing the “click” concept, Cu(I) catalysts and ligands, as well as its applications.<sup>4</sup>

Recovery of Cu species is a long-term exploration in “click” reaction.<sup>5</sup> In this work, a MNPs-supported tris(triazolyl)-CuBr catalyst, with a diameter of approximately 25 nm was synthesized. This magnetically recyclable catalyst smoothly promoted “click” reactions of terminal alkynes in water at room temperature. Inductively coupled plasma (ICP) analysis revealed that the Cu leaching is almost negligible. This work was carried out in collaboration with Laetitia Etienne (determination of copper traces in the products by ICPMS), and with Mar í Echeverria and Dr. Sergio Moya (TEM).

### References:

1. V. V. Rostovtsev, L. G. Green, V. V. Fokin, K. B. Sharpless, *Angew. Chem. Int. Ed.* **2002**, *41*, 2596.
2. C. W. Tornøe, C. Christensen, M. Meldal, *J. Org. Chem.* **2002**, *67*, 3057.
3. L. Liang, J. Ruiz, D. Astruc, *Adv. Syn. Catal.* **2011**, *353*, 3434.
4. L. Liang, D. Astruc, *Coord. Chem. Rev.* **2011**, *255*, 2933.
5. B. Dervaux, F. D. Prez, *Chem. Sci.* **2012**, *3*, 959.

## Click Chemistry

A Highly Active and Magnetically Recoverable Tris(triazolyl)-Cu<sup>I</sup> Catalyst for Alkyne–Azide Cycloaddition ReactionsDong Wang,<sup>[a]</sup> Laetitia Etienne,<sup>[b]</sup> María Echeverría,<sup>[c]</sup> Sergio Moya,<sup>[c]</sup> and Didier Astruc\*<sup>[a]</sup>

**Abstract:** Nanoparticle-supported tris(triazolyl)-CuBr, with a diameter of approximately 25 nm measured by TEM spectroscopy, has been easily prepared, and its catalytic activity was evaluated in the copper-catalyzed azide–alkyne cycloaddition (CuAAC) reaction. In initial experiments, 0.5 mol% loading successfully promoted the CuAAC reaction between benzyl azide and phenylacetylene, in water at room temperature (25 °C). During this process, the iron oxide nanoparticle-supported tris(triazolyl)-CuBr displayed good monodispersity, excellent recoverability, and outstanding reusability. Indeed, it was simply collected and separated from the reaction medium by using an external magnet, then used for an-

other five catalytic cycles without significant loss of catalytic activity. Inductively coupled plasma (ICP) analysis for the first cycle revealed that the amount of copper leached from the catalyst into the reaction medium is negligible (1.5 ppm). The substrate scope has been examined, and it was found that the procedure can be successfully extended to various organic azides and alkynes and can also be applied to the one-pot synthesis of triazoles, through a cascade reaction involving benzyl bromides, alkynes, and sodium azide. In addition, the catalyst was shown to be an efficient CuAAC catalyst for the synthesis of allyl- and TEG-ended (TEG = triethylene glycol) 27-branch dendrimers.

## Introduction

The copper-catalyzed 1,3-dipolar cycloaddition reaction between alkynes and azides (CuAAC), yielding 1,4-disubstituted 1,2,3-triazoles,<sup>[1]</sup> is undoubtedly the most representative example of a “click” reaction<sup>[2]</sup> to date. The CuAAC reaction demonstrates excellent atom economy, exclusive regioselectivity, a high tolerance to a range of functional groups, and the use of mild reaction conditions. In addition, 1,2,3-triazoles possess many interesting properties, such as antibacterial,<sup>[3]</sup> antiallergic,<sup>[4]</sup> anti-HIV,<sup>[5]</sup> and antineoplastic<sup>[6]</sup> activity. 1,2,3-triazoles also have the potential for coordinating to metal centers, which can be useful for sensing and in further catalytic reactions.<sup>[7]</sup> Therefore, the CuAAC reaction has been extensively applied in organic synthesis, biology, and materials science<sup>[8]</sup> since its discovery by the groups of Sharpless<sup>[1a]</sup> and Meldal<sup>[1b]</sup> in 2002.

However, the majority of reported CuAAC systems, in particular the systems that use homogeneous catalysts, have been susceptible to contamination by the cytotoxic Cu<sup>I</sup> ion, which

restricts the application of such systems in electronics and biomedicine. To overcome this drawback, a wide range of strategies have been investigated. Chromatographic purification of the crude product, washing the crude product with ethylenediaminetetraacetic acid (EDTA) or ammonia, and performing CuAAC reactions under continuous flow conditions (quadrature<sup>TM</sup>, thiourea resin, or activated charcoal as the metal scavenger) are all acceptable methods, but they are scavenger-, energy-, and time-consuming procedures. The development of an astute copper-free click strategy has been proposed, but this strategy has only been used for the CuAAC reactions of cyclooctyne reagents.<sup>[9]</sup> The heterogenization of click-chemistry catalysts appears to be a logical solution; the use of heterogeneous catalysts could result in easy removal, recovery, and reusability of the copper catalyst; thereby, minimizing copper contamination of the reaction products. Until now, several supports have been employed for immobilization of copper species, such as polymers,<sup>[10]</sup> zeolites,<sup>[11]</sup> activated carbon,<sup>[12]</sup> alumina,<sup>[11a,13]</sup> resin,<sup>[14]</sup> carbon nanotubes,<sup>[15]</sup> and silica.<sup>[16]</sup>

In a related context, functionalized magnetic nanoparticles have emerged as viable alternatives.<sup>[17]</sup> Magnetic nanosized catalysts can easily be separated from reaction mixtures by using an external magnet. They display better stability and reusability, more efficient catalytic activity, lower preparation costs, and lower toxicities in comparison with other materials that are used as supported heterogeneous catalysts. These properties are due to their insoluble, paramagnetic, and nanosized nature.<sup>[18]</sup> In addition, the size, shape, morphology, and dispersity of magnetic nanosized catalysts are controllable. Therefore it is possible to design different magnetic nanocatalysts for specific catalytic applications.<sup>[19]</sup>

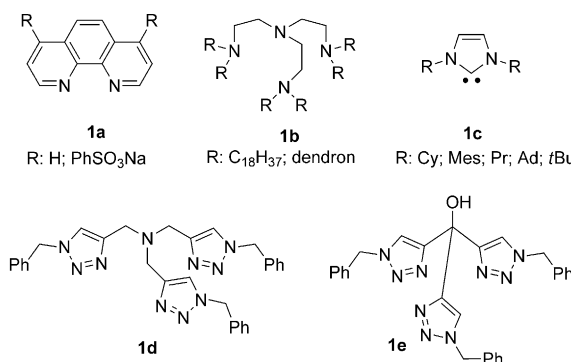
[a] Dr. D. Wang, Prof. Dr. D. Astruc  
ISM, Université Bordeaux  
351 Cours de la Libération, 33405 Talence Cedex (France)  
E-mail: d.astruc@ism.u-bordeaux1.fr

[b] L. Etienne  
ICMCB, UPR CNRS No. 9048  
87 Avenue, Pey-berland, 33608 Pessac Cedex (France)

[c] M. Echeverría, Prof. S. Moya  
CIC biomaGUNE, Unidad Biosuperficies  
Paseo Miramón 182, Edif. “C”, 20009 Donostia-San Sebastián (Spain)

Supporting information for this article is available on the WWW under <http://dx.doi.org/10.1002/chem.201304536>.

Among the various copper sources for CuAAC reactions, including  $\text{Cu}^{\text{II}}$  salt/reductant mixtures,  $\text{Cu}^{\text{I}}$  salts, copper nanoparticles,  $\text{Cu}^{\text{I}}$  complexes, and  $\text{Cu}^0$ /oxidant mixtures,  $\text{Cu}^{\text{I}}$  complexes represent the most efficient copper source in terms of product yield and catalyst turn-over numbers (TONs). The use of  $\text{Cu}^{\text{I}}$ -ligand complexes was shown to both accelerate the catalytic process, in comparison with the ligand-free  $\text{Cu}^{\text{I}}$  species, and stabilize  $\text{Cu}^{\text{I}}$  intermediates. Moreover, it is relatively straightforward to graft  $\text{Cu}^{\text{I}}$  complexes onto a support in hybrid material assemblies. Indeed, nitrogen-based ligands and N-heterocyclic carbenes (**1a–e**, Figure 1) were found to be excellent ligands



**Figure 1.** A selection of ligands currently used in CuAAC reactions. Cy = cyclohexyl; Mes = mesityl; Pr = *n*-propyl; Ad = adamantyl.

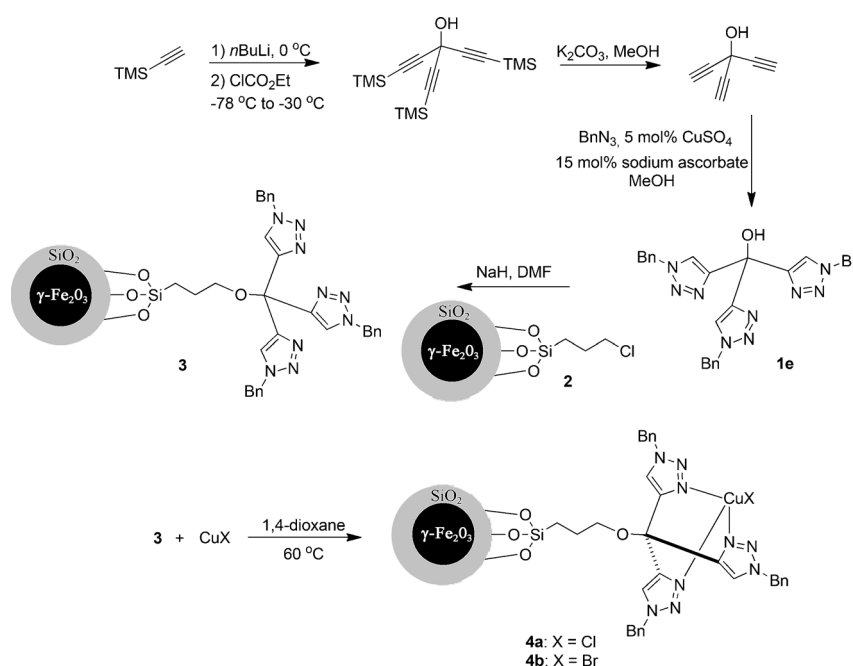
for CuAAC reactions.<sup>[20]</sup> Fokin et al. designed polytriazoles **1d** that showed outstanding activity for click reactions with various substrates.<sup>[21a,b]</sup> Subsequently, Pericàs et al. prepared tris(1-benzyl-1*H*-1,2,3-triazol-4-yl)methanol ligand, **1e**, and  $\text{CuCl}\cdot\mathbf{1e}$ , which efficiently catalyzed CuAAC reactions in water, or under neat conditions, in a short reaction time with a low catalyst loading. In addition, the hydroxyl group of **1e** proved to be a very promising anchoring point for immobilization, allowing the assembly of heterogeneous CuAAC catalysts.<sup>[21c]</sup> Our group synthesized  $\text{Cu}^{\text{I}}$  complexes with (hexabenzyl)tren **1b**, and dendritic analogues with 18- or 54-branch termini that are powerful catalysts for click reactions. The catalytically active metallodendrimers provided a rare positive dendritic effect that was also mechanistically very useful.<sup>[22]</sup> Herein, we present the synthesis of a magnetic  $\text{Cu}^{\text{I}}\cdot\mathbf{1e}$  complex, in which **1e** was not only used as the chelating framework for the  $\text{Cu}^{\text{I}}$  salt, but also as a linker to  $\text{SiO}_2$ -coated  $\gamma\text{-Fe}_2\text{O}_3$  nanoparticles. Both the catalytic activity

and the reusability of the catalyst, for CuAAC reactions, have been investigated.

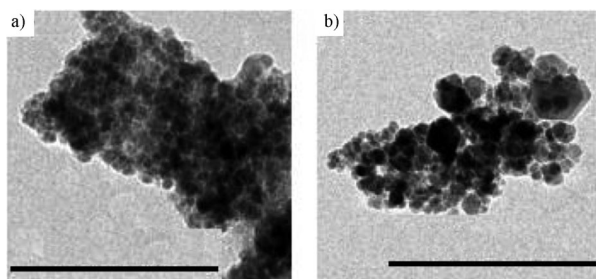
## Results and Discussion

### Synthesis of magnetic iron oxide nanoparticle-supported tris(triazolyl)- $\text{Cu}^{\text{I}}$ complexes

The primary step for the synthesis of the iron oxide nanoparticle-supported tris(triazolyl)- $\text{Cu}^{\text{I}}$  complexes was the synthesis of tris(1-benzyl-1*H*-1,2,3-triazol-4-yl)methanol, **1e** (Scheme 1). The CuAAC reactions were conducted, in the presence of copper sulfate and sodium ascorbate (a catalytic system developed by Sharpless et al.),<sup>[1a]</sup> between three equivalents of benzyl azide and a tris(alkynyl)carbinol intermediate. This intermediate was readily prepared by the addition of trimethylsilylacetylide to ethyl chloroformate, followed by removal of the trimethylsilyl (TMS) groups. The 3-chloropropyltriethoxysilane-functionalized magnetic nanoparticles, **2**, were obtained through immobilization of 3-chloropropyltriethoxysilane on the surface of robust  $\text{SiO}_2/\gamma\text{-Fe}_2\text{O}_3$ <sup>[23]</sup> by means of heterogenization with the Si–OH binding sites of  $\text{SiO}_2/\gamma\text{-Fe}_2\text{O}_3$  in toluene heated at reflux. Magnetic nanoparticle-supported tris(1-benzyl-1*H*-1,2,3-triazol-4-yl)methanol, **3**, was prepared by alkylation of **2** with **1e**.<sup>[14b]</sup> The loading of **3** was calculated by determination of the nitrogen content (C, H, N elemental analysis), the result indicated that the content was approximately  $0.068\text{ mmol g}^{-1}$ . Finally, complexation of **3** with  $\text{CuCl}$  or  $\text{CuBr}$  (1.1 equivalents) resulted in the assembly of magnetic nanoparticle-supported tris(triazolyl)- $\text{CuCl}$ , **4a**, or tris(triazolyl)- $\text{CuBr}$ , **4b**, respectively. Transmission electron microscopy (TEM) images showed that the diameter of **4b** was approximately 25 nm (Figure 2a).



**Scheme 1.** Synthesis of  $\text{CuX}\cdot\mathbf{1e}/\text{SiO}_2/\gamma\text{-Fe}_2\text{O}_3$  (**4**). Bn = benzyl.



**Figure 2.** a) TEM image of CuBr-1 e/SiO<sub>2</sub>/γ-Fe<sub>2</sub>O<sub>3</sub> (**4b**) before the CuAAC reactions; b) TEM image of **4b** after eight reaction cycles. Scale bars = 200 nm.

### Optimization of the conditions for alkyne-azide cycloadditions catalyzed by **4**

The catalytic applications of magnetically recyclable catalyst **4** in the cycloaddition reaction between benzyl azide and phenylacetylene, yielding the corresponding 1,4-disubstituted 1,2,3-triazoles, was investigated under various conditions (Table 1). In these preliminary experiments, CuAAC reactions

Table 1. Screening of solvents and catalysts for CuAAC. <sup>[a]</sup>				
Entry	Cat. ([mol %])	Solvent Ratio ([mL]:[mL])	Time [h]	Yield [%] <sup>[b]</sup>
1	<b>4a</b> (0.17)	MeOH/H <sub>2</sub> O (1:1)	4	28
2	<b>4a</b> (0.2)	MeOH/H <sub>2</sub> O (1:1)	24	61
3	<b>4a</b> (0.5)	MeOH/H <sub>2</sub> O (1:1)	68	98
4	<b>4a</b> (1)	MeOH/H <sub>2</sub> O (1:1)	24	91
5	<b>4a</b> (1)	EtOH/H <sub>2</sub> O (1:1)	24	90
6	<b>4a</b> (1)	H <sub>2</sub> O (1)	24	90
7	<b>4b</b> (0.5)	H <sub>2</sub> O (1)	12	89
8	<b>4b</b> (0.5)	H <sub>2</sub> O (1)	20	97

[a] The reaction was carried out with phenylacetylene (1 mmol) and benzyl azide (1.05 mmol) in the presence catalysts **4a** or **4b**, in the stated solvent at room temperature, under a nitrogen atmosphere. [b] Isolated yields after column chromatography.

were conducted in a mixture of MeOH and H<sub>2</sub>O (1:1), with various loadings of **4a**, under a nitrogen atmosphere at room temperature. Increasing yields of 1,2,3-triazoles were obtained with increasing catalyst loading, in the range 0.17–1.0 mol%. The reactions proceeded in excellent yields (91 %) in the presence of 1 mol% **4a** (entry 4), and replacing the mixed solvent MeOH/H<sub>2</sub>O by H<sub>2</sub>O alone or by EtOH/H<sub>2</sub>O did not affect the catalytic efficiency. Catalyst **4b** was then evaluated in CuAAC reactions and demonstrated superior catalytic activity compared with that of **4a** (0.5 mol% **4b** provided 1,2,3-triazoles with 97 % yield, in water, within 20 h at room temperature) Considering our goal of an economic and environmentally friendly reaction, these aqueous conditions are clearly favorable. Moreover, the excellent catalytic performances of **4a** and **4b** benefited from the good monodispersity of the SiO<sub>2</sub>-coated iron oxide nanoparticles in water.

### Investigation of the reusability of **4b** in the CuAAC reaction between benzyl azide and phenylacetylene

The reusability of the highly active magnetic nanoparticle-supported Cu<sup>I</sup> complex, **4b**, was tested by using the model reaction between benzyl azide and phenylacetylene, with 0.5 mol% [Cu] in water at room temperature, under a nitrogen atmosphere. Catalyst **4b** showed excellent magnetic properties and monodispersity. After completion of the first reaction, the catalyst was collected by using an external magnet, successively washed with CH<sub>2</sub>Cl<sub>2</sub> and methanol, and dried under vacuum for 2 h. A new reaction was then performed with fresh reactants under the same conditions. The results are summarized in Table 2; **4b** could be reused six times without significant

**Table 2.** Reusability test for catalyst **4b** in the cycloaddition reaction between phenylacetylene and benzyl azides.<sup>[a]</sup>

Run	Yield [%] <sup>[b]</sup>	Yield [%] <sup>[c]</sup>
1	97	96
2	95	93
3	94	72
4	92	39
5	92	–
6	92	–
7	84	–
8	67 <sup>[d]</sup>	–

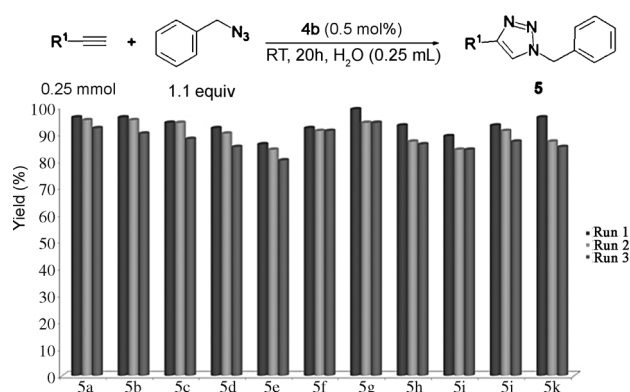
[a] The reaction was carried out with phenylacetylene (1 mmol) and benzyl azide (1.05 mmol) in the presence of **4b** (74 mg, 0.005 mmol copper), at room temperature in water for 20 h. [b] Isolated yields after column chromatography. The reaction was carried out in nitrogen-purged H<sub>2</sub>O (for 10 min) under a nitrogen atmosphere. [c] Isolated yields after column chromatography. The reaction was carried out in air. [d] The reaction time was 45 h.

loss of its catalytic activity, a decrease in the yield of the reaction only being observed after six cycles. The TEM image revealed that the morphology and size of **4b** changed over time, and a particle aggregation problem emerged after eight reaction cycles (Figure 2b). In addition, the leaching of copper species from the initial catalyst into the reaction media, a key issue for evaluating heterogeneous catalysts for CuAAC reactions, was investigated. After the first cycle, inductively coupled plasma (ICP) analysis revealed that 0.04 % of copper species was released from the initial catalyst into the reaction media, and the amount of residual copper species in the crude reaction product was approximately 1.5 ppm, compared with 5–15 ppm for other catalysts in the literature.<sup>[7,8]</sup> Thus, copper species leaching into the crude product was not completely eliminated, but appeared to be negligible.<sup>[17c]</sup> As anticipated, the tris(triazolyl) fragment proved to be a stable chelating framework for the adsorption of the Cu<sup>I</sup> salt, and a good linker for the SiO<sub>2</sub>-coated γ-Fe<sub>2</sub>O<sub>3</sub> nanoparticles through straightforward C–O bond formation. Magnetic catalyst **4b** also performed well in the presence of air, but became deactivated after the second run, probably caused by aerobic oxidation of the Cu<sup>I</sup> species into a Cu<sup>II</sup> species.

We then questioned whether CuBr did not coordinate with the tris(triazolyl) ligand to form a copper complex, but was simply caged in the iron oxide nanoparticles. In order to answer this point, a control experiment was performed by mixing SiO<sub>2</sub>-coated  $\gamma$ -Fe<sub>2</sub>O<sub>3</sub>, without the tris(triazolyl) ligand, with CuBr (three equivalents according to the amount of CuBr used in synthesis of **4b**).<sup>[14b]</sup> The obtained mixture was used for promoting the cycloaddition reaction of benzyl azide with phenylacetylene. To achieve a clear comparison, the amount of the mixture corresponded to the weight of **4b** at the same scale. The results showed that a 54% yield was obtained in the first run, and only 18% in the second run. Therefore, it is reasonable to infer that the iron oxide supported tris(triazolyl)-CuBr complex is the actual catalytic species.

### Investigation of the substrate scope for CuAAC reactions catalyzed by **4b**

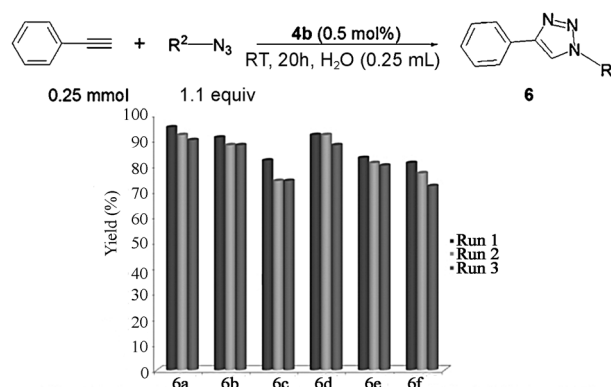
Encouraged by the efficiency of the reaction protocol described above, the scope of the reaction was examined with magnetic catalyst **4b** (0.5 mol% [Cu]), in water under a nitrogen atmosphere, at room temperature. Firstly, various terminal alkynes were investigated in reactions with benzyl azide. For each substrate, the reusability of **4b** was examined for the first three runs. As shown in Figure 3, on carrying out the CuAAC reaction between benzyl azide and phenylacetylene on a 0.25 mmol scale, the desired 1,4-disubstituted 1,2,3-triazole, **5a**, was produced in 96% yield with 100% selectivity (the selectivity was determined by using <sup>1</sup>H NMR spectroscopy), and a slight decrease in the yield was observed from runs one to three (down to 92%). Electron-donating (CH<sub>3</sub>O, NH<sub>2</sub>) and electron-withdrawing (CHO) groups on the alkynes were tolerated, and no direct correlation could be drawn between the electronic nature of the terminal alkynes and the outcome of the reaction. Heteroatom-containing alkynes, 2-ethynylpyridine and 3-ethynylpyridine, were suitable cycloaddition partners,



**Figure 3.** Substrate scope of terminal alkynes in the presence of catalyst **4b**. The bar graph shows the yield of isolated products. **5a**: R<sup>1</sup> = C<sub>6</sub>H<sub>5</sub> (yield of the first three runs: 96, 95, and 92%); **5b**: R<sup>1</sup> = 4-CHOC<sub>6</sub>H<sub>4</sub> (96, 95, and 90%); **5c**: R<sup>1</sup> = 4-CH<sub>3</sub>OC<sub>6</sub>H<sub>4</sub> (94, 94, and 88%); **5d**: R<sup>1</sup> = 4-NH<sub>2</sub>C<sub>6</sub>H<sub>4</sub> (92, 90, and 85%); **5e**: R<sup>1</sup> = pyridine-2-yl (86, 84, and 80%); **5f**: R<sup>1</sup> = pyridine-3-yl (92, 91, and 91%); **5g**: R<sup>1</sup> = C<sub>4</sub>H<sub>9</sub> (99, 94, and 94%); **5h**: R<sup>1</sup> = C<sub>5</sub>H<sub>11</sub> (93, 87, and 86%); **5i**: R<sup>1</sup> = HOC(CH<sub>3</sub>)<sub>2</sub> (89, 84, and 84%); **5j**: R<sup>1</sup> = HOC(C<sub>6</sub>H<sub>5</sub>)<sub>2</sub> (93, 91, and 87%); **5k**: R<sup>1</sup> = ferrocenyl (96, 87, and 85%).

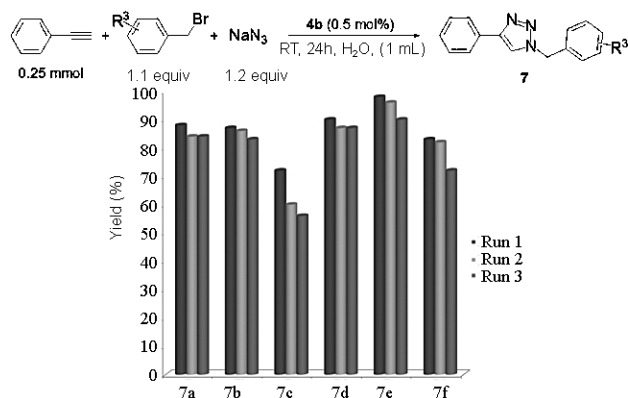
and the corresponding 1,2,3-triazoles, **5e** and **5f**, were obtained in 86 and 92% yields, respectively. The somewhat lower yield of the former reaction is probably attributable to the relatively bulky structure. Aliphatic alkynes containing linear chains were also suitable substrates, producing 1,4-disubstituted 1,2,3-triazoles **5g** and **5h** in excellent yields (99 and 93%, respectively). It was found that longer-chain aliphatic terminal alkynes resulted in the lowest yields. The products **5i** and **5j** were separated with high conversions when aliphatic terminal alkynes with hydroxyl groups were employed in CuAAC reaction. This procedure has been successfully extended to include ferrocenylacetylene as a substrate, the yield of the obtained product, **5k**, being 96%. The reusability of **4b** was also verified with all substrates, as shown in Figure 3.

The substrate scope of organic azides was then further investigated (Figure 4). The results indicated that benzyl, alkyl, and aryl azides could be successfully employed to assemble 1,2,3-triazoles through the CuAAC reaction with phenylacetylene. The yields decreased steadily upon increasing the alkyl-chain length of the organic azides (**6a–6c**). When phenyl azide was used, **4b** smoothly promoted the formation of 1,2,3-triazole **6d** with a 92% yield. However, organic azides with electron-donating (CH<sub>3</sub>) or electron-withdrawing (I) substituents resulted in lower yields. For each substrate, **4b** was recovered and reused three times with good catalytic activity.



**Figure 4.** Substrate scope of organic azides in the presence of catalyst **4b**. The bar graph shows the yield of isolated products. **6a**: R<sup>2</sup> = C<sub>6</sub>H<sub>13</sub> (yield of the first three runs: 95, 92, and 90%); **6b**: R<sup>2</sup> = C<sub>6</sub>H<sub>17</sub> (91, 88, and 88%); **6c**: R<sup>2</sup> = C<sub>18</sub>H<sub>37</sub> (82, 74, and 74%); **6d**: R<sup>2</sup> = C<sub>6</sub>H<sub>5</sub> (92, 92, and 88%); **6e**: R<sup>2</sup> = 4-CH<sub>3</sub>OC<sub>6</sub>H<sub>4</sub> (83, 81, and 80%); **6f**: R<sup>2</sup> = 4-IC<sub>6</sub>H<sub>4</sub> (81, 77, and 72%).

Cascade-reaction strategies display significant advantages over classical stepwise methods and have frequently been used as a powerful method in organic synthesis. Cascade reactions offer rapid and convergent construction of molecules from commercially available starting materials, without the isolation and purification of any intermediates, resulting in saving time, cost, and energy. In this context, taking into account the interest in avoiding storage and manipulation of organic azides, which can be hazardous, a three-component one-pot process was investigated by testing an azido reaction/1,3-dipolar cycloaddition of alkynes, sodium azide, and benzyl bromides (Figure 5). This process performed smoothly with



**Figure 5.** One-pot azide formation and subsequent CuAAC reaction mediated by **4b**. **7a**:  $R^3 = 4\text{-Br}$  (yield of the first three runs: 88, 84, and 84%); **7b**:  $R^3 = 3\text{-I}$  (87, 86, and 83%); **7c**:  $R^3 = 4\text{-CN}$  (72, 60, and 56%); **7d**:  $R^3 = 4\text{-NO}_2$  (90, 87, and 87%); **7e**:  $R^3 = 3\text{-CH}_3$  (98, 96, and 90%); **7f**:  $R^3 = 1\text{-CH}_2\text{-4-C}_6\text{H}_5\text{-1H-[1,2,3]triazole}$  (83, 82, and 72%).

0.5 mol% **4b**, without other additives, in water for 24 h at room temperature. Both electron-donating (3- $\text{CH}_3$ ) and electron-withdrawing (4-Br, 3-I, and 4- $\text{NO}_2$ ) substituents on benzylbromide showed good reactivity with sodium azide and phenylacetylene, producing the corresponding 1,2,3-triazoles in excellent yields. When 4-cyano benzylbromide was involved in the reaction, a lower yield (72%) was obtained, attributable to the coordination behavior of 4-cyano benzylbromide with the active copper center, resulting in deactivation of the catalyst. The double-azido CuAAC reaction of 1,2-dibromomethylbenzene proceeded well in the presence of 1 mol% **4b**, yielding product **7f**, which contains two triazole fragments, in 83% yield, and only a trace amount of the single triazole product. The reusability of **4b** was also investigated in the cascade-reaction strategy. Thus, it was shown that **4b** could be recovered and reused three times with only a slight decrease in the yield of the reaction. We also attempted the same tandem reactions, but with a linear-chain alkyl bromide (1-bromooctane), sodium azide, and phenylacetylene. Unfortunately, only a trace of desired product was obtained, probably because of the poor reactivity of 1-bromooctane with sodium azide in water at room temperature. Also, no triazole was produced when an aryl bromide (phenyl bromide) was employed, owing to the inability of phenyl bromide to undergo  $\text{S}_\text{N}2$  reactions.

Encouraged by the efficiency of the reaction protocol described above, **4b** was probed as a CuAAC catalyst for the synthesis of 27-branch dendrimers by 1→3 connectivity between dendritic nona-azide polymer **8** and two propargylated phenol dendrons (**9a** and **9b**). In a previous report,<sup>[8e,24]</sup> it was indicated that these reactions reached completion only in the presence of a quantitative amount of the catalyst developed by Sharpless et al. We found that 8 mol% of **4b** per branch successfully catalyzed the quantitative synthesis of 27-allyl and 27-TEG dendrimers (**10a** and **10b**, respectively) over 26 h or two days, respectively (Scheme 2). Moreover, after the first cycle of the synthesis of **10a**, **4b** was recharged and completed another synthesis of **10a**, within approximately three days, under ambient conditions.

## Conclusion

The syntheses of iron oxide nanoparticle-supported tris(triazolyl)- $\text{Cu}^{\text{I}}$  complexes, **4**, has been shown to be straightforward and convenient. The CuBr version of the magnetic nanoparticle catalyst, **4b**, showed, with low loading (0.5 mol%), good catalytic activity, recoverability, and reusability in CuAAC reactions. The catalyst was easily separated from the reaction medium by using an external magnet and showed good catalytic activity for six cycles. The amount of leaching copper species from the initial catalyst into the reaction media, determined by inductively coupled plasma (ICP) analysis, is negligible. This system has a broad substrate scope, and 25 1,4-disubstituted 1,2,3-triazoles were synthesized in good to excellent yields, including 27-allyl and 27-TEG dendrimers. For each small molecular substrate, **4b** was reused three times with either the same catalytic efficiency or only a slight decrease in yield. The outstanding performance of **4b** benefited from the excellent inherent properties of iron oxide nanoparticles and the powerful chelating nature of the tris(triazolyl) ligand with  $\text{Cu}^{\text{I}}$  centers. The above-mentioned results show that the reported procedure is easy-to-operate, economical, and environmentally friendly, as well as being in accordance with the principles of click chemistry and green chemistry. Magnetic catalyst **4b** could potentially be applied to CuAAC reactions for the synthesis of macromolecules, biomolecules, and nanoparticles.

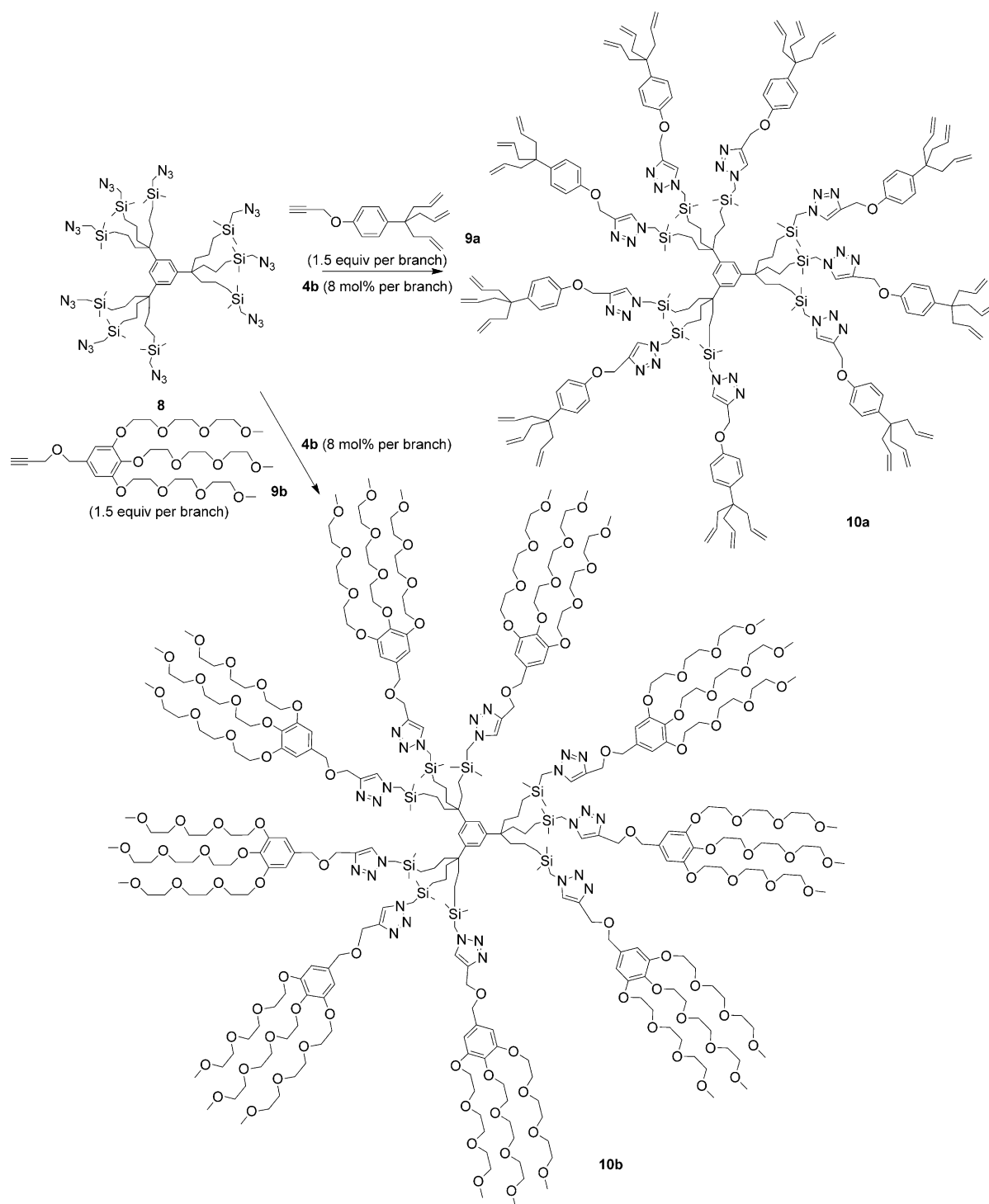
## Experimental Section

### General

All reactions were performed under nitrogen by using standard Schlenk techniques, unless otherwise noted. DMF was freshly distilled from calcium hydroxide, 1,4-dioxane was dried over Na foil, and distilled from sodium benzophenone under nitrogen immediately prior to use. CuBr was purified by stirring in glacial acetic acid overnight, followed by filtration, washing with ethanol and then drying under vacuum; it was stored under nitrogen and in the dark. All commercially available reagents were used as received, unless indicated otherwise. Flash column chromatography was performed using silica gel (300–400 mesh).  $^1\text{H}$  NMR spectra were recorded by using a 300 MHz spectrometer, and  $^{13}\text{C}$  NMR spectra were recorded at 75 MHz by using a 300 MHz spectrometer. Elemental analyses were performed by the Center of Microanalyses of the CNRS at Lyon Villeurbanne, France. The infrared spectra were recorded on an ATI Mattson Genesis series FTIR spectrophotometer. The inductively coupled plasma optical emission spectroscopy (ICP-OES) analyses were carried out using a Varian ICP-OES 720ES apparatus. Room temperature throughout the paper is 23–25 °C.

### Synthesis of tris(triazolyl)methanol (**1e**)<sup>[21c]</sup>

A solution of trimethylsilylacetylene (2.3 mL, 16.6 mmol) in anhydrous THF (20 mL) was cooled to  $-78^\circ\text{C}$ . Then, 2.5 M *n*BuLi in hexane (6.1 mL, 15.2 mmol) was added dropwise, and the solution was stirred for 4 h. Ethyl chloroformate (442  $\mu\text{L}$ , 4.61 mmol) was added, and the reaction was stirred overnight while warming to  $-30^\circ\text{C}$ . The reaction was quenched with saturated  $\text{NH}_4\text{Cl}$  solution, diluted with water, and extracted with  $\text{Et}_2\text{O}$  (3×30 mL). The com-



**Scheme 2.** Synthesis of dendrimers **10a** and **10b** through CuAAC reactions catalyzed by **4b**.

binded organic phase was dried over  $\text{Na}_2\text{SO}_4$ , and the solvent was removed under reduced pressure. The crude product was further purified by silica-gel chromatography (petroleum ether/ethyl acetate as eluent) to yield tris(trimethylsilylethynyl)methanol in 67% yield (1.0 g).  $^1\text{H NMR}$  (300 MHz,  $\text{CDCl}_3$ ):  $\delta = 2.82$  (s, 1H), 0.18 ppm (s, 27H).<sup>[21c]</sup> In a round-bottomed flask, the obtained tris(trimethylsilylethynyl)methanol in methanol (10 mL) was stirred in the presence of  $\text{K}_2\text{CO}_3$  (4.20 g, 37.5 mmol) at room temperature overnight. The solution was filtered to remove excess  $\text{K}_2\text{CO}_3$  and added to a solu-

tion of benzyl azide (1.25 g, 9.40 mmol) in methanol (10 mL).  $\text{CuSO}_4 \cdot 5\text{H}_2\text{O}$  (38.9 mg, 0.156 mmol) and sodium ascorbate (93.0 mg, 0.468 mmol) were added, and the mixture was stirred for 14 h at room temperature. The solvent was removed under reduced pressure. The residue was dissolved in dichloromethane (50 mL) and washed with saturated  $\text{Na}_2\text{CO}_3$  solution ( $5 \times 30$  mL). The organic phase was dried over  $\text{Na}_2\text{SO}_4$  and the solvent removed under reduced pressure. Purification was performed by flash column chromatography, with petroleum ether/ethyl acetate as eluent, and

product **1e** was obtained in 37% yield (0.58 g). <sup>1</sup>H NMR (300 MHz, CDCl<sub>3</sub>): δ = 7.64 (s, 3H), 7.24–7.38 (m, 15H), 5.47 (s, 6H), 5.04 ppm (s, 1H).<sup>[21c]</sup>

### Synthesis of iron oxide nanoparticle-supported tris(triazolyl)methanol ligand (**3**)<sup>[14b]</sup>

A solution of **1e** (252 mg, 0.5 mmol) in DMF (2 mL) was added dropwise into a suspension of NaH (15 mg) in anhydrous DMF (2 mL) at 0 °C. After stirring for 45 min at room temperature, the suspension became a clear solution and was cooled to 0 °C and the added through a syringe to a sonicated DMF solution of **2** (400 mg). The reaction mixture was allowed to warm to room temperature, and dried at 80 °C for 96 h. After this time the reaction mixture was cooled down to room temperature, and the magnetic solid was separated by using an external magnet and then successively washed with DMF (20 mL), THF (20 mL), MeOH (20 mL), and Et<sub>2</sub>O (20 mL). The resulting magnetic nanoparticles were dried in a vacuum at 45 °C overnight. The amount of tris(triazolyl) ligand in the functionalized magnetic nanoparticles, **3**, was 0.068 mmol g<sup>-1</sup>, which was calculated from the results of elemental nitrogen analysis (found: N 0.8582%).

### Synthesis of iron oxide nanoparticle-supported tris(triazolyl)methanol catalyst (**4**)

In a round-bottomed flask, a mixture of CuX (0.15 mmol, X = Br or Cl) and iron oxide nanoparticle-supported tris(triazolyl)methoxy ligand **3** (2 g) in anhydrous 1,4-dioxane (40 mL) was sonicated for approximately 15 min and stirred at 45 °C overnight. The iron oxide nanoparticle-supported tris(triazolyl)methanol–CuX catalysts **4** were successively washed with 1,4-dioxane (20 mL), toluene (20 mL), and Et<sub>2</sub>O (20 mL), then dried at 45 °C overnight under vacuum and stored before use.

### General procedures for the **4b**-catalyzed cycloaddition of alkynes and organic azides

A dried Schlenk tube equipped with a magnetic stirring bar was charged, under a nitrogen atmosphere, with alkyne (0.25 mmol), organic azide (0.275 mmol), catalyst **4b** (18.4 mg), and nitrogen-purged H<sub>2</sub>O (0.25 mL). The mixture was stirred at room temperature for 20 h, and CH<sub>2</sub>Cl<sub>2</sub> (5 mL) was added. The catalyst was collected by using a magnet and washed with CH<sub>2</sub>Cl<sub>2</sub> (3 × 5 mL) and MeOH (5 mL), then dried at room temperature under vacuum. During the above-mentioned treatment for the reaction, the catalyst was always kept under a nitrogen atmosphere. The combined organic phase was dried over Na<sub>2</sub>SO<sub>4</sub> and filtered, the filtrate was removed under reduced pressure in order to obtain the crude product, which was further purified by silica-gel chromatography (petroleum ether/ethyl acetate as eluent) to yield the corresponding 1,4-disubstituted 1,2,3-triazole. The recovered catalyst was then used for the next reaction cycle.

### General procedures for one-pot azide formation and subsequent CuAAC reaction catalyzed by **4b**

Alkyne (0.25 mmol), benzyl bromide (0.275 mmol), sodium azide (0.3 mmol), nitrogen purged H<sub>2</sub>O (1 mL), and **4b** (18.4 mg) were added to a flask with a stirrer bar, and the mixture was stirred for 24 h at room temperature under nitrogen. CH<sub>2</sub>Cl<sub>2</sub> (5 mL) was added to the mixture, and the catalyst was collected by using a magnet and washed with CH<sub>2</sub>Cl<sub>2</sub> (3 × 5 mL) and MeOH (5 mL), then dried at room temperature under vacuum. The combined or-

ganic phase was dried over Na<sub>2</sub>SO<sub>4</sub> and filtered, the filtrate was removed under reduced pressure in order to obtain the crude product, which was further purified by silica-gel chromatography (petroleum ether/ethyl acetate as eluent) to yield the corresponding 1,4-disubstituted 1,2,3-triazole. The recovered catalyst was then used for the next reaction cycle.

### Acknowledgement

Helpful discussions with Dr. J. Ruiz and financial support from the China Scholarship Council (CSC) of the People's Republic of China (Ph. D. grant to D.W.), the Université de Bordeaux, and the Centre National de la Recherche Scientifique (CNRS) are gratefully acknowledged.

**Keywords:** click chemistry · copper · green chemistry · magnetic nanoparticles

- [1] a) V. V. Rostovtsev, L. G. Green, V. V. Fokin, K. B. Sharpless, *Angew. Chem.* **2002**, *114*, 2708–2711; *Angew. Chem. Int. Ed.* **2002**, *41*, 2596–2599; b) C. W. Tornøe, C. Christensen, M. Meldal, *J. Org. Chem.* **2002**, *67*, 3057–3064.
- [2] H. C. Kolb, M. G. Finn, K. B. Sharpless, *Angew. Chem.* **2001**, *113*, 2056–2075; *Angew. Chem. Int. Ed.* **2001**, *40*, 2004–2021.
- [3] a) M. J. Genin, D. A. Allwine, D. J. Anderson, M. R. Barbachyn, D. E. Emmert, S. A. Garmon, D. R. Graber, K. C. Grega, J. B. Hester, D. K. Hutchinson, J. Morris, R. D. Reischer, D. Stper, B. H. Yagi, *J. Med. Chem.* **2000**, *43*, 953–970; b) B. S. Holla, M. Mahalinga, M. S. Karthikeyan, B. Poojary, P. M. Akberali, N. S. Kumari, *Eur. J. Med. Chem.* **2005**, *40*, 1173–1178.
- [4] a) D. R. Buckle, D. J. Outred, C. J. M. Rockell, H. Smith, B. A. Spicer, *J. Med. Chem.* **1983**, *26*, 251–254; b) D. R. Buckle, C. J. M. Rockell, H. Smith, B. A. Spicer, *J. Med. Chem.* **1986**, *29*, 2262–2267.
- [5] R. Alvarez, S. Velazquez, A. San-Felix, S. Aquaro, E. De Clercq, C.-F. Perno, A. Karlsson, J. Balzarini, M. J. Camarasa, *J. Med. Chem.* **1994**, *37*, 4185–4194.
- [6] N. A. Al-Masoudim, Y. A. Al-Soud, *Tetrahedron Lett.* **2002**, *43*, 4021–4022.
- [7] For selected examples, see: a) R. M. Meudtner, M. Ostermeier, R. Goddard, C. Limberg, S. Hecht, *Chem. Eur. J.* **2007**, *13*, 9834–9840; b) D. Schweinfurth, K. I. Hardcastle, U. H. F. Bunz, *Chem. Commun.* **2008**, 2203–2205; c) O. Fleischel, N. Wu, A. Petitjean, *Chem. Commun.* **2010**, 46, 8454–8456; d) S. Warsink, R. M. Drost, M. Lutz, A. L. Spek, C. J. Elsevier, *Organometallics* **2010**, *29*, 3109–3116; e) D. Urankar, B. Pinter, A. Pevce, F. De Proft, I. Turel, J. Košmrlj, *Inorg. Chem.* **2010**, *49*, 4820; f) A. Poulain, D. Canseco-Gonzalez, R. Hynes-Roche, H. Muller-Bunz, O. Schuster, H. Stoeckli-Evans, A. Neels, M. Albrecht, *Organometallics* **2011**, *30*, 1021–1029; g) K. F. Donnelly, A. Petronilho, M. Albrecht, *Chem. Commun.* **2013**, 49, 1145–1159.
- [8] a) A. E. Speers, G. C. Adam, B. F. Cravatt, *J. Am. Chem. Soc.* **2003**, *125*, 4686–4687; b) K. D. Bodine, D. Y. Gin, M. S. Gin, *J. Am. Chem. Soc.* **2004**, *126*, 1638–1639; c) P. Wu, A. K. Feldman, A. K. Nugent, C. J. Hawker, A. Scheel, B. Voit, J. Pyun, J. M. J. Fréchet, K. B. Sharpless, V. V. Fokin, *Angew. Chem.* **2004**, *116*, 4018–4022; *Angew. Chem. Int. Ed.* **2004**, *43*, 3928–3932; d) L. D. Pachón, J. H. van Maarseveen, G. Rothenberg, *Adv. Synth. Catal.* **2005**, *347*, 811–815; e) D. J. V. C. van Steenis, O. R. P. David, G. P. F. van Strijdonck, J. H. van Maarseveen, J. N. H. Reek, *Chem. Commun.* **2005**, 4333–4335; f) V. D. Bock, H. Hiemstra, J. H. van Maarseveen, *Eur. J. Org. Chem.* **2006**, 51–68; g) M. A. White, J. A. Johnson, J. T. Koberstein, N. J. Turro, *J. Am. Chem. Soc.* **2006**, *128*, 11356–11357; h) C. Ornelas, J. Ruiz, E. Cloutet, S. Alves, D. Astruc, *Angew. Chem.* **2007**, *119*, 890–895; *Angew. Chem. Int. Ed.* **2007**, *46*, 872–877; i) M. Meldal, C. W. Tornøe, *Chem. Rev.* **2008**, *108*, 2952–3015; j) S. Berndl, N. Herzig, P. Kele, D. Lachmann, X. Li, O. S. Wolfbeis, H.-A. Wagenknecht, *Bioconjugate Chem.* **2009**, *20*, 558–564; k) H. Lahlali, K. Jobe, M. Watkinson, S. M. Goldup, *Angew. Chem.* **2011**, *123*, 4237–4241; *Angew. Chem. Int. Ed.* **2011**, *50*, 4151–4155; l) M. Empting, O. Avrutina, R. Mensinger, S. Fabritz, M. Reinwarth, M. Biesalski, S. Voigt, G. Buntkowsky, H. Kolmar,

- Angew. Chem.* **2011**, *123*, 5313–5317; *Angew. Chem. Int. Ed.* **2011**, *50*, 5207–5211; m) L. Liang, D. Astruc, *Coord. Chem. Rev.* **2011**, *255*, 2933–2945.
- [9] a) J. M. Baskin, C. R. Bertozzi, *QSAR Comb. Sci.* **2007**, *26*, 1211–1219; b) J. C. Jewett, C. R. Bertozzi, *Chem. Soc. Rev.* **2010**, *39*, 1272–1279.
- [10] a) C. Girard, E. Önen, M. Aufort, S. Beauvière, E. Samson, J. Herscovici, *Org. Lett.* **2006**, *8*, 1689–1692; b) A. Sarkar, T. Mukherjee, S. Kapoor, J. Phys. Chem. C **2008**, *112*, 3334–3340.
- [11] a) S. Chassaing, M. Kumarraja, A. S. S. Sido, P. Pale, J. Sommer, *Org. Lett.* **2007**, *9*, 883–886; b) S. Chassaing, A. S. S. Sido, A. Alix, M. Kumarraja, P. Pale, J. Sommer, *Chem. Eur. J.* **2008**, *14*, 6713–6721; c) P. Kuhn, A. Alix, M. Kumarraja, B. Louis, P. Pale, J. Sommer, *Eur. J. Org. Chem.* **2009**, 423–429.
- [12] H. Sharghi, R. Khalifeh, M. M. Doroodmand, *Adv. Synth. Catal.* **2009**, *351*, 207–218.
- [13] B. H. Lipshutz, B. R. Taft, *Angew. Chem.* **2006**, *118*, 8415–8418; *Angew. Chem. Int. Ed.* **2006**, *45*, 8235–8238.
- [14] a) T. R. Chan, V. V. Fokin, *QSAR Comb. Sci.* **2007**, *26*, 1274–1279; b) E. Ozkal, S. Özçubukçu, C. Jimeno, M. A. Pericàs, *Catal. Sci. Technol.* **2012**, *2*, 195–200.
- [15] H. Sharghi, M. H. Beyzavi, A. Safavi, M. M. Doroodmand, R. Khalifeh, *Adv. Synth. Catal.* **2009**, *351*, 2391–2410.
- [16] a) T. Miao, L. Wang, *Synthesis* **2008**, 363–368; b) A. Coelho, P. Diz, O. Caamaño, E. Sotelo, *Adv. Synth. Catal.* **2010**, *352*, 1179–1192.
- [17] a) E. M. Claesson, N. C. Mehendale, R. J. M. Klein Gebbink, G. van Koten, A. P. Philipse, *J. Magn. Magn. Mater.* **2007**, *311*, 41–45; b) A. Megia-Fernandez, M. Ortega-Muñoz, J. Lopez-Jaramillo, F. Hernandez-Mateo, F. Santoyo-Gonzalez, *Adv. Synth. Catal.* **2010**, *352*, 3306–3320; c) R. B. Nasir Baig, R. S. Varma, *Green Chem.* **2012**, *14*, 625–632; d) J.-M. Collinson, J. D. E. T. Wilton-Ely, S. Díez-González, *Chem. Commun.* **2013**, *49*, 11358–11360.
- [18] For selected reviews on nanocatalysis, see: a) C. Burda, X. Chen, R. Narayanan, M. A. El-Sayed, *Chem. Rev.* **2005**, *105*, 1025–1102; b) D. Astruc, F. Lu, J. Ruiz, *Angew. Chem.* **2005**, *117*, 8062–8083; *Angew. Chem. Int. Ed.* **2005**, *44*, 7852–7872; c) D. Astruc, K. Heuze, S. Gatard, D. Méry, S. Nlate, L. Plault, *Adv. Synth. Catal.* **2005**, *347*, 329–338; d) A. Schätz, O. Reiser, W. J. Stark, *Chem. Eur. J.* **2010**, *16*, 8950–8967; e) P. Chen, X. Zhou, H. Shen, N. M. Andoy, E. Choudhary, K.-S. Han, G. Liu, W. Meng, *Chem. Soc. Rev.* **2010**, *39*, 4560–4570; f) *Nanomaterials and Catalysis* (Eds.: P. Serp, K. Philippot), Wiley-VCH, Weinheim, **2013**.
- [19] a) B. Berkovski in *Magnetic Fluids and Applications Handbook* (Eds.: B. Berkovski, V. Bashtovoy), Begell House, Inc., New York, Wallingford, **1996**, pp. 1–250; b) R. B. Bedford, M. Bentham, D. W. Bruce, S. A. Davis, R. M. Frost, M. Hird, *Chem. Commun.* **2006**, 1398–1400; c) V. Polshettiwar, R. Luque, A. Fihri, H. Zhu, M. Bouhrara, J.-M. Basset, *Chem. Rev.* **2011**, *111*, 3036–3075; d) A. Fihri, M. Bouhrara, B. Nekoueishahari, J.-M. Basset, V. Polshettiwar, *Chem. Soc. Rev.* **2011**, *40*, 5181–5203; e) D. Wang, L. Salmon, J. Ruiz, D. Astruc, *Chem. Commun.* **2013**, *49*, 6956–6958.
- [20] a) P. L. Golas, N. V. Tsarevsky, B. S. Sumerlin, K. Matyjaszewski, *Macromolecules* **2006**, *39*, 6451–6457; b) P. L. Golas, N. V. Tsarevsky, K. Matyjaszewski, *Macromol. Rapid Commun.* **2008**, *29*, 1167–1171.
- [21] a) T. R. Chan, R. Hilgraf, K. B. Sharpless, V. V. Fokin, *Org. Lett.* **2004**, *6*, 2853–2855; b) J. E. Hein, J. C. Tripp, L. B. Krasnova, K. B. Sharpless, V. V. Fokin, *Angew. Chem.* **2009**, *121*, 8162–8165; *Angew. Chem. Int. Ed.* **2009**, *48*, 8018–8021; c) S. Özçubukçu, E. Ozkal, C. Jimeno, M. A. Pericàs, *Org. Lett.* **2009**, *11*, 4680–4683.
- [22] For a discussion of the mechanism (mono versus bimetallic) of the CuAAC reaction, see: a) J. E. Hein, V. V. Fokin, *Chem. Soc. Rev.* **2010**, *39*, 1302–1315; b) L. Liang, J. Ruiz, D. Astruc, *Adv. Synth. Catal.* **2011**, *353*, 3434–3450.
- [23] S. Shylesh, L. Wang, W. R. Thiel, *Adv. Synth. Catal.* **2010**, *352*, 425–432.
- [24] A. K. Diallo, E. Boisselier, L. Liang, J. Ruiz, D. Astruc, *Chem. Eur. J.* **2010**, *16*, 11832–11835.

Received: November 19, 2013

Published online on February 26, 2014

**Chapter 4**  
**Magnetically Recyclable PdNPs in C-C Coupling Reactions**

## 4.1 Introduction

This chapter concerns our approaches of magnetic catalysts, i.e. palladium nanoparticle catalysts that are immobilized on magnetic iron oxide  $\gamma\text{-Fe}_2\text{O}_3$  in various ways. Two submitted papers with the collaboration of Christophe Deraedt (PhD student in our group) are included in this chapter.

The first work that we have conducted with some collaboration of Christophe Deraedt concerns the preparation, characterization and catalytic applications of MNPs-immobilized PEGylated  $\gamma\text{-Fe}_2\text{O}_3$ -Pd nanoparticle catalysts. The basis for this work lies in a variety of studies of dendritic catalysts and nanoparticles (NPs) catalysts that have been previously conducted by our research group. Indeed, recently Elodie Boisselier (former PhD student)<sup>1</sup> and Christophe Deraedt<sup>2</sup> prepared triethylene glycol (TEG)-terminated “click” dendrimers containing Percec-type dendrons, and successively used them for assembling dendrimer-encapsulated metal nanoparticles (DENs) and dendrimer-stabilized NPs (DSNs) involving AuNPs and PdNPs. Moreover, these PdNPs displayed impressive catalytic activity in carbon-carbon cross coupling reactions.<sup>2,3,4,5</sup>

Considering the advantages of MNPs in catalyst recovery, in the present work dendritic “click” ligands terminated by TEG groups were immobilized on iron oxide MNPs and utilized in the synthesis of PdNPs. These MNPs exhibited high catalytic activity and recyclability in Suzuki, Sonogashira and Heck reactions. In addition, five pharmacologically relevant or natural compounds were also readily obtained through the above-mentioned coupling reactions using these magnetic PdNP catalysts. The comparison of the PdNPs with related PdNPs supported on magnetic linear ligands indicated positive dendritic effects in terms of ligand loading, catalyst loading, catalytic activity and recyclability.

The second work conducted essentially by Christophe Deraedt work with whom we have collaborated introduces a simple method of impregnating pre-synthesized PdNPs stabilized by TEG-terminated “click” dendrimers into iron oxide MNPs, by stirring the mixture of MNPs and PdNPs. The presence of MNPs largely improved the activity, stability and recyclability in carbon-carbon cross coupling reactions and oxidation

reaction of benzyl alcohol to benzaldehyde.

**References:**

1. E. Boisselier, A. K. Diallo, L. Salmon, C. Ornelas, J. Ruiz, D. Astruc, *J. Am. Chem. Soc.* **2010**, *132*, 2729.
2. C. Deraedt, L. Salmon, L. Etienne, J. Ruiz, D. Astruc, *Chem. Commun.* **2013**, *49*, 8169.
3. C. Deraedt, L. Salmon, D. Astruc, *Adv. Syn. Catal.* **2014**, *356*, DOI 10.1002/adsc.201400153.
4. C. Deraedt, L. Salmon, J. Ruiz, D. Astruc, *Adv. Synth. Catal.* **2013**, *355*, 2992.
5. C. Deraedt, A. Rapakousiou, Y. Wang, L. Salmon, M. Bousquet, D. Astruc, *Angew. Chem., Int. Ed.* **2014**, *52*, DOI: 10.1002/anie.201403062.

## Highly efficient and magnetically recoverable “click” PEGylated $\gamma$ -Fe<sub>2</sub>O<sub>3</sub>-Pd nanoparticle catalysts for Suzuki-Miyaura, Sonogashira, and Heck reactions: Dendritic effects

Dong Wang,<sup>†</sup> Christophe Deraedt,<sup>†</sup> Lionel Salmon,<sup>‡</sup> Laetitia Etienne,<sup>§</sup> Christine Labrugère,<sup>†</sup> Jaime Ruiz,<sup>†</sup> Didier Astruc\*<sup>†</sup>

<sup>†</sup> ISM, Univ. Bordeaux, 351 Cours de la Libération, 33405 Talence Cedex, France.

<sup>‡</sup> LCC, CNRS, 205 Route de Narbonne, 31077 Toulouse Cedex, France.

<sup>§</sup> ICMCB, UPR CNRS No. 9048, 87 Avenue, Pey-Berland, 33608 Pessac Cedex, France.

<sup>†</sup> PLACAMAT UMS 3626, CNRS-Université de Bordeaux, 87 av. Albert Schweitzer, 33608 Pessac Cédex, France.

### ABSTRACT

The engineering of novel catalytic nanomaterials that are both highly active for crucial carbon-carbon bond formations, easily recoverable many times and biocompatible is highly desirable in terms of sustainable and green chemistry. It is in this spirit that new catalysts comprising dendritic “click” ligands immobilized on a magnetic nanoparticle (MNP) core, terminated by triethylene glycol (TEG) groups and incorporating Pd nanoparticles (PdNPs) are characterized by transmission electron microscopy (TEM), high-resolution transmission electron microscopy (HRTEM), inductively coupled plasma analysis (ICP), Fourier transform infrared spectroscopy (FT-IR), and energy-dispersive X-ray spectroscopy (EDX) and shown to be highly active, dispersible and magnetically recoverable many times in Suzuki, Sonogashira and Heck reactions. In addition, a series of pharmacologically relevant or natural products were successfully synthesized using these magnetic PdNPs as catalyst. For comparison, related PdNP catalysts deposited on MNPs bearing linear “click” PEGylated ligands are also prepared, and strong positive dendritic effects concerning ligand loading, catalyst loading, catalytic activity and recyclability are observed, i.e. the dendritic catalysts are much more efficient than the non-dendritic analogues.

## INTRODUCTION

Accompanied with the rapid development of modern industry, environmental concerns are increasing day by day. Maximization of synthetic efficiency and minimization of waste generation are basic constraints to solve the environmental problems.<sup>1</sup> In a related context, the use of heterogeneous catalysts appears to be one of the promising methodologies in developing environmentally friendly organic transformation process, due to their separability, reusability, and unique activity provided through the interaction between the catalytic species and supports.<sup>2</sup> Among transition metal nanoparticle (NP) catalysts,<sup>3</sup> magnetic nanoparticles (MNPs) have recently received a lot of attention as excellent supports.<sup>4</sup> MNPs catalysis is nowadays undergoing an explosive development, because MNPs-immobilized catalysts perfectly combine the advantages of catalytically active NPs and magnetic NPs. NP catalysts benefit from activity, selectivity and stability, resulting from the large surface-to-volume ratio, tunable size, shape, composition, electronic structure, and solubility whereas MNPs are easily assembled, accessible and reusable with an external magnetic field. Therefore MNP catalysts fully embody the principles of green chemistry and sustainability.

Dendrimers, dendrons, dendronized and dendritic polymers, a family of nanosized three-dimensional well-defined highly branched molecular frameworks, have been demonstrated to have essential and promising applications in catalysis.<sup>5-9</sup> In particular, dendrimer-encapsulated metal nanoparticles (DENs) and dendrimer-stabilized NPs (DSNs) have proved to be efficient catalysts for a variety of reactions<sup>10</sup> since Crook's group pioneered catalysis by polyamidoamine (PAMAM)-encapsulated Pd nanoparticles (PdNPs).<sup>11</sup> The DENs and DSNs possess a variety of key properties including tunable size due to the predictable number of metal atoms in the precatalyst, solubility and stability caused by the functional groups and steric embedding effects, loose binding to the NP surface, and the possibility of heterogenization by fixation on a solid support. PAMAM dendrimers,<sup>12</sup> polypropyleneimine (PPI) dendrimers<sup>13</sup> and phenylazomethine dendrimers<sup>14</sup> are the most used dendrimers for the stabilization of

metal NPs. It was recently reported that triethylene glycol (TEG)-terminated “click” dendrimers containing Percec-type dendrons,<sup>15</sup> constructed using Newkome-type 1→3 connectivity,<sup>16</sup> were remarkably powerful for assembling DENs and DSNs involving AuNPs and PdNPs.<sup>17</sup> The latter exhibited unprecedented catalytic performance in both C-C cross-coupling reactions and reduction of 4-nitrophenol, owing to smooth complexation of triazole to Pd atoms, water solubility provided by TEG termini, and the formation of dendritic nanoreactors containing hydrophilic periphery and hydrophobic interior.

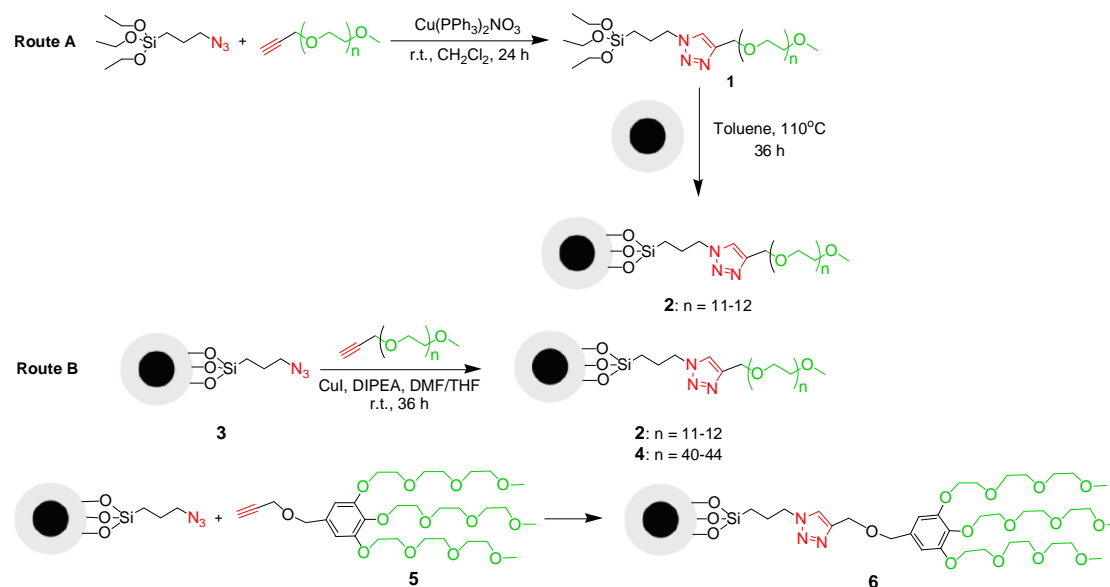
The introduction of dendritic fragments into MNPs has been utilized during the past few years, and this engineering considerably increased the number of functional groups on the surface of MNPs and strongly improves the dispersion of MNPs in organic or aqueous solvent.<sup>4e,18</sup> These MNPs-immobilized dendritic fragments are promising catalysts,<sup>18</sup> reusable adsorbents of metal ions,<sup>18c</sup> and potential drug carriers.<sup>18d</sup> In the field of catalysis, most of these MNPs catalysts bearing dendritic frameworks were MNP-anchored metal complexes, organocatalysts, and biocatalysts. To the best of our knowledge, the only example on magnetic DENs or DSNs has been reported by Bronstein’s group.<sup>18g</sup> These authors used polyphenylenepyridyl dendrons as capping molecules to successively stabilize iron oxide NPs and PdNPs, and the obtained magnetically recoverable Pd catalyst afforded excellent catalytic performance in the selective hydrogenation of dimethylethynylcarbinol to dimethylvinylcarbinol.

Herein, we report the engineering, synthesis, characterization and catalytic efficiency and recyclability of PdNPs supported on new MNPs containing dendritic “click” PEGylated ligands. High efficiency of these PdNP catalysts is found in Suzuki–Miyaura, Sonogashira, and Heck reactions, and positive dendritic effects are demonstrated in terms of the loading amount of catalyst, catalytic activity, and in particular recyclability.

## RESULTS AND DISCUSSION

**Syntheses of MNP-immobilized PEGylated triazolyl ligands 2, 4, 6, 9.** The syntheses of MNPs-immobilized linear and dendritic PEGylated triazolyl ligands were the primary steps of this project. Magnetic linear PEG550-triazoles **2** was prepared through two strategies (Scheme 1): grafting pre-synthesized Si(OEt)<sub>3</sub>-functionalized PEG-triazole on the surface of iron oxide MNPs (Route A), or direct “click” synthesis of PEG-triazole on the surface of iron oxide MNPs after the introduction of azido groups (Route B). In route A, the “click” reaction of (3-azidopropyl)triethoxysilane with PEG550 alkyne was readily conducted in the presence of [Cu(PPh<sub>3</sub>)<sub>2</sub>NO<sub>3</sub>] in anhydrous CH<sub>2</sub>Cl<sub>2</sub> at room temperature (r.t.) giving Si(OEt)<sub>3</sub>-functionalized PEG-triazoles **1** that was further immobilized on the surface of MNPs via the heterogenization with the Si–OH binding sites of SiO<sub>2</sub>/γ-Fe<sub>2</sub>O<sub>3</sub> NPs. In route B, the “click” reaction was successfully carried out between PEG550 alkyne and azido-modified iron oxide NPs. The loading of the ligands in **2** was calculated by determination of the nitrogen content (C, H, N elemental analysis), and the result revealed that the loadings were 0.17 mmol g<sup>-1</sup> and 0.26 mmol g<sup>-1</sup> for routes A and B, respectively. The lower ligand loading of route A seems attributable to the low efficiency of the heterogenization process caused by the bulky chain of compound **1**. In order to obtain higher ligand loading, route B was used in the preparations of MNPs-immobilized linear PEG2000-triazole ligand **4** and Percec-type dendron-triazole ligand **6** (Scheme 1). The former contains a longer hydrophilic PEG chain than **2**, and the latter possesses a TEG-terminated dendritic framework.

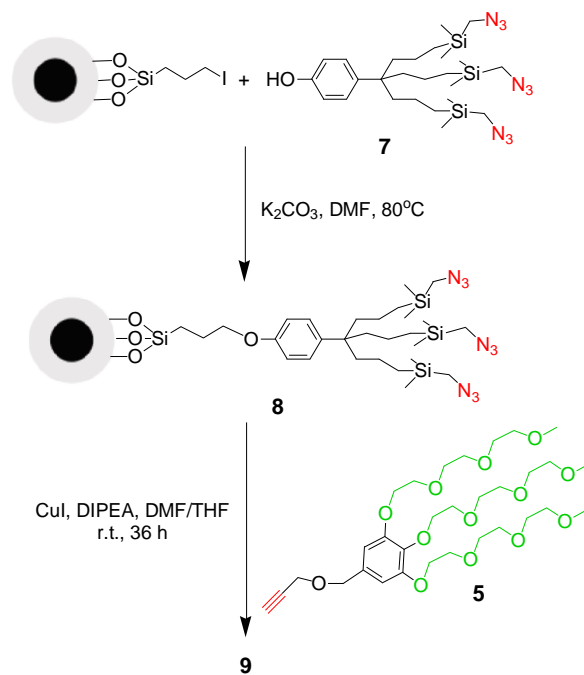
**Scheme 1.** Syntheses of MNPs-immobilized linear and dendritic PEGylated triazolyl ligands **2**, **4**, and **6**

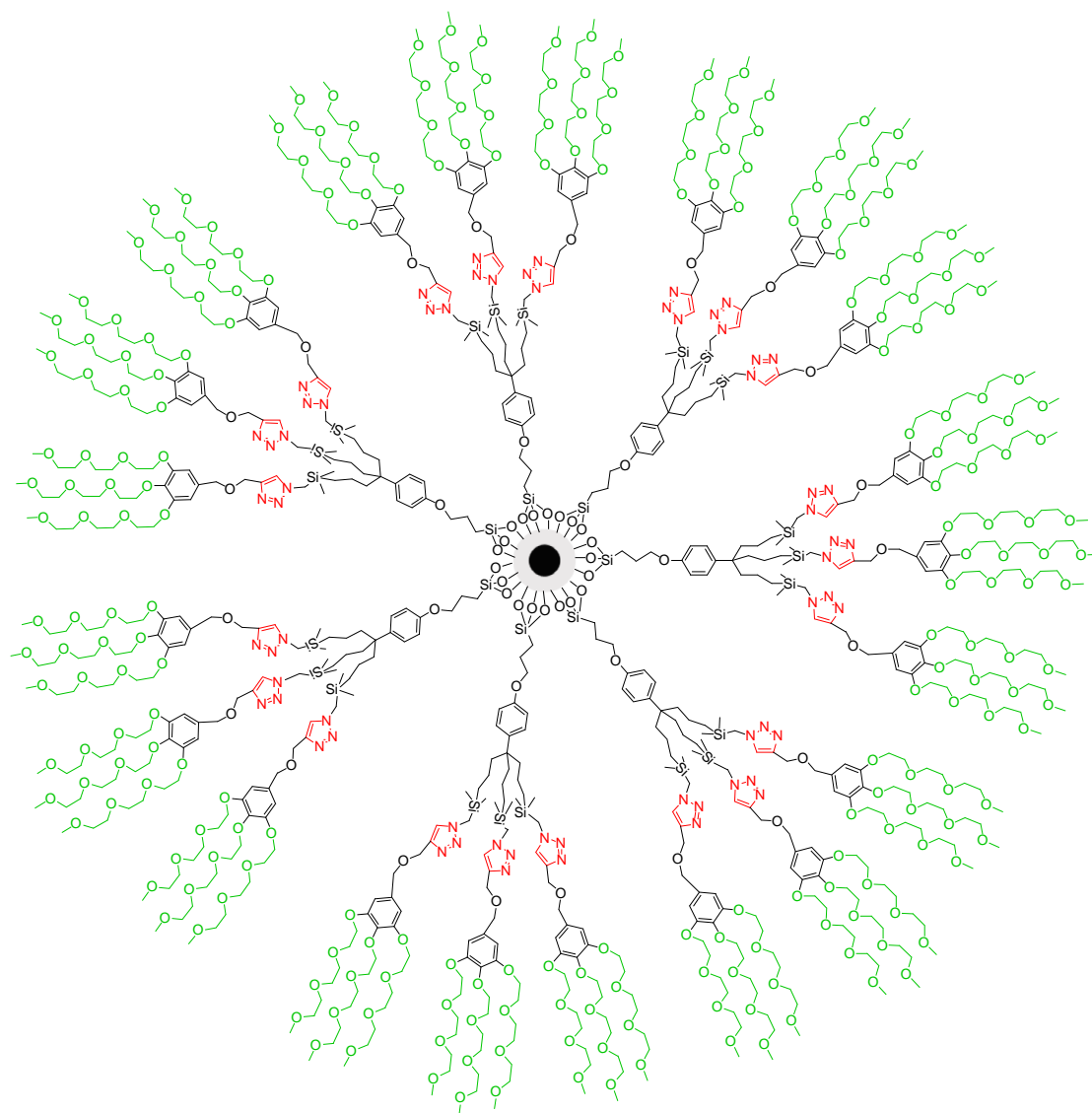


There are basically two strategies for the modification of MNPs with dendritic fragments:<sup>4c</sup> (i) the divergent synthesis of dendritic fragments on the surface of MNPs after the introduction of a linker, and (ii) the grafting of pre-synthesized dendritic fragments. The synthesis of MNPs-immobilized dendritic tris-triazole ligand **9** was achieved through both strategies. The divergent synthesis approach is shown in Scheme 2. Iodo-functionalized MNPs were derived by coupling of  $\text{SiO}_2/\gamma\text{-Fe}_2\text{O}_3$  NPs with pre-synthesized (3-iodopropyl)triethoxysilane.<sup>19</sup> The dendritic precursor **7** bearing a phenol and three azido groups has been reported earlier.<sup>20</sup> Newkome-type 1 $\rightarrow$ 3 connectivity<sup>16</sup> was then applied using nucleophilic substitution of the terminal iodine by the phenolate group of **7** in the presence of  $\text{K}_2\text{CO}_3$  in DMF.<sup>20</sup> This reaction provided dendritic azide-functionalized MNPs **8** in which the existence of azido groups was verified by the appearance of the  $\text{N}_3$  band at  $2102 \text{ cm}^{-1}$  in the FT-IR spectra. The loading amount of azido groups was  $0.86 \text{ mmol g}^{-1}$ , as measured by elemental analysis (EA). Finally, the “click” reaction of **8** with the Percec-type dendron **5** efficiently proceeded to afford MNP-anchored dendritic the TEG-triazole ligand **9** (Figure 1). In the process, the reaction was monitored by FT-IR as indicated

by the almost complete disappearance of the IR signal of  $2102\text{ cm}^{-1}$  that stands for the azido group.

**Scheme 2.** Divergent synthesis of MNP-immobilized dendritic tris-triazole ligand with TEG tethers.

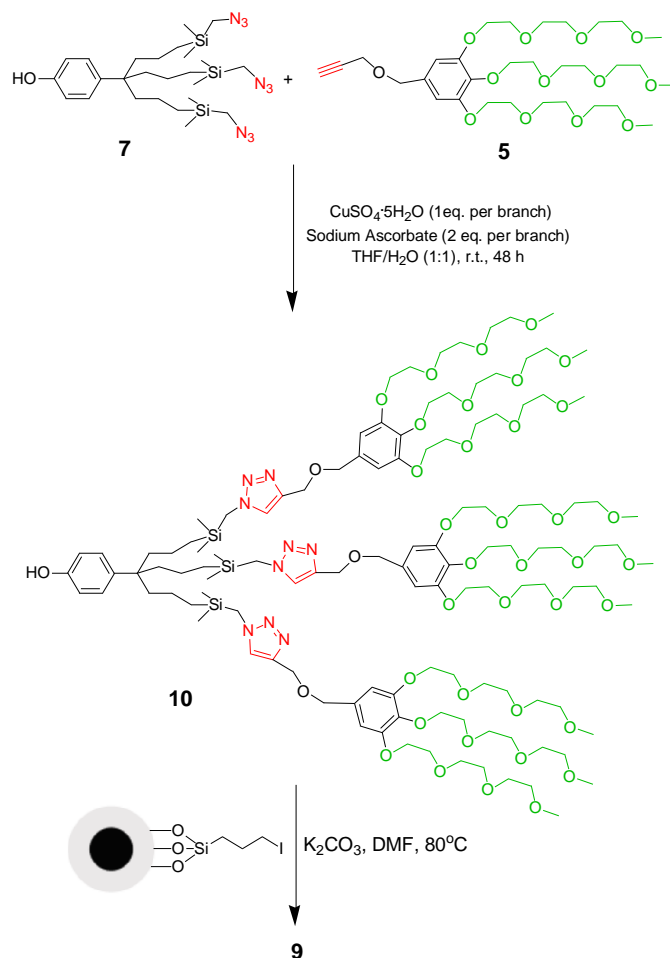




**Figure 1.** Schematic structure of MNP **9**.

Scheme 3 represents the other synthetic method for grafting the pre-synthesized dendritic fragments. The “click” reaction of dendritic azide **7** with Percec-type<sup>15</sup> dendron **5** was successfully performed using the “Sharpless-Fokin” catalyst<sup>21</sup> in mixed solvent of THF and H<sub>2</sub>O, providing phenolic hydroxy group-functionalized tris-triazole dendron **10**. Thereafter, the desired MNP-immobilized dendritic tris-triazole ligand **9** was constructed via the Williamson reaction between **10** and iodo-modified MNPs.<sup>20</sup>

**Scheme 3.** Synthesis of MNPs-immobilized dendritic tris-triazole ligand with triethylene glycol (TEG) tethers through the grafting of pre-synthesized dendrons.

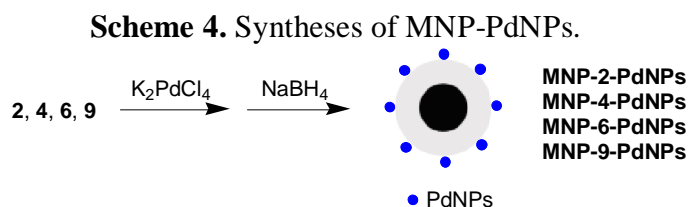


EA showed that the triazole loading amounts of **9** were 0.63 and 0.42 mmol g<sup>-1</sup>, for the divergent synthesis and the grafting of pre-synthesized unit method, respectively. It was thus clear that the divergent synthesis was more efficient than the grafting of pre-synthesized unit method, considering that the amount of loaded functional groups is a very key issue for the evaluation of loading protocols. In addition, the obtained MNPs **9** possessed much higher ligand loading than that of MNPs-immobilized linear ligands **2** and **4** (Table 1). This result shows that the introduction of a dendritic structure could remarkably increase the density of functional groups around the MNPs, which is the indication of a positive dendritic effect.

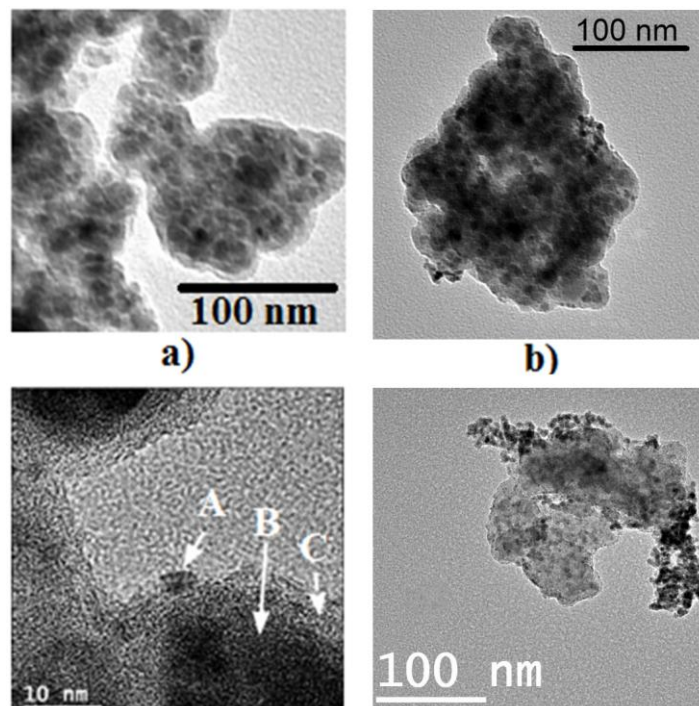
Transmission electron microscopy (TEM) images revealed that all of MNPs **2**, **4**, **6**, **9** presented core-shell morphology with an average particle size of about 25 nm ranging from 10 to 40 nm (Fig, S1, 2a).

Note that in the synthetic processes of these magnetic PEGylated triazolyl ligands, the magnetic separation was repeatedly used in purifying operation as an efficient, time saving, “green” and easy-to-operate protocol.

**Preparation and characterization of iron oxide NP-immobilized PdNPs: MNP-2-PdNPs, MNP-4-PdNPs, MNP-6-PdNPs, MNP-9-PdNPs.** MNPs **2, 4, 6, 9** are highly dispersible and even partially soluble in water owing to the presence of PEG or TEG, providing the possibility that MNPs **2, 4, 6, 9** are used as supports for efficient immobilization of PdNPs in water. First, the coordination of Pd(II) with triazolyl fragment was achieved by adding 2 equiv. of  $K_2PdCl_4$  per triazolyl group into a suspension of MNPs-immobilized PEGylated triazolyl ligands in water. The complexation process of triazole to Pd(II) has been confirmed in earlier reports.<sup>10o,17b,c</sup> PdNPs were then loaded onto the MNPs supports following by the reduction of Pd(II) to Pd(0) using 10 equiv.  $NaBH_4$  per triazole group (Scheme 4). These MNP-PdNPs were characterized by TEM, HRTEM, EDX, FT-IR, and ICP-OES.

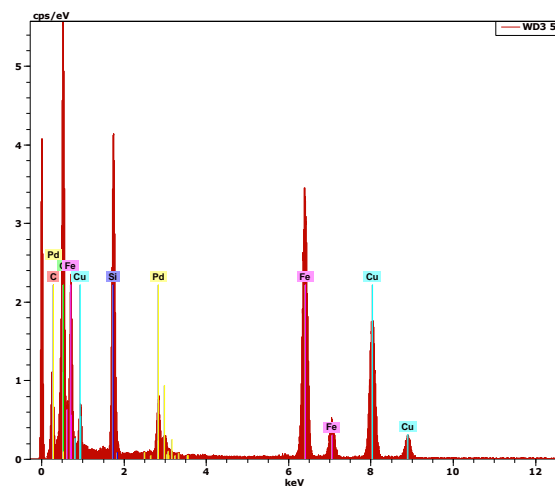


Taking **MNP-9-PdNPs** as an example, the production was performed upon utilizing the MNP **9** as support that was prepared by the divergent synthesis method. TEM image of **MNP-9-PdNPs** revealed the core-shell structure and the almost unchanged size compared to unloaded MNP **9** (Figure 2b). Moreover, HRTEM pictures showed that the sizes of formed PdNPs were smaller than 5 nm with an average size of approximately 3.0 nm (Fig S1, 2c).

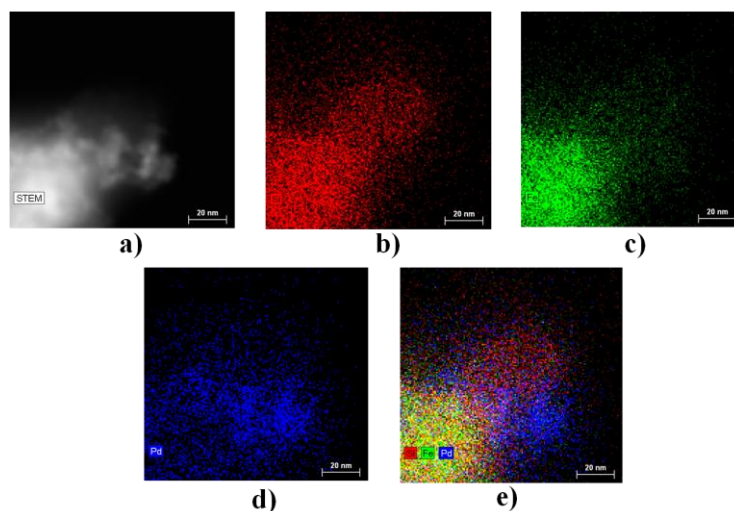


**Figure 2.** (a) TEM image of MNPs **9**. (b) TEM image of **MNP-9-PdNPs**. (c) HRTEM image of **MNP-9-PdNPs** (A: PdNP; B:  $\gamma$ -Fe<sub>2</sub>O<sub>3</sub> core; C: SiO<sub>2</sub> shell). (d) TEM image of **MNP-9-PdNPs** after 8 reaction cycles in the Suzuki-Miyaura reaction.

The elemental composition was determined by EDX analysis, and the results shown in Figure 3 indicate Si, O, Fe and Pd signals that are provided by the **MNP-9-PdNPs**. For further characterization of the sample, high resolution scanning transmission electron microscopy coupled quantified energy dispersive X-ray spectroscopy (HRSTEM-EDX) mapping of the sample was also investigated (**Figure 4, S2**). Looking at the compositional maps of Si, Fe, Pd and mainly the combined composition image, the presence of the iron oxide nanoparticles is clearly distinguished in the core of the MNP that is encapsulated by the silicon oxide shell while the palladium nanoparticles are localized at the border.

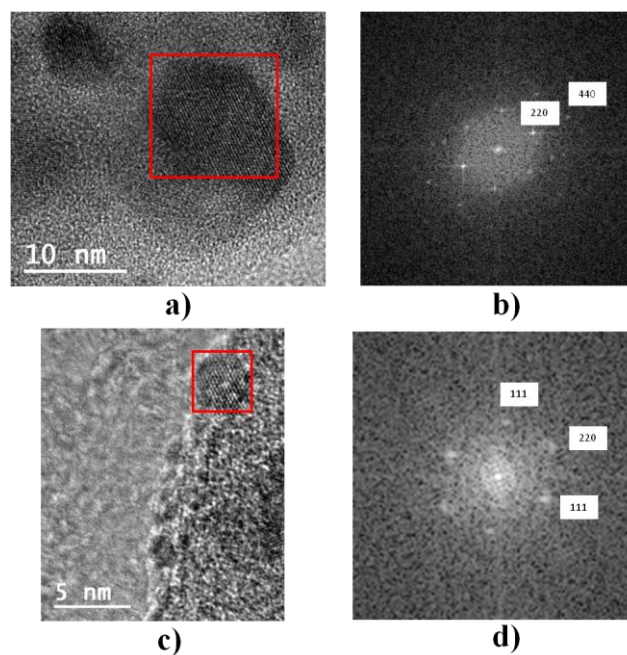


**Figure 3.** EDX spectrum of **MNP-9-PdNPs**.



**Figure 4.** STEM dark-field image (a) and elemental maps of **MNP-9-PdNPs** for Si (b), Fe (c), Pd (d), and mixture of Si, Fe, Pd (e) obtained by EDX.

Thanks to the HRTEM images it was also possible to observe the atomic arrangements in several Pd and Fe<sub>2</sub>O<sub>3</sub> particles. Figure 5b shows the atomic planes for a  $\gamma$ -Fe<sub>2</sub>O<sub>3</sub> nanoparticle and the corresponding selected-area electron diffraction (SAED) pattern showing a [111] orientation of a face centered cubic (fcc) structure. Similar treatment for a selected Pd nanoparticle revealed a [011] orientation of a face centered cubic (fcc) structure (Figure 5d).



**Figure 5.** (a) HRTEM image of the Fe<sub>2</sub>O<sub>3</sub> nanoparticles, (b) the corresponding SAED of Fe<sub>2</sub>O<sub>3</sub> nanoparticles, (c) HRTEM image of the Pd nanoparticles, (d) the corresponding SAED of Pd nanoparticles.

ICP-OES analysis showed that the Pd loading of **MNP-9-PdNPs** is 0.21 mmol g<sup>-1</sup>, which is approximately 3 times larger than that of **MNP-2-PdNPs** and 4 times larger than that of **MNP-4-PdNPs** (Table 1) and signifies a positive dendritic effect regarding catalyst loading.

**Table 1. Loading Amounts of Triazolyl Ligand in MNPs 2, 4, 6, 9; and Loading Amounts of PdNP in MNP-2-PdNPs, MNP-4-PdNPs, MNP-6-PdNPs, MNP-9-PdNPs.**

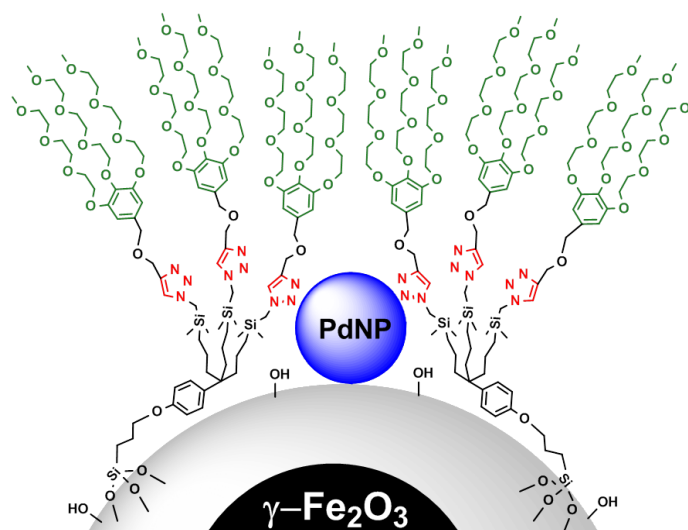
MNPs	Triazole loading (mmol/g)	Pd loading (mmol/g)
MNP 2 <sup>a</sup>	0.26	
MNP 4 <sup>a</sup>	0.14	
MNP 6 <sup>a</sup>	0.27	
MNP 9 <sup>b</sup>	0.63	
<b>MNP-2-PdNPs</b>		0.072
<b>MNP-4-PdNPs</b>		0.048
<b>MNP-6-PdNPs</b>		0.082
<b>MNP-9-PdNPs</b>		0.210

<sup>a</sup> The MNPs were prepared through route B. <sup>b</sup> The MNPs were prepared through the divergent method.

We know that in dendrimers containing triazole ligands, these ligands quantitatively coordinate to Pd(II) according to a 1:1 stoichiometry, which was demonstrated by cyclic voltammetry with ferrocenyltriazole-terminated dendrimers.<sup>20a</sup> In the case of **MNP-9-PdNPs** the approximate average number of ligands around one iron oxide NP is of the order of 10000. The average number of PdNPs loaded on one iron oxide NP is approximately 3.6 (see calculations in SI).

In arene-cored dendrimers, PdNP are trapped inside dendrimers upon weak interaction with the triazole ligand. We also know that this interaction is weak, because these nitrogen ligands are not  $\pi$ -acceptors for metal(0), and indeed triazole ligands are very easily displaced from the PdNP surface for instance in metal surface catalysis of nitrophenol reduction. In the present case, the SiOH groups of the silica core are a dense assembly of ligands for PdNP stabilization, which has already been suggested. The HRTEM of figures 2c and 5c clearly shows PdNPs sitting on the silica surface. Thus it

is believed that the PdNPs are stabilized on the silica surface on one (inner) side and by bakfolding triazole ligands on the other (outer) side (Figure 6).<sup>22</sup> Indeed the silica core-triazole ligand distance is adequate for such stabilization. In this way, the stabilization of the PdNPs is double and stronger, but leaves the outer surface available for easy triazole displacement by substrates in catalysis experiments.



**Figure 6.** The proposed schematic structure of **MNP-9-PdNPs**.

**Investigation of the activities, recyclabilities, and substrate scope of MNP-PdNPs in the Suzuki-Miyaura reaction.** Pd-catalyzed Suzuki-Miyaura reactions for the construction of C-C bonds are crucial in modern chemical transformations involving the syntheses of pharmaceuticals, functional materials, and natural compounds. The catalytic activities of these MNPs-PdNPs were evaluated in Suzuki-Miyaura reactions using bromobenzene and phenylboronic acid as model substrates. In these preliminary experiments, **MNPs-9-PdNPs** was chosen as the catalyst for optimizing investigations that were first conducted in aqueous media (mixture of EtOH and H<sub>2</sub>O) with various catalytic amount of [Pd], using K<sub>2</sub>CO<sub>3</sub> as a base at 80 °C under nitrogen atmosphere (Table 2). Increasing yields of desired biphenyl product were observed with increasing catalytic amount, in the range of 0.063 – 0.315 mol%. The reaction reached a yield of 91%, using 0.315 mol% of [Pd] (corresponding to 15 mg of **MNP-9-PdNPs**), within 24 h. Attempts involving the replacement of K<sub>2</sub>CO<sub>3</sub> by others

bases including Na<sub>2</sub>CO<sub>3</sub>, KOH and K<sub>3</sub>PO<sub>4</sub>, decrease of the reaction temperature, or reduction the reaction time caused lower yields (Table 2).

**Table 2. Optimization of the Suzuki-Miyaura Reaction Between Bromobenzene and Phenylboronic Acid Using MNP-9-PdNPs as Catalyst.<sup>a</sup>**

Entry	Amount (mol%)	Solvent (mL)	Base	Temperature (°C)	Time (h)	Yield <sup>c</sup> (%)
1	0.063	EtOH/H <sub>2</sub> O (10:10)	K <sub>2</sub> CO <sub>3</sub>	80	24	31
2	0.189	EtOH/H <sub>2</sub> O (10:10)	K <sub>2</sub> CO <sub>3</sub>	80	24	63
<b>3</b>	<b>0.315<sup>b</sup></b>	<b>EtOH/H<sub>2</sub>O (10:10)</b>	<b>K<sub>2</sub>CO<sub>3</sub></b>	<b>80</b>	<b>24</b>	<b>91</b>
4	0.625	EtOH/H <sub>2</sub> O (10:10)	K <sub>2</sub> CO <sub>3</sub>	80	24	93
5	0.315	EtOH/H <sub>2</sub> O (10:10)	K <sub>2</sub> CO <sub>3</sub>	45	24	45
6	0.315	EtOH/H <sub>2</sub> O (10:10)	K <sub>2</sub> CO <sub>3</sub>	80	2	34
7	0.315	EtOH/H <sub>2</sub> O (10:10)	K <sub>2</sub> CO <sub>3</sub>	80	10	66
8	0.315	EtOH/H <sub>2</sub> O (3:3)	K <sub>2</sub> CO <sub>3</sub>	80	24	80
9	0.315	EtOH/H <sub>2</sub> O (10:10)	Na <sub>2</sub> CO <sub>3</sub>	80	24	79
10	0.315	EtOH/H <sub>2</sub> O (10:10)	KOH	80	24	64
11	0.315	EtOH/H <sub>2</sub> O (10:10)	K <sub>3</sub> PO <sub>4</sub>	80	24	72

<sup>a</sup> The reaction was carried out with bromobenzene (1 mmol) and phenylboronic acid (1.5 mmol) in the presence of the catalyst **MNPs-9-PdNPs** and base (2 equiv) in EtOH/H<sub>2</sub>O under a nitrogen atmosphere. <sup>b</sup> 15 mg of **MNPs-9-PdNPs**. <sup>c</sup> Isolated yields after column chromatography.

The recyclability, a key issue of heterogeneous catalysts from both the practical and environment points of view, was tested for all MNP-PdNPs under optimized conditions. As shown in Table 3, the reactions catalyzed by **MNP-2-PdNPs** and **MNP-4-PdNPs** containing linear ligands were smoothly performed with 0.315 mol% of [Pd], and the biphenyl product was isolated in 80% and 82% yields, respectively. Then, these two catalysts were readily separated from the reaction medium using an external magnet and reused for the next cycles (Fig S3). An obvious decrease in activity was found in the second and third reaction cycles (Table 3). **MNP-6-PdNPs** bearing mono-triazole Percec-type dendron, however, showed a good catalytic performance in terms of activity and recyclability. The magnetically recoverable catalyst produced a yield of 87% in the first run and maintained a similar activity in the next three cycles. Interestingly, **MNP-9-PdNPs** containing tris-triazole dendrons was a superior catalyst. Remarkably, its catalytic activity did not deteriorate during 8

successive runs presenting yields of 87 - 91 %, a steady loss of activity only being detected from the ninth cycle (Table 3). The TEM analysis of the recovered catalyst revealed that the size and morphology of both **MNP-9-PdNPs** and the corresponding PdNPs after 8 cycles had no apparent change (Figure 2d). ICP analysis indicated that only 0.24 and 0.95 ppm Pd leached out from the initial **MNP-9-PdNPs** catalyst after the first and the eighth cycles respectively, which implied that **MNP-9-PdNPs** was highly stable. In addition, **MNP-9-PdNPs** maintained the same catalytic activity for months following storage at r.t. in air.

In the case of the Suzuki-Miyaura reactions, the comparison among these MNP-PdNPs catalysts clearly indicated positive dendritic effects regarding both activity and recyclability, in particular in recyclability issue. It seems reasonable to infer that the improved catalytic performance benefited from the presence of the dendritic framework that efficiently stabilized the PdNP and played a crucial role as a barrier to inhibit the release of the PdNP or part of it from the MNP support.

**Table 3. Investigation of the Recyclabilities of MNP-PdNPs in the Suzuki-Miyaura Reaction Between Bromobenzene and Phenylboronic Acid<sup>a</sup>**

	Cycle <sup>b</sup>									
	1	2	3	4	5	6	7	8	9	10
<b>MNP-2-PdNPs</b>	80	62	25							
<b>MNP-4-PdNPs</b>	82	82	66	35						
<b>MNP-6-PdNPs</b>	87	87	83	83	40					
<b>MNP-9-PdNPs</b>	91	91	89	89	88	87	87	87	80	69

<sup>a</sup> The reaction was carried out with bromobenzene (1 mmol) and phenylboronic acid (1.5 mmol) in the presence of the catalyst MNP-PdNPs (0.315 mol%) and K<sub>2</sub>CO<sub>3</sub> (2 equiv) under a nitrogen atmosphere for 24 h. <sup>b</sup> Isolated yields (% ± 2%) were provided for each cycle.

In order to check whether the catalytic activity originated from the immobilized PdNPs or from leached Pd, a control experiment was performed. Therefore the Suzuki-Miyaura reaction between bromobenzene and phenylboronic acid in the presence of **MNP-9-PdNPs** was allowed to proceed for 2 h under the optimized conditions providing the desired cross-coupling product in 34% yield. Subsequently,

the catalyst was magnetically separated at 80 °C; the remained reaction solution was transferred to another Schlenk flask and was stirred again for another 22 h. Then the biphenyl product was isolated in 36% yield, showing that almost no yield increase was observed after removing the immobilized PdNPs catalyst. The result of the hot-magnetic separation experiment<sup>23</sup> confirmed the heterogeneous nature of the catalyst.

Encouraged by the efficiency of the reaction protocol described above, the scope of the Suzuki-Miyaura reaction was examined with **MNP-9-PdNPs** (0.315 mol% of [Pd]) in the mixture of EtOH and H<sub>2</sub>O under nitrogen atmosphere at 80 °C, and the results are gathered in Table 4. A series of bromobenzenes bearing various substituents were tested in reactions with phenylboronic acid. Bromobenzenes containing electron-withdrawing (NO<sub>2</sub>, CHO, CH<sub>3</sub>CO, CH<sub>3</sub>CH<sub>2</sub>OCO) as well as electron-donating (NH<sub>2</sub>, CHO, CH<sub>3</sub>) groups in *para*-position were suitable coupling partners, and the corresponding coupling products (**11b-h**) were efficiently synthesized in 83-94% yields. No direct correlation could be drawn between the outcome and the electronic nature of bromobenzene substituents. The challenging reaction with 2,4,6-trimethyl bromobenzene generated the corresponding product in 91% yield (Table 4, entry 9). Substituted arylboronic acids were also investigated, and they all reacted smoothly with bromobenzene to provide the desired products in good yields (Table 4, entries 10, 11). The steric effect was also observed, however. Moreover, the reaction of 4-nitrochlorobenzene smoothly proceeded with 1 mol% of **MNP-9-PdNPs**, producing the corresponding coupling product in 88% yield.

**Table 4. Investigation of the Substrate Scope in the Presence of MNP-PdNPs in the Suzuki-Miyaura Reaction<sup>a</sup>**

Entry	R <sup>1</sup>	X	R <sup>2</sup>	Products	Yield (%) <sup>b</sup>
1	H	Br	H	<b>11a</b>	91
2	4-NO <sub>2</sub>	Br	H	<b>11b</b>	92
3	4-CHO	Br	H	<b>11c</b>	94
4	4-CH <sub>3</sub> CO	Br	H	<b>11d</b>	94
5	4-CH <sub>3</sub> CH <sub>2</sub> OCO	Br	H	<b>11e</b>	83
6	4-NH <sub>2</sub>	Br	H	<b>11f</b>	89
7	4-CH <sub>3</sub> O	Br	H	<b>11g</b>	92
8	4-CH <sub>3</sub>	Br	H	<b>11h</b>	90
9	2,4,6-TrisCH <sub>3</sub>	Br	H	<b>11i</b>	91 <sup>c</sup>
10	H	Br	4-CH <sub>3</sub>	<b>11j</b>	89
11	H	Br	2-CH <sub>3</sub>	<b>11k</b>	74
12	4-NO <sub>2</sub>	Cl	H	<b>11b</b>	88 <sup>d</sup>

<sup>a</sup> The reaction was carried out with bromobenzene (1 mmol) and phenylboronic acid (1.5 mmol) in the presence of catalysts **MNP-9-PdNPs** (0.315 mol%) and K<sub>2</sub>CO<sub>3</sub> (2 equiv) in EtOH/H<sub>2</sub>O (10 mL/10mL) under a nitrogen atmosphere for 24 h. <sup>b</sup> Isolated yields (%) were provided for each cycle. <sup>c</sup> The reaction time is 86 h. <sup>d</sup> The reaction was carried out in the presence of 1 mol% of [Pd] in 72 h.

**Investigation of the activities and recyclabilities of MNP-PdNPs in Sonogashira and Heck reactions.** The Sonogashira and Heck coupling reactions are also two common strategies of C-C bonds construction respectively forming conjugated compounds and arylated olefins. **MNP-2-PdNPs**, **MNP-6-PdNPs** and **MNP-9-PdNPs** were all used as catalysts in both Sonogashira and Heck reactions.

The Sonogashira reaction of iodobenzene and phenylacetylene was chosen to test the recyclability of the MNP-PdNPs bearing linear or dendritic PEGylated triazolyl ligands. The reactions were performed with 1.5 mol% of [Pd] using Et<sub>3</sub>N as base in THF at 65 °C for 24 h. After each reaction cycle, the catalyst has been separated from the reaction mixture using a magnet and successively washed with CH<sub>2</sub>Cl<sub>2</sub> and acetone and then re-used in a subsequent run. As shown in Table 5, the yields of the first reaction cycle catalyzed by **MNP-2-PdNPs**, **MNP-6-PdNPs**, and **MNP-9-PdNPs** were 78%, 82%, 85%, respectively. The recyclability results showed that an obvious loss in activity of **MNP-2-PdNPs** bearing linear PEG550-triazole

ligand was observed in the second run; **MNP-6-PdNPs** with the small dendron could be easily recycled three times with slight loss of catalytic activity. It is particularly gratifying, however, that **MNP-9-PdNPs** containing dendritic tris-triazole ligands maintained almost the same catalytic activity from the first to the sixth cycle. The results of Table 5 show that the catalytic recyclability was significantly influenced by the structure of PEGylated triazolyl ligands, the dendritic frame greatly improving the recyclability.

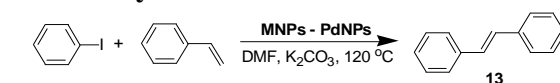
**Table 5. Investigation of the Recyclabilities of MNP-PdNPs in the Sonogashira Reaction Between Iodobenzene and Phenylacetylene.<sup>a</sup>**

	Cycle <sup>b</sup>						
	1	2	3	4	5	6	7
<b>MNP-2-PdNPs</b>	78	65					
<b>MNP-6-PdNPs</b>	82	80	79	63			
<b>MNP-9-PdNPs</b>	85	83	83	81	80	80	75

<sup>a</sup> The reaction was carried out with iodobenzene (1 mmol), phenylacetylene (1.2 mmol) in the presence of catalysts MNP-PdNPs (1.5 mol%) and Et<sub>3</sub>N (2 equiv) in THF (5 mL) at 65 °C under a nitrogen atmosphere for 24 h. <sup>b</sup> Isolated yields (%) were provided for each cycle. Yields: ±2%.

The recyclability test of **MNP-2-PdNPs**, **MNP-6-PdNPs**, and **MNP-9-PdNPs** was also carried out for the Heck cross-coupling reaction of iodobenzene with styrene utilizing 1.5 mol% of [Pd] and 2 equiv. of K<sub>2</sub>CO<sub>3</sub> at 120 °C in DMF (Table 6). The desired (*E*)-1,2-diphenylethene was isolated in good yields and 100% selectivity in the first run in all cases with these MNP-PdNPs. A superior activity and recyclability were also found with increase of the dendritic grade of ligands around the MNPs (Table 6). The recycling performances of these MNP-PdNPs in the Heck reaction were generally not as good as that of both Suzuki and Sonogashira reactions, which was caused by the harsher conditions of the Heck reaction. Nevertheless, the recyclability was good again with **MNP-9-PdNPs** and much superior to those of the other catalysts, showing another dramatically positive dendritic effect.

**Table 6. Investigation of the Recyclabilities of MNP-PdNPs in the Heck Reaction Between Iodobenzene and Styrene<sup>a</sup>**



	Cycle <sup>b</sup>				
	1	2	3	4	5
<b>2 - PdNPs</b>	73	36			
<b>6 - PdNPs</b>	81	77	57		
<b>9 - PdNPs</b>	85	84	84	82	74

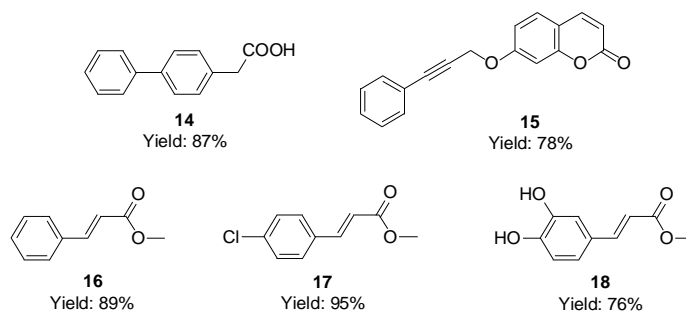
<sup>a</sup> The reaction was carried out with iodobenzene (0.6 mmol), styrene (0.5 mmol) in the presence of the catalyst MNP-PdNPs (1.5 mol%) and K<sub>2</sub>CO<sub>3</sub> (2 equiv) in DMF (5 mL) at 120 °C under a nitrogen atmosphere for 24 h. <sup>b</sup> Isolated yields (% ± 1.5%) were provided for each cycle.

**Syntheses of pharmacologically relevant or natural products based on Suzuki-Miyaura, Sonogashira, and Heck reactions.** Synthesis of pharmacologically interesting or natural products is one of the most important applications of C-C coupling reactions. The impressive ability of Pd catalysts to create C-C bonds provides many new avenues for designing medicinal candidates.

Inspired by its high efficiency, excellent recyclability, negligible Pd-leaching and the biocompatibility of iron, **MNP-9-PdNPs** was utilized in the syntheses of pharmacologically important or natural products through Suzuki-Miyaura, Sonogashira, and Heck reactions, as shown in Figure 7.

Felbinac **14**, a commercial nonsteroidal anti-inflammatory drug, is used to treat arthritis and inflammation.<sup>24</sup> The Suzuki reaction of 4-bromophenylacetic acid with phenylboronic acid was smoothly conducted upon using **MNP-9-PdNPs** as catalyst under the optimized conditions, providing Felbinac in 87% yield. Coumarine (2*H*-chromen-2-one) is naturally occurring constituent of many plants and essential oils. Coumarine and its derivatives have been proved to be useful for treating various ailments including cancer, spasm, brucellosis, burns, and rheumatic disease.<sup>25</sup> Internal alkyne **15** containing coumarine fragment was synthesized with 78% yield through Sonogashira reaction between ethyne-functionalized coumarine and iodobenzene in the presence of 1.5 mol% of [Pd] and 1 equiv. of Et<sub>3</sub>N at 40 °C. Diverse derivatives of

cinnamic acid possesses different pharmacological activities,<sup>26</sup> for example, methyl cinnamate **16** is used as a flavoring agent and a composition of soap; methyl-4-chlorocinnamate **17** has antifungal activity; methyl caffeate **18** exhibits antitumor activity against Sarcoma 180 as well as antimicrobial activity. Heck reactions involving these corresponding aromatic iodides and methyl acrylate were carried out under the optimal conditions. Compounds **16**, **17** and **18** were successfully isolated with 76-95% yield and almost 100% selectivity.



**Figure 7.** Syntheses of pharmacologically relevant or natural products using MNP-9-PdNPs as catalyst.

## CONCLUSION

The investigations of catalyst engineering around a MNP has led here to disclose favorable dendritic loading according to a divergent synthesis compared to a grafting of pre-synthesized unit method, which is new kind of positive dendritic effect. Other design features that have involved TEG termini and click syntheses were also favorable because of the advantageous NP dispersity and Pd(II) binding respectively, leading upon reduction to efficient 3-nm-sized PdNPs in the  $\gamma$ -Fe<sub>2</sub>O<sub>3</sub>-Pd catalysts. MNP-6-PdNPs and MNP-9-PdNPs containing dendritic frames provided impressive and superior performances concerning both activity and recyclability in Suzuki-Miyaura, Sonogashira, and Heck reactions compared to the linear counterparts in star-shaped MNP catalysts. In particular, MNPs-9-PdNPs that were decorated with larger dendrons containing tris-triazole groups showed the best catalytic results among these catalysts. In addition, in the case of MNP-9-PdNPs-catalyzed Suzuki-Miyaura reactions, ICP analysis revealed that the amount of Pd leached from the initial catalyst is negligible after 8 cycles. Finally, the morphology and size of MNP-9-PdNPs did

not significantly vary over time.

A new lesson regarding the design and engineering of catalysts deposited on MNPs is that MNPs decorated with dendritic frame are clearly favorable concerning the goal of efficiency for practical and environmentally friendly reactions. Indeed, it is impressive that **MNP-9-PdNPs** remains stable for months in air and is recyclable many times without significant yield decrease or morphology/size change, which is attributed the barrier formed by the dendronic frame at the dendrimer periphery that protects the intradendritic PdNP catalyst. The principles and results presented here should thus open a gate for more applications of MNPs-Den-NP catalysts in “green” chemistry.

## **EXPERIMENTAL SECTION**

### **General**

All reactions were performed under nitrogen by using standard Schlenk techniques, unless otherwise noted. Anhydrous DMF and CH<sub>2</sub>Cl<sub>2</sub> were freshly distilled from calcium hydroxide; anhydrous toluene was dried over Na foil and distilled under nitrogen immediately prior to use. All commercially available reagents were used as received, unless indicated otherwise. Flash column chromatography was performed using silica gel (300–400 mesh). <sup>1</sup>H NMR spectra were recorded by using a 300 MHz spectrometer, and <sup>13</sup>C NMR spectra were recorded at 75 MHz by using a 300 MHz spectrometer. Elemental analyses were performed by the Center of Microanalyses of the CNRS at Lyon Villeurbanne, France. The infrared spectra were recorded on an ATI Mattson Genesis series FT-IR spectrophotometer. The inductively coupled plasma optical emission spectroscopy (ICP-OES) analyses were carried out using a Varian ICP-OES720ES apparatus. Room temperature (r.t.) throughout the article is 23–25°C.

**Synthesis of compound 1.** The freshly prepared tetraethoxy silane-functionalized azide (0.5 mmol), polyethylene glycol ethyne (n = 11-12) (0.5 mmol), Cu(PPh<sub>3</sub>)<sub>2</sub>NO<sub>3</sub> (0.01 mmol) were placed into a dried Schlenk tube equipped with a magnetic stirring bar. The Schlenk tube was purged with nitrogen and 2.5 mL of dry CH<sub>2</sub>Cl<sub>2</sub> was added.

The mixture was stirred overnight at room temperature. Then the solvent was removed *in vacuo*, the obtained residue was dissolved in 20 mL of anhydrous diethyl ether, and filtered, and CH<sub>2</sub>Cl<sub>2</sub> of the filtrate was removed and dried *in vacuo*. The obtained compound **1** (375 mg, 89.8% of yield) was kept under an atmosphere of nitrogen for further application. <sup>1</sup>H NMR (300 MHz, CDCl<sub>3</sub>): δ<sub>H</sub> 7.54 (s, 1H), 5.27 (s, 2H), 4.64 (s, 2H), 3.74-3.81 (m, 2H), 3.60-3.64 (m, 53H), 3.34 (s, 3H), 1.92-2.03 (m, 2H), 1.18 (t, *J* = 7.1 Hz, 9H), 0.54-0.60 (m, 2H). <sup>13</sup>C NMR (75 MHz, CDCl<sub>3</sub>): δ<sub>C</sub> 144.86, 122.59, 71.83, 70.45, 69.55, 64.58, 58.89, 58.37, 52.29, 24.13, 18.20, 7.38. MS (*m/z*), calcd. for C<sub>35</sub>H<sub>71</sub>N<sub>3</sub>O<sub>15</sub>Si (*n* = 11) or C<sub>37</sub>H<sub>75</sub>N<sub>3</sub>O<sub>16</sub>Si (*n* = 12): 801.5 or 845.5, found: MNa<sup>+</sup> 824.5 and 868.5.

#### **Synthesis of iron oxide nanoparticle-immobilized PEGylated triazolyl ligand 2.**

**Route A.** Under an atmosphere of nitrogen, 0.3 g of **1** in 2 mL of anhydrous CH<sub>2</sub>Cl<sub>2</sub> was added to a suspension of 0.3 g of MNPs SiO<sub>2</sub>/γ-Fe<sub>2</sub>O<sub>3</sub> in 30 mL of anhydrous toluene. The mixture was then stirred at 110°C under nitrogen atmosphere for 36 h. The dark brown solid material obtained was magnetically separated, washed repeatedly with toluene (2 × 10 mL), CH<sub>2</sub>Cl<sub>2</sub> (10 mL), diluted aqueous solution of ammonia (until there is no blue color in the solution), <sup>17b</sup> H<sub>2</sub>O (2 × 20 mL), and acetone (2 × 10 mL) to remove any unanchored species and then dried *in vacuo*.

**Route B.** Compound PEG550 alkyne (1.12 mmol) and 3-azidopropyltriethoxysilane-functionalized MNP **3** (1 g) were mixed with CuI (8 mg), in DMF-THF (1:1, 40 mL) under nitrogen. *N,N*-Diisopropylethylamine (2 mL) was injected into the mixture that was then stirred at r.t. for 36 h. The reaction was monitored by FT-IR as indicated by the almost complete disappearance of IR signal of 2104 cm<sup>-1</sup> with stand for the azide group. Then the mixture was submitted to magnetic separation, and the MNPs were washed sequentially with DMF (20 mL), THF (20 mL), CH<sub>2</sub>Cl<sub>2</sub> (20 mL), diluted aqueous solution of ammonia (until there is no blue color in the solution), <sup>17b</sup> H<sub>2</sub>O (2 × 20 mL), and acetone (20 mL), and finally dried *in vacuo*.

#### **Synthesis of iron oxide nanoparticle-immobilized PEGylated triazolyl ligand 4.**

The synthesis was conducted as for the ligand **2** following the route B except that PEG550 alkyne was replaced by PEG2000 alkyne.

### Synthesis of iron oxide nanoparticle-immobilized dendritic mono-triazole ligand

**6.** The synthesis was carried out as for the ligand **2** following the route B except that PEG550 alkyne was replaced by Percec-type dendron **5**.

**Synthesis of iron oxide nanoparticles-immobilized dendritic azide 8.** In a dried Schlenk tube, a mixture of 3-iodopropyltriethoxysilane-functionalized MNP (0.5 g), dendron **7** (350 mg),  $K_2CO_3$  (0.8 g) in anhydrous DMF (40 mL) was sonicated for approximately 15 min and stirred at 80 °C under nitrogen for 48 h. Then, the mixture was submitted to magnetic separation, and the MNPs were washed sequentially with DMF (20 mL),  $CH_2Cl_2$  (20 mL),  $Na_2S_2O_3$ -saturated solution ( $2 \times 20$  mL),  $H_2O$  ( $3 \times 20$  mL), and acetone ( $2 \times 20$  mL), and finally dried *in vacuo*.

**Synthesis of compound 10.** The azido dendron **7** (0.1 mmol) and alkyne-functionalized Percec-type dendron **5** (0.3 mmol) were dissolved in tetrahydrofuran (THF), and water was added (5 mL: 5 mL, THF/water). At r.t.  $CuSO_4 \cdot 5H_2O$  was added (1 equiv. *per* branch, 1M aqueous solution), followed by the dropwise addition of a freshly prepared solution of sodium ascorbate (2 equiv. *per* branch, 1M aqueous solution). The solution was allowed to stir for 48 hours at r.t. After removing THF under vacuum, dichloromethane and an aqueous solution of ammonia were added. The mixture was allowed to stir for 10 min in order to remove all the  $Cu^I$  trapped inside the dendrimer as  $Cu(NH_3)_6^+$ . The organic phase was washed twice with water (20mL), dried with sodium sulphate, filtered under paper and the solvent was removed *in vacuo*. The dendrimer **10** was obtained as a viscous brown liquid in 86% yield.  $^1H$  NMR (300 MHz,  $CDCl_3$ ):  $\delta_H$  7.27 (s, 2H), 7.26 (s, 1H), 6.91 (d,  $J = 7.8$  Hz, 2H), 6.65 (d,  $J = 7.8$  Hz, 2H), 6.48 (s, 6H), 4.52 (s, 6H), 4.36 (s, 6H), 4.04 (18H), 3.41-3.74 (m, 102H), 3.26 (27H), 1.45 (s, 6H), 0.93 (s, 6H), 0.47 (s, 6H), 0.05 (s, 18H).  $^{29}Si$  NMR ( $CDCl_3$ , 79.5 MHz):  $\delta_{Si}$  2.75, 2.70.  $^{13}C$  NMR (75 MHz,  $CDCl_3$ ): 154.24, 152.52, 144.49, 138.18, 137.87, 137.76, 133.29, 127.11, 123.27, 114.97, 114.87, 107.28, 106.27, 72.18, 71.80, 70.65, 70.56, 70.39, 69.62, 68.70, 63.47, 58.88, 42.89, 42.76, 41.80, 41.57, 40.79, 17.31, 14.85, 14.66, -4.04. MS (MALDI-TOF;  $m/z$ ), calcd. for  $C_{118}H_{203}N_9O_{40}Si_3$ : 2471.3, found:  $MNa^+$  2494.0. Anal. calcd for  $C_{118}H_{203}N_9O_{40}Si_3$  C 57.33, H 8.28, N 5.10, found (%) C 56.99, H 8.01, N 5.06.

**Synthesis of iron oxide nanoparticle-immobilized dendritic tris-triazole ligand 9 through the divergent synthesis method.** MNP 8 (0.5 g), Percec-type dendron 5 (455 mg), were mixed with CuI (8 mg), in DMF-THF (1:1, 20 mL) under nitrogen. *N,N*-Diisopropylethylamine (2 mL) was injected into the mixture that was then sonicated for approximately 15 min and stirred at r.t. for 36 h. The reaction was monitored by FT-IR as indicated by the almost complete disappearance of IR signal of  $2102\text{ cm}^{-1}$  with stand for the azide group. Then the mixture was submitted to magnetic separation, and the MNPs were washed sequentially with DMF (10 mL), THF (10 mL),  $\text{CH}_2\text{Cl}_2$  (10 mL),  $\text{H}_2\text{O}$  ( $2 \times 10\text{ mL}$ ), and acetone (10 mL), and finally dried *in vacuo*.

**Synthesis of iron oxide nanoparticle-immobilized dendritic tris-triazole ligand 9 through the method of grafting of pre-synthesized dendron.** The synthesis was carried out as for the synthesis of MNPs 8 except that dendron 7 was replaced by dendron 10.

**Synthesis of iron oxide nanoparticle-immobilized PdNPs (taking MNP-9-PdNPs as an example).** In a Schlenk flask, the suspension of MNP 9 (200 mg, 0.126 mmol triazole) in 15 mL of  $\text{H}_2\text{O}$  was sonicated for approximately 10 min under nitrogen. Then, an orange solution of  $\text{K}_2\text{PdCl}_4$  (0.252 mmol, 82 mg, 2 eq. per triazole) in 15 mL Milli-Q  $\text{H}_2\text{O}$  was added to the Schlenk flask. The mixture was stirred at r.t. for 2 h, then submitted to magnetic separation, and the MNPs were washed with Milli-Q  $\text{H}_2\text{O}$  (10 mL) under nitrogen. After the addition of 20 mL of Milli-Q  $\text{H}_2\text{O}$ , a 10 mL aqueous solution containing 1.26 mmol of  $\text{NaBH}_4$  was injected. The mixture was stirred at r.t. for 2 h, the color of the mixture changed to black from brown, which indicated the reduction of  $\text{Pd}^{2+}$  to  $\text{Pd}^0$  and PdNP formation. The mixture was submitted to magnetic separation, and the MNPs were washed with Milli-Q  $\text{H}_2\text{O}$  ( $2 \times 10\text{ mL}$ ), and acetone (10 mL) under nitrogen, and the catalyst was dried at  $45\text{ }^\circ\text{C}$  for at least 4 h *in vacuo* and stored under nitrogen before use.

**General procedures for the MNP-PdNPs-catalyzed Suzuki reaction of bromobenzene and phenylboronic acid.** A dried Schlenk tube equipped with a magnetic stirring bar was charged, under a nitrogen atmosphere, with bromobenzene

(1 mmol), phenylboronic acid (1.5 mmol), MNP-PdNPs (0.00315 mmol [Pd]),  $K_2CO_3$  (276 mg, 2 mmol) and EtOH/H<sub>2</sub>O (1:1, 20 mL). The mixture was sonicated for approximately 5 min and stirred at 80 °C for 24 h. The catalyst was collected by using a magnet and washed successively with EtOH (3 × 15 mL), H<sub>2</sub>O (2 × 5 mL) and acetone (5 mL), then dried at r.t. *in vacuo*. The combined organic phase was washed with H<sub>2</sub>O (2 × 5 mL), and dried over Na<sub>2</sub>SO<sub>4</sub> and filtered, the filtrate was removed *in vacuo* in order to obtain the crude product that was further purified by silica-gel chromatography (petroleum ether as eluent) to yield biphenyl. The recovered catalyst was then used for the next reaction cycle.

**General procedures for the MNP-PdNPs-catalyzed Sonogashira reaction of iodobenzene and phenylacetylene.** A dried Schlenk tube equipped with a magnetic stirring bar was charged, under a nitrogen atmosphere, with iodobenzene (1 mmol), phenylacetylene (1.2 mmol), MNP-PdNPs (0.015 mmol [Pd]), Et<sub>3</sub>N (2 mmol, 0.28 mL), and THF (5 mL). The mixture was sonicated for approximately 5 min and stirred at 65 °C for 24 h. The catalyst was collected using a magnet and washed successively with CH<sub>2</sub>Cl<sub>2</sub> (3 × 15 mL) and acetone (5 mL), then dried at r.t. *in vacuo*. The combined organic phase was washed with H<sub>2</sub>O (2 × 5 mL), and dried over Na<sub>2</sub>SO<sub>4</sub> and filtered, the filtrate was removed *in vacuo* in order to obtain the crude product that was further purified by silica-gel chromatography (petroleum ether/ethyl acetate as eluent) to yield 1,2-diphenylethyne. The recovered catalyst was then used for the next reaction cycle.

**General procedures for the MNP-PdNPs-catalyzed Heck reaction of iodobenzene and styrene.** A dried Schlenk tube equipped with a magnetic stirring bar was charged, under a nitrogen atmosphere, with iodobenzene (0.6 mmol), styrene (0.5 mmol), MNP-PdNPs (0.015 mmol [Pd]),  $K_2CO_3$  (2 mmol, 276 mg), and DMF (5 mL). The mixture was sonicated for approximately 5 min and stirred at 120 °C for 24 h. The catalyst was collected using a magnet and washed successively with CH<sub>2</sub>Cl<sub>2</sub> (3 × 15 mL), H<sub>2</sub>O (2 × 10 mL) and acetone (5 mL), then dried at r.t. *in vacuo*. The combined organic phase was washed with H<sub>2</sub>O (2 × 5 mL), and dried over Na<sub>2</sub>SO<sub>4</sub> and filtered, the filtrate was removed *in vacuo* in order to obtain the crude product that was further

purified by silica-gel chromatography (petroleum ether/ethyl acetate as eluent) to yield (*E*)-1,2-diphenylethene. The recovered catalyst was then used for the next reaction cycle.

## AUTHOR INFORMATION

### Corresponding Authors

[d.astruc@ism.u-bordeaux1.fr](mailto:d.astruc@ism.u-bordeaux1.fr)

### Notes

The authors declare no competing financial interest.

## ACKNOWLEDGMENTS

Financial support from the China Scholarship Council (CSC) of the People's Republic of China (Ph. D. grant to D.W.), the Université de Bordeaux, the Centre National de la Recherche Scientifique (CNRS) and L'Oréal are gratefully acknowledged.

**Supporting Information Available:** STEM dark-field image and elemental maps of **MNP-9-PdNPs**, pictures of catalyst separation using an external magnet, calculation of nanoparticle ratios, NMR spectra and data of the C-C coupling reactions products, and mass spectra of compounds **1** and **10**. This material is available free of charge via the internet at <http://pubs.acs.org>.

## REFERENCES

1. (a) Anastas, P. T.; Warner, J. C. *Green Chemistry: Theory and Practice*, Oxford University Press, New York, 1998. (b) Doble, M.; Kruthiventi, A. K. *Green Chemistry and Engineering*, Academic Press, London, 2007. (c) Sharma, S. K.; Mudhoo, A. *Green Chemistry for Environmental Sustainability*. CRC Press, Boca Raton, FL, USA, 2010.
2. (a) Somorjai, G. A. *Introduction to Surface Chemistry and Catalysis*, Wiley, New York, 1994. (b) Corma, A. *Chem. Rev.* **1995**, *95*, 559-614. (c) Haruta, M. *Catal. Today* **1997**, *36*, 153-166. (d) *Handbook of Heterogeneous Catalysis*; Ertl, G.; Knozinger, H.; Weitkamp, J. Eds., Wiley-VCH, Weinheim, Germany, 1997. (e) Corma, A. *Chem. Rev.* **1997**, *97*, 2373-2419. (f) Haruta, M.; Date, M. *Appl. Catal. A: Gen.* **2001**, *222*, 427-437. (g) *Modern Surface Organometallic Chemistry*;

- Basset, J.-M.; Psaro, R.; Roberto, D.; Ugo, R. Eds., Wiley-VCH, Weinheim, 2009.
- (h) Corma, A.; Garc ía, H.; Llabr és i Xamena, F. X. *Chem. Rev.* **2010**, *110*, 4606-4655.
3. (a) Burda, C.; Chen, X.; Narayanan, R.; El-Sayed, M. A. *Chem. Rev.* **2005**, *105*, 1025-1102. (b) Astruc, D.; Lu, F.; Ruiz, J.; *Angew. Chem. Int. Ed.* **2005**, *44*, 7852-7872. (c) *Nanoparticles and Catalysis*; Astruc, D. Ed., Wiley-VCH, Weinheim, 2008. (d) Chen, P.; Zhou, X.; Shen, H.; Andoy, N. M.; Choudhary, E.; Han, K.-S.; Liu, G.; Meng, W. *Chem. Soc. Rev.* **2010**, *39*, 4560-4570. (e) Arp ád, M. *Chem. Rev.* **2011**, *111*, 2251-2320. (f) Mondloch, J. E.; Bayram, E.; Finke, R. G. *J. Mol. Catal. A: Chem.* **2012**, *355*, 1-38. (g) Bronstein, L. M.; Shifrina, Z. B. *Chem. Rev.* **2011**, *111*, 5301-5344; (h) Bai, C.; Liu, M. *Nano Today* **2012**, *7*, 258-281. (i) *Nanomaterials and Catalysis*; Serp, P.; Philippot, K. Eds., Wiley-VCH, Weinheim, 2013.
4. (a) Lu, A. H.; Salabas, E. L.; Schüth, F. *Angew. Chem., Int. Ed.* **2007**, *46*, 1222-1244. (b) Shylesh, S.; Schünemann, V.; Thiel, W. R. *Angew. Chem., Int. Ed.* **2010**, *49*, 3428-3459. (c) Zhu, Y.; Stubbs, L. P.; Ho, F.; Liu, R.; Ship, C. P.; Maguire, J. A.; Hosmane, N. S. *ChemCatChem* **2010**, *2*, 365-374. (d) Polshettiwar, V.; Luque, R.; Fihri, A.; Zhu, H.; Bouhrara, M.; Basset, J. M. *Chem. Rev.* **2011**, *111*, 3036-3075. (e) Kainz, Q. M.; Reiser, O. *Acc. Chem. Res.* **2014**, *47*, 667-677. (f) Wang, D.; Astruc, D. *Molecules* **2014**, *19*, 4635-4653. (g) Wang, D.; Astruc, D. *Chem. Rev.* 2014, doi: org/10.1021/cr500134h.
5. (a) Newkome, G. R.; He, E.; Moorefield, C. N. *Chem. Rev.* **1999**, *99*, 1689-1746. (b) Astruc, D.; Chardac, F. *Chem. Rev.* **2001**, *101*, 2991-3023. (c) van Heerbeek, R.; Kamer, P. C. J.; van Leeuwen, P. W. N. M.; Reek, J. N. H. *Chem. Rev.* **2002**, *102*, 3717-3756. (d) Twyman, L. J.; King, A. S. H.; Martin, I. K. *Chem. Soc. Rev.* **2002**, *31*, 69-82. (e) Astruc, D.; Heuze, K.; Gatard, S.; Méry, D.; Nlate, S.; Plault, S. *Adv. Synth. Catal.* **2005**, *347*, 329-338. (f) Helms, B.; Fréchet, J. M. J. *Adv. Synth. Catal.* **2006**, *348*, 1125-1148. (g) de Jesús, E.; Flores, J. C. *Ind. Eng. Chem. Res.* **2008**, *47*, 7968-7081. (h) Astruc, D.; Boisselier, E.; Ornelas, C. *Chem. Rev.* **2010**, *110*, 1857-1959. (i) Astruc, D. *Nat. Chem.* **2012**, *4*, 255-267. (j) Caminade,

- A. M.; Ouali, A.; Keller, M.; Majoral, J. P. *Chem. Soc. Rev.* **2012**, *41*, 4113-4125.
- (k) Wang, D.; Astruc, D. *Coord. Chem. Rev.* **2013**, *257*, 2317–2334.
6. Piotti, M. E.; Rivero, F.; Bond, R.; Hawker, C. J.; Fréchet, J. M. J. *J. Am. Chem. Soc.* **1999**, *121*, 9471-9472.
7. Fréchet, J. M. J. *J. Polym. Sci. Part A: Polym. Chem.* **2003**, *41*, 3713-3725.
8. Helms, B.; Liang, C. O.; Hawker, C. J.; Fréchet, J. M. J. *Macromolecules* **2005**, *38*, 5411-5415.
9. Helms, B.; Fréchet, J. M. J. *Adv. Synth. Catal.* **2006**, *348*, 1125-1148.
10. (a) Balogh, L.; Tomalia, D. A. *J. Am. Chem. Soc.* **1998**, *120*, 7355–7356. (b) Crooks, R. M.; Zhao, M.; Sun, L.; Chechik V.; Yeung, L. K. *Acc. Chem. Res.* **2001**, *34*, 181-190. (c) Yeung, L. K.; Crooks, R. M. *Nano Lett.* **2001**, *1*, 14–17. (d) Rahim, E. H.; Kamounah, F. S.; Frederiksen, J.; Christensen, J. B. *Nano Lett.* **2001**, *1*, 499–503. (e) Higushi, M.; Shiki, S.; Ariga, S.; Yamamoto, K. *J. Am. Chem. Soc.* **2001**, *123*, 4414–4420. (f) Yamamoto, K.; Higushi, M.; Shiki, S.; Tsuruta, M.; Chiba, H. *Nature* **2002**, *415*, 509–511. (g) Satoh, N.; Cho, J. S.; Higushi, M.; Yamamoto, K. *J. Am. Chem. Soc.* **2003**, *125*, 8104–8105. (h) Scott, R. W. J.; Datye, A. K.; Crooks, R. M. *J. Am. Chem. Soc.* **2003**, *125*, 3708–3709. (i) Scott, R. W.; Wilson, O. M.; Oh, S.-K.; Kenik, E. A.; Crooks, R. M. *J. Am. Chem. Soc.* **2004**, *126*, 15583–15591. (j) Ooe, M.; Murata, M.; Mizugaki, T.; Ebitani, K. *J. Am. Chem. Soc.* **2004**, *126*, 1604–1608. (k) Wilson, O. M.; Scott, R. W. J.; Garcia-Martinez, J. C.; Crooks, R. M. *J. Am. Chem. Soc.* **2005**, *127*, 1015–1024. (l) Scott, R. W. J.; Sivadiranarayana, C.; Wilson, O. M.; Yan, Z.; Goodman, D. W.; Crooks, R. M. *J. Am. Chem. Soc.* **2005**, *127*, 1380–1381. (m) Gomez, M. V.; Guerra, J.; Velders, A. H.; Crooks, R. M. *J. Am. Chem. Soc.* **2008**, *131*, 341–350. (n) Satoh, N.; Nakashima, T.; Kamikura, K.; Yamamoto, K. *Nat. Nanotechnol.* **2008**, *3*, 106–111. (o) Deraedt, C.; Astruc, D. *Acc. Chem. Res.* **2014**, *47*, 494-503.
11. (a) Zhao, M.; Sun, L.; Crooks, R. M. *J. Am. Chem. Soc.* **1998**, *120*, 4877–4878. (b) Zhao, M.; Crooks, R. M. *Angew. Chem. Int. Ed.* **1999**, *38*, 364-366. (c) Myers, V. S.; Weier, M. W.; Carino, E. V.; Yancey, D. F.; Pande, S.; Crooks, R. M. *Chem. Sci.* **2011**, *2*, 1632-1646.

12. Tomalia, D. A.; Baker, H.; Dewald, J.; Hall, M.; Kallos, G.; Martin, S.; Roeck, J., Ryder, J.; Smith, P. *Polym. J.* **1985**, *17*, 117-132. (b) Tomalia, D. A.; Naylor, A. M.; Goddard III, W. *Angew. Chem., Int. Ed.* **1990**, *29*, 138-175.
13. (a) de Brabander-van den Berg, E. M. M.; Meijer, E. W. *Angew. Chem., Int. Ed. Engl.* **1993**, *32*, 1308-1311. (b) Bosman, A. W.; Janssen, H. M.; Meijer, E. W. *Chem. Rev.* **1999**, *99*, 1665-1688.
14. (a) Higushi, M.; Shiki, S.; Ariga, S.; Yamamoto, K. *J. Am. Chem. Soc.* **2001**, *123*, 4414-4420. (b) Yamamoto, K.; Higushi, M.; Shiki, S.; Tsuruta, M.; Chiba, H. *Nature* **2002**, *415*, 509-511. (c) Satoh N.; Nakashima T.; Kamikura K.; Yamamoto, K. *Nat. Nanotechnol.* **2008**, *3*, 106-111.
15. (a) Percec, V.; Johansson, G.; Ungar, G.; Zhou, J. *J. Am. Chem. Soc.* **1996**, *118*, 9855-9866. (b) Balagurusamy, V. S. K.; Ungar, G.; Percec, V.; Johansson, G. *J. Am. Chem. Soc.* **1997**, *119*, 1539-1555. (c) Percec, V.; Peterca, M.; Dulcey, A. E.; Imam, M. R.; Hudson, S. D.; Nummelin, S.; Adelman, P.; Heiney, P. A. *J. Am. Chem. Soc.* **2008**, *130*, 13079-13094.
16. (a) Newkome, G. R.; Yao, Z.; Baker, G. R.; Gupta, V. K. *J. Org. Chem.* **1985**, *50*, 2003-2004. (b) Newkome, G. R.; Moorefield, C. N. *Aldrichim. Acta* **1992**, *25*, 31-38. (c) Newkome, G. R. *Pure Appl. Chem.* **1998**, *70*, 2337-2343. (d) Newkome, G. R.; Shreiner, C. *Chem. Rev.* **2010**, *110*. (e) Moulines, F.; Djakovitch, L.; Boese, R.; Gloaguen, B.; Thiel, W.; Fillaut, J.-L.; Delville, M.-H.; Astruc, D. *Angew. Chem., Int. Ed. Engl.* **1993**, *32*, 1075-1077.
17. (a) Boisselier, E.; Diallo, A. K.; Salmon, L.; Ornelas, C.; Ruiz, J.; Astruc, D. *J. Am. Chem. Soc.* **2010**, *132*, 2729-2742. (b) Deraedt, C.; Salmon, L.; Etienne, L.; Ruiz, J.; Astruc, D. *Chem. Commun.* **2013**, *49*, 8169-8171. (c) Deraedt, C.; Salmon, L.; Astruc, D. *Adv. Syn. Catal.* 2014, DOI: 10.1002/adsc.201400153.
18. (a) Abu-Reziq, R.; Alper, H.; Wang, D.; Post, M. L. *J. Am. Chem. Soc.* **2006**, *128*, 5279-5282. (b) Uzun, K.; Çevik, E.; Şenel, M.; Sözeri, H.; Baykal, A.; Abasıyanık, M. F.; Toprak, M. S. *J. Nanopart. Res.* **2010**, *12*, 3057-3067. (c) Chou, C. M.; Lien, H. L. *J. Nanopart. Res.* **2011**, *13*, 2099-2107. (d) Kainz, Q. M.; Schätz, A.; Zöpfl, A.; Stark, W. J.; Reiser, O. *Chem. Mater.* **2011**, *23*, 3606-3613. (e)

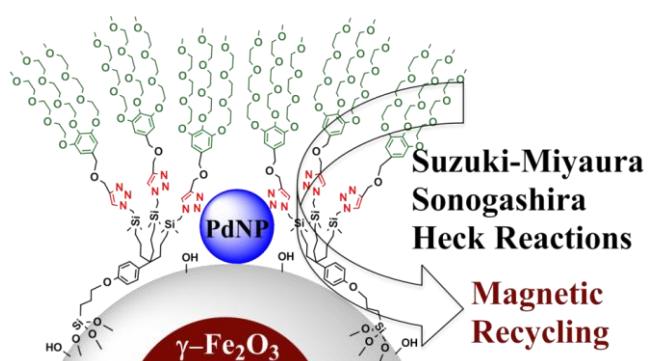
- Pourjavadi, A.; Hosseini, S. H.; Hosseini, S. T.; Aghayeemeibody, S. A. *Catal. Commun.* **2012**, *28*, 86–89. (f) Wang, H.; Shentu, B.; Zhang, W.; Gu, C.; Weng, Z. *Eur. Polym. J.* **2012**, *48*, 1205-1211. (g) Kuchkina, N. V.; Yuzik-Klimova, E. Y.; Sorokina, S. A.; Peregudov, A. S.; Antonov, D. Y.; Gage, S. H.; Boris, B. S.; Nikoshvili, L. Z.; Sulman, E. M.; Morgan, D. G.; Mahmoud, W. E.; Al-Ghamdi, A. A.; Bronstein, L. M.; Shifrina, Z. B. *Macromolecules* **2013**, *46*, 5890-5898.
19. Guo, W.; Monge-Marcet, A.; Catto ̈n, X.; Shafir, A.; Pleixats, R.; *React. Funct. Polym.* **2013**, *73*, 192-199.
20. (a) Ornelas, C.; Ruiz, J.; Cloutet, E.; Alves, S.; Astruc, D. *Angew Chem., Int. Ed.* **2007**, *46*, 872-877. (b) Djeda, R.; Rapakousiou, A.; Liang, L.; Guidolin, N.; Ruiz, J.; Astruc, D. *Angew Chem., Int. Ed.* **2010**, *49*, 8152-8156. (c) Rapakousiou, A.; Wang, Y.; Belin, C.; Pinaud, N.; Ruiz, J.; Astruc, D. *Inorg. Chem.* **2013**, *52*, 6685-6693.
21. Rostovtsev, V. V.; Green, L. G.; Fokin, V. V.; Sharpless, K. B. *Angew. Chem. Int. Ed.* **2002**, *41*, 2596-2599.
22. Costa, N. J. S.; Kiyohara, P. K.; Monteiro, A. L.; Coppel, Y.; Philippot, K.; Rossi, L. M. *J. Catal.* **2010**, *276*, 382-389. (b) Zhu, M.; Diao, G. *J. Phys. Chem. C* **2011**, *115*, 24743-24749. (c) Li, W.; Zhang, B.; Li, X.; Zhang, H.; Zhang, Q. *Appl. Catal. A: Gen.* **2013**, *459*, 65-72. (d) Wang, J.; Xu, B.; Sun, H.; Song, G. *Tetrahedron Lett.* **2013**, *54*, 238-241. (e) de Rivera, F. G.; Angurell, I.; Rossell, M. D.; Erni, R.; Llorca, J.; Divins, N. J.; Muller, G.; Seco, M.; Rossell, O. *Chem.-Eur. J.* **2013**, *19*, 11963-11974. (f) Beygzadeh, M.; Alizadeh, A.; Khodaei, M. M.; Kordestani, D. *Catal. Commun.* **2013**, *32*, 86-91.
23. (a) Sch ̈az, A.; Long, T. R.; Grass, R. N.; Stark, W. J.; Hanson, P. R.; Reiser, O. *Adv. Funct. Mater.* **2010**, *20*, 4323-4328. (b) Hu, J.; Wang, Y.; Han, M.; Zhou, Y.; Jiang, X.; Sun, P. *Catal. Sci. Technol.* **2012**, *2*, 2332-2340. (c) de Rivera, F. G.; Angurell, I.; Rossell, M. D.; Erni, R.; Llorca, J.; Divins, N. J.; Muller, G.; Seco, M.; Rossell, O. *Chem. Eur. J.* **2013**, *19*, 11963-11974. (d) Zhang, Q.; Su, H.; Luo, J.; Wei, Y. *Catal. Sci. Technol.* **2013**, *3*, 235-243.
24. Kohler, C.; Tolman, E.; Wooding, W.; Ellenbogen, L. *Arzneim.-Forsch.* **1980**, *30*,

702-707.

25. Egan, D.; O'Kennedy, R.; Moran, E.; Cox, D.; Prosser, E.; Thornes, R. D. *Drug. Metab. Rev.* **1990**, *22*, 503-529.

26. Sharma, P. *J. Chem. Pharm. Res.* **2011**, *3*, 403-423.

### Table of Contents (TOC)



# Impregnation of dendritically preformed Pd nanoparticles on magnetic nanoparticles for improved catalyst robustness, efficiency and recyclability

Christophe Deraedt,<sup>[a]</sup> Dong Wang,<sup>[a]</sup> Lionel Salmon,<sup>[b]</sup> Laetitia Etienne,<sup>[c]</sup> Jaime Ruiz,<sup>[a]</sup> Didier Astruc\*<sup>[a]</sup>

[a] ISM, UMR CNRS N°5255, Univ. Bordeaux, 33405 Talence, Cedex (France) Fax: (+33)5-4000-2994 E-mail: [d.astruc@ism.u-bordeaux.fr](mailto:d.astruc@ism.u-bordeaux.fr)

[b] Laboratoire de Chimie de Coordination, CNRS UPR-8241 and Université de Toulouse ; UPS, INP ; F-31077 Toulouse (France)

[c] ICMCB, UPR CNRS N°9048, 87 avenue, Pey-Berland, 33608 Pessac Cedex (France)

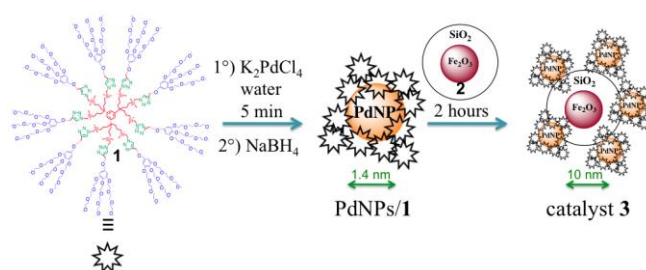
**Abstract:** The simple impregnation of  $\gamma$ -Fe<sub>2</sub>O<sub>3</sub>(core)/SiO<sub>2</sub>(shell) magnetic nanoparticles with a dendrimer containing stabilized Pd nanoparticles, a new method producing a highly efficient heterogeneous catalyst, provides much better stability, recyclability and activity in C-C cross coupling reactions and selective oxidation in water of benzyl alcohol to benzaldehyde than unsupported Pd nanoparticles.

The quest of improved catalysts and strategies for catalyst efficiency and recyclability is presently more challenging than ever toward better sustainability. Supported metal nanoparticles (NPs) have recently been shown to be excellent catalysts for a variety of reactions owing to their large surface-to-volume ratio, remarkable efficiency and topological properties and their heterogenization on various oxide and carbon supports that allow their recovery.<sup>[1]</sup> In particular, iron oxide magnetic nanoparticles (MNPs) have received considerable attention recently,<sup>[2]</sup> because they are biocompatible and most easily recovered from reaction mixtures using a simple external magnetic field.

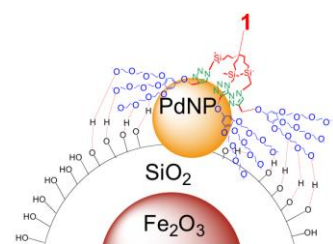
Classically the fixation of NPs on supports mostly uses reduction of metal salts in the presence of the support followed by an adequate thermal treatment.<sup>[3]</sup> Here we

propose a novel very efficient method involving PdNPs that are pre-stabilized by a water-soluble “clicked” dendrimer **1**,<sup>[4]</sup> then deposited on silica-coated maghemite  $\gamma$ -Fe<sub>2</sub>O<sub>3</sub> MNPs **2** by simple mixing and stirring with the aqueous solution of PdNPs/**1**. This simple preparation provides the new heterogeneous PdNP/**1**/MNP catalyst, **3** (Figure 1). Catalytic tests for which quantitative or nearly quantitative yields of desired products were obtained here with relatively high turnover frequencies and unusually low amounts of Pd involving carbon-carbon cross coupling reactions<sup>[3,5]</sup> (Suzuki-Miyaura, copper-free Sonogashira and Heck reactions of bromoarenes) and selective aerobic oxidation of benzylic alcohol to benzaldehyde.<sup>[6]</sup> Another crucial aspect of these new catalysts is their robustness and recyclability.

The driving force of the strong PdNP fixation onto the silica shell is provided by the multiple supramolecular H-bonding interactions between the TEG (triethylene glycol) termini of **1** and surface OH groups of the silica shell of **2** in synergy with the backfolding of intradendritic triazole groups of **1** that interact with the other side of the PdNP surface (Figure 2).

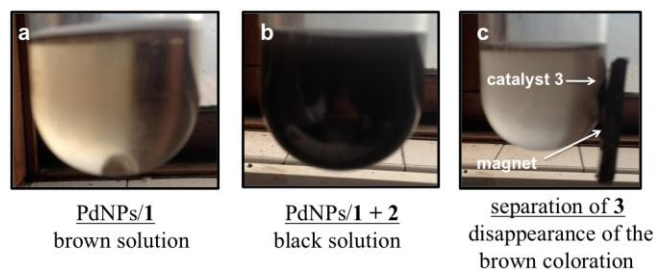


**Figure 1.** Preparation of the new catalyst PdNPs/MNP, **3**, starting from the arene-cored dendrimer **1** that contains nine 1,2,3-triazolyl groups connected to nine Percec-type dendrons terminated by 27 triethylene glycol groups.



**Figure 2.** Schematic picture of the stabilization of the dendrimer **1** on the silica surface and fixation of the PdNPs by supramolecular H bonding interactions between the TEG termini of **1** and the OH groups at the surface of **2**.

The detailed preparation of **3** and its characterization are as follows. An aqueous solution of small PdNPs ( $1.4 \pm 0.7$  nm) was synthesized in the presence of the dendrimer **1** that contains nine 1,2,3 triazolyl groups with 27 TEG termini **1** (1.1 mg of  $K_2PdCl_4$  and 2.59 mg of dendrimer **1**). After the coordination of one equiv.  $Pd^{II}$  per triazolyl group (9 triazolyl groups *per* dendrimer) in water, an aqueous  $NaBH_4$  solution was subsequently added causing the instantaneous formation of PdNPs. Dynamic light scattering (DLS) allowed concluding that each PdNP was stabilized and surrounded in average by about ten dendrimers **1**.<sup>[4b]</sup>  $\gamma$ - $Fe_2O_3$  MNPs of approximately 10 nm diameter were synthesized by the co-precipitation method described by Shylesh et al.<sup>[7a]</sup> These MNPs were subsequently coated with a dense silica layer using tetraethoxysilane (TEOS) as the silica source and aqueous  $NH_3$  as hydrolyzing agent. In order to well disperse **2** in the water solution of PdNPs/**1**, the solution was plunged into an ultrasonic bath. Ultrasons also favor the ligandation of PdNP at the  $SiO_2$  surface.<sup>[7b]</sup> After 2 hours of ultrasons (entry 1 and 2 of Table 1), **3** was separated from the aqueous solution using a simple magnet (Figure 3). The resulting aqueous solution was analyzed by inductively coupled plasma optical electron spectrometry (ICP-OES) and compared to the ICP-OES result of the initial aqueous solution of PdNPs/**1** in order to investigate the Pd loading. ICP-OES revealed that 94% of the starting Pd was loaded on the MNPs **2** (entry 2). With only 5 min of ultrasons and 2 hours of stirring Pd loading reached 97.5% (entry 3) and 99.9% in 16 hours of stirring (entry 4). When the amount of **2** was reduced from 120 mg to 50 mg (entry 6) or 25 mg (entry 7), the Pd loading was less important, respectively 60% and 40%. As expected, a larger amount of **2** (700 mg instead of 120 mg) led to a quantitative loading (entry 5).



**Figure 3.** a) (pictures same size) Brown aqueous solution of PdNPs/**1**. b) After addition of **2** to the aqueous solution of PdNPs/**1** (black color). c) After 2 hours of stirring, the catalyst was separated with a magnet (disappearance of the brown color of the solution).

**Table 1.** Impregnation of PdNPs/**1** onto **2** for the synthesis of catalyst **3**.

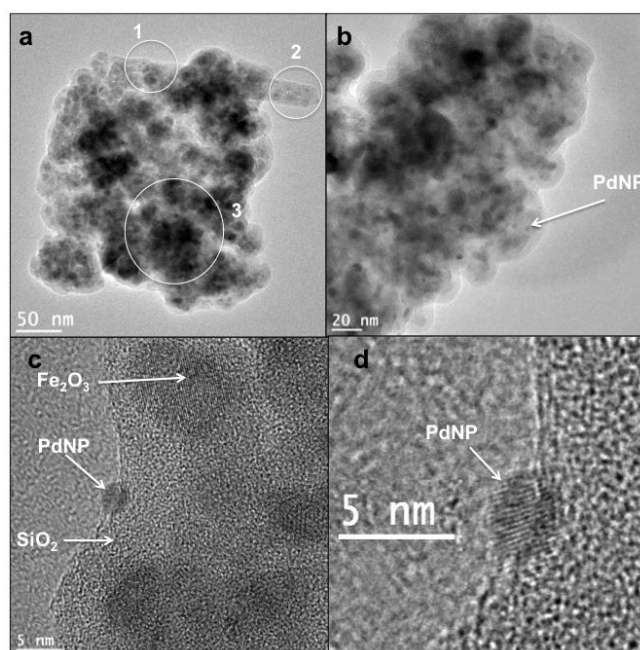
Entry <sup>[a]</sup>	<b>2</b> (mg)	Ultrason (hour)	Stirring (hour)	Temp. ( °C)	Pd loading on <b>3</b> (%) <sup>[b]</sup>
1	120	2	0	50	75.0
2	120	2	0	20	94.0
3	120	0.08	2	20	97.5
4	120	0.08	16	20	99.9
5	700	0.08	2	20	99.9
6	50	0.08	2	20	60.0
7	25	0.08	2	20	40.0

[a] Reactions were carried out using 33 mL of an aqueous solution of PdNPs/**1** (2.6 mg of **1** + 1.1 mg of  $K_2PdCl_4$  + 1.1 mg of  $NaBH_4$ ). [b] Pd loading was determined by ICP-OES.

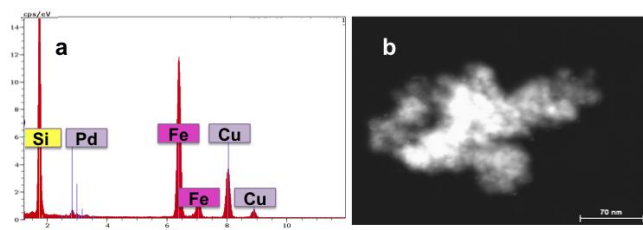
In conclusion, it was possible to obtain a quantitative loading of Pd upon mixing pre-formed PdNPs/**1** and MNPs coated with silica under optimized conditions. After the separation of the new magnetic catalyst **3** from the aqueous solution, the aqueous solution was evaporated, and the resulting residue was analyzed by  $^1H$  NMR in  $CDCl_3$  (or  $D_2O$ ) in order to check if only PdNP or PdNP@**1** was loaded onto the MNPs **2**. In the case of entry 4 (quantitative impregnation), no trace of dendrimer **1** was observed in the  $^1H$  NMR spectrum, which was not the case of entry 6 (only 60% of Pd was loaded in this case).  $^1H$  NMR spectroscopy indicates that PdNPs@dendrimer **1** were completely loaded onto the MNPs (in the case of entry 4). Elemental analysis showed that **3** was composed of an organic phase (presence of C, N, O atoms) leading to the

same conclusion as upon  $^1\text{H}$  NMR analysis. Moreover **2** was used in large amount (120 or 700 mg) in comparison with Pd (1.1 mg of  $\text{K}_2\text{PdCl}_4$ ), and the PdNPs were somewhat wedged by **2**.

Catalyst **3** was characterized by high-resolution transmission electron microscopy (HRTEM) and by energy-dispersive X-ray (EDX) spectroscopy. The size of the iron core was between 5 and 10 nm as described by the authors,<sup>[7a]</sup> and small monodispersed PdNPs were localized on the silica shell with an average size of  $2.0 \pm 0.7$  nm. EDX spectroscopy was conducted in three independent zones (shown in Figure 4a) of an aggregate of **3**. In all cases, the presence of Pd, Fe and Si was evidenced. Zones 1 and 2 are localized at the periphery of the assembly and contain 2-3% weight of Pd (vs. 97-98%  $\text{Fe}_2\text{O}_3\text{-SiO}_2$ ), whereas zone 3 that is located more inside the assembly contains only 0.5% weight of Pd. This is in agreement with the fact that supramolecular interactions allow the stabilization/impregnation of PdNPs/**1** on the silica shell surface of **2**.



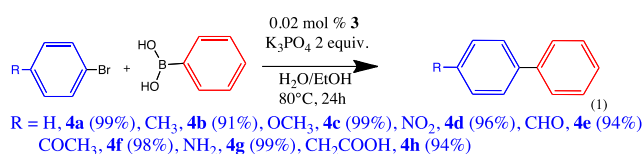
**Figure 4.** a) General view of an assembly of **3** by HRTEM microscopy. The three encircled zones correspond to the zones of EDX analysis; see below. b) HRTEM of **3** at 20 nm scale. Small PdNPs are observed at the periphery of **3**. c) Distinction between  $\text{Fe}_2\text{O}_3$ ,  $\text{SiO}_2$  and Pd NPs in the HRTEM picture (5 nm scale). d) Zoom on a PdNP.



**Figure 5.** EDX analysis of **3**. a) EDX spectrum showing the presence of Pd, Fe and Si in the assembly of NPs **3** (zone 1). b) HRTEM dark field image in which PdNPs at the periphery of the aggregate are better distinguished.

Catalytic Suzuki-Miyaura reactions were conducted in H<sub>2</sub>O/EtOH at 80 °C within 24h with 0.02 mol % of Pd from **3** in the presence of K<sub>3</sub>PO<sub>4</sub> as a base (Scheme 1). Eight substrates were tested, and yields were in the range of 91% - 99%. The results obtained are comparable with those obtained using the homogeneous catalyst PdNPs/**1** alone or even better, which is remarkable. For instance, under the same conditions **4f** was obtained with a yield < 50% with 0.02 mol % of PdNPs/**1**, whereas a yield of 98% was obtained with the same amount of Pd from **3**. Moreover, felbinac **4h** (R = CH<sub>2</sub>CO<sub>2</sub>H in Scheme 1), a nonsteroidal anti-inflammatory drug used to treat arthritis and inflammation was synthesized in this way, the Suzuki-Miyaura reaction providing a 94% yield.

In order to determine the optimal amount of **3** necessary for the Suzuki-Miyaura reaction between bromobenzene and phenyl boronic acid, some items including yields, turnover numbers (TONs) and TOFs were measured in the presence of different amounts of **3**. With only 20 ppm of Pd after 2 days, the reaction yielded 88 % of coupled product, i.e. a TON of 44000 with a TOF of nearly 10<sup>3</sup> h<sup>-1</sup> (Table 2).



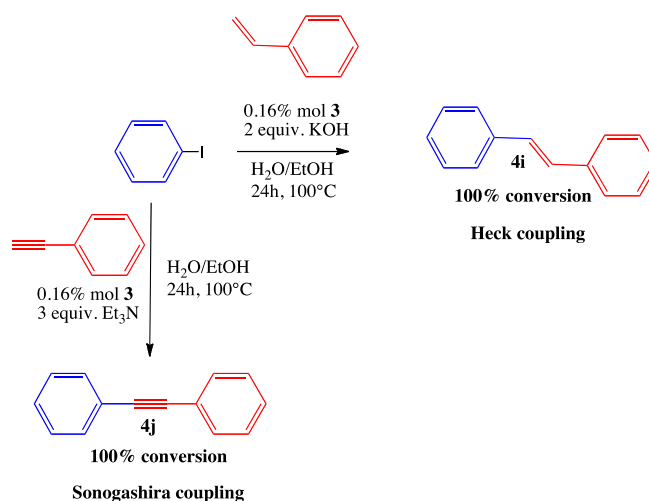
**Scheme 1.** Suzuki-Miyaura reaction of various substrates with 200 ppm of Pd from **3** in H<sub>2</sub>O/EtOH at 80 °C during 24h carried out with 1 mmol of bromoarene, 1.5 mmol of phenyl boronic acid and 2 mmol of K<sub>3</sub>PO<sub>4</sub>.

**Table 2.** Suzuki-Miyaura reactions between bromobenzene and phenyl boronic acid with various amount of catalyst **3**.<sup>[a]</sup>

Entry	Pd amount ( <b>3</b> ) (mol %)	Time (h)	Yield (%)	TON	TOF (h <sup>-1</sup> )
1	0.2	24	99	495	20.6
2	0.02	24	99	4 950	206
3	0.005	24	60	12 000	500
4	0.005	36	99	19 000	550
5	0.003	48	91	30 333	632
6	0.002	48	88	44 000	917

[a] The reactions have been carried out in with 1 mmol of bromobenzene, 1.5 mmol of phenyl boronic acid, 2 mmol of K<sub>3</sub>PO<sub>4</sub> in a mixture solvent H<sub>2</sub>O/EtOH (10 mL/10 mL) at 80 °C.

Another major interest of this catalyst is that by applying a simple magnet, **3** is totally recovered. The catalyst **3** was used at least five times without much loss of activity. For instance, in the synthesis of **4a**, yields decreased from 99% yield (1<sup>st</sup> run) to 91% (5<sup>th</sup> run). ICP-OES showed that only 0.3% of Pd composing **3** was lost after the first run. The catalytic activity was also tested for the Heck and copper-free Sonogashira reactions (Scheme 2).

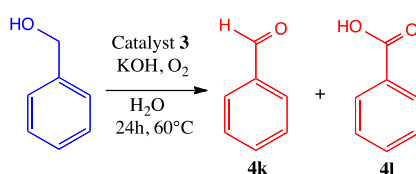


**Scheme 2.** Heck coupling (right) and Sonogashira coupling (bottom).

The efficiency of **3** with only 0.16% mol % Pd for the copper-free Sonogashira reaction was evaluated for the coupling between iodobenzene and phenylacetylene in the presence of Et<sub>3</sub>N as a base. Within 24h at 100 °C in a mixture of H<sub>2</sub>O/EtOH as solvent, the desired product was isolated quantitatively.

The Heck reaction between iodobenzene and styrene was also performed under the same conditions as those of the Sonogashira reaction but with KOH as base instead of Et<sub>3</sub>N. Only the *E* isomer of stilbene was formed quantitatively in the reaction.

In order to evaluate the robustness, selectivity and efficiency of **3**, the widely studied oxidation of benzyl alcohol by dioxygen to benzaldehyde **4k** was investigated. This reaction was selected, because in the presence of only PdNPs/**1** the reaction did not work at all, and PdNPs directly precipitated when O<sub>2</sub> was bubbled into the reaction medium. Now with **3** instead of **1**, the aerobic oxidation of benzylic alcohol in water with KOH as base occurred very efficiently with only 0.09-0.20 mol % of Pd from **3**. The reaction requires the presence of KOH as base and 5 min of O<sub>2</sub> bubbling (excess of O<sub>2</sub> leads to the side product **4l**). Moreover, the use of molecular O<sub>2</sub> instead of stoichiometric organic oxidant is highly valuable and much researched.<sup>[8]</sup> The reaction performed in water, at relatively low temperature (60 °C) with only 0.2 % mol of Pd (maximum) led to quantitative conversion of the alcohol into the aldehyde (Table 3, entry 13).



**Scheme 3.** Selective benzyl alcohol oxidation with the catalyst **3**.

**Table 3.** Investigation of the aerobic benzyl alcohol oxidation in water

Entry <sup>[a]</sup>	Pd (3) amount (mol %)	KOH	Side product	NMR <sup>[d]</sup> Conversion (%)
7	0.09	2 equiv.	No	74
8	0.09	0 equiv.	No	0
9 <sup>[b]</sup>	0.09	2 equiv.	No	33
10 <sup>[c]</sup>	0.09	2 equiv.	<b>4l</b>	74
11	0.045	2 equiv.	No	24
12	0.022	2 equiv.	No	4
13	0.20	2 equiv.	No	98

[a] The reactions have been carried out with 1 mmol of benzyl alcohol in H<sub>2</sub>O (3 mL) during 24h at 60 °C, and 5 min of O<sub>2</sub> was bubbled before starting the reaction. [b] The reaction was performed under air. [c] O<sub>2</sub> was present during the entire reaction. [d] The NMR conversion corresponds that of benzylic alcohol to benzaldehyde **4k**.

These results show that **3** is much more robust than PdNPs/**1** and permits to extend the use of the PdNPs as efficient and reusable catalyst in **3** to reactions that are different from cross C-C coupling.

In conclusion, the new concept of impregnation of dendritically preformed PdNPs on MNPs was shown to be highly productive for large improvements in terms of catalyst robustness, efficiency and recyclability. The dendrimer-stabilized and encapsulated PdNPs/**1** were quantitatively impregnated upon heterogeneization on silica-coated maghemite  $\gamma$ -Fe<sub>2</sub>O<sub>3</sub> MNPs **2** by simple mixing and stirring with the aqueous solution of PdNPs/**1**. This preparation produced a highly stabilized magnetic catalyst **3** that was active even with only 20 ppm of Pd for the Suzuki-Miyaura reaction of bromoarenes in the mixture of green solvent H<sub>2</sub>O/EtOH and reusable. To the best of our knowledge, this activity has never been reached for the Suzuki-Miyaura reaction with magnetic heterogeneous PdNPs. Actually, lots of magnetic PdNP systems has been used for the Suzuki-Miyaura coupling, but most of them require 0.1-2% mol of Pd<sup>[9a-9g]</sup>, and only a few examples work below this amount.<sup>[9h]</sup> Moreover, the leaching amount of only 0.3% for a run led to only 0.6 ppm Pd contamination of products, which is very valuable for the synthesis of biological molecules such as the felbinac **4h** as described above. This magnetic catalyst was so robust that the selective oxidation of benzylic alcohol by O<sub>2</sub> was quantitative at 60 °C

in water with only 0.09-0.2 % mol of Pd from **3**, which was not possible with non-impregnated PdNPs/**1** because of the instantaneous aggregation of PdNPs in the presence of O<sub>2</sub>. Finally, another advantage is that **3** is a solid, and catalysis does not necessarily have to be conducted in water unlike with PdNPs/**1**, which was a limitation. In summary, this method produced a highly stable, versatile, efficient and recyclable magnetic catalyst for a variety of crucial reactions under sustainable conditions.

## Experimental Section

Synthesis of the catalyst **3**.

MNP **2** (25, 50, 120 or 700 mg) is added to the water solution of PdNPs/**1** ( $3.2 \times 10^{-3}$  mmol of Pd). Ultrasonic is applied during 5min or 2h. When only 5 min of ultrasons is used, the mixture is stirred during 2 hours or 16 hours (see Table 1 of the main text). Catalyst **3** is then separated from the water with a magnet. The water phase is kept and **3** is dried other night at 35-40 °C. In order to know the percentage of Pd loading, the water phase is analyzed by ICP-OES and compared to the initial ICP-OES value determined for the solution of PdNPs/**1** (see Table).

## Acknowledgements

Financial support from the Univ. Bordeaux, the CNRS, the Ministère de l'Enseignement Supérieur et de la Recherche (PhD grant to C.D.) and L'Oréal are gratefully acknowledged.

**Keywords:** Magnetic nanoparticle • palladium nanoparticle • C-C cross coupling • oxidation • green chemistry

[1] a) M. Haruta, M. Date, *Appl. Catal. A General* **2001**, 222, 427-437; b) *Nanotechnology in Catalysis, Vol.1 and 2 (Nanostructure Science and Technology)*, (Eds.; B. Zhou, S. Hermans, G. A. Somorjai), **2003**; c) A. T. Bell, *Science* **2003**, 299, 1688-1691; d) D. Astruc, F. Lu, J.

- Ruiz, *Angew. Chem.* **2005**, *117*, 8062-8083; *Angew. Chem. Int. Ed.* **2005**, *44*, 7852-7872; e) A. Corma, H. Garcia, *Chem. Soc. Rev.* **2008**, *37*, 2096-2126; f) J.-M. Basset, R. Psaro, D. Roberto, R. Ugo, Ed. *Modern Surface Organometallic Chemistry*. Wiley-VCH, Weinheim, **2009**; g) A. Corma, H. García, F. X. Llabres i Xamena, *Chem. Rev.* **2010**, *110*, 4606-4655; h) L. M. Bronstein, Z. B. Shifrina, *Chem. Rev.* **2011**, *111*, 5301-5344; i) *Nanomaterials in Catalysis*; (Eds.: P. Serp, K. Philippot), Wiley-VCH, Weinheim, **2013**; j) M. Haruta, *Angew. Chem., Int. Ed.* **2014**, *53*, 52-56.
- [2] a) A.-H. Lu, E. L. Salabas, F. Schüth, *Angew. Chem., Int. Ed.* **2007**, *46*, 1222-1244; b) S. Roy, M. A. Pericas, *Org. Biomol. Chem.* **2009**, *7*, 2669-2677; c) S. Shylesh, V. Schünemann, W. R. Thiel, *Angew. Chem., Int. Ed.* **2010**, *49*, 3428-3459; c) Y. Zhu, L. P. Stubbs, F. Ho, R. Liu, C. P. Ship, J. A. Maguire, N. S. Hosmane, *ChemCatChem* **2010**, *2*, 365-374; d) C. W. Lim, I. S. Lee, *Nano Today* **2010**, *5*, 412-434; e) V. Polshettiwar, R. Luque, A. Fihri, H. Zhu, M. Bouhrara, J.-M. Basset, *Chem. Rev.* **2011**, *111*, 3036-3075; f) L. M. Rossi, A. S. Garcia, L. L. R. Vono, *J. Braz. Chem. Soc.* **2012**, *23*, 1959-1971; g) M. B. Gawande, P. S. Branco, R. S. Varma, *Chem. Soc. Rev.* **2013**, *42*, 3371-3393; h) D. Wang, D. Astruc, *Chem. Rev.* **2014**, DOI: 10.1021/cr500134h.
- [3] M. T. Reetz, W. Helbig, S. A. Quaiser, in *Active metals: preparation, characterizations, applications*, (Ed.: A. Fürstner), Wiley-VCH, Weinheim, **1996**, p. 279; b) H. Bönemann, R. Richards, *Eur. J. Inorg. Chem.* **2001**, *10*, 2455-2480; c) Yonezawa, T.; Toshima, N. *Polymer-Stabilized Metal Nanoparticles: Preparation, Characterization and Applications, in Advanced Functional Molecules and Polymers*; H. S. Nalwa, Ed.; OPA N.V., 2001, Vol. 2, Chap. 3, pp. 65-86; d) *Nanoparticles and Catalysis* (Ed.: D. Astruc) Wiley-VCH, Weinheim, **2008**.
- [4] a) E. Boisselier, A. K. Diallo, L. Salmon, C. Ornelas, J. Ruiz, D. Astruc, *J. Am. Chem. Soc.* **2010**, *132*, 2729-2742; b) C. Deraedt, L. Salmon, J. Ruiz, D. Astruc, *Chem. Commun.* **2013**, *49*, 8169-8171. c) C. Deraedt, D. Astruc, *Acc. Chem. Res.* **2014**, *47*, 494-503; d) V. Percec, C. Mitchell, W.-D. Cho, S. Uchida, M. Glodde, G. Ungar, X. Zeng, Y. Liu, V. S. K. Balagurusamy, *J. Am. Chem. Soc.* **2004**, *126*, 6078-6094.
- [5] a) N. Miyaura, A. Suzuki, *Chem. Rev.* **1995**, *95*, 2457-2483; b) I. P. Beletskaya, A. V. Cheprakov, A. V. *Chem. Rev.* **2000**, *100*, 3009-3066; c) R. M. Crooks, M. Zhao, L. Sun, V.

- Chechik, L. K. Yeung, *Acc. Chem. Res.* **2001**, *34*, 181-190; d) J. Hassan, M. Sévignon, C. Gozzi, E. Schulz, M. Lemaire, *Chem. Rev.* **2002**, *12*, 1359-1469; e) R. W. J. Scott, O. M. Wilson, R. M. Crooks, *Phys. Chem. B* **2005**, *109*, 692-704; f) J. G. de Vries, *Dalton Trans.* **2006**, 421-429 g) V. S. Myers, M. W. Weier, E. V. Carino, D. F. Yancey, S. Pande, R. M. Crooks, *Chem. Sci.* **2011**, *2*, 1632-1646; h) R. Chinchilla, C. Najera, *Chem. Soc. Rev.* **2011**, *40*, 5084-5121.
- [6] a) M. I. Fernandez, G. Tojo, *Oxidation of Alcohols to Aldehydes and Ketones: A Guide to Current Common Practice*, Springer, New York, **2006**; b) M. J. Schultz, M. S. Sigman, *Tetrahedron* **2006**, *62*, 8227-8241; c) N. Dimitratos, J. A. Lopez-Sanchez, G. J. Hutchings, *Chem. Sci.* **2012**, *3*, 20-44; d) Z. Shi, C. Zhang, C. Tang, N. Jiao, *Chem. Soc. Rev.* **2012**, *41*, 3381-3430; e) C. Parmeggiani, F. Cardona, *Green Chem.* **2012**, *14*, 547-564.
- [7] a) S. Shylesh, L. Wang, W. R. Thiel, *Adv. Synth. Catal.* **2010**, *352*, 425-432; b) Ultrasonication has proved to be an efficient method for impregnation of Pd ions on magnetic support: U. Laska, C. G. Frost, G. J. Price, P. K. Plucinski, *J. Catal.* **2009**, *268*, 318-328.
- [8] a) K. Yamaguchi, N. Mizumo, *Angew. Chem., Int. Ed.* **2002**, *41*, 4538-4542; b) A. Tashiro, A. Mitsuishi, R. Irie, T. Katsuki, *Synlett* **2003**, *12*, 1868-1870.
- [9] a) P. Wang, F. Zhang, Y. Long, M. Xie, R. Li, J. Ma, *Catal. Sci. Technol.* **2013**, *3*, 1618-1624; b) W. Tang, J. Li, X. Jin, J. Sun, J. Huang, R. Li, *Catal. Commun.* **2014**, *43*, 75-78; c) J. Sun, Z. Dong, X. Sun, P. Li, F. Zhang, Wuquan Hu, Haidong Yang, H. Wang, R. Li, *J. Mol. Catal. A: Chem.* **2013**, *367*, 46-51; d) M. Shokouhimehr, J. E. Lee, S. I. Han, T. Hyeon, *Chem. Commun.* **2013**, *49*, 4779-4781; e) J. Wang, B. Xu, H. Sun, G. Song, *Tetrahedron Lett.* **2013**, *54*, 238-241; Q. Zhang, H. Su, J. Luo, Y. Wei, *Catal. Sci. Technol.* **2013**, *3*, 235-243; f) A. S. Singh, U. B. Patil, J. M. Nagarkar, *Catal. Commun.* **2013**, *35*, 11-16; g) M. Shokouhimehr, T. Kim, S. W. Jun, K. Shin, Y. Jang, B. H. Kima, J. Kim, T. Hyeon, *App. Catal. A: General* **2014**, *476*, 133-139; h) B. Karimi, F. Mansouri, H. Vali, *Green Chem.* **2014**, *16*, 2587-2596.

**Chapter 5**  
**Mono- and Polymetallic Palladium Complexes Containing**  
**2-Pyridyl-1,2,3-triazole Ligand or Nonabranched-derived Ligands**

## 5.1 Introduction

After the publication of the concept of “click” chemistry by Sharpless, our group provided noteworthy contributions in the area. The first “click” metallodendrimers containing 1,2,3-triazoles were reported by Catia Ornelas et al from our group in 2007<sup>1</sup> together with the first uses in molecular recognition and sensing of anions and cations. In parallel, Abdou Diallo and Catia Ornelas, two former PhD students of our group, disclosed also in 2007 the first use of dendritic 1,2,3-triazoles in stabilizing extremely active Pd nanoparticles in catalysis of Suzuki-Miyaura reactions (“homeopathic” catalysis).<sup>2-5</sup>

In continuation of this line of research on “click” chemistry, we have designed “clicked” pyridyltriazol ligands for catalytic applications. The work of this chapter concerns the catalytic application of palladium complexes containing single or nona-branched 2-pyridyl-1,2,3-triazole ligands. The pyridyl-triazole ligand and its nona-branched analogue were prepared, then used for the complexation of Pd(OAc)<sub>2</sub>. In this way, a series of mono- and polymetallic pincer-type palladium complexes were obtained in which the triazole fragment does not act as a linker but also as one of the coordinating groups. Surprisingly, these polymetallic palladium complexes exhibited various solubilities with various loading amounts of Pd atoms, resulting in homogeneous or heterogeneous properties in organic solvents. The catalytic activity of these complexes was evaluated in carbon-carbon cross coupling reactions. This indicated that of Suzuki-Miyaura, Sonogashira, and Heck reactions involving aryl halides including activated aryl chlorides or acyl chloride proceeded smoothly in the presence of these catalysts. This work was done with the collaboration of Dr. Dominique Denux (thermogravimetric analysis) and Dr. Jaime Ruiz. (cyclic voltammetry measurement).

Recently, a review of 1,2,3-triazole-metal complexes in catalysis was authored in collaboration by the research group of Pengxiang Zhao, former student of our group.<sup>6</sup>

### References:

1. C. Ornelas, J. Ruiz, E. Cloutet, S. Alves, D. Astruc, *Angew. Chem. Int. Ed.* **2007**,

46, 872.

2. C. Ornelas, L. Salmon, J. Ruiz Aranzaes, D. Astruc, *Chem. Commun.* **2007**, 4946.
3. A. K. Diallo, C. Ornelas, L. Salmon, J. Ruiz, D. Astruc, *Angew. Chem. Int. Ed. Engl.* **2007**, *46*, 8644.
4. C. Ornelas, L. Salmon, J. Ruiz Aranzaes, D. Astruc, *Chem. Eur. J.* **2008**, *14*, 50.
5. C. Ornelas, J. Ruiz, L. Salmon, D. Astruc, *Adv. Syn. Catal.* **2008**, *350*, 837.
6. D. Huang, P. Zhao, D. Astruc, *Coord. Chem. Rev.* **2014**, *272*, 145.

# The Clicked Pyridyl-Triazole Ligand: From Homogeneous to Robust, Recyclable Heterogeneous Mono- and Polymetallic Palladium Catalysts for Efficient Suzuki–Miyaura, Sonogashira, and Heck Reactions

Dong Wang,<sup>a</sup> Dominique Denux,<sup>b</sup> Jaime Ruiz,<sup>a</sup> and Didier Astruc<sup>a,\*</sup>

<sup>a</sup> ISM, UMR CNRS N° 5255, Univ. Bordeaux, 351 Cours de la Libération, 33405 Talence Cedex, France  
Fax: (+33)-5-4000-6994; e-mail: d.astruc@ism.u-bordeaux1.fr

<sup>b</sup> ICMCB-CNRS, UPR9048, 87, Avenue du Docteur Schweitzer, 33608 Pessac Cedex, France

Received: July 13, 2012; Revised: October 12, 2012; Published online: January 4, 2013

Supporting information for this article is available on the WWW under <http://dx.doi.org/10.1002/adsc.201200619>.

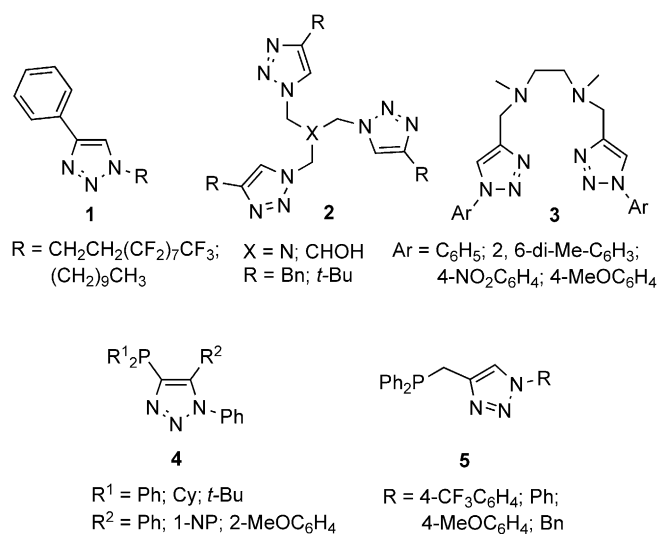
**Abstract:** Various mono- and polymetallic palladium complexes containing a 2-pyridyl-1,2,3-triazole (pyta) ligand or a nonbranch-derived (nonapyta) ligand have been synthesized by reaction of palladium acetate with these ligands according to a 1:1 metal-ligand stoichiometry and used as catalysts for carbon-carbon cross-coupling including the Suzuki–Miyaura, Sonogashira and Heck reactions. The unsubstituted monopalladium and nonapalladium complexes were insoluble in all the reaction media, whereas tri- and tetranuclear palladium complexes were soluble, which allowed conducting catalysis under either homogeneous or heterogeneous conditions. The organopalladium complexes were characterized by standard analytical and spectroscopic

methods and by thermogravimetry showing decomposition above 110 °C. Both types of catalysts showed excellent activity for these cross carbon-carbon bond formations involving aryl halides including activated aryl chlorides or acyl chloride. Besides the comparison between homogeneous and heterogeneous catalysis, the key feature of these catalysts is their remarkable robustness that allowed recycling at least ten times in the example of the Heck reaction with excellent yields and without significant reduction of the conversion.

**Keywords:** catalysis; click chemistry; cross C–C coupling; palladium; pyridine; recycling; triazoles

## Introduction

Click chemistry has proven to be a powerful concept allowing one to assemble molecular fragments under green conditions,<sup>[1]</sup> the Cu-catalyzed alkyne–azide (CuAAC) reaction being the most popular example with the regioselective formation of 1,4-disubstituted 1,2,3-triazoles.<sup>[2,3]</sup> This click CuAAC reaction is all the more useful as the 1,2,3-triazole heterocycle also is an excellent ligand,<sup>[4]</sup> which brings about potential applications of 1,2,3-triazole complexes. Such applications have already appeared in optics,<sup>[5]</sup> redox sensing<sup>[6]</sup> and catalysis.<sup>[7]</sup> In the latter area, the clicked 1,2,3-triazole ligand has proven useful for the mild stabilization of catalytically very efficient nanoparticles.<sup>[6]</sup> On the other hand, in molecular catalysis, examples using 1,2,3-triazole-derived ligands are scarce (Figure 1).<sup>[8–13]</sup> Zhu and Yi<sup>[8]</sup> synthesized two efficient triazole ligands **1** for the palladium-catalyzed Suzuki–Miyaura and



**Figure 1.** 1,2,3-triazolyl ligands used in molecular catalysis (see text).<sup>[8–13]</sup>

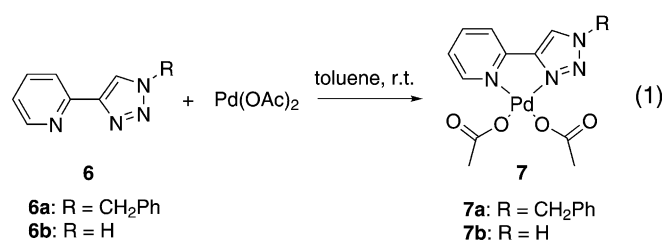
Heck reactions. Fokin<sup>[4c,9]</sup> and Pericàs<sup>[10]</sup> designed polytriazoles **2** that were powerful stabilizing ligands for “click” reactions. A series of triazole-based N<sub>4</sub> tetradenate ligands **3** was synthesized by Hao and Wang,<sup>[11]</sup> and Mn(II) complexes containing these ligands showed efficient catalytic activities in the epoxidation of various aliphatic terminal olefins with peracetic acid. Phosphino-1,2,3-triazoles **4**<sup>[12]</sup> and phosphinomethylene-1,2,3-triazoles **5**<sup>[13]</sup> have been used by Zhang and Reek’s research groups, respectively, as remarkable ligands for Suzuki–Miyaura, amination, and allylic alkylation reactions. The 2-pyridyl-1,2,3-triazole (pyta) complexes that compare to 2,2′-bipyridine have already provided luminescent properties,<sup>[5]</sup> but catalytic functions have so far been overlooked.

Here we report that the easily prepared pyta ligand and a new, nona-branch analogue nonapyta coordinate in 1:1 stoichiometry to Pd(OAc)<sub>2</sub>, and that the monomeric and three nonapyta Pd complexes corresponding to the progressive loading of the nonapyta ligand with Pd(II) provided efficient catalysts for cross carbon-carbon coupling reactions. Examples of the Suzuki–Miyaura,<sup>[14]</sup> Sonogashira<sup>[15]</sup> and Heck<sup>[16]</sup> reactions illustrate these catalytic applications. Moreover, the great robustness and various solubilities of the pyta- and nonapyta-Pd catalysts allowed conducting both homogeneous and heterogeneous reactions with recyclability of the heterogeneous catalysts. Indeed, efficient catalysts are well known for these Pd-catalyzed cross-coupling reactions,<sup>[14–16]</sup> but the interest for the pyta-Pd and nonapyta-Pd complexes resides in their robustness and recyclability and on the comparison among the catalysts of various nuclearities and solubilities.<sup>[17,18]</sup>

## Results and Discussion

### Synthesis of the Monometallic Palladium 2-Pyridyl-1,2,3-triazoles (Pd-pyta) Complexes

Reactions between the known 2-pyridyl-1,2,3-triazoles (pyta) **6a** and **6b** and palladium acetate, conducted in toluene under ambient conditions, lead to the 1:1 ligand-metal complexes **7a** and **7b**, respectively [Eq. (1)]. The five-membered chelate ring structures were

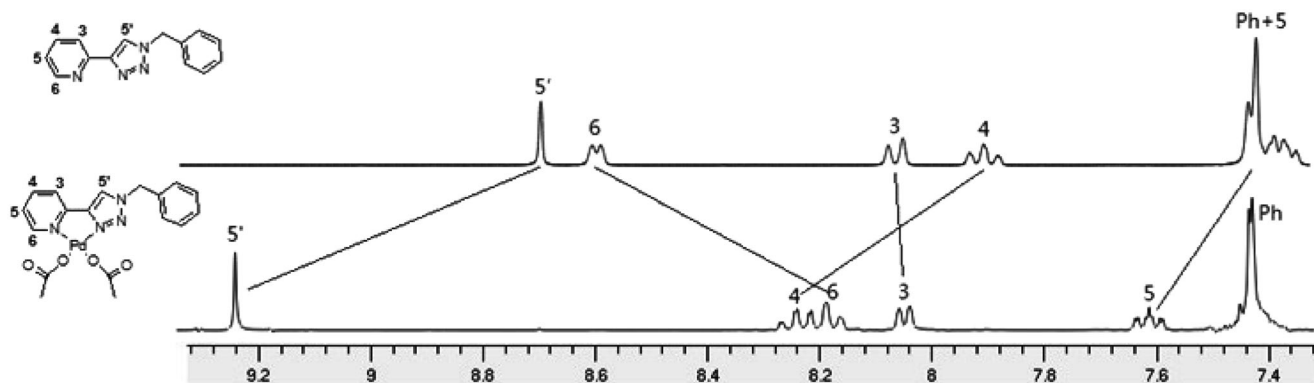


synthesis of monomeric palladium complexes **7**

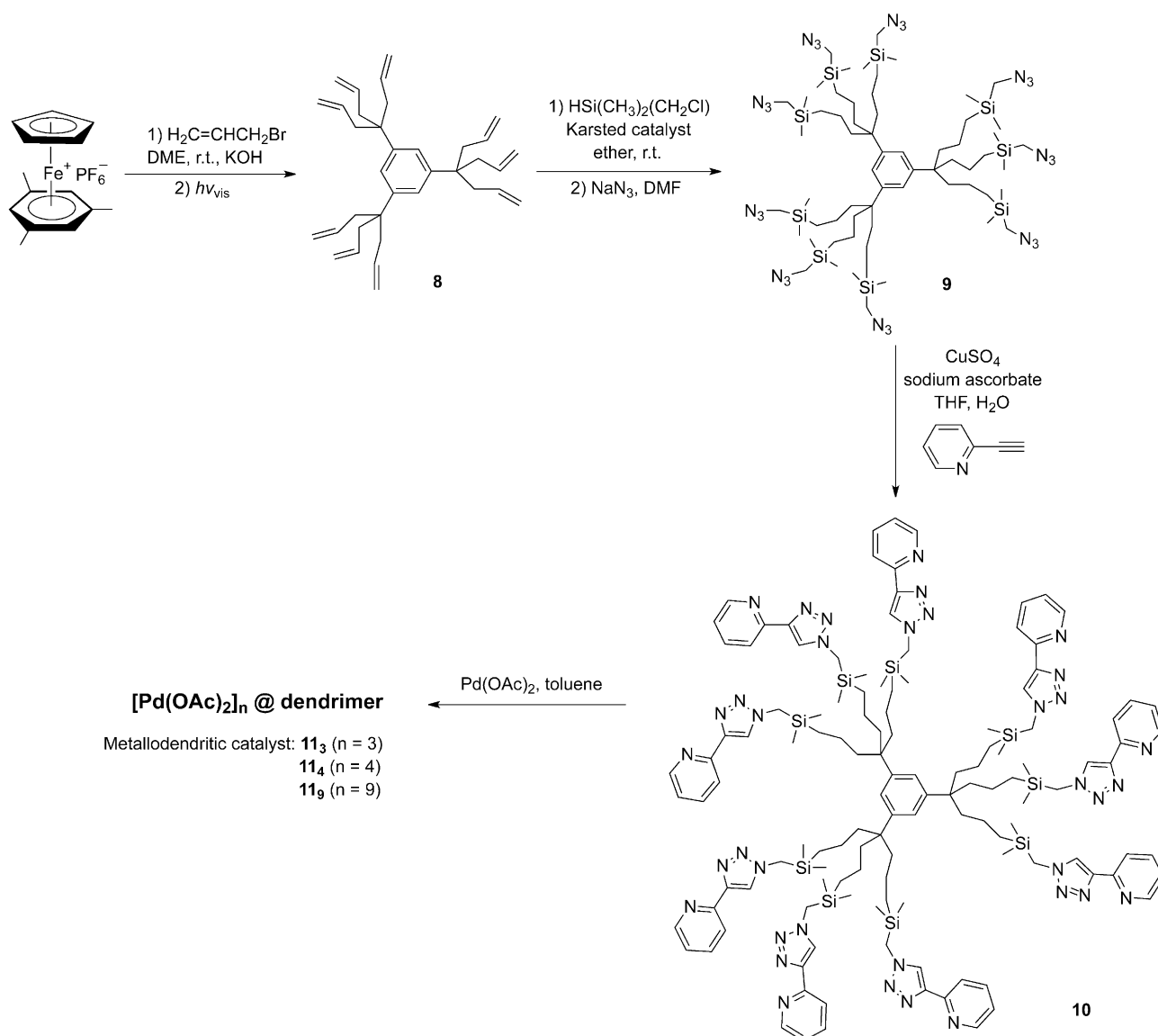
confirmed by the NMR spectra of **7a** and **7b** in which the ratio of pyta and palladium ion was 1 to 1, and by elemental analysis. The proton signals of both pyridine and 1,2,3-triazole were shifted, which indicated that both of them were coordinated to the palladium ion (Figure 2). The solubility of the palladium complex **7b**, unlike that of **7a**, was very low, which was a message indicating that **7b** has the potential of being a heterogeneous catalyst.

### Synthesis of the Polymetallic Palladium-Nonapyta Complexes

A new nona-branched ligand **10** was prepared, involving three tripods that resulted from the known CpFe<sup>+</sup>-induced nona-allylation of mesitylene in [FeCp(η<sup>6</sup>-mesitylene)][PF<sub>6</sub>] followed by visible-light-induced decomplexation, hydrosilylation of **8** and re-



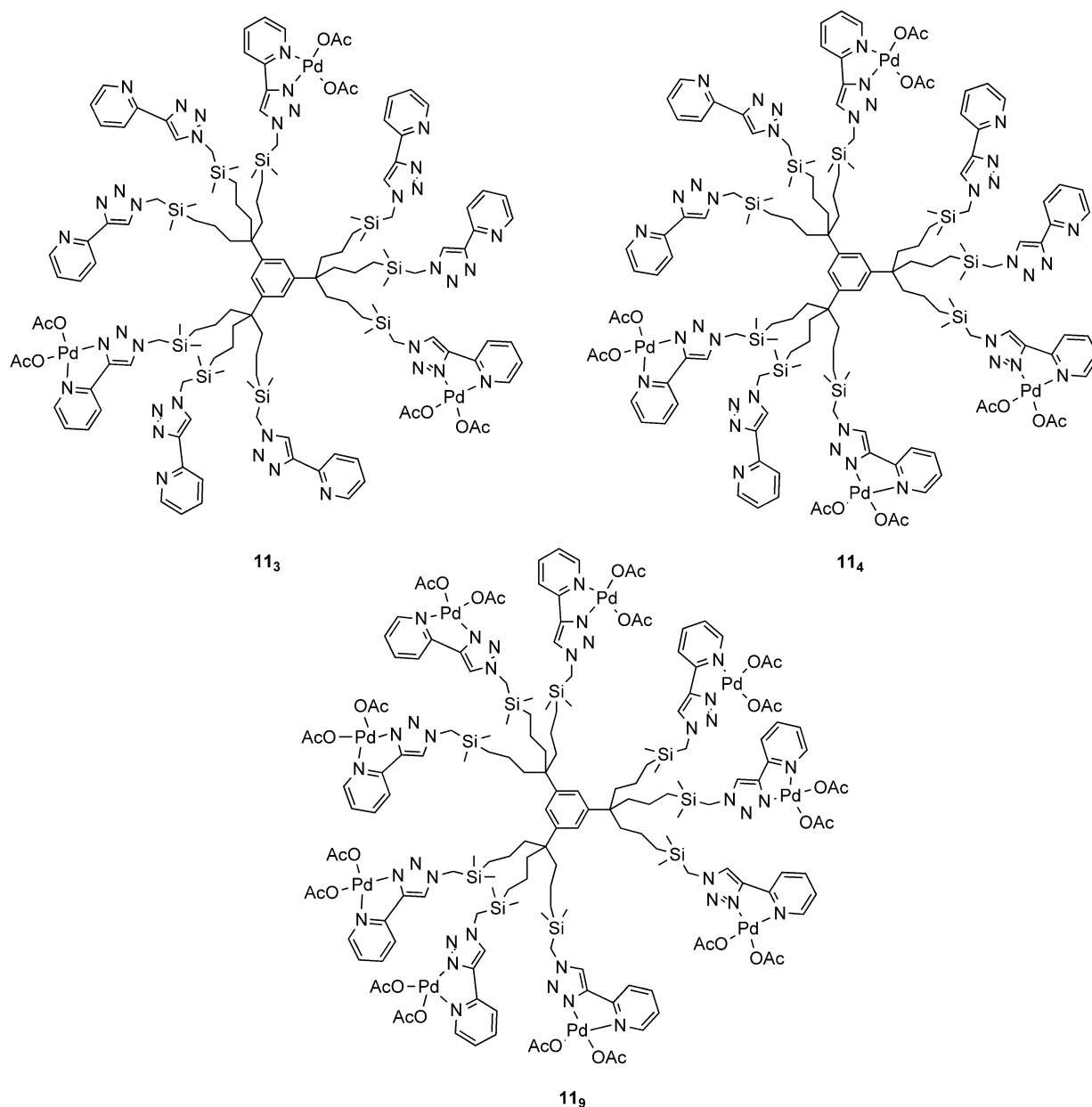
**Figure 2.** Magnified <sup>1</sup>H NMR spectra of **6a** (top) and **7a** (bottom).



**Scheme 1.** Synthesis of the nona-branched ligand **10** and metallodendritic catalysts **11**.

action with  $\text{NaN}_3$  yielding **9**<sup>[6]</sup> (Scheme 1). Click CuAAC reactions in toluene between **9** and ethynylpyridine provided **10**. Reactions of **10** with  $\text{Pd}(\text{OAc})_2$  under ambient conditions yielded various polymetallic palladium complexes **11<sub>x</sub>** depending on the reaction time. After 2 to 5 min of reaction, only the soluble trimetallic complex **11<sub>3</sub>** was formed, then the tetrametallic complex **11<sub>4</sub>**, somewhat less soluble, was synthesized after 20 to 30 min of reaction. Finally, the synthesis of the insoluble nonametallated complex **11<sub>9</sub>**, required one to two days for completion under the same reaction conditions (Figure 3). All the attempts to form a monometallic or bimetallic complex by lowering the reaction time, the temperature or the amount of  $\text{Pd}(\text{OAc})_2$  resulted in the formation of mixtures of **11<sub>3</sub>** together with unreacted ligand **10**, indicating that the second and third metallations were faster

than the first one. This and the fact that the fourth metallation step is slower than the three first ones strongly argues in favor of a fast monometallation of each of the three tripods and slower second metallation of each tripod. The solubilities of the complexes also drop after the third metallation, thus the synergistic steric and solubility effects provide a rationalization for the fact that the second metallation of the tripods is slower than the monometallation, and the lack of steric effect among the three tripods and the good solubility of **11<sub>3</sub>** explain why the three tripods of **10** are rapidly monometallated at comparable rates. The structures of the complexes **11<sub>3</sub>** and **11<sub>4</sub>** were shown by  $^1\text{H}$  NMR upon comparison of the relative intensities of the methyl peaks of the core  $\text{SiMe}_2$  and  $\text{Pd}-\text{OAc}$  groups, respectively, and the structures of the three polymetallic complexes were confirmed by



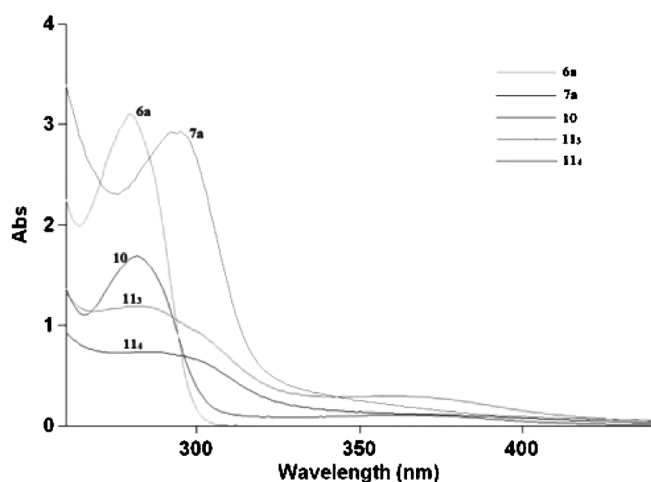
**Figure 3.** Metallo-dendritic catalysts **11<sub>3</sub>**, **11<sub>4</sub>**, and **11<sub>9</sub>**.

elemental analysis. Given the remarkable robustness of the Pd-*tpya* and Pd-*nonatypa* bonds at high temperatures, the catalytic activities of **7a**, **7b**, **11<sub>3</sub>**, **11<sub>4</sub>** and **11<sub>9</sub>**, were then evaluated for the Suzuki–Miyaura, Sonogashira, and Heck reactions.

#### UV-Vis Spectroscopy of the Ligands and Palladium Complexes

Figure 4 shows the UV-vis spectra of the ligands **6a** and **10** and palladium complexes **7a**, **11<sub>3</sub>**, **11<sub>4</sub>**. Before

the metallation reactions, the ligands **6a** and **10** showed a distinct  $\pi$ - $\pi^*$  transition around 280 nm. After coordination, a slight red shift from 280 to 293 nm was observed from the spectra of the mono-palladium complexes **6a** and **7a**, which was probably assigned to the ligand-to-metal charge-transfer transition (LMCT).<sup>[19]</sup> Similar results were obtained for the complexes of the nonaligand, the UV bands of the **11<sub>3</sub>** and **11<sub>4</sub>** are located at 286 and 287 nm through red shifts, respectively. The corresponding  $\lambda$ , A, and  $\epsilon$  values are listed in Table 1.



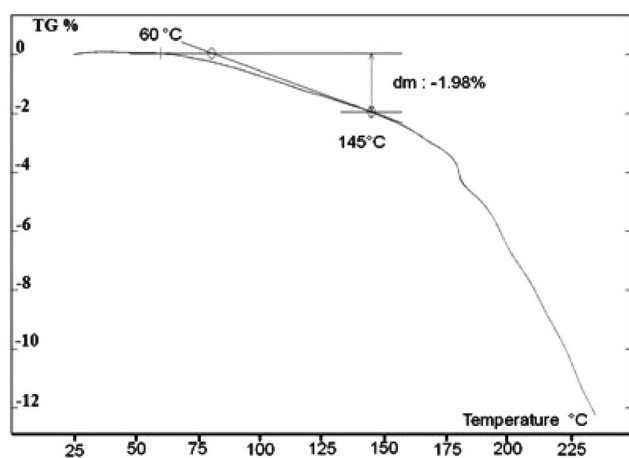
**Figure 4.** UV-vis spectra of the ligands and palladium complexes.

**Table 1.** UV-vis characteristics of the ligands and palladium complexes.

Compound	C [molL <sup>-1</sup> ]	λ [nm]	A	ε [M <sup>-1</sup> cm <sup>-1</sup> ]
<b>6a</b>	3.3 × 10 <sup>-4</sup>	280	3.103	9.31 × 10 <sup>3</sup>
<b>7a</b>	3.3 × 10 <sup>-4</sup>	293	2.934	8.80 × 10 <sup>3</sup>
<b>10</b>	1.3 × 10 <sup>-5</sup>	281	1.688	1.27 × 10 <sup>5</sup>
<b>11<sub>3</sub></b>	1.3 × 10 <sup>-5</sup>	286	1.188	0.89 × 10 <sup>5</sup>
<b>11<sub>4</sub></b>	1.3 × 10 <sup>-5</sup>	287	0.775	0.58 × 10 <sup>5</sup>

### Thermogravimetric Analysis of the Palladium Complexes **7b** and **11<sub>3</sub>**

In order to determine the thermal stability of the mono- and nona-Pd complexes, thermogravimetric analysis

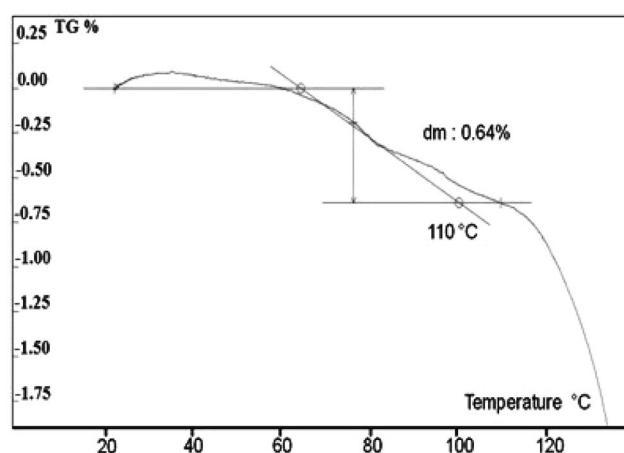


sis (Figure 5) coupled with mass spectrometry (see the Supporting Information) has been carried out for both samples under Ar. For the mono-Pd complex **7b**, a first weight loss corresponding successively to residual water and then solvent is observed. The slope change for the fragment group of organic compounds formed from decomposition starts at 130°C and are clearly visible without ambiguity after 145°C (for coupling with mass spectrometry, see the Supporting Information).

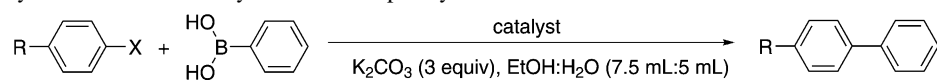
The nona-Pd complex **11<sub>3</sub>**, shows a slight weight loss up to 110°C that corresponds to traces of residual water, and decomposition begins above this temperature.

### Catalysis of the Suzuki–Miyaura Cross-Coupling Reactions

The Suzuki–Miyaura reactions were carried out homogeneously in H<sub>2</sub>O/EtOH with the palladium complexes **11<sub>3</sub>**, **11<sub>4</sub>**, and heterogeneously with the insoluble palladium complexes **7b**, **11<sub>3</sub>**, as catalysts. K<sub>2</sub>CO<sub>3</sub> (3 equiv.) was used as base in all the reactions (Table 2). We tested the influence of the EtOH/H<sub>2</sub>O volume ratios for Suzuki–Miyaura reactions conducted at 50°C. Using the catalyst **7b**, the yields of cross carbon-carbon coupling products were 82% and 88% with EtOH/H<sub>2</sub>O ratios of 1:1 and 3:2, respectively (Table 3, entries 2 and 3), showing the slight yield increase upon increasing the EtOH content in this solvent mixture. The heterogeneous catalysts **7b** and **11<sub>3</sub>**, also provided excellent yields that compared to those of the homogeneous catalysts **11<sub>3</sub>** and **11<sub>4</sub>**. The aryl chloride *p*-NO<sub>2</sub>-C<sub>6</sub>H<sub>4</sub>Cl also provided the cross-coupling product in good yield upon reaction with PhB(OH)<sub>2</sub> using the heterogeneous catalyst **7b** (entry 13).



**Figure 5.** Thermogravimetric analysis of **7b** (left) and **11<sub>3</sub>** (right).

**Table 2.** Suzuki–Miyaura reactions of aryl halide with phenylboronic acid.<sup>[a]</sup>


Entry	X	R	Catalyst (mol%)	Temp. [°C]	Time [h]	C [%] <sup>[b]</sup>	TON
1	I	CH <sub>3</sub> O	<b>7b</b> (0.5)	r.t.	48	77	154
2	I	CH <sub>3</sub> O	<b>7b</b> (0.5)	50	48	82 <sup>[c]</sup>	164
3	I	CH <sub>3</sub> O	<b>7b</b> (0.5)	50	48	88	176
4	I	CH <sub>3</sub> O	<b>11<sub>3</sub></b> (0.5)	50	48	96	192
5	I	CH <sub>3</sub> O	<b>11<sub>4</sub></b> (0.5)	50	48	91	182
6	I	CH <sub>3</sub> O	<b>11<sub>9</sub></b> (0.5)	50	48	85	170
7	Br	CH <sub>3</sub> O	<b>7b</b> (0.5)	80	48	91	182
8	Br	CH <sub>3</sub> O	<b>7b</b> (0.5)	50	96	96	192
9	Br	CH <sub>3</sub> O	<b>11<sub>3</sub></b> (0.5)	50	48	93	186
10	Br	CH <sub>3</sub> O	<b>11<sub>3</sub></b> (0.5)	80	48	97	194
11	Br	CH <sub>3</sub> O	<b>11<sub>4</sub></b> (0.5)	50	48	91	182
12	Br	CH <sub>3</sub> O	<b>11<sub>9</sub></b> (0.5)	50	48	88	176
13	Cl	NO <sub>2</sub>	<b>7b</b> (2)	120	120	74	37
14	Cl	NO <sub>2</sub>	<b>11<sub>9</sub></b> (2)	120	120	57	29

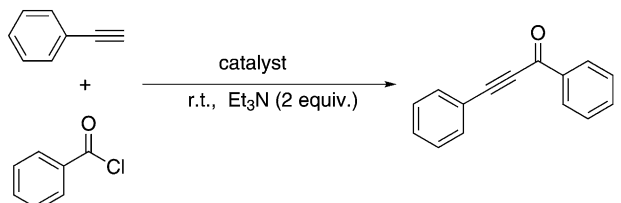
<sup>[a]</sup> Reaction conditions: aryl halide (0.5 mmol), phenylboronic acid (0.75 mmol), K<sub>2</sub>CO<sub>3</sub> (1.5 mmol, 207 mg), EtOH (7.5 mL), H<sub>2</sub>O (5 mL).

<sup>[b]</sup> C: conversion (yield of isolated product).

<sup>[c]</sup> Solvent: EtOH (5 mL) and H<sub>2</sub>O (5 mL).

### Catalysis of the Sonogashira Reactions

The complexes **7b**, **11<sub>3</sub>**, **11<sub>4</sub>**, **11<sub>9</sub>** catalyze the cross-coupling reaction between benzoyl chloride and phenylacetylene in a simple one-pot procedure without cocatalyst and at low catalyst concentrations (Table 3). All the reactions were carried out using two equiv. triethylamine as both the base and solvent at room

**Table 3.** Sonogashira coupling of benzoyl chloride with phenylacetylene.<sup>[a]</sup>


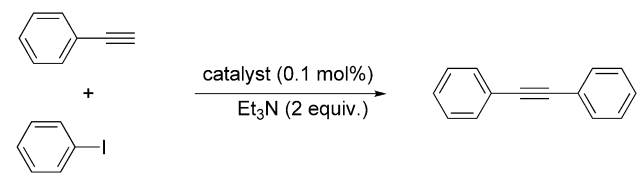
Entry	Catalyst (mol%)	Time [h]	C [%] <sup>[b]</sup>	TON
1	<b>7a</b> (0.1)	48	90	900
2	<b>7b</b> (0.01)	48	44	4400
3	<b>7b</b> (0.05)	48	76	1620
4	<b>7b</b> (0.1)	24	86	860
5	<b>11<sub>3</sub></b> (0.1)	12	95	950
6	<b>11<sub>4</sub></b> (0.1)	12	93	930
7	<b>11<sub>9</sub></b> (0.1)	24	87	870
8	<b>11<sub>9</sub></b> (0.1)	48	89	890

<sup>[a]</sup> Reaction conditions: benzoyl chloride (1.2 mmol), phenylacetylene (1 mmol), Et<sub>3</sub>N (2 mmol).

<sup>[b]</sup> C: conversion (yield of isolated product).

temperature. The reaction proceeded well with all these catalysts. The catalyst **11<sub>3</sub>** was soluble in Et<sub>3</sub>N and showed better catalytic activities than the insoluble catalysts **7b** and **11<sub>9</sub>**. The catalyst **11<sub>4</sub>** was partly soluble and also provided a good result. A significant drop in the yield was detected upon lowering the catalyst content (entries 2–4).

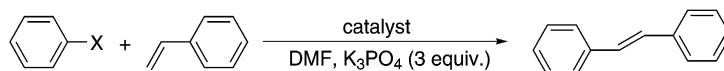
Iodobenzene was also used as a substrate for Sonogashira reactions with phenylacetylene. When the reaction was carried out at room temperature, a low yield was obtained, and increasing the reaction temperature to 50 °C improved the yield (Table 4, en-

**Table 4.** Sonogashira coupling of iodobenzene with phenylacetylene.<sup>[a]</sup>


Entry	Catalyst	Temp. [°C]	Time [h]	C [%] <sup>[b]</sup>	TON
1	<b>7b</b>	r.t.	48	58	580
2	<b>7b</b>	50	24	83	830
3	<b>11<sub>3</sub></b>	50	24	88	880
4	<b>11<sub>4</sub></b>	50	24	86	860
5	<b>11<sub>9</sub></b>	50	24	83	830
6	<b>11<sub>9</sub></b>	50	48	87	870

<sup>[a]</sup> Reaction conditions: iodobenzene (1.2 mmol), phenylacetylene (1 mmol), Et<sub>3</sub>N (2 mmol).

<sup>[b]</sup> C: conversion (yield of isolated product).

**Table 5.** Mizoroki–Heck reaction of aryl halide substrates with styrene.<sup>[a]</sup>

Entry	X	Catalyst (mol%)	Temp. [°C]	Time	Conversion [%] <sup>[b]</sup>	TON
1	I	<b>7b</b> (2)	100	24 h	79	40
2	I	<b>7b</b> (2)	100	48 h	86	43
3	I	<b>7b</b> (5)	100	48 h	96	19
4	I	<b>11<sub>3</sub></b> (2)	100	48 h	93	47
5	I	<b>11<sub>4</sub></b> (2)	100	48 h	92	46
6	I	<b>11<sub>9</sub></b> (5)	100	48 h	94	19
7	Br	<b>7b</b> (5)	120	7 d	64	13
8	Br	<b>11<sub>9</sub></b> (5)	120	7 d	55	11

<sup>[a]</sup> Reaction conditions: aryl halide (0.5 mmol), styrene (1 mmol), K<sub>3</sub>PO<sub>4</sub> (1.5 mmol, 318 mg), DMF (2 mL).

<sup>[b]</sup> Yield of isolated product.

tries 1 and 2). Homogeneous catalysis with **11<sub>3</sub>** smoothly catalyzed the reaction with somewhat better yield than under heterogeneous conditions with **7b** and **11<sub>9</sub>**. The yield gap was not as large as in the reaction with benzoyl chloride, however, possibly due to partial solubilization of these heterogeneous catalysts at high temperature. In addition, in general, benzoyl chloride showed higher reactivity than iodobenzene.

### Catalysis of the Heck Reaction

Mizoroki–Heck coupling reactions between halogenobenzenes and styrene using these palladium complexes were successful (Table 5). Both types, heterogeneous (**7b**, **11<sub>9</sub>**) and homogeneous catalysts (**11<sub>3</sub>**, **11<sub>4</sub>**), catalyzed the reaction between iodobenzene and styrene in 92–96% yields. Meanwhile, either 2 mol% of homogeneous catalyst (**11<sub>3</sub>** or **11<sub>4</sub>**) or 5 mol% of heterogeneous catalyst (**7b** or **11<sub>9</sub>**) provided excellent yields. The reaction between stilbene and the less reactive bromobenzene gave a moderate yield, a longer reaction time and higher temperature than with iodobenzene being required.

Taking the Heck reaction as example, the recovery and reuse of the heterogeneous catalysts **7b** and **11<sub>9</sub>** were investigated. They could be recharged with iodobenzene and styrene at least ten times without significant loss of their catalytic activity (Table 6), which showed the interest (easy catalyst recovery, high turnover numbers) of these heterogeneous catalysts.

### Comparison of the Catalytic Activities with Literature Examples

We compared the catalytic activity of our catalyst **7b** with literature examples that were published in 2011 or 2012. The reaction conditions and TON numbers

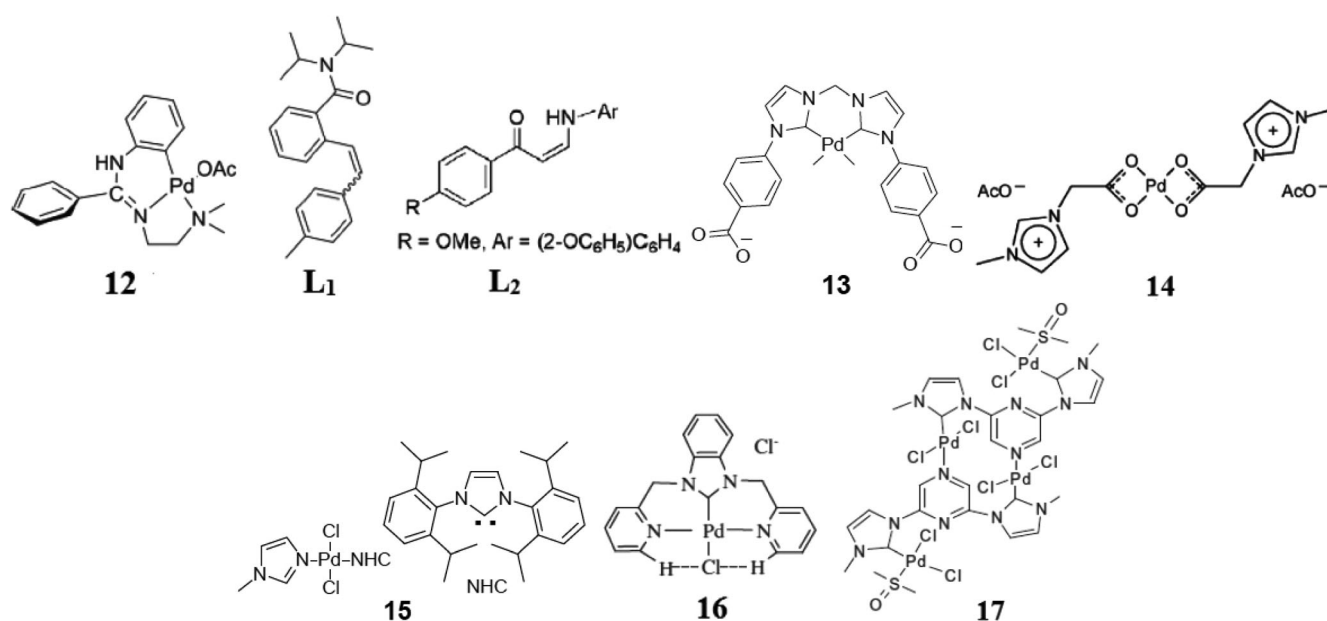
**Table 6.** Recharging of the dendritic catalysts **7b** and **11<sub>9</sub>** for the Heck reactions of iodobenzene with styrene.

Recharging run <sup>[a]</sup>	1	2	3	4	5	6	7	8	9	10
Catalyst <b>7b</b> [conversion (%)] <sup>[b]</sup>	96	93	93	92	92	93	91	91	91	91
Catalyst <b>11<sub>9</sub></b> [conversion (%)] <sup>[b]</sup>	94	93	91	91	92	91	89	87	84	78

<sup>[a]</sup> Recharging the catalysts for the reactions of entry 3 and 6 in Table 5.

<sup>[b]</sup> Yield of isolated product.

are listed in Table 6 (Figure 6), Table 7 (Figure 7) and Table 8 (Figure 8), which correspond to Suzuki–Miyaura, Sonogashira, and Heck reactions, respectively. From Table 7, it appears that **7b** showed good catalytic activity for the Suzuki reaction, but comparing with the others, the advantage is not remarkable, even some catalytic systems are much better than ours. It is worth noting, however, that heterogeneous **7b** has the potential of recharge. Among the copper-free systems for Sonogashira reactions, the ones containing phosphine or ionic liquid exhibited more significant activities. The TON of **7b** is larger than those of most phosphine- or ionic liquid-containing catalysts, which means that **7b** is an outstanding catalyst for Sonogashira reactions. Although **7b** does not show a very good activity for the Heck reaction (Table 9), the high-temperature stable and heterogeneous properties render it rechargeable for ten times without significant loss of catalytic activity. The possibility of conversion between homogeneous and heterogeneous catalysts upon change of substituent and palladium nuclearity and the property of recharge make this catalyst family containing the pyridyl-triazole ligand original and useful.

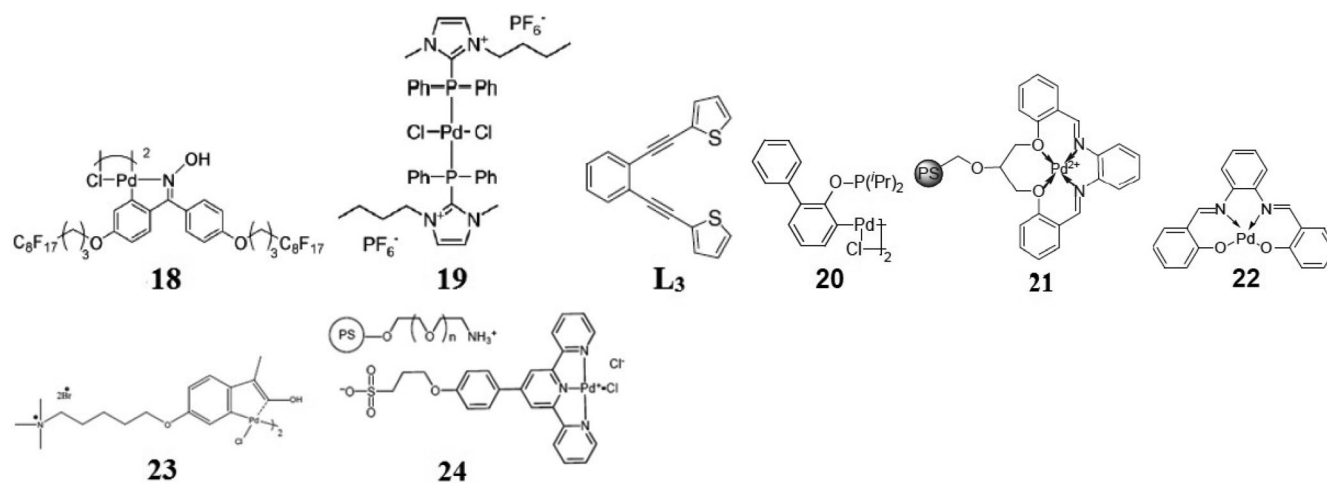


**Figure 6.** Catalysts and ligands from the literature for the Suzuki–Miyaura reaction.

**Table 7.** Comparison of catalytic activities with literature examples (Figure 6) for the Suzuki reaction between 4-methoxyhalobenzene and phenylboronic acid.

Entry	X	Catalyst (and ligand) (mol%)	Solvent	Base	Other additive	Time and temperature	Yield [%]	TON
1	Br	<b>7b</b> (0.5)	EtOH/H <sub>2</sub> O	K <sub>2</sub> CO <sub>3</sub>	no	48 h, 50 °C	91	182
2	Cl	<b>7b</b> (0.5)	EtOH/H <sub>2</sub> O	K <sub>2</sub> CO <sub>3</sub>	no	120 h, 120 °C	74	37
3 <sup>[20]</sup>	Br	<b>12</b> (1)	toluene	K <sub>3</sub> PO <sub>4</sub>	no	2 h, 100 °C	70	70
4 <sup>[21]</sup>	Br	Pd(OAc) <sub>2</sub> (2)/ <b>L1</b> (4)	dioxane	Cs <sub>2</sub> CO <sub>3</sub>	no	3 h, 80 °C	77	39
5 <sup>[22]</sup>	Br	PdCl <sub>2</sub> (1)/ <b>L2</b> (1)	EtOH/H <sub>2</sub> O	K <sub>2</sub> CO <sub>3</sub>	no	6 h, 60 °C	96	96
6 <sup>[23]</sup>	Br	<b>13</b> (0.1)	H <sub>2</sub> O	K <sub>2</sub> CO <sub>3</sub>	TBAB	2 h, 100 °C	96	960
7 <sup>[24]</sup>	Br	<b>14</b> (1)	MeOH	K <sub>3</sub> PO <sub>4</sub>	no	4 h, 130 °C	100	100
8 <sup>[25]</sup>	Cl	<b>15</b> (1)	THF/H <sub>2</sub> O	K <sub>3</sub> PO <sub>4</sub> ·3 H <sub>2</sub> O	no	24 h, r.t.	95	95
9 <sup>[26]</sup>	Br	<b>16</b> (0.2)	DMF/H <sub>2</sub> O	KOH	no	24 h, 60 °C	89	445
10 <sup>[27]</sup>	Br	[PdL <sub>3</sub> Cl] <sup>+</sup> PF <sub>6</sub> <sup>-</sup> (1) <sup>[a]</sup>	DMF/PhMe	Cs <sub>2</sub> CO <sub>3</sub>	no	10 h, 110 °C	54	54
11 <sup>[28]</sup>	Br	<b>17</b> (0.5)	DMSO	Cs <sub>2</sub> CO <sub>3</sub>	no	18 h, 85 °C	88	176

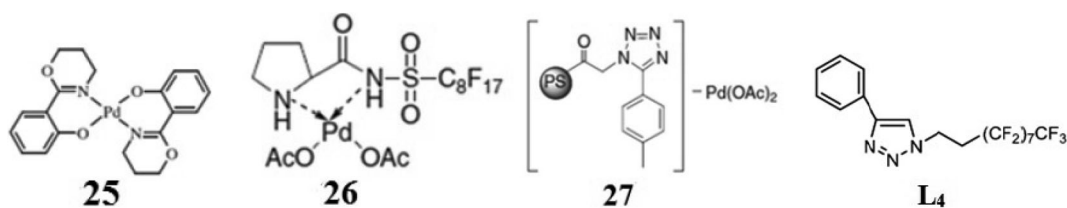
<sup>a</sup> L = P(*p*-Tol)<sub>3</sub>.



**Figure 7.** Catalysts and ligands from literature for the Sonogashira reaction.

**Table 8.** Comparison of catalytic activities with literature examples (Figure 7) for the Sonogashira reaction between iodobenzene and phenylacetylene.

Entry	Catalyst (and ligand) (mol%)	Base	Solvent	Other additive	Time and temperature	Yield [%]	TON
1	<b>7b</b> (0.1)	Et <sub>3</sub> N	Et <sub>3</sub> N	no	24 h, 50 °C	83	830
2 <sup>[29]</sup>	<b>18</b> (0.1)	K <sub>2</sub> CO <sub>3</sub>	H <sub>2</sub> O	TBAB	2.5 h, 100 °C	82	820
3 <sup>[30]</sup>	<b>19</b> (2)	Et <sub>3</sub> N	[Bmim]PF <sub>6</sub>	no	2 h, 80 °C	100	50
4 <sup>[31]</sup>	[PdCl <sub>2</sub> (PPh <sub>3</sub> ) <sub>2</sub> ] (2)/ <b>L</b> <sub>3</sub> (2)	Et <sub>3</sub> N	CH <sub>3</sub> CN	no	17 h, > 81 °C	84	42
5 <sup>[32]</sup>	<b>20</b> (0.1)	Et <sub>3</sub> N	H <sub>2</sub> O	no	6 h, 40 °C	93	930
6 <sup>[33]</sup>	PdEnCat <sup>TM</sup> 30 (0.4)	KOH	EtOH	no	24 h, 70 °C	84	210
7 <sup>[34]</sup>	<b>21</b> (0.5)	Piperidine	H <sub>2</sub> O	no	0.5 h, 100 °C	87	174
8 <sup>[35]</sup>	<b>22</b> (0.3)	Et <sub>3</sub> N	Et <sub>3</sub> N	no	5 h, r.t.	97	323
10 <sup>[36]</sup>	<b>23</b> (0.047)	Et <sub>3</sub> N	[TMBA]NTf <sub>2</sub>	no	12 h, 80 °C	92	1957
11 <sup>[37]</sup>	<b>24</b> (5)	Et <sub>3</sub> N	H <sub>2</sub> O	no	12 h, 60 °C	78	16

**Figure 8.** Catalysts and ligands from the literature for the Heck reaction.**Table 9.** Comparison of catalytic activities with literature examples (Figure 8) for the Heck reaction between iodobenzene and styrene.

Entry	Catalyst (mol%)	Base	Solvent	Other additive	Time and temperature	Yield [%]	TON
1	<b>7b</b> (2)	K <sub>3</sub> PO <sub>4</sub>	DMF	no	48 h, 100 °C	86	43
2 <sup>[24]</sup>	<b>14</b> (1)	K <sub>2</sub> CO <sub>3</sub>	MeOH	no	24 h, 110 °C	100	100
3 <sup>[38]</sup>	<b>21</b> (0.5)	K <sub>2</sub> CO <sub>3</sub>	DMF	no	2 h, 100 °C	88	176
4 <sup>[37]</sup>	<b>24</b> (5)	DBU	H <sub>2</sub> O	no	6 h, 100 °C	90	18
5 <sup>[39]</sup>	<b>25</b> (0.4)	K <sub>2</sub> CO <sub>3</sub>	DMAc	no	8 h, 120 °C	73	182
6 <sup>[40]</sup>	<b>26</b> (0.1)	K <sub>2</sub> CO <sub>3</sub>	H <sub>2</sub> O	TBAB	6 h, 100 °C	69	690
7 <sup>[41]</sup>	<b>27</b> (1)	K <sub>2</sub> CO <sub>3</sub>	DMF	no	1 h, 125 °C	87	87
8 <sup>[8]</sup>	Pd(OAc) <sub>2</sub> (1)/ <b>L</b> <sub>4</sub> (4)	K <sub>2</sub> CO <sub>3</sub>	DMF	no	12 h, 100 °C	77	77
9 <sup>[42]</sup>	Pd(L-proline) <sub>2</sub> (2)	NaOAc	H <sub>2</sub> O	TBAB	MW (200–300 W), 80 °C, 10 min	94	47
10 <sup>[43]</sup>	PdCl <sub>2</sub> (1)	K <sub>2</sub> CO <sub>3</sub>	PEG-400	no	12 min, 120 °C (10 W of MW)	74	74
11 <sup>[44]</sup>	Pd(OAc) <sub>2</sub> (5)	K <sub>2</sub> CO <sub>3</sub>	H <sub>2</sub> O	PEG-200	20 min, 80 °C (ultrasound irradiation)	75	15

## Conclusions

A new family of palladium complexes is shown to be excellent as homogeneous or heterogeneous catalysts for the Suzuki–Miyaura, Sonogashira and Heck reactions of haloarenes. This family includes two monometallic 2-pyridyl-1,2,3-triazole (pyta) complexes, **7a**, that is soluble, and **7b** that is almost insoluble in most solvents, and three polymetallic nonapyta complexes, the soluble trimetallic complex **11<sub>3</sub>**, the less soluble tetrametallic complex **11<sub>4</sub>** and the completely insoluble nonametallated complex **11<sub>9</sub>**. Thus, the synthesis of the new nonbranched nonapyta ligand allowed us to delineate a strategy of progressive insolubilization of the catalysts upon progressive loading with Pd(OAc)<sub>2</sub>

whereby the two OAc ligands change their coordination type from chelate to monodentate, forming extremely robust, yet catalytically efficient nonapyta complexes.

The independence of the three tripods of the nonaligand **10** induces large complexation rates that are similar among the three tripods, with a complexation rate that even increases from the first to the third metallation. It is obviously the bulk introduced by the second metallation of each tripod that provokes the progressive insolubilization of the complexes containing more than three Pd(OAc)<sub>2</sub> units, before further metallation very slowly proceed heterogeneously up to the nonametallation. Altogether, this family of catalysts comprises mono- and polymetallic catalysts

containing almost identical catalytic sites and share the property of robustness.

The monomeric complex **7b** and the nonmetallic complex **11**, are efficient heterogeneous catalysts that can be recharged at least ten times without significant loss of their catalytic activity, taking the Heck reaction as example. Thus although these catalysts are not as efficient with chloroarenes as some specific alkylphosphine-containing catalysts such as the closely related 2-phosphino-1,2,3-triazolyl and 2-phosphinomethyl-1,2,3-triazolyl palladium catalysts that have not been recycled, they are extremely robust, which allowed their efficient recycling. In conclusion, in addition to the synthesis of a new remarkable family of polynuclear complexes, this study brings about the rare duality of catalyst efficiency and robustness for cross carbon-carbon coupling reactions with recycling applications.

## Experimental Section

### General Data

Reagent-grade diethyl ether (used in hydrosilylation reactions) was predried over sodium foil and distilled from sodium-benzophenone anion under argon immediately prior to use. Anhydrous toluene was dried from sodium. Triethylamine was dried from calcium hydride. Other solvents and chemicals were used as received.

Only hydrosilylation reactions were carried out using Schlenk techniques or in a nitrogen-filled Vacuum Atmosphere drylab. Kartsted catalyst and Pd(OAc)<sub>2</sub> (98% or ≥99.9%) were purchased from Aldrich. Compounds **8**, **9** were synthesized according to ref.<sup>[45]</sup>

Flash column chromatography was performed using silica gel (300–400 mesh). <sup>1</sup>H NMR spectra were recorded with a 300 or 400 MHz spectrometer, <sup>29</sup>Si NMR spectra were obtained at 59.6 MHz with a 300 MHz spectrometer, and <sup>13</sup>C NMR spectra were recorded at 50, 75 or 100 MHz with 200, 300 or 400 MHz spectrometers. Copies of <sup>1</sup>H NMR, <sup>29</sup>Si and <sup>13</sup>C NMR spectra are provided (see Supporting Information). The soluble complex **1** was examined by cyclic voltammetry in CH<sub>2</sub>Cl<sub>2</sub> at 20 °C with 0.1 M [*n*-Bu<sub>4</sub>N][PF<sub>6</sub>] as supporting electrolyte on a Pt electrode, and a chemically irreversible reduction wave was observed at 0.95 V vs. the internal reference decamethylferrocene<sup>[46]</sup> at a scan rate of 0.1 V.s<sup>-1</sup> (see the Supporting Information). Elemental analyses were performed by the Center of Microanalyses of the CNRS at Lyon Villeurbanne, France.

For the thermogravimetric analysis, the samples have been previously degassed under primary vacuum during 45 min to reach 5·10<sup>-2</sup> mbar, and the device has been filled with pure argon with less than 2 ppm of O<sub>2</sub>. Experiments have been performed under argon flux and with a 2.5 °Cmin<sup>-1</sup> ramp temperature (TGA Setaram TAG2400 device coupled with a Thermostat quadrupolar mass spectrometer from Balzer).

**Caution: Sodium azide is potentially explosive. Great care is needed when handling this compound.**

### Synthesis of 1-Benzyl-4-phenyl-1H-[1,2,3]triazole (**6a**)<sup>[47]</sup>

2-Ethynylpyridine (0.5 mmol), benzyl azide (0.5 mmol) and [Cu(phen)(PPh<sub>3</sub>)<sub>2</sub>][NO<sub>3</sub>] (0.005 mmol, 4.27 mg) were added to a test tube with a stir bar, and the mixture was stirred at room temperature (25–28 °C) without exclusion of air under solvent-free conditions. After 10 min, the mixture was diluted with ethyl acetate and filtered. The filtrate was evaporated under reduced pressure to obtain the crude product, which was further purified by silica-gel chromatography (petroleum ether/ethyl acetate as eluent) to afford 1-benzyl-4-phenyl-1H-[1,2,3]triazole (**6a**); yield: (114 mg (97%)). <sup>1</sup>H NMR (300 MHz, DMSO-*d*<sub>6</sub>): δ = 8.70 (s, 1H, CH of triazole), 8.60 (d, *J* = 4.8 Hz, 1H, CH of pyridyl), 8.05 (d, *J* = 8.1 Hz, 1H, CH of pyridyl), 7.86–7.91 (m, 1H, CH of pyridyl), 7.32–7.41 (m, 6H, CH of pyridyl and CH of phenyl), 5.69 (s, 2H, CH<sub>2</sub>-triazole).

### Synthesis of Complex **7a**

**6a** (70.5 mg, 0.3 mmol) and palladium acetate (67.4 mg, 0.3 mmol) were dissolved in anhydrous toluene (8.0 mL). The mixture was stirred at room temperature for one day. After the reaction, the solid was isolated by filtration and washed successively with 20 mL toluene and 20 mL ether to give **7a** as a yellow solid; yield: 125 mg (91%). <sup>1</sup>H NMR (300 MHz, DMSO-*d*<sub>6</sub>): δ = 9.24 (s, 1H, CH of triazole), 8.21–8.27 (m, 1H, CH of pyridyl), 8.18 (d, *J* = 6.9 Hz, 1H, CH of pyridyl), 8.05 (d, *J* = 5.7 Hz, 1H, CH of pyridyl), 7.59–7.64 (m, 1H, CH of pyridyl), 7.39–7.45 (m, 5H, CH of phenyl), 5.83 (s, 2H, CH<sub>2</sub>-triazole), 1.93 (s, 3H, COCH<sub>3</sub>), 1.84 (s, 3H, COCH<sub>3</sub>); <sup>13</sup>C NMR (100 MHz, CDCl<sub>3</sub>): δ = 176.42 (C=O), 176.24 (C=O), 149.95, 148.47, 147.61, 141.88, 134.69, 129.73, 129.56, 129.12, 126.40, 126.34, 122.70 (C of Ar), 55.83 (CH<sub>2</sub>-triazole), 24.05, 23.69 (COCH<sub>3</sub>); MS (ESI): *m/z* = 461.0619 [M<sup>+</sup>], calcd. For C<sub>18</sub>H<sub>18</sub>N<sub>4</sub>O<sub>4</sub>Pd: 460.7799; anal. calcd. for C<sub>18</sub>H<sub>18</sub>N<sub>4</sub>O<sub>4</sub>Pd: C 46.92, H 3.94, N 12.16; found: C 46.43, H 3.87, N, 11.86.

### Synthesis of 2-(1H-[1,2,3]triazol-4-yl)-pyridine (**6b**)<sup>[48]</sup>

Trimethylsilyl azide (0.2 mL, 1.5 mmol) was added to a DMF and MeOH solution (2 mL, 9:1) of CuI (9.6 mg, 0.05 mmol) and 2-ethynylpyridine (103 mg, 1 mmol) under nitrogen. The reaction mixture was stirred at 100 °C overnight. After consumption of 2-ethynylpyridine, the mixture was cooled to room temperature and filtered through a short column of silica and concentrated. The residue was purified with silica gel column chromatography (petroleum ether/ethyl acetate, 10:1 to 1:1) to afford 2-(1H-[1,2,3]triazol-4-yl)-pyridine **6b**; yield: 95 mg (65%). <sup>1</sup>H NMR (300 MHz, DMSO-*d*<sub>6</sub>): δ = 15.27 (s, 1H, NH of triazole), 8.63 (d, *J* = 3.6 Hz, 1H, CH of pyridyl), 8.38 (s, 1H, CH of triazole), 8.00 (d, *J* = 7.8 Hz, 1H, CH of pyridyl), 7.87–7.93 (m, 1H, CH of pyridyl), 7.35–7.39 (m, 1H, CH of pyridyl).

**Caution: This reaction produces explosive and toxic hydrogen azide (HN<sub>3</sub>) in situ and must therefore be conducted behind a safety shield in a hood.**

## Synthesis of 7b

**6b** (73 mg, 0.5 mmol) and palladium acetate (112.3 mg, 0.5 mmol) were dissolved in anhydrous toluene (10.0 mL), and the mixture was stirred at room temperature for one day. After the reaction, the solid was isolated by filtration and washed successively with 20 mL toluene and 20 mL ether to give **7b** as a yellow solid; yield: 165 mg (89%). Anal. calcd. for  $C_{11}H_{12}N_4O_4Pd$ : C 35.64, H 3.26, N 15.12; found: C 35.47, H 3.23, N 15.63.

## Synthesis of the Dendritic Ligand 10

The azido dendrimer **9** (455.2 mg, 0.3 mmol) and 2-ethynylpyridine (417 mg, 4.05 mmol) were dissolved in tetrahydrofuran (THF), and water was added (20 mL:20 mL, THF/water). At room temperature,  $CuSO_4 \cdot 5H_2O$  was added (1 equiv *per* branch, 1 M aqueous solution), followed by the dropwise addition of a freshly prepared solution of sodium ascorbate (2 equiv *per* branch, 1 M aqueous solution). The solution was allowed to stir for 48 h at room temperature. After removing THF under vacuum, dichloromethane and an aqueous solution of ammonia were added. The mixture was allowed to stir for 10 min in order to remove all the Cu(I) trapped inside the dendrimer as  $Cu(NH_3)_6^+$ . The organic phase was washed twice with water (20 mL), dried with sodium sulfate, filtered on paper and the solvent was removed under vacuum. The product was washed with pentane (10 mL) in order to remove the excess of 2-ethynylpyridine and precipitated using dichloromethane/pentane. The dendrimer **10** was obtained as a brown solid; yield: 595 mg (81%).  $^1H$  NMR (300 MHz,  $CDCl_3$ ):  $\delta$  = 8.56 (d,  $J$  = 4.5 Hz, 9H, CH of pyridyl), 8.16 (d,  $J$  = 7.8 Hz, 9H, CH of pyridyl), 8.08 (s, 9H, CH of triazole), 7.76 (t,  $J$  = 7.2 Hz, 9H, CH of pyridyl), 6.98 (s, 3H, CH of Ar), 3.96 (s, 18H,  $SiCH_2$ -triazole), 1.64 (s, 18H,  $CH_2CH_2CH_2Si$ ), 1.11 (s, 18H,  $CH_2CH_2CH_2Si$ ), 0.65 (t,  $J$  = 7.5 Hz, 18H,  $CH_2CH_2CH_2Si$ ), 0.09 [s, 54H,  $Si(CH_3)_2$ ];  $^{13}C$  NMR (50 MHz,  $CDCl_3$ ):  $\delta$  = 150.64, 149.38, 148.07, 145.91, 137.00, 122.95, 122.79, 121.65, 120.22 (C of pyridyl, triazole, and phenyl), 44.04 ( $CH_2$ -triazole), 41.85 and 41.38 (benzylic quaternary C and  $CH_2CH_2CH_2Si$ ), 17.79 ( $CH_2CH_2CH_2Si$ ), 14.97 ( $CH_2CH_2CH_2Si$ ), -3.70 [ $Si(CH_3)_2$ ];  $^{29}Si$  NMR ( $CDCl_3$ , 59.62 MHz):  $\delta$  = 2.87; MS (MALDI-TOF):  $m/z$  = 2467.8 [ $MNa^+$ ], calcd. for  $C_{126}H_{174}N_{36}Si_9$ : 2445.7; anal. calcd. for  $C_{126}H_{174}N_{36}Si_9$ : C 61.88, H 7.17, N 20.62; found: C 61.67, H 7.02, N 20.38.

## Synthesis of the Metallodendritic Catalysts

### [Pd(OAc)<sub>2</sub>]<sub>n</sub>@dendrimer (11)

The dendritic palladium complexes were prepared by using  $Pd(OAc)_2$  and dendritic ligand **10** in freshly distilled toluene at the given concentrations for a period of time indicated in the Supporting Information. Then, the solution was filtered, the filter residues were washed with large amounts of toluene and ether to give the catalysts **11<sub>3</sub>**, **11<sub>4</sub>**, and **11<sub>9</sub>** as yellow or brown solids.

**[Pd(OAc)<sub>2</sub>]<sub>3</sub>@dendrimer (11<sub>3</sub>):** Dendrimer **10** (48.9 mg, 0.02 mmol) and palladium acetate (40.4 mg, 0.18 mmol) were dissolved in anhydrous toluene (15 mL). The mixture was stirred at less than 25 °C for 2–5 min, a bright yellow solid precipitated out from the solution. The solid was iso-

lated immediately by filtration and washed successively 40 mL toluene and 40 mL ether to give **11<sub>3</sub>** as a yellow solid. The filtrate can continue to be stirred under the same conditions, repeating above-mentioned operation, **11<sub>3</sub>** was obtained after drying under vacuum; yield: 20 mg (32%). The product was kept under nitrogen.  $^1H$  NMR (300 MHz,  $CDCl_3$ ):  $\delta$  = 0.03 (s, 54H), 0.51 (s, 18H), 1.02 (s, 18H), 1.55 (s, 18H), 1.83 (s, 9H), 1.97 (s, 9H), 4.03–4.24 (m, 18H), 6.93 (s, 3H), 7.30–7.45 (m, 8H), 7.85–8.05 (m, 18H), 8.39 (s, 6H), 8.55–8.61 (m, 6H), 9.42 (s, 3H);  $^{13}C$  NMR (75 MHz,  $CDCl_3$ ):  $\delta$  = 176.49, 176.24, 172.88, 150.74, 150.25, 149.97, 148.94, 148.53, 147.95, 147.18, 141.00, 137.84, 127.25, 126.28, 124.77, 123.57, 122.53, 120.03, 37.16, 24.07, 23.67, 22.04, 0.03, -0.24;  $^{29}Si$  NMR ( $CDCl_3$ , 59.62 MHz):  $\delta$  = 11.14, 2.89; MS (MALDI-TOF):  $m/z$  = 2764.8 [ $M-(OAc)_6$ ], calcd. for  $C_{138}H_{192}N_{36}O_{12}Pd_3Si_9$ : 3119.3; anal. calcd. for  $C_{138}H_{192}N_{36}O_{12}Pd_3Si_9$ : C 53.14, H 6.20, N 16.17; found: C 53.53, H 5.97, N 16.63.

**[Pd(OAc)<sub>2</sub>]<sub>4</sub>@dendrimer (11<sub>4</sub>):** Dendrimer **10** (48.9 mg, 0.02 mmol) and palladium acetate (18.0 mg, 0.08 mmol) were dissolved in toluene (15 mL). The mixture was stirred at less than 25 °C for 20–30 min, a bright yellow solid precipitated out from the solution. The solid was isolated immediately by filtration and washed successively with 40 mL toluene and 40 mL ether to give **11<sub>4</sub>** as a light brown solid; yield: 34 mg (51%). The product was kept under nitrogen.  $^1H$  NMR (300 MHz,  $CDCl_3$ ):  $\delta$  = 9.48 (s, 4H), 8.55–8.62 (m, 5H), 8.40 (s, 5H), 7.87–8.09 (m, 20H), 7.29–7.44 (m, 8H), 6.96 (s, 3H), 4.05–4.24 (m, 18H), 1.97 (s, 12H), 1.85 (s, 12H), 1.59 (s, 18H), 1.05 (s, 18H), 0.59 (s, 18H), 0.02 (s, 54H);  $^{13}C$  NMR (75 MHz,  $CDCl_3$ ):  $\delta$  = 176.46, 176.18, 172.97, 150.87, 150.75, 150.27, 150.14, 149.97, 148.49, 147.96, 147.60, 147.15, 137.84, 137.73, 124.78, 124.24, 123.57, 123.43, 120.04, 119.93, 44.19, 44.12, 37.15, 31.37, 24.07, 23.66, 22.20, 19.50, 17.80, 1.11, 0.96, -3.27, -3.30;  $^{29}Si$  NMR ( $CDCl_3$ , 59.62 MHz):  $\delta$  = 11.12, 6.65, 2.86, anal. calcd. for  $C_{142}H_{198}N_{36}O_{16}Pd_4Si_9 \cdot 2H_2O$ : C 50.46, H 6.02, N 14.92; found: C 50.71, H 5.87, N 14.60.

**[Pd(OAc)<sub>2</sub>]<sub>9</sub>@dendrimer (11<sub>9</sub>):** Dendrimer **10** (48.9 mg, 0.02 mmol) and palladium acetate (40.4 mg, 0.18 mmol) were dissolved in anhydrous toluene (25 mL). The mixture was allowed to stir for 48 h at room temperature. The solid was isolated by filtration and washed successively with 20 mL toluene and 20 mL ether to give **11<sub>9</sub>** as a brown solid; yield: 80.4 mg (90%); anal. calcd. for  $C_{162}H_{228}N_{36}O_{36}Pd_9 \cdot 5H_2O$ : C 42.70, H 5.26, N 11.07; found: C 42.69, H 5.18, N 10.87.

## General Procedure for the Sonogashira Reaction

A round-bottom flask (10 mL) containing monomeric or dendritic catalyst (0.001 mmol) was subjected to the Schlenk-line procedures of evacuation and purging of nitrogen for three cycles. Phenylacetylene (1 mmol), benzoyl chloride or iodobenzene (1.2 mmol), and 2 equiv.  $Et_3N$  (2 mmol) were successively added, and the mixture was stirred at room temperature or 50 °C. After the reaction was finished, the mixture was diluted with dichloromethane and filtered. The filtrate was removed under reduced pressure to provide the crude product that was further purified by silica gel chromatography (petroleum ether/ethyl acetate as

eluent) to yield the corresponding Sonogashira coupling products.

**1,3-Diphenyl-propynone:**  $^1\text{H NMR}$  (300 MHz,  $\text{CDCl}_3$ ):  $\delta = 8.22\text{--}8.23$  (m, 1H), 8.20 (t,  $J = 1.8$  Hz, 1H), 7.65–7.69 (m, 2H), 7.58–7.63 (m, 1H), 7.36–7.53 (m, 5H).

**1,2-Diphenylethyne:**  $^1\text{H NMR}$  (300 MHz,  $\text{CDCl}_3$ ):  $\delta = 7.51\text{--}7.56$  (m, 4H), 7.30–7.38 (m, 6H).

### General Procedure for the Suzuki Reaction

A round-bottom flask containing monomeric or dendritic catalyst (0.0025 mmol),  $\text{K}_2\text{CO}_3$  (1.5 mmol), and borophenyl acid (0.75 mmol) was subjected to the Schlenk-line procedures of evacuation and purging of nitrogen for three cycles. Halobenzene (if halobenzene was liquid) (0.5 mmol),  $\text{H}_2\text{O}$  (5 mL), and ethanol (7.5 mL) were successively added using syringes, and the mixture was stirred under controlled conditions. After cooling to room temperature, the mixture was diluted with dichloromethane and filtered. The filtrate was washed with water and the organic phase was dried using sodium sulfate, filtered on paper and the solvent was removed under vacuum to provide the crude product that was further purified by silica gel chromatography (petroleum ether as eluent) to yield the corresponding Suzuki reaction products.

**4-Methoxybiphenyl:**  $^1\text{H NMR}$  (300 MHz,  $\text{CDCl}_3$ ):  $\delta = 7.59\text{--}7.64$  (m, 4H), 7.49 (t,  $J = 7.7$  Hz, 2H), 7.37 (t,  $J = 7.4$  Hz, 1H), 7.05 (d,  $J = 9.0$  Hz, 2H), 3.91 (s, 3H).

### General Procedure for the Heck Reaction

A round-bottom flask containing monomeric or dendritic catalyst (0.025 mmol) and  $\text{K}_3\text{PO}_4$  (1.5 mmol) was subjected to the Schlenk-line procedures of evacuation and purging of nitrogen for three cycles. Iodobenzene or bromobenzene (0.5 mmol), styrene (1 mmol), and DMF (3 mL) were successively added using syringes, and the mixture was stirred under controlled conditions. After cooling to room temperature, the mixture was diluted with diethyl ether and filtered. The filtrate was washed with water and the organic phase was dried using sodium sulfate, filtered on paper and the solvent was removed under vacuum to provide the crude product, which was further purified by silica gel chromatography (petroleum ether as eluent) to yield corresponding Heck reaction products.

**(E)-1,2-Diphenylethene:**  $^1\text{H NMR}$  (300 MHz,  $\text{CDCl}_3$ ):  $\delta = 7.59$  (d,  $J = 7.2$  Hz, 4H), 7.43 (t,  $J = 7.5$  Hz, 4H), 7.30–7.36 (m, 2H), 7.19 (s, 2H).

### Procedure for Recycling the Catalysts

A round-bottom flask containing catalyst **7b** or **11**, (0.025 mmol) and  $\text{K}_3\text{PO}_4$  (1.5 mmol) was subjected to the Schlenk-line procedures of evacuation and purging of nitrogen for three cycles. Iodobenzene (0.5 mmol), styrene (1 mmol), and DMF (3 mL) were successively added using syringes, and the mixture was stirred at  $100^\circ\text{C}$  for 48 h. After cooling to room temperature, the mixture was diluted with diethyl ether and stood until the cloudy mixture became clear. Then the clear solution was poured into a glass through a paper filter and the solid was left in the flask as much as possible, and this operation was repeated three times. Then the collected solution was washed with

water, and the organic phase was dried using sodium sulphate, filtered on paper, and the solvent was removed under vacuum. This provided the crude product that was further purified by silica gel chromatography (petroleum ether as eluent) to yield the corresponding Heck reaction products. 0.5 mmol  $\text{K}_3\text{PO}_4$  was added to the flask containing the solid, and the Schlenk-line procedures of evacuation and purging of nitrogen for three cycles was conducted. Iodobenzene (0.5 mmol), styrene (1 mmol), and DMF (3 mL) were successively added using syringes, and the mixture was stirred at  $100^\circ\text{C}$  for 48 h. The process can be repeated at least ten times, and the yields indicated in table 6 were obtained.

### Acknowledgements

Financial support from the China Scholarship Council (CSC) from the People's Republic of China (Ph. D. grant to DW), the Université Bordeaux I, and the Centre National de la Recherche Scientifique (CNRS) is gratefully acknowledged.

### References

- [1] H. C. Kolb, M. G. Finn, K. B. Sharpless, *Angew. Chem.* **2001**, *113*, 2056–2075; *Angew. Chem. Int. Ed.* **2001**, *40*, 2004–2021.
- [2] a) V. V. Rostovtsev, L. G. Green, V. V. Fokin, K. B. Sharpless, *Angew. Chem.* **2002**, *114*, 2708–2711; *Angew. Chem. Int. Ed.* **2002**, *41*, 2596–2599; b) C. W. Tornøe, C. Christensen, M. Meldal, *J. Org. Chem.* **2002**, *67*, 3057–3064.
- [3] Reviews: a) D. Fournier, R. Hoogenboom, U. S. Schubert, *Chem. Soc. Rev.* **2007**, *36*, 1369–1380; b) M. V. Gil, M. J. Arévalo, Ó. López, *Synthesis* **2007**, 1589–1620; c) W. H. Binder, R. Sachsenhofer, *Macromol. Rapid Commun.* **2007**, *28*, 15–54; d) M. Meldal, C. W. Tornøe, *Chem. Rev.* **2008**, *108*, 2952–3015; e) G. Franc, A. Kakkar, *Chem. Commun.* **2008**, 5267–5276; f) J. F. Lutz, Z. Zarafshani, *Adv. Drug Delivery Rev.* **2008**, *60*, 958–970; g) J. F. Lutz, H. G. Börner, *Prog. Polym. Sci.* **2008**, *33*, 1–39; h) B. Droumaguet, K. Velonia, *Macromol. Rapid Commun.* **2008**, *29*, 1073–1089; i) W. H. Binder, R. Zirbs, *Click chemistry in Macromolecular Synthesis*, in: *Encyclopedia of Polymer Science and Technology*, Wiley, New York, **2009**; H. R. Marsden, A. Kros, *Macromol. Biosci.* **2009**, *9*, 939–951; j) P. L. Golas, K. Matyjaszewski, *Chem. Soc. Rev.* **2010**, *39*, 1338–1354; k) J. E. Hein, V. V. Fokin, *Chem. Soc. Rev.* **2010**, *39*, 1302–1315; l) B. S. Sumerlin, A. P. Vogt, *Macromolecules* **2010**, *43*, 1–13; m) H. Struthers, T. L. Mindt, R. Schibli, *Dalton Trans.* **2010**, *39*, 675–696; n) U. Mansfeld, C. Pietsch, R. Hoogenboom, C. R. Becer, U. S. Schubert, *Polym. Chem.* **2010**, *1*, 1560–1598; o) D. Best, *Biochemistry* **2009**, *48*, 6571–6584; p) D. G. Mullen, D. Q. McNerny, A. Desai, X. Cheng, S. C. DiMaggio, A. Kotlyar, Y. Zhong, S. Qin, C. V. Kelly, T. P. Thomas, I. Majoros, B. G. Orr, J. R. Baker, M. M. B. Holl, *Bioconjugate Chem.* **2011**, *22*, 679–689; q) L. Liang, D. Astruc, *Coord. Chem. Rev.* **2011**, *255*, 2933–2945.
- [4] For seminal studies, see: a) M. Barz, E. Herdtweck, W. R. Thiel, *Angew. Chem.* **1998**, *110*, 2380–2383;

- Angew. Chem. Int. Ed.* **1998**, *37*, 2262–2265; b) S. Komeda, M. Lutz, A. L. Spek, Y. Yamanaka, T. Sato, M. Chikuma, J. Reedijk, *J. Am. Chem. Soc.* **2002**, *124*, 4738–4746; c) T. R. Chan, R. Hilgraf, K. B. Sharpless, V. V. Fokin, *Org. Lett.* **2004**, *6*, 2853–2855; d) S. Badèche, J.-C. Daran, J. Ruiz, D. Astruc, *Inorg. Chem.* **2008**, *47*, 4903–4908.
- [5] a) M. Felici, P. Contreras-Carballada, Y. Vida, J. M. M. Smits, R. J. M. Nolte, L. D. Cola, R. M. Williams, M. C. Feiters, *Chem. Eur. J.* **2009**, *15*, 13124–13134; b) M. Obata, A. Kitamura, A. Mori, C. Kameyama, J. A. Czaplewski, R. Tanaka, I. Kinoshita, T. Kusumoto, H. Hashimoto, M. Harada, Y. Mikata, T. Funabiki, S. Yano, *Dalton Trans.* **2008**, 3292–3300; c) D. Maity, T. Govindaraju, *Inorg. Chem.* **2010**, *49*, 7229–7231; d) M. Felici, P. Contreras-Carballada, Y. Vida, J. M. M. Smits, R. J. M. Nolte, L. D. Cola, R. M. Williams, M. C. Feiters, *Chem. Eur. J.* **2009**, *15*, 13124–13134; e) D. Schweinfurth, K. I. Hardcastle, U. H. F. Bunz, *Chem. Commun.* **2008**, 2203–2205.
- [6] a) C. Ornelas, J. Ruiz, E. Cloutet, S. Alves, D. Astruc, *Angew. Chem.* **2007**, *119*, 890–895; *Angew. Chem. Int. Ed.* **2007**, *46*, 872–877; b) C. Ornelas, L. Salmon, J. Ruiz, D. Astruc, *Chem. Eur. J.* **2008**, *14*, 50–64.
- [7] a) A. K. Diallo, C. Ornelas, L. Salmon, J. Ruiz, D. Astruc, *Angew. Chem.* **2007**, *119*, 8798–8802; *Angew. Chem. Int. Ed.* **2007**, *46*, 8644–8648; b) C. Ornelas, J. Ruiz, L. Salmon, D. Astruc, *Adv. Syn. Catal.*, **2008**, *350*, 837–845.
- [8] Y.-W. Zhu, W.-B. Yi, C. Cai, *Catal. Commun.* **2011**, *15*, 118–122.
- [9] a) T. R. Chan, R. Hilgraf, K. B. Sharpless, V. V. Fokin, *Org. Lett.* **2004**, *6*, 2853–2855; J. E. Hein, J. C. Tripp, L. B. Krasnova, K. B. Sharpless, V. V. Fokin, *Angew. Chem.* **2009**, *121*, 8162; *Angew. Chem. Int. Ed.* **2009**, *48*, 8018–8021.
- [10] S. Özçubukçu, E. Ozkal, C. Jimeno, M. A. Pericàs, *Org. Lett.* **2009**, *11*, 4680–4683.
- [11] E. Hao, Z. Wang, L. Jiao, S. Wang, *Dalton Trans.* **2010**, 39, 2660–2666.
- [12] For phosphinotriazole in catalysis, see: a) D. Liu, W. Gao, Q. Dai, X. Zhang, *Org. Lett.* **2005**, *7*, 4907–4910; b) Q. Dai, W. Gao, D. Liu, L. M. Kapes, X. Zhang, *J. Org. Chem.* **2006**, *71*, 3928–3934; c) S. M. Spinella, Z.-H. Guan, J. Chen, X. Zhang, *Synthesis* **2009**, 3094–3098.
- [13] For phosphinomethylenetriazole in catalysis, see: R. J. Detz, S. A. Heras, R. de Gelder, P. W. N. M. van Leeuwen, H. Hiemstra, J. N. H. Reek, J. H. van Maarseveen, *Org. Lett.* **2006**, *8*, 3227–3230.
- [14] a) N. Miyaura, K. Yamada, A. Suzuki, *Tetrahedron Lett.* **1979**, *20*, 3437–3440; b) A. Suzuki, *Chem. Commun.* **2005**, 4759–4763; c) L. Yin, J. Liebscher, *Chem. Rev.* **2007**, *107*, 133–173; d) R. Martin, S. L. Buchwald, *Acc. Chem. Res.* **2008**, *41*, 1461–1473; e) A. Fihri, M. Bouhrara, B. Nekoueshahraki, J.-M. Basset, V. Polshettiwar, *Chem. Soc. Rev.* **2011**, *40*, 5181–5203; f) M. Pérez-Lorenzo, *J. Phys. Chem. Lett.* **2012**, *3*, 167–174; g) R. Rossi, F. Bellina, M. Lessi, *Adv. Synth. Catal.* **2012**, *354*, 1181–1255; h) M. M. Heravi, E. Hashemi, *Monatsh. Chem.* **2012**, *143*, 861–880; i) L. C. C. Vieira, M. W. Paixão, A. G. Corrêa, *Tetrahedron Lett.* **2012**, *53*, 2715–2718.
- [15] a) K. Sonogashira, Y. Tohda, N. Hagihara, *Tetrahedron Lett.* **1975**, 4467–4470; b) R. Chinchilla, C. Nájera, *Chem. Rev.* **2007**, *107*, 874–922; c) H. Doucet, J.-C. Hierso, *Angew. Chem.* **2007**, *119*, 850–888; *Angew. Chem. Int. Ed.* **2007**, *46*, 834–871; d) R. Chinchilla, C. Nájera, *Chem. Soc. Rev.* **2011**, *40*, 5084–5121; e) T. J. Colacot, *Platinum Met. Rev.* **2012**, *56*, 110–116; f) F. Bellina, M. Lessi, *Synlett* **2012**, 773–777.
- [16] a) R. F. Heck, *J. Am. Chem. Soc.* **1968**, *90*, 5518–5526; b) L. Lavenot, C. Gozzi, K. Ilg, I. Orlova, V. Penalva, M. Lemaire, *J. Organomet. Chem.* **1998**, *567*, 49–55; c) I. P. Beletskaya, A. V. Cheprakov, *Chem. Rev.* **2000**, *100*, 3009–3066; d) M. M. Heravi, A. Fazeli, *Heterocycles* **2010**, *81*, 1979–2026; e) A. Balanta, C. Godard, C. Claver, *Chem. Soc. Rev.* **2011**, *40*, 4973–4985; f) J. L. Bras, J. Muzart, *Chem. Rev.* **2011**, *111*, 1170–1214; g) D. M. Cartney, P. J. Guiry, *Chem. Soc. Rev.* **2011**, *40*, 5122–5150; h) M.-T. Ma, J.-M. Lu, *Appl. Organomet. Chem.* **2012**, *26*, 175–179; i) C. C. C. J. Seechurn, M. O. Kitching, T. J. Colacot, V. Snieckus, *Angew. Chem.* **2012**, *124*, 5150–5174; *Angew. Chem. Int. Ed.* **2012**, *51*, 5062–5085.
- [17] For palladodendrimers in catalysis, see: a) R. A. Kleij, P. W. N. M. van Leeuwen, A. W. van der Made, European Patent EP0456317, **1991**; *Chem. Abstr.* **1992**, *116*, 129870; b) G. E. Oosterom, J. N. H. Reek, P. C. J. Kramer, P. W. N. M. van Leeuwen, *Angew. Chem.* **2001**, *113*, 1878; *Angew. Chem. Int. Ed.* **2001**, *40*, 1828; c) D. Astruc, F. Chardac, *Chem. Rev.* **2001**, *101*, 2991–3031; d) R. van Heerbeek, P. C. J. Kamer, P. W. N. M. van Leeuwen, J. N. H. Reek, *Chem. Rev.* **2002**, *102*, 3717; e) H. P. Dijkstra, G. P. M. van Klink, G. van Koten, *Acc. Chem. Res.* **2002**, *35*, 798; f) D. Astruc, K. Heuze, S. Gatard, D. Méry, S. Nlate, L. Plault, *Adv. Synth. Catal.* **2005**, *347*, 329–338; g) J. N. H. Reek, S. van Arevalo, R. Heerbeek, P. C. J. Kamer, P. W. N. M. van Leeuwen, *Adv. Catal.* **2006**, *49*, 71–151; h) L. Gade, (Ed.), *Dendrimers in Catalysis*, Springer, Heidelberg, **2006**; i) S.-H. Hwang, C. D. Shreiner, C. N. Moorefield, C. N. Newkome, *New J. Chem.* **2007**, *31*, 1192–1217; j) R. Andrés, E. de Jesus, J. C. Flores, *New J. Chem.* **2007**, *31*, 1161–1191; k) E. de Jesus, J. C. Flores, *Ind. Eng. Chem. Res.* **2008**, *47*, 7968–7981; l) C. Ornelas, J. Ruiz, L. Salmon, D. Astruc, *Adv. Synth. Catal.* **2008**, *350*, 837–845; m) F. Martínez-Olíd, J. M. Benito, J. C. Flores, E. de Jesus, *Isr. J. Chem.* **2009**, *49*, 99–108; n) D. Astruc, E. Boisselier, C. Ornelas, *Chem. Rev.* **2010**, *110*, 1857–1959; o) D. Astruc, *Tetrahedron: Asymmetry* **2010**, *21*, 1041–1054; p) Y.-H. Tang, A. Y.-T. Huang, P.-Y. Chen, H.-T. Chen, C.-L. Kao, *Curr. Pharm. Des.* **2011**, *17*, 2308–2330.
- [18] For reviews on homogeneous and heterogeneous catalysis, see: a) J. Hassan, M. Sévignon, C. Gozzi, E. Schulz, M. Lemaire, *Chem. Rev.* **2002**, *102*, 1359–1469; b) F. Fache, E. Schulz, M. L. Tommasino, M. Lemaire, *Chem. Rev.* **2000**, *100*, 2159–2231.
- [19] R. Schweinfurth, S. Pattacini, S. Strobel, B. Sarkar, *Dalton Trans.* **2009**, 9291.
- [20] M.-T. Chen, K.-M. Wu, C.-T. Chen, *Eur. J. Inorg. Chem.* **2012**, 720–726.

- [21] L.-W. Xu, X.-H. Chen, H. Shen, Y. Deng, J.-X. Jiang, *Eur. J. Org. Chem.* **2012**, 290–297.
- [22] K. Jiang, G.-Q. Lai, C.-Q. Sheng, *Eur. J. Org. Chem.* **2012**, 290–297.
- [23] Z.-Z. Zhou, F.-S. Liu, D.-S. Shen, C. Tan, L.-Y. Liu, *Inorg. Chem. Commun.* **2011**, *14*, 659–662.
- [24] L. Li, J. Wang, C. Zhou, R. Wang, M. Hong, *Green Chem.* **2011**, *13*, 2071–2077.
- [25] F. F. D. Oliveira, M. R. dos Santos, P. M. Lalli, E. M. Schmidt, P. Bakuzis, A. A. M. Lapis, A. L. Monteiro, M. N. Eberlin, B. A. D. Neto, *J. Org. Chem.* **2011**, *76*, 10140–10147.
- [26] Y.-Q. Tang, J.-M. Lu, L.-X. Shao, *J. Organomet. Chem.* **2011**, *696*, 3741–3744.
- [27] Q.-X. Liu, H.-L. Li, X.-J. Zhao, S.-S. Ge, M.-C. Shi, G. Shen, Y. Zang, X.-G. Wang, *Inorg. Chim. Acta* **2011**, *376*, 437–445.
- [28] G. Roymahapatra, S. Giri, A. A. Danopoulos, P. K. Chattaraj, A. Mahapatra, V. Bertolasi, J. Dinda, *Inorg. Chim. Acta* **2012**, *383*, 83–90.
- [29] W. Susanto, C.-Y. Chu, W. J. Ang, T.-C. Chou, L.-C. Lo, Y. Lam, *Green Chem.* **2012**, *14*, 77–80.
- [30] J. Zhang, M. Đaković, Z. Popović, H. Wu, Y. Liu, *Catal. Commun.* **2012**, *17*, 160–163.
- [31] S. Atobe, M. Sonoda, Y. Suzuki, H. Shinohara, T. Yamamoto, A. Ogawa, *Chem. Lett.* **2011**, *40*, 925–927.
- [32] A. N. Marziale, J. Schlüter, J. Eppinger, *Tetrahedron Lett.* **2011**, *52*, 6355–6358.
- [33] J. C. Barros, R. S. Yaunner, A. L. F. de Souza, J. F. M. da Silva, O. A. C. Antunes, *Appl. Organomet. Chem.* **2011**, *25*, 820–823.
- [34] Y. He, C. Cai, *J. Organomet. Chem.* **2011**, *696*, 2689–2692.
- [35] B. Bahramian, M. Bakherad, A. Keivanloo, Z. Bakherad, B. Karrabi, *Appl. Organometal. Chem.* **2011**, *25*, 420–423.
- [36] V. Singh, R. Ratti, S. Kaur, *J. Mol. Catal. A: Chem.* **2011**, *334*, 13–19.
- [37] T. Suzuka, K. Kimura, T. Nagamine, *Polymers* **2011**, *3*, 621–639.
- [38] Y. He, C. Cai, *Appl. Organomet. Chem.* **2011**, *25*, 799–803.
- [39] M. Bagherzadeh, M. Amini, A. Ellern, L. K. Woo, *Inorg. Chim. Acta* **2012**, *383*, 46–51.
- [40] L. Wan, C. Cai, *Transition Met. Chem.* **2011**, *36*, 747–750.
- [41] Y. He, C. Cai, *Transition Met. Chem.* **2011**, *36*, 113–117.
- [42] B. K. Allam, K. N. Singh, *Synthesis* **2011**, 1125–1131.
- [43] Z. Du, W. Zhou, L. Bai, F. Wang, J.-X. Wang, *Synlett* **2011**, 369–372.
- [44] G. An, X. Ji, J. Han, Y. Pan, *Synth. Commun.* **2011**, *41*, 1464–1471.
- [45] C. Ornelas, J. Ruiz, E. Cloutet, S. Alves, D. Astruc, *Angew. Chem.* **2007**, *119*, 890; *Angew. Chem. Int. Ed.* **2007**, *46*, 872.
- [46] J. Ruiz, D. Astruc, *C. R. Acad. Sci. Paris, Série II* **1998**, 21–27.
- [47] D. Wang, M. Zhao, X. Liu, Y. Chen, N. Li, B. Chen, *Org. Biomol. Chem.* **2012**, *10*, 229–231.
- [48] T. Jin, S. Kamijo, Y. Yamamoto, *Eur. J. Org. Chem.* **2004**, 3789–3791.

## Conclusion and Perspective

In this thesis, our investigations have concerned the design and catalytic applications of recoverable catalysts, specifically focusing on two aspects:

- (i) the synthesis, functionalization and catalytic application of magnetically recyclable dendritic catalysts;
- (ii) the design, synthesis and catalytic properties of monomeric and dendritic palladium complexes containing the 2-pyridyl-1,2,3-triazole ligand;

In a review of MNPs-immobilized RuNPs and Ru complex catalysts, we emphasized the significance of magnetically recoverable ruthenium catalysts and figured out the recent developments, breakthroughs, trends and unsolved problems in this area. This review inspired us to synthesize novel MNPs-Ru catalysts, and evaluate their catalytic performance in some key reactions. Based on these literature reviews, the experimental work led to immobilization of homogeneous pentamethylcyclopentadienyl (Cp\*) ruthenium complex onto SiO<sub>2</sub>/γ-Fe<sub>2</sub>O<sub>3</sub> shell-core nanoparticles, forming heterogeneous analogues. It was observed that Cp\*(PPh<sub>3</sub>)<sub>2</sub>Ru/SiO<sub>2</sub>/γ-Fe<sub>2</sub>O<sub>3</sub> is highly efficient for regioselective synthesis of a series of 1,5-disubstituted 1,2,3-triazoles through ruthenium-catalyzed alkyne-azide cycloaddition (RuAAC). More importantly, the catalyst was simply recovered with an external magnet and reused for at least five times without significant decrease in activity and selectivity. Considering the wide uses of Cp\*Ru(II) catalysts in organic synthesis, the principles and results presented here should open a field of applications in “green” chemistry involving the recycling of such catalysts.

A MNPs-anchored tris(triazolyl)-CuBr catalyst was prepared. This catalyst was shown to be obtained with a good monodispersity and successfully catalyzes the copper-catalyzed cycloaddition between terminal alkynes and azides (CuAAC) including a broad substrate scope in aqueous solution at room temperature. Several 1,4-disubstituted 1,2,3-triazoles including allyl- and triethylene glycol-ended 27-branch dendrimers were obtained in good to excellent yields and 100% selectivity. In addition, the procedure was extended to “one-pot” synthesis of 1,4-disubstituted

1,2,3-triazoles through a cascade reaction involving benzyl bromides, alkynes, and sodium azide. The catalyst was easily separated from the reaction medium by using an external magnet and recycled for six cycles with only a slight decrease of activity and small leaching of copper, when phenylacetylene and benzyl azide were chosen as model substrates. This magnetic catalyst could potentially be applied to CuAAC reactions for the synthesis of macromolecules, biomolecules, and nanoparticles.

The investigation of MNPs-anchored PdNPs decorated by TEG-terminated “click” dendrimers indicates various positive dendritic effects in terms of ligand loading, catalyst loading, catalytic activity and recyclability. This work provides a new lesson regarding the design and engineering of catalysts deposited on MNPs, i.e. MNPs decorated with dendritic frame are clearly favorable concerning the efficiency for practical and environmentally friendly reactions. Moreover, the protocol of impregnation of pre-synthesized PdNPs stabilized by TEG-terminated “click” dendrimer into iron oxide MNPs, is an excellent complementarity for classic synthesis method of MNPs-metal NPs. The principles and results presented here should thus open a gate for more applications of MNPs-DEN-NP catalysts in “green” chemistry.

A new family of polynuclear Pd complexes bearing the triazolyl pyridine ligand exhibited the rare duality of catalyst efficiency and robustness for cross carbon-carbon coupling reactions with recycling applications. The result brings a solid argument indicating that triazole compounds are promising ligands for transition metals in catalysis.

In sum, our thesis has led to advances in development of current knowledge on catalytic applications of recyclable catalysts. Dendrimer catalysts and magnetic catalysts are two key components in catalysis science. Both of them bring about the rare duality of catalyst efficiency and catalyst recovery, and each of dendrimer catalysts and magnetic catalysts hold several characteristics.

The catalytic properties of dendrimer catalysts can be easily tuned through the adjustment of their structure, size, shape, chemical functionality, and solubility. Moreover, dendrimer catalysts possess a monodisperse nature that retains the advantage of homogeneous catalysts in terms of showing fast kinetic behavior, easy

tenability and rationalization. However, dendrimer catalysts also have some disadvantages, such as complicated synthesis procedure, inconvenient recovery process, negative dendritic effects that were often observed (i.e. poorer catalytic activity when the dendrimer generation was increased).

Magnetic catalysts perfectly combine the advantages of heterogeneous catalysts (easy recovery and regeneration), nanocatalysts (such as a large surface-to-volume ratio relative to bulk materials, excellent activity, great selectivity, and high stability), and inherent properties of MNPs (such as biocompatibility, low preparation cost, simple synthesis procedure, and magnetic separability).

Although both dendrimer catalysts and magnetic catalysts can fill the gap between homogeneous catalysis and heterogeneous catalysis, in our views, magnetic catalysts are more economic and practical. Nevertheless, dendritic frameworks were shown to improve the efficiency of MNP-supported Pd catalysts. Magnetic catalysts fully embody the principles of “green” chemistry and sustainability and most probably represent the future of recyclable catalysts.

Concerning the increasing environmental problem, the development of “green” and economic catalysts involving MNPs-supported catalysts is still urgently required. Further research in the area will be mainly concentrated in explorations of new magnetic multifunctionalized catalysts, magnetic bimetallic catalysts, magnetic plasmonic photocatalysts, Fe, Co, Mo and Ni catalyst, and their use in multikilogram-scale synthesis toward industrial production.

## List of Published or Submitted Thesis Publications

1. **D. Wang**, L. Etienne, M. E. Igartua, S. Moya, D. Astruc, A highly active and magnetically recoverable tris(triazolyl) Cu(I) catalyst for “click” alkyne-azide cycloaddition reactions, *Chem.-Eur. J.* **2014**, *20*, 4047-4054.
2. **D. Wang**, L. Salmon, J. Ruiz, D. Astruc. Recyclable ruthenium (II) complex supported on magnetic nanoparticles: A regioselective catalyst for alkyne azide cycloaddition, *Chem. Comm.* **2013**, *49*, 6956-6958.
3. **D. Wang**, D. Denux, J. Ruiz, D. Astruc. The Clicked Pyridyl-Triazole Ligand: From Homogeneous to Robust, Recyclable Heterogeneous Mono- and Polymetallic Palladium Catalysts for Efficient Suzuki-Miyaura, Sonogashira, and Heck Reactions, *Adv. Synth. Catal.* **2013**, *355*, 129-142.
4. **D. Wang**, C. Deraedt, L. Salmon, L. Etienne, J. Ruiz, D. Astruc. Highly efficient and magnetically recoverable “click” PEGylated  $\gamma$ -Fe<sub>2</sub>O<sub>3</sub>-Pd nanoparticle catalysts for Suzuki-Miyaura, Sonogashira, and Heck reactions, **2014**, submitted.
5. C. Deraedt, **D. Wang**, L. Salmon, L. Etienne, J. Ruiz, D. Astruc, Impregnation of dendritically preformed Pd nanoparticles on magnetic nanoparticles for improved catalyst robustness, efficiency and recyclability, **2014**, to be submitted.
6. **D. Wang**, D. Astruc, Dendritic catalysis-Basic concepts and recent trends. *Coord. Chem. Rev.* **2013**, *257*, 2317–2334.
7. **D. Wang**, D. Astruc. Fast-growing Field of Magnetically Recyclable Nanocatalysts, *Chem. Rev.* **2014**, DOI: 10.1021/cr500134h.
8. **D. Wang**, D. Astruc. Magnetically Recoverable Ruthenium Catalysts in Organic Synthesis, *Molecules* **2014**, *19*, 4635-4653.

# **Nouveaux Catalyseurs Recyclables pour les Réactions de Formation de Liaisons Carbone-Carbone et Carbone-Azote**

## **Résumé**

Les catalyseurs supportés sur des dendrimères et nanoparticules magnétiques acquièrent actuellement une importance accrue dans le contexte de la chimie verte et du développement durable car ils sont séparés facilement des produits de réaction par filtration ou à l'aide d'un aimant et recyclables. Dans cet esprit, la thèse a été dédiée à la synthèse, à la caractérisation et aux applications catalytiques de catalyseurs moléculaires, nano- et dendritiques immobilisés impliquant le ruthénium, le cuivre et le palladium. Les catalyseurs magnétiquement recyclables de ruthénium (II), de cuivre (I) et des nanoparticules de palladium ont produit d'excellentes performances en terme d'activité, de stabilité et de recyclabilité pour les réactions de cycloaddition entre les alcynes et les azotures et les réactions de couplage croisé carbone-carbone. Enfin, la synthèse de complexes mono- et polymétalliques du palladium contenant les ligands 2-pyridyl-1,2,3-triazole a également été réalisée et leurs propriétés catalytiques ont été étudiées.

## **Mots-clés:**

Catalyse, nanoparticule magnétique, dendrimère, catalyseur recyclable, réactions de couplage carbone-carbone, réaction "click"

# **New Recyclable Catalysts for the formations of Carbon-Carbon and Carbon-Nitrogen Bonds**

## **Abstract:**

Catalysts based on dendrimers and magnetic nanoparticles are becoming increasingly utilized in the context of green and sustainable chemistry, because they are easily separated by precipitation or by using a simple magnet respectively, and they are recyclable. In this spirit, the thesis has been devoted to the synthesis, characterization and catalytic applications of iron oxide magnetic nanoparticles-immobilized molecular, nano- and dendritic catalysts involving Ru, Cu and Pd. Magnetically recyclable ruthenium(II) and Cu(I) complexes and Pd nanoparticles have provided excellent catalytic performances in terms of activity, stability and recyclability, using alkyne-azide cycloaddition and carbon-carbon cross coupling reactions. The synthesis of mono- and polymetallic palladium complexes containing the 2-pyridyl-1,2,3-triazole ligand or nonbranch-derived ligands has also been carried out, and their catalytic properties in coupling reactions has been studied.

## **Keywords:**

Catalysis, magnetic nanoparticle, dendrimer, catalyst recovery, C-C coupling reactions, "click" reaction